

University of Strathclyde
Department of Pure and Applied Chemistry

The development of analytical approaches to profile
Scotch Whisky colour

Megan Holden

A thesis submitted to the Department of Pure and Applied
Chemistry, University of Strathclyde, Glasgow, in part
fulfilment of the regulations for the degree of Doctor of
Philosophy

September 2015

Copyright

This thesis is the result of the author's original research. It has been composed by the author and has not been previously submitted for examination which has led to the award of a degree.

The copyright of this thesis belongs to the author under the terms of the United Kingdom Copyright Acts as qualified by University of Strathclyde Regulation 3.50. Due acknowledgement must always be made of the use of any material contained in, or derived from, this thesis.

Signed:

Dated:

For my family – *per asepera ad astra*

Sláinte!

Acknowledgements

Firstly I would like to thank my supervisor, Dr. Alison Nordon for all of her expertise and guidance throughout my PhD. She has been a constant source of support and always made time for me whether to advise, encourage or simply reassure – it's safe to say I couldn't have got through this project without you and I feel privileged to have worked with you. Thank you Alison!

I would also like to thank my second and third supervisors, Professor David Littlejohn and Professor Walter Johnstone. Both have generously contributed their time to this project and their informative discussions throughout my research have provided me with advice and suggestions that have helped me progress my work.

I would also like to acknowledge the outstanding support from my supervisors at the Scotch Whisky Research Institute (SWRI) and all of the staff members I have come to know there. I was always made to feel welcome at the SWRI and cannot praise everyone enough for the help and guidance I received there. In particular I would like to thank Ian Goodall, Craig Owen and Shona Glancy – their knowledge and expertise in the Scotch Whisky industry have been invaluable throughout this project.

I would like to further extend my gratitude to Gary Golquhoun, Trevor Whittle and all members of Fibre Photonics. Their expertise in all aspects of ATR-MIR spectrometry was invaluable and I am extremely grateful for all of their advice and support during this project.

Thanks must also be given to: Piotr Gromski, for your expertise in chemometrics and the PC-DFA work you completed, both were invaluable for my studies; Simon Cubbon of Waters Ltd., for the UPLC-MS analysis undertaken for this project and the generous time you spent instructing me through the workings of the MarkerLynx software; and also to Gemma Gardiner, you never failed to keep me smiling during the struggles of final year and the work you completed on caramel fade was an extremely important addition to this research. It was a pleasure to work with you all!

This project was made possible by joint funding from the SWRI, Fibre Photonics and the University of Strathclyde and so I would like to thank each of them for the opportunity to undertake this novel research in such a stimulating field.

Finally but by no means least, I would like to thank my colleagues, friends and family. To all of those from the analytical group, thanks for all the tea and chats – I wouldn't have made it without your support! To all of my friends and family, thank you for always sticking by me when times have been hardest – thank you especially to my wife Diane, words cannot describe how important you are to me and I want to thank you for all of your support and understanding throughout this PhD.

Abstract

Attenuated total reflectance mid-infrared (ATR-MIR) spectrometry and liquid chromatography – mass spectrometry (LC-MS) have been investigated as techniques for profiling Scotch Whisky colour (naturally derived and that originating from E150a caramel).

ATR-MIR was initially implemented to investigate caramel colourants and it was found that profiles dominated by colour constituents could be obtained by analysing dried residues of caramel solutions. Using this approach, it was possible to differentiate between legally permitted E150a caramels and the three other EU recognised classes (not permitted in Scotch). It was also possible to obtain unique profiles for different E150a formulations. These distinctions between caramels were maintained when dissolved in a typical blend whisky, a finding that could provide the opportunity to use E150a caramels as inherent authenticity markers in Scotch. Additional factors such as changing caramel concentration, varying the blend matrix, and caramel fade were also investigated in this work and found in some cases to influence spectra.

Work progressed from the above findings to compare multivariate data analysis tools for the prediction of caramel identities, based on their characteristic spectra. PCA with GLSW and PC-DFA were found to be most successful but would require background whisky matrices to be accounted for during calibration.

Analysis of LC-MS data complemented that of ATR-MIR, showing the potential to distinguish between caramel materials as described above. The advantage of ATR-MIR over LC-MS is its adaptability for field studies as a portable device, LC-MS on the other hand has the ability to identify components responsible for sample distinctions and it was possible in this work to find components characteristic of different caramels. Advanced software also enabled tentative structures to be assigned to some components. Additional studies using LC-MS highlighted its potential for other applications relating to Scotch, for example components characteristic of different cask histories and maturation ages were found.

Contents

Copyright	i
Dedication	ii
Acknowledgements	iii
Abstract	v
Contents	vi
1.0 INTRODUCTION	1
1.1 The History of Scotch Whisky.....	1
1.2 Current Scotch Whisky Legislation	5
1.3 Current Manufacturing Process	7
1.3.1 Malting	7
1.3.2 Mashing.....	8
1.3.3 Fermentation	9
1.3.4 Distillation.....	10
<i>1.3.4.1 Pot-still for distillation of malt whiskies</i>	13
<i>1.3.4.2 Coffey still for distillation of grain whiskies</i>	16
1.3.5 Maturation	19
1.3.6 Blending and Bottling	22
1.4 The Origins of Colour in Scotch Whisky.....	24
1.4.1 Natural Colour.....	24
<i>1.4.1.1 Cask history</i>	25
<i>1.4.1.2 Other variables</i>	26
1.4.2 Caramel Colour	27
1.5 General Thesis Scope and Aims	31
1.6 References	34
2.0 THEORY	38
2.1 ATR-MIR Spectrometry	38
2.1.1 MIR Spectrometry.....	38
2.1.2 ATR-MIR Spectrometry	43
<i>2.1.2.1 Optical fibres</i>	44

2.1.2.2 ATR-MIR probe technology	48
2.1.2.3 ATR probe design	50
2.1.3 Fourier Transform Infrared Spectrometry.....	53
2.2 Liquid Chromatography – Mass Spectrometry	57
2.2.1 Liquid Chromatography	57
2.2.2 Mass Spectrometry.....	62
2.2.2.1 Ion source.....	63
2.2.2.2 Mass analyser	64
2.2.2.3 Detector.....	67
2.2.3 MarkerLynx XS™ Software.....	68
2.3 Data Analysis	70
2.3.1 Principal Component Analysis (PCA).....	70
2.3.2 Clustering and Classification Tools	73
2.3.2.1 Hierarchical cluster analysis (unsupervised)	74
2.3.2.2 k-nearest neighbour (k-NN) classification	77
2.3.2.3 Principal components – discriminant function analysis (PC- DFA).....	79
2.3.3 Data Preprocessing Tools.....	81
2.3.3.1 Derivatisation.....	81
2.3.3.2 Normalisation.....	83
2.3.3.3 Generalised least squares weighting preprocessing.....	84
2.4 References	85

3.0 ATR-MIR SPECTROMETRY FOR PROFILING CARAMEL COLOUR IN SCOTCH WHISKY 90

3.1 Introduction	90
3.1.1 Basis of this Study.....	90
3.1.2 Profiling Caramel Colourants in Foodstuffs – A Literature Review.....	91
3.1.3 Study Objectives	96
3.2 Experimental	98
3.2.1 Samples and Materials	98
3.2.1.1 Caramels and colourant materials	98

3.2.1.2	<i>Blends for discrimination study</i>	99
3.2.2	Mid-infrared Spectrometry	99
3.2.3	UV-Visible Spectrometry	99
3.2.4	Methods of Analysis	100
3.2.4.1	<i>Samples spiked in 40% ethanol</i>	100
3.2.4.2	<i>Samples spiked in blended Scotch Whisky</i>	100
3.2.4.3	<i>Caramel concentration study</i>	101
3.2.4.4	<i>Caramel fade study</i>	102
3.2.4.5	<i>Blend discrimination study</i>	103
3.2.5	Data Analysis	103
3.3	Results and Discussion	105
3.3.1	ATR-MIR for Profiling Caramel Colourants	105
3.3.1.1	<i>Assessment of the ATR-MIR method</i>	105
3.3.1.2	<i>Profiling caramels in 40% ethanol</i>	113
3.3.1.3	<i>Profiling caramels in blended Scotch Whisky</i>	123
3.3.2	Scenarios relevant to ‘Real’ Whisky Products	131
3.3.2.1	<i>Caramel concentration study</i>	131
3.3.2.2	<i>Caramel fade study</i>	136
3.3.3	Blend Discrimination Study	141
3.4	Conclusions	145
3.5	References	147

4.0 THE APPLICATION OF CLASSIFICATION TOOLS FOR THE PREDICTION OF CAMEL IDENTITIES..... 150

4.1	Introduction	150
4.1.1	Basis of this Study	150
4.1.2	Classification Tools for Profile Prediction – A Literature Review	151
4.1.2.1	<i>GLSW preprocessing</i>	151
4.1.2.2	<i>HCA</i>	153
4.1.2.3	<i>k-NN classification</i>	155
4.1.2.4	<i>PC-DFA</i>	156
4.1.3	Study Objectives	158

4.2 Experimental	160
4.2.1 Samples	160
4.2.1.1 Calibration samples/data	160
4.2.1.2 Test samples/data	162
4.2.2 Data Analysis	165
4.2.2.1 Data preparation/pre-treatment	165
4.2.2.2 PCA with GLSW preprocessing	165
4.2.2.3 HCA.....	166
4.2.2.4 k-NN classification	166
4.2.2.5 PC-DFA	167
4.3 Results and Discussion.....	168
4.3.1 PCA with GLSW Preprocessing	168
4.3.1.1 Optimisation of the weighting parameter (and model validation)	168
4.3.1.2 Predicting the caramel class and E150a formulation of test data.....	173
4.3.1.3 Summary.....	190
4.3.2 HCA	191
4.3.3 k-NN Classification.....	196
4.3.3.1 Predicting the caramel class and E150a formulation of test data.....	196
4.3.3.2 Summary.....	204
4.3.4 PC-DFA	205
4.3.4.1 Assigning caramel class and E150a formulation to test data.....	205
4.3.4.1 Summary.....	215
4.3.5 Prediction of Blend Whisky Identities using Classification Tools.....	215
4.4 Conclusions	217
4.5 References	220

5.0 UPLC TOF MS IN COMBINATION WITH STATISTICAL DATA ANALYSIS FOR THE IDENTIFICATION OF CARMEL COMPONENTS	225
--	------------

5.1 Introduction	225
5.1.1 Basis of this Study.....	225
5.1.2 UPLC-MS in Combination with Statistical Data Analysis for Differentiating Caramel Materials	226
5.1.3 Study Objectives	230
5.2 Experimental	231
5.2.1 Samples	231
5.2.2 UPLC-MS	231
5.2.3 Data Analysis	233
5.2.3.1 <i>Pareto scaling</i>	233
5.2.4 Elemental Composition Analysis (ECA)	234
5.3 Results and Discussion.....	235
5.3.1 UPLC-MS in Combination with PCA to Profile Caramel Composition	235
5.3.1.1 <i>Caramels in 40% ethanol</i>	235
5.3.1.2 <i>Caramels in whisky matrix (Blend W)</i>	251
5.3.2 The Application of MarkerLynx Software for Structural Elucidation	257
5.3.2.1 <i>Elemental composition analysis</i>	257
5.3.2.2 <i>Structural elucidation</i>	260
5.4 Conclusions	267
5.5 References	269

**6.0 UPLC TOF MS IN COMBINATION WITH STATISTICAL DATA
ANALYSIS FOR PROFILING NON VOLATILE COMPONENTS IN
SCOTCH WHISKY 272**

6.1 Introduction	272
6.1.1 Basis of this Study.....	272
6.1.2 UPLC in Combination with MS as a Tool for Profiling Scotch Whisky	272
6.1.3 Study Objectives	276
6.2 Experimental	277
6.2.1 Samples	277

6.2.2.1 Preparation of the solvent extracts (samples 9-11)	279
6.2.2 UPLC-MS	279
6.2.3 Data Analysis	279
6.3 Results and Discussion.....	281
6.3.1 Profiling Whiskies with Different Cask History – ‘Subset A’.....	281
6.3.2 Profiling Whiskies with Different Maturation Ages – ‘Subset B’.	288
6.3.3 Comparison of ‘Authentic’ vs. ‘Simulated’ Maturation Profiles – ‘Subset C’	295
6.3.4 Detecting Common Adulterants and Understanding the Affect of Fade	301
6.3.5 Blend Discrimination – ‘Subset E’	307
6.4 Conclusions	315
6.5 References	317
7.0 CONCLUSIONS AND FUTURE WORK.....	319
7.1 Conclusions	319
7.2 Comments and Suggestions for Future Work	322
8.0 APPENDICES	326
8.1 Calculating Reconstitution Volume	326
8.2 Scores and Loadings Data for Additional PCs.....	328
8.3 Considerations and Recommendations for ATR-MIR Instrument Development	330

1.0 INTRODUCTION

1.1 The History of Scotch Whisky

The word 'whisky' comes from the Gaelic term '*uisge beatha*', which translates in English as 'water of life' and in Latin as '*aqua vitae*'.¹ This name ties in nicely with the early history of distilled alcoholic beverages, which were regarded as having powerful medicinal properties, and whose recipes were primarily entrusted to the religious clerics of the time.² Whisky has since grown to be one of the most popular drinks of leisure, with Scotch Whisky in particular being considered as the international spirit of choice. The success of Scotch is entwined with its extensive history, in its time being exposed to ever changing laws of taxation and legislation that have ultimately shaped the industry as it is known today.

Whisky is produced by the art of distilling and the earliest documented record of the craft in Scotland dates as far back as 1494. In this year an entry in the Scottish Exchequer Rolls refers to "eight bolls of malt to Friar John Cor wherewith to make aquavitae".³ This quantity is sufficient to produce almost 1500 bottles of whisky and so clearly indicates that distillation was already a well established technique by this time. In fact, the earliest roots of distillation can be traced back as far as the ancient Egyptians, who introduced the art to Western Europe. It is generally considered, that distilling was then brought to Scotland by missionary monks from Ireland, where monastic distilleries were already in operation in the later twelfth century.⁴

The first record of control in place over whisky in Scotland dates back to 1505, where a monopoly was granted to the Guild of Surgeon barbers in Edinburgh over the manufacture and sale of what they called 'aqua vite'.^{3,4} These being the medical practitioners of the time, this supports the early use of whisky for medicinal purposes and a clear attempt to control distilling for this use only. Closely following this, a reference to whisky being acquired for drinking pleasure is noted in the Treasury Accounts of King James IV during a stay at Inverness in September of 1506. Two entries were made on the 15th and 17th of the month reading 'For aqua vite to the

King...' and 'For ane flacat of aqua vite to the King...' respectively and record payment to the local barber.⁵

The production of whisky in these early stages used primitive equipment and lacked scientific expertise making the spirit potent and potentially harmful. It was not until the mid sixteenth century that an improvement in the quality of Scotch began to develop, due to advances in still designs and the dissolution of the monasteries. Monks had no choice but to put their distilling skills to use causing the knowledge of whisky production to spread rapidly to others.⁶ A shortage of grain for food became evident in the months to follow and alerted the authorities to the widespread practice of whisky distillation. The lack of availability of grain caused by the clear violation of the 1505 monopoly led to the first subjection of Scotch Whisky to government control in 1597.²

The government Act of 1597 stated that production of the distilled product was to be restricted to Earls, Lords, Barons and Gentlemen, who could distil for their own use only.³ Despite these regulations, the drinking of whisky in Scotland for social purposes had widely increased in popularity, leading to many breaches of the law and further government attention. An Act of Excise was consequently passed by the Scots Parliament in 1644, fixing the duty as 2s. 8d. per pint of aquavita or other strong liquor. Taxation continued for the remainder of the seventeenth century, although it was not strongly imposed. There were many variations made to the types and amounts of duty collected and at one point collection was even allowed to lapse.²

Taxation began to have a larger impact on the production of Scotch Whisky after the Act of the Union with England in 1707. An English malt tax was extended north across the border in 1713 meeting strong opposition in Scotland by those arguing that it directly contradicted the terms of the Treaty of Union. When an attempt was then made to increase the tax to 3d per bushel of malt in 1725, a series of violent riots resulted. The government backed off after such a strong reaction and over the next hundred years the excise laws were in confusion with no two distilleries being taxed at the same rate.^{2,7-8}

Legitimate distilling did however develop and from 1751 the Parliament in London increasingly subjected whisky production to taxation. The extent of this meant that by 1756 the duty paid on spirits had now reached eight times that of 1708. The resulting outcome in Scotland was a thriving trade in illicit distilling and although 14000 illegal stills were being confiscated every year, more than half of the whisky being enjoyed in Scotland had not contributed a penny to duty.^{6,8}

Smuggling also became common, with the perpetrators going to extreme measures to prevent detection. Cases exist of smugglers transporting whisky in pig's bladders hidden under clothing and on some occasions concealing whisky in coffins while imitating funeral processions.⁹ This extreme flouting of the law eventually prompted the Duke of Gordon, one of the largest landowners in central Scotland, to push through the Excise Act of 1823, making it profitable for distillers to produce whisky legally. Licensed distillers were now able to produce spirit of strength equal to that of the smugglers in return for a licence fee of £10 annually and a payment of 2s. 3d. per gallon of spirit made in stills of capacity greater than 40 gallons. Illicit distilling began to subside and virtually disappeared over the next decade.^{3,5}

The 1823 legislation laid the foundations for the Scotch Whisky industry as it is known today, with a few points of interest boosting it further. Up until this point Scotch Whisky had been made by the fermentation of only malted barley, using copper pot stills for distillation. In 1826 Robert Stein patented a new still, which was soon superseded by an improved version in 1830 by Aeneas Coffey, known today as the 'Coffey' still. This important development enabled whisky to be distilled in a continuous operation, with the resulting whisky providing a milder and less intense spirit, irrespective of the quality of malt utilised. This invention introduced the opportunity to ferment other sources of sugar to obtain alcohol, mainly cereals such as wheat, maize and rye. Whiskies produced in this manner became termed grain whiskies. Around the 1860s blending was pioneered by Andrew Usher and constitutes mixing grain whiskies with the higher quality malts. Although this primarily reduced the costs of production, the lighter flavours of the products also extended the appeal of Scotch Whisky to a considerably larger market and even today over 90% of Scotch sold worldwide is in the blended form.^{3,8}

A second development assisting the popularity and sales of Scotch Whisky came about in 1863 when the vineyards of France became devastated by plagues of the phylloxera beetle. By the 1880s the whole of Europe was affected, resulting in significant shortages in wine and brandy. The Scots were quick to take advantage and the Scotch Whisky industry was presented with the opportunity to capture international markets, which it did, replacing brandy with whisky as the preferred spirit. Over the following years the industry slumped slightly due to economic depression but Scotch Whisky still maintained its status as the spirit of choice.⁸

By the beginning of the twentieth century an issue had surfaced among distillers regarding clarification of what should be classified as 'whisky'. Malt distillers, grain distillers and the blended whisky producers all had conflicting ideas as to the correct definition and this turned into a confrontation in 1901. This year saw the Pattison brothers, owners of a successful distillery at the time, on trial for fraud after mixing large quantities of grain whisky with a minute amount of malt and attempting to pass the product off as high quality malt.² This prompted the malt distillers to demand action to limit the term 'whisky' to malt whiskies alone and in 1905 two wine and spirit merchants were prosecuted by the Islington Borough Council for retailing whisky 'not of the nature, substance and quality demanded'.^{1,2}

The debate had gone in favour of malt whisky and was strongly appealed by the grain distillers and blenders over the next few years. In 1908 the government appointed the Royal Commission, comprised of scientists and medical men, the task of settling the debate. Their findings were what first encompassed both grain and malt whiskies as being authentically Scotch. In the years that followed, legislation continued to build from this decision, providing legal definitions of Scotch Whisky and the beginnings of restrictions on production materials, geographical location of manufacture and a minimum time frame for maturation.^{1,3}

1.2 Current Scotch Whisky Legislation

Scotch Whisky is currently legislated under the Scotch Whisky Regulations (SWR) of 2009 and has come a long way since the first account of ‘aquavita’ in Scotland from 1494.¹⁰ In the present day Scotch Whisky is exported to over 200 countries worldwide and in 2014 generated £3.95 billion for the UK balance of trade.¹¹ Effective legislation of Scotch Whisky is therefore of crucial importance for the UK economy, as well as for the protection of brand authenticity and reputation. The SWR replace the Scotch Whisky Act of 1988, and one of the most prominent additions is the introduction of 5 distinct new categories of Scotch Whisky:¹⁰

- **‘Single Malt Scotch Whisky’**: which means a Scotch Whisky that has been distilled in one or more batches at a single distillery; from water and malted barley without the addition of any other cereals; and in pot stills.
- **‘Single Grain Scotch Whisky’**: which means a Scotch Whisky that has been distilled at a single distillery; from water, malted barley and other malted or un-malted cereals; and so does not comply with the definitions of ‘Single Malt Scotch Whisky’ or ‘Blended Scotch Whisky’.
- **‘Blended Malt Scotch Whisky’**: which means a blend of two or more Single Malt Scotch Whiskies that have been distilled at more than one distillery.
- **‘Blended Grain Scotch Whisky’**: which means a blend of two or more Single Grain Scotch Whiskies that have been distilled at more than one distillery.
- **‘Blended Scotch Whisky’**: which means a blend of one or more Single Malt Scotch Whiskies with one or more Single Grain Scotch Whiskies.

The remaining contents of the SWR provide for the control of the manufacture, marketing, movement and labelling of Scotch Whisky. In these regulations ‘Scotch Whisky’ is therefore defined as a whisky produced in Scotland:¹⁰

- (a) that has been distilled at a distillery in Scotland from water and malted barley (to which only whole grains of other cereals may be added) all of which have been –*
 - I. processed at that distillery into a mash;*
 - II. converted at that distillery into a fermentable substrate only by endogenous enzyme systems; and*
 - III. fermented at that distillery only by the addition of yeast*
- (b) that has been distilled at an alcoholic strength by volume of less than 94.8 per cent so that the distillate has an aroma and taste derived from the raw materials used in, and the method of its production;*
- (c) that has been matured only in oak casks of a capacity not exceeding 700 litres;*
- (d) that has been matured in Scotland*
- (e) that has been matured for a period of not less than three years;*
- (f) that has been matured only in an excise warehouse or a permitted place;*
- (g) that retains the colour, aroma and taste derived from the raw materials used in, and the method of, its production and maturation;*
- (h) to which no substance has been added, or to which no substance has been added except –*
 - I. water;*
 - II. plain spirit caramel colouring; or*
 - III. water and plain spirit caramel colouring; and*
- (i) that has a minimum alcoholic strength by volume of 40%.*

If the whisky product does not comply with these strict stipulations then it cannot be labelled, packaged, sold or advertised as Scotch or marketed in any way which implies a Scotch product. Neither can it be moved between countries while still in the wooden casks used for maturation or any other wooden container.

1.3 Current Manufacturing Process

The production of Scotch Whisky is not the result of a single discovery; the manufacture has instead developed throughout its history. In the present day the process is now established as having five main steps: malting, mashing, fermentation, distillation and maturation. These stages are utilised both in the production of grain and malt whiskies, however there are a number of differences between the two that will be outlined where appropriate.⁵

1.3.1 Malting

Malting is the process by which barley is converted into malted barley, to generate enzymes which will later be used to convert starch into fermentable sugars. Barley (Figure 1.1) consists of two main components: the embryo which is the living structure that develops into a new plant; and the endosperm which is the store of starch from where the new plant draws its food supplies.¹²

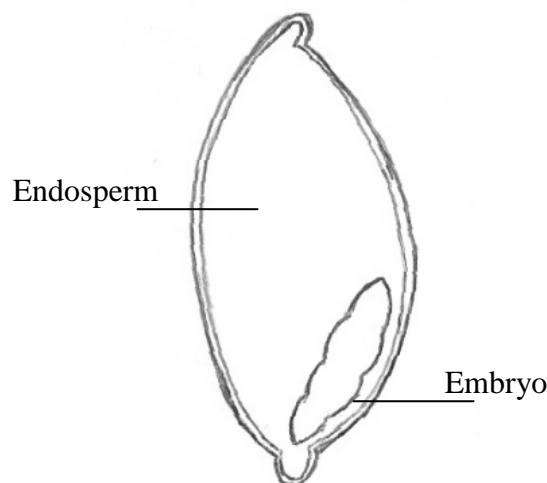


Figure 1.1: Cross section of a barley grain illustrating embryo and endosperm.

Malting is a three step process consisting of steeping, germination and drying. Steeping involves the immersion of barley grains in water for a period of typically two to three days, the cycle depending on the time taken for the moisture content of the barley to rise to the desired level. This process triggers the growth mechanism of the embryo, prompting the barley to germinate. Germination involves the activation of enzymes which begin to convert the barley's starch into sugar, providing energy

for the developing shoot. Traditionally, the barley was laid out on a stone or tiled malting floor for seven to fourteen days for this step, where it was required to be turned regularly to allow an even process and prevent the build up of heat. The large amount of space required and the need for skilled workers however, has led to the development of more modern techniques and large drums are now commonly used. The barley is slowly turned in these drums allowing all grains to receive similar treatment and the air conditions can also be controlled to provide the ideal environment for germination. Once complete, the malt is then transferred into kilns for drying, which halts the germination to leave behind a source of enzymes.¹²⁻¹³

The heat for drying is provided by a furnace at the base of the kiln and is evenly distributed by a hot air chamber to the kiln surface. The temperature however must always be kept below 70 °C or the enzymes will be destroyed.² The fuel source for the furnace was traditionally peat, which has now been gradually replaced by coal. Peat can still be added to the furnace in small amounts however, as it is well known for imparting a recognizable smoky flavour on the final whisky.¹⁴ After the drying process the malt is removed from the kiln and stored for several weeks to allow heat to dissipate naturally – hot malt would prove counterproductive at later stages in production. In the present day there are only a small number of distilleries which use their own malting systems as consistent malt can instead be acquired from a specialised maltster.¹²

1.3.2 Mashing

In preparation for mashing the dried malt is ground into a coarse flour known as grist. When grain whiskies are being manufactured, other cooked unmalted cereals are incorporated into the flour. The mashing process then involves mixing the grist with hot water in a vessel known as the Mash-Tun and typically includes three additions of water. The first addition of water is at approximately 63 °C and the purpose is to rupture the starch cells and allow the enzymes generated during malting to convert the starch into sugars. The result of this step is the formation of a sugary liquid known as ‘wort’, which is drained from the Mash-Tun to a vessel known as the underback.

The second addition of water to the grist occurs at about 78°C and assists in the solubilisation of any starch not converted at the lower temperature. The Mash-Tun is then drained for a second time to allow a sufficient quantity of wort to progress forward for fermentation. The final water is added to the Mash-Tun at even higher temperatures of between ~ 80 – 90°C. The primary function of this is to strip away any last remaining sugars into a Sparge tank, with the resulting liquid being recycled and used for the first application of water to the next mash. The solid grist which remains in the Mash-Tun after draining is called ‘draff’ and this is sold on as cattle feed.^{2,12,15}

1.3.3 Fermentation

Before fermentation can begin the wort needs to be cooled to a temperature of around 22 - 24°C. Once this is achieved the sugary liquid can then be transferred to fermentation vessels known as washbacks, where yeast is added and the fermentation process starts. The particular species of yeast utilised in the production of Scotch Whisky is generally ‘*Saccharomyces cerevisiae*’ and its primary purpose is to convert the sugars in the wort to ethanol. The liquid resulting after fermentation (typically 2 - 5 days) is known as the wash and has an ethanol content of approximately 8 - 10%.^{16,17} Although the remaining bulk of the wash is water, small quantities of other components, termed congeners, are present and their production depends on factors such as:¹⁶

- the genetic properties of the yeast strain;
- the viability and vitality of the yeast;
- initial aeration of the wort;
- the temperature profile during fermentation; and
- microbial contamination.

Typical congeners produced during fermentation include: higher alcohols such as butyl alcohol and propyl alcohol; aldehydes and ketones such as acetaldehyde, diacetyl and furfural; sulphur compounds for example dimethyl sulphide; acid compounds; and esters like ethyl acetate and iso-amyl-acetate. These components are

very important in the production of whisky, influencing the unique flavour and organoleptic qualities of the final distilled product.¹⁷

1.3.4 Distillation

The low ethanol content wash from fermentation (containing its various congeners) is next passed on to the distillation stage of production; distillation being a process that allows the separation of components from a liquid mixture (or partial separation that increases the concentration of a component) by exploiting differences in the boiling points and/or volatility of the mixture components. This process in Scotch Whisky production therefore enables the alcoholic strength of the spirit to be increased from ~8 – 10% to a level adequate for classification as a Scotch Whisky (>40% in the final product as laid out by the SWR).¹⁰

When considered individually, pure ethanol boils at 78.5°C whilst water boils at 100°C. When mixed together however, the resulting liquid will typically possess a boiling point at a temperature somewhere between the two; the value of which depends on the relative concentrations of ethanol and water. This can be explained with reference to Raoult's Law, which states that the vapour pressure of each component of an ideal solution will be equal to the vapour pressure of the pure component (at the same temperature) scaled by an amount proportional to the mole fraction of that component. This has been depicted within Figure 1.2a for an ideal mixture of two liquids, showing how the total vapour pressure would change depending on the mole fractions.^{18,19}

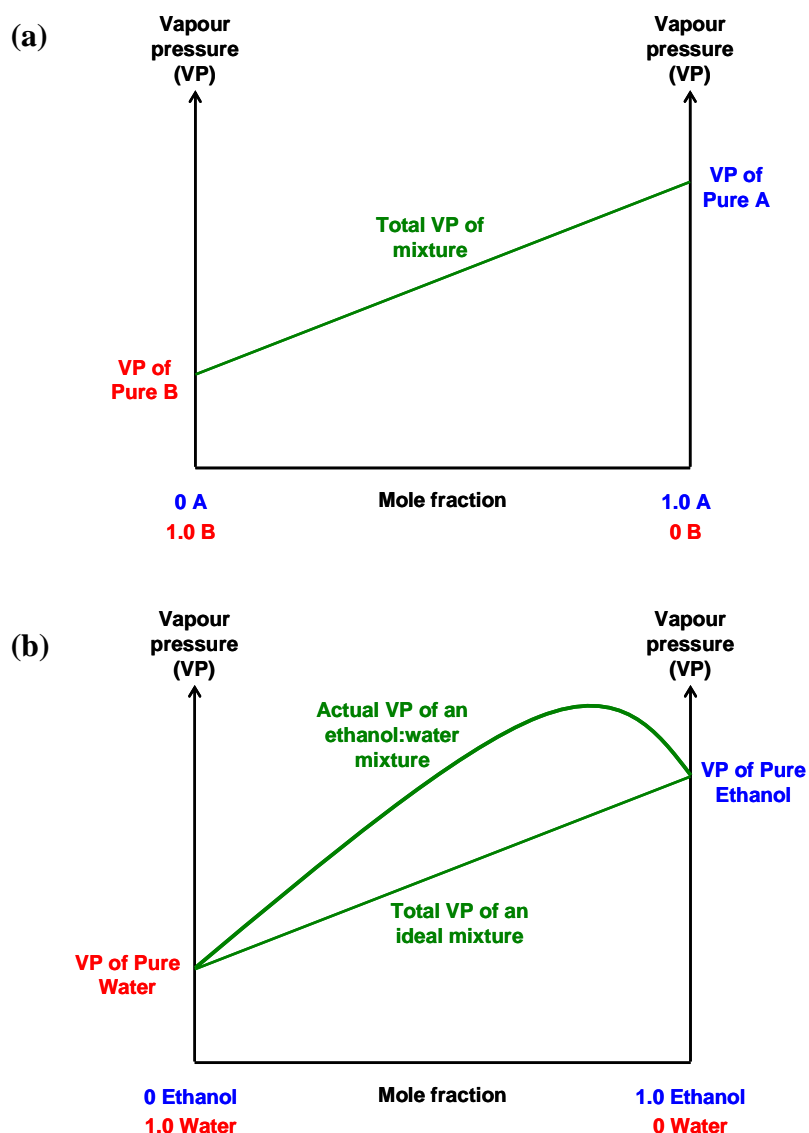


Figure 1.2: (a) Plot depicting the total vapour pressure for an ideal mixture of two components at different mole fractions and (b) plot showing a positive deviation from Raoult's Law as observed for a non ideal mixture of two components such as ethanol and water.¹⁸

It is important to note at this point, that Raoult's Law is only true for ideal mixtures, whereby the forces between the particles in solution are exactly the same as those in the pure liquids. A mixture of ethanol and water is not an ideal solution and will result in a positive deviation from Raoult's Law as depicted within Figure 1.2b. It is clear from Figure 1.2b that the maximum vapour pressure of an ethanol:water mixture is actually greater than that of either of the individual components. This occurs because when in solution, the intermolecular forces between the molecules of ethanol and water are less than those observed for the pure components. At certain compositions therefore, the molecules of a non-ideal mixture can be liberated from

solution more easily than they would be from the pure liquids. The maximum vapour pressure for a mixture of ethanol and water is known to occur at a composition of 95.6% ethanol.

The higher the vapour pressure of a mixture the lower its boiling point will be, as less heat is required to overcome the intermolecular attractions between molecules. For a mixture of ethanol and water therefore (where the vapour pressure varies depending on the relative concentrations of these components) the boiling point will change in accordance with composition as illustrated within Figure 1.3.^{18,19}

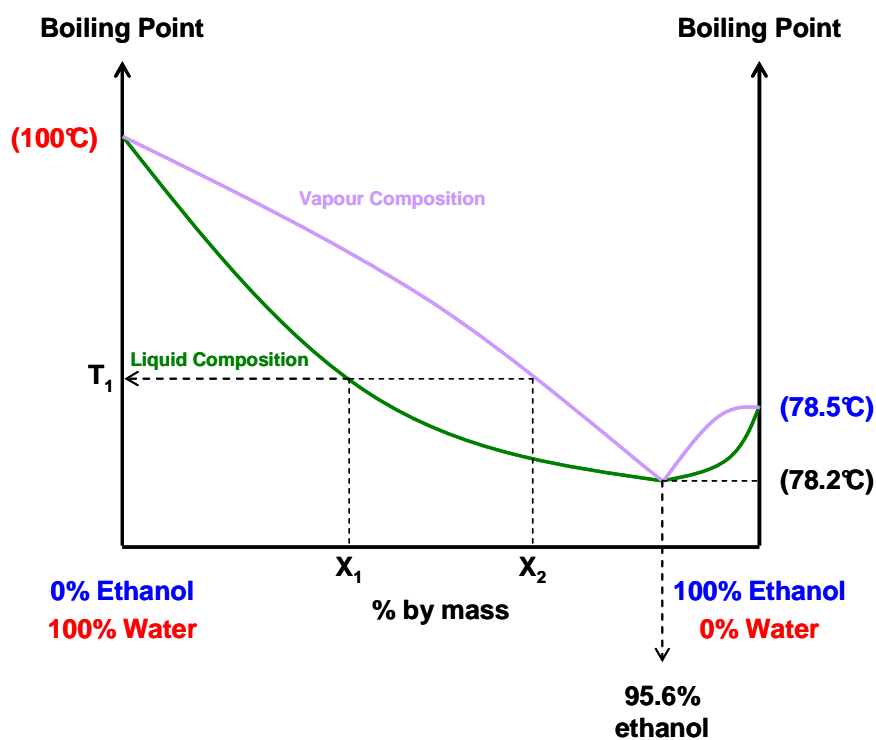


Figure 1.3: Plot illustrating the relationship between boiling point and composition (% by mass) for an ethanol and water mixture. The affect on vapour composition by heating an ethanol:water mixture of composition X_1 is also demonstrated.¹⁸

It is clearly demonstrated by this figure that the boiling point of the liquid mixture generally decreases as the percentage of ethanol increases. Figure 1.3 also demonstrates how the vapour composition is affected when a solution of ethanol and water is distilled. A liquid ethanol:water mixture with composition X_1 will boil at a temperature (T_1) given by the liquid composition curve and the vapour produced will have a composition of X_2 , which has a higher concentration of ethanol compared to

the starting liquid. This is due to the fact that the molecules of ethanol, which are more volatile than water, can be liberated more easily from solution in this non-ideal mixture than they can from pure ethanol. When condensed, the vapour will maintain the composition of X_2 and if the boiling-condensing sequence were continued, the concentration of ethanol can be increased until a liquid of 95.6% ethanol is obtained. At this point an azeotropic mixture is obtained and it is no longer possible to increase the concentration of ethanol by boiling.^{18,19}

This is the process by which the low ethanol content wash from fermentation (with ethanol content of ~8-10%) is concentrated to provide a spirit of adequate ethanol concentration to be acquired for maturation (the next step in Scotch Whisky production). Congeners present in the original wash will also be present within the resulting spirit: those of high volatility vaporising to a greater extent earlier on during distillation and those with lower volatilities preferentially vaporising later in the process.^{20,21}

Scotch whiskies are distilled in apparatus known as ‘stills’ and there are currently two types used by the industry: the pot still, which has been traditionally used for the production of malt whiskies; and the Coffey still which was developed later and is now used in the manufacture of grain whiskies.²² Each method of distillation will be discussed separately over the following sections.

1.3.4.1 Pot-still for distillation of malt whiskies

The distillation of malt whiskies takes place using a pair of copper pot-stills. Copper was traditionally chosen for this purpose due to its good malleability and high conductance of heat; however more recently it is appreciated for its ability to remove unwanted sulphurous compounds, which provide unpleasant flavours and aromas.^{22,23} The pot still can assume many shapes, heights and sizes and it is believed that the structure is important for determining the individual characteristics of a malt due to variations in contact with the copper.²² The pot still therefore varies from one distillery to another, although the generic components remain the same and are illustrated by Figure 1.4. Although a pot still consists of a number of components,

the major ones include: a broad pot, where the liquid to be distilled is contained; the swan neck bending at the head to the lyne arm, along which vapours from the pot are directed; and the condenser, where these vapours revert into a liquid distillate.²⁴

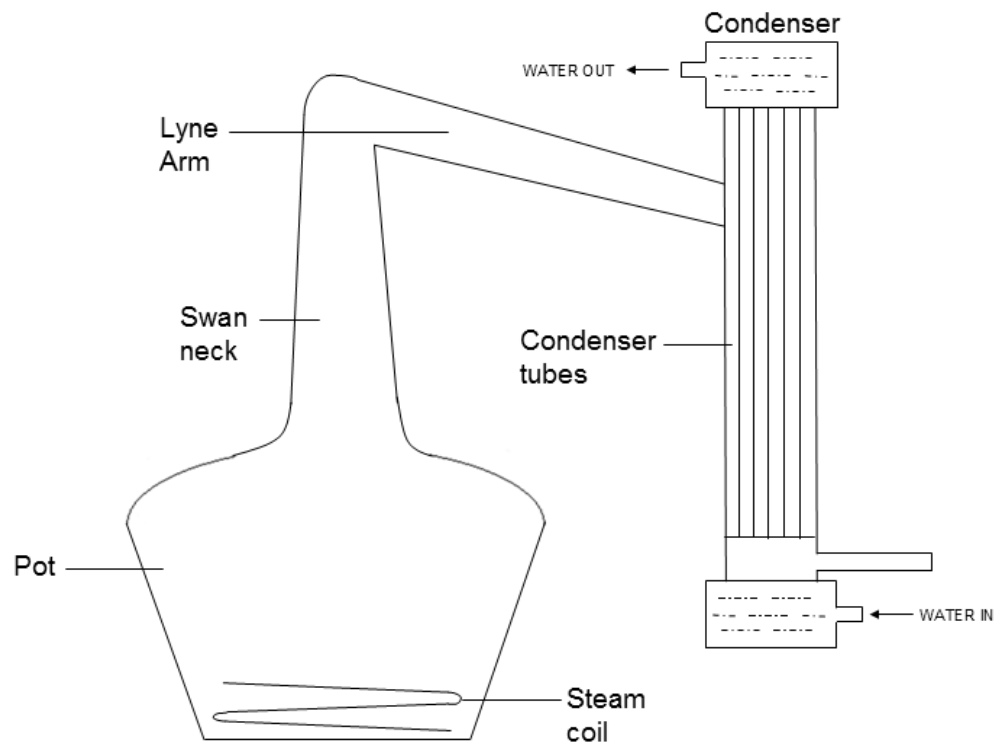


Figure 1.4: Schematic illustrating the general components of a pot still.²⁴

The distillation process begins by heating the wash from fermentation in the first of the two pot stills, referred to as the wash still. Originally the still would have been heated by peat or coal fires, however this commonly resulted in burnt solids adhering to the bottom of the still, tainting the distillate. Metal chains known as ‘rummagers’ were fitted as a solution to this, rotating around the base of the wash still to prevent the build up of charred material. Most distilleries today employ steam coils for heating which avoid these problems and give more accurate heat control. The wash is therefore steam heated and maintained at a temperature just below the boiling point of water, allowing the alcohol and other components that are most volatile to vaporise and pass over the still neck and lyne arm into the condenser.²³⁻²⁵

Many modern distilleries utilise a shell and tube condenser design (as shown in Figure 1.4), which consists of multiple straight copper tubes through which a

constant flow of water runs from bottom to top. When the vapours from the wash reach the top of the tubes they condense and flow downwards where the resulting distillate, known as the low wines, is collected in a vessel termed the low wines receiver. Alternatively the more traditional worm tub condenser can be incorporated (Figure 1.5) where the vapours are condensed while travelling along a ‘worm’ shaped copper tube which is completely immersed in a tank of cooling water, entering at the base of the tub.^{25,26}

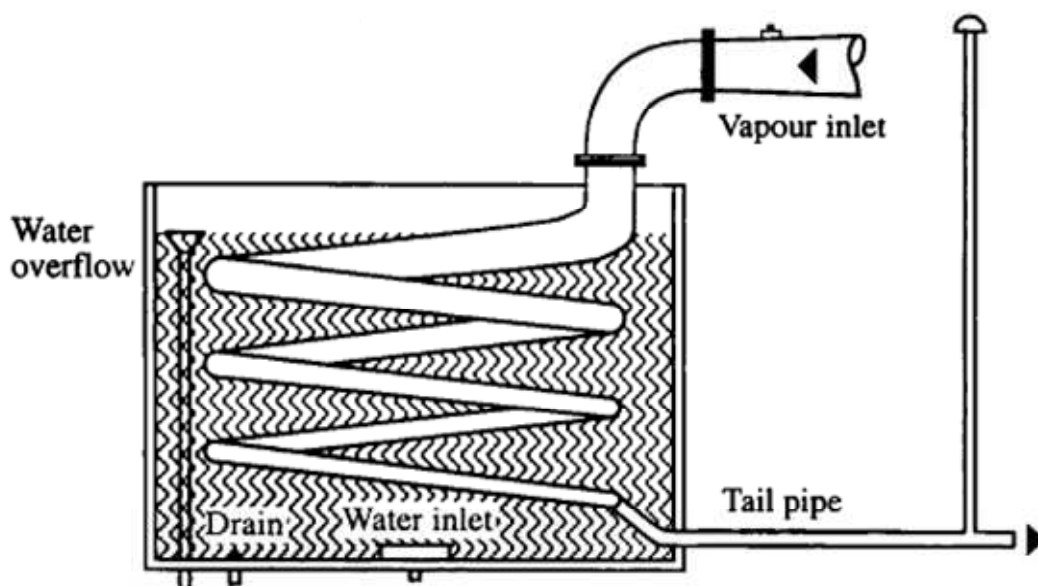


Figure 1.5: Illustration of a worm tub condenser.²⁶

Distillation in the wash still usually takes between 5 – 8 hours to complete, with the exact time depending on the shape and size of the still. The resulting low wine has an approximate ethanol content of 20% v/v and now constitutes around a third of the original volume. At this point the low wines are transferred into the second of the pair of stills, the spirit still, where distillation is undertaken again but with a great deal more control.²³

This second distillation can be considered as fractionated and is separated into three parts known as the foreshots, the middle cut and the feints.²³⁻²⁶

- **The foreshots** consist of the most volatile components and include many of the congener compounds mentioned in the fermentation section. There are

also a number of residues present from the first distillation, mainly fatty acids and their esters, which are not highly volatile but become soluble more quickly at the higher alcohol concentration. These foreshots tend to have pungent, unpleasant flavours with some components being dangerous to health. For these reasons they are not retained as part of the final spirit and are transferred back to the low wines receiver.

- **The middle cut** is the portion of the distillate that is of the quality required to progress onwards for maturation. The changeover of the distillate from the foreshots to the middle cut is typically monitored by the addition of water to the distillate, which will appear cloudy until the foreshots have mostly passed. The middle cut, referred to as 'new-make' is collected in a vessel called the spirit receiver where the alcohol concentration is regularly monitored until reaching the desired value, approximately 65 – 75 % v/v being typical.
- **The feints** make up the final fraction and consist of the components of lowest volatility. Like the foreshots, the feints fraction contains compounds harmful to the aroma of the final whisky and so is also directed back to the low wines receiver to be reused in the next spirit still distillation. The feints portion isn't completely unwanted however and is rich in phenols and certain compounds responsible for smoky aromas, all of which benefit the final spirit. The cut off point for this fraction therefore has to be carefully determined to permit the addition of some flavours but not others.

1.3.4.2 Coffey still for distillation of grain whiskies

The production of grain whiskies incorporates continuous distillation and the scale of operations is such that one grain distillery can be responsible for six times the annual output of the large malt distilleries. The development of continuous distillation links back to 1827 when Robert Stein devised and patented the first still for this use. His design was however rather complex and became superseded in 1830 by Aeneas Coffey, whose invention is known as the Patent or Coffey still.²⁷

The Coffey still is in use today for the manufacture of grain whisky in a form that has remained fundamentally unchanged since 1830. The general construction of the Coffey still entails two tower sections, an analyser and a rectifier column, the purpose of the former being to separate the alcohol from the wash obtained during fermentation and the latter designed to allow removal of unwanted flavour compounds from the final spirit. The essential features of the Coffey still are highlighted by Figure 1.6.²⁰

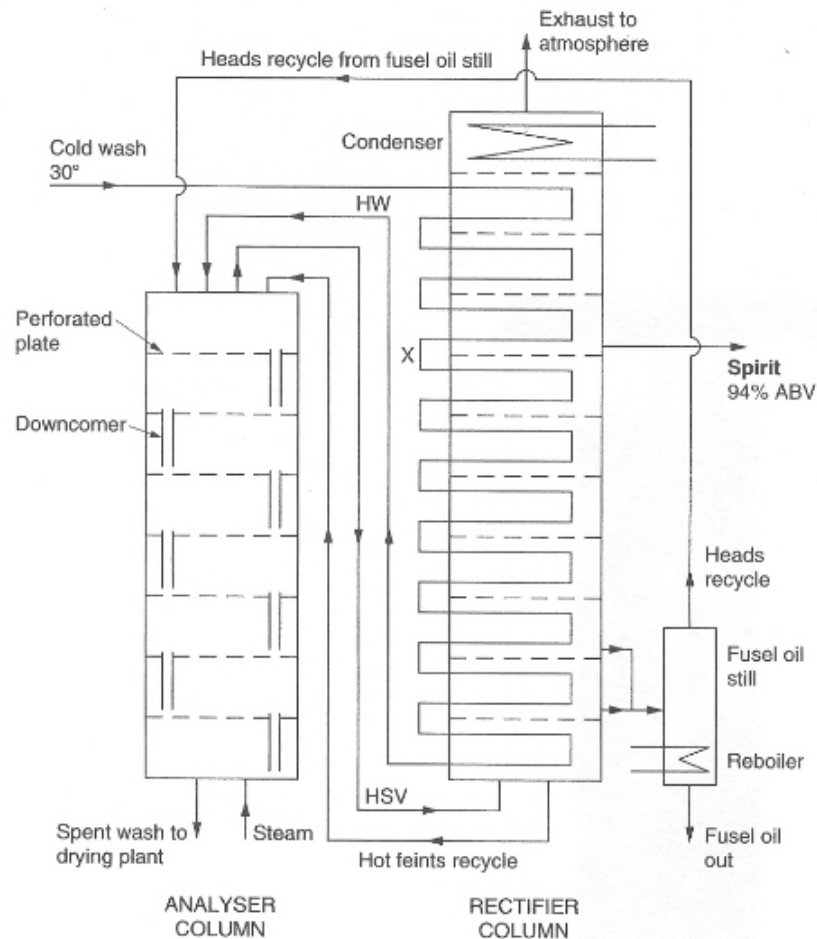


Figure 1.6: Diagram showing the essential features of a Coffey still: HW, hot wash; X, wash coil; HSV, hot spirit vapour.²⁰

Both columns of the Coffey still stand side by side and can be up to 60 feet in height. Internally the two columns consist of a series of compartments separated by a large number of plates, usually 35-40 make up the analyser and up to 60 for the rectifier.^{20,27} Firstly the wash is pumped along a copper pipe into the top of the rectifier column, coming straight from the fermentation vessel at a temperature of

about 30 °C. The wash travels downwards between the rectifier plates, *via* bends in the wash coil, constantly rising in temperature due to contact with vapour from the analyser. By the time the wash reaches the bottom of the rectifier it has reached about 94 °C and is directed into the top of the analyser column.^{20,21} Some other still designs used in grain whisky production do not require this process and pre-heat the wash in a separate container before discharging it at the top of the analyser.²⁰

The hot wash flows out of the piping at the top of the analyser and across the top plate where it can flow through the downpipe (labelled ‘downcomer’ in Figure 1.6) and cascade through the subsequent compartments all the way to the bottom. Steam is fed into the analyser from its base allowing heating of the entire column and the vapour pressure is sufficient to allow it to bubble into the liquid wash *via* perforations in each tray, while preventing any liquid falling through them. The principle of operation of the analyser is to separate the wash components by the countercurrent flow of liquid and vapour. The way this works is that when the vapour passes through the liquid some of the less volatile components begin to condense and transfer latent heat to the wash. This causes the more volatile components of the liquid to boil and so enriches the rising vapours with alcohol. The alcohol and other components of sufficient volatility, make their way to the top of the analyser column where they are passed into the rectifier tower *via* its base. The hot spirit vapour from the analyser rises through the rectifier and progressively condenses on contact with the pipeline coiling through the column. This again results in a countercurrent flow as while the vapour is rising, the condensing liquid descends.^{20,21,23,27}

The temperature gradient of the rectifier column causes less volatile components in the vapour to collect in the lower plates and the more volatile components to reform into liquid in the higher trays where temperatures are lower. Liquid of different composition is therefore obtained in different compartments of the rectifier tower and collection of the grain spirit is taken from the plate which corresponds to a concentration of about 94% alcohol. By law, the upper limit of ethanol content from continuous distillation cannot exceed 94.8%.^{10,28} Most unwanted congeners have consequently been separated out onto different plates at this point, allowing the production of a milder and less intense whisky product following maturation.

1.3.5 Maturation

On completion of the distillation process, the virtually colourless new make spirit is transferred to oak casks for maturation. It is these oak casks which are acknowledged as being one of the most important factors influencing the final quality of a Scotch Whisky. During maturation the pungent and often unpleasant aromas of the distillate transform into the typical mellow characteristics associated with a mature whisky and the spirit changes colour from being virtually clear to a golden brown.^{2,23}

The oak casks used by the Scotch Whisky industry vary in wood variety and size but cannot legally exceed 700 L, as enforced by the SWR.¹⁰ Traditionally casks consisting of Spanish oak, previously used for the fermentation and shipment of sherry, were preferred for the maturation of Scotch and they are still highly sought after today due to their excellent maturation potential and longer lifespan. The sherry casks used are mainly 500 L butts, however they have been in short supply since the early 20th century when containers for sherry transportation were gradually replaced by bulk tankers.^{23,29} As a consequence, processes such as wine-treatment and wine-seasoning have since been developed as alternative procedures to emulate the conditions of the originally used sherry casks.^{23,30,31}

The main supplies of oak casks in the present day are therefore imported from the USA and consist of ex-bourbon casks manufactured using American oak. There are two different barrels of this type: the standing barrel, with a capacity of about 180 L; and the hogshead barrel, which is built from disassembled casks, using a larger number of staves, to hold an increased volume of approximately 250 L.²⁹ These casks are relatively easy to acquire due to regulations in the USA which specify that only newly charred oak casks can be used for the maturation of bourbon. Therefore rather than the casks being disposed of after one use, they can be re-used by distilleries in Scotland.³² One final type of cask that is relatively rare is the puncheon, which has similar capacity to a butt. These are typically prepared using American oak and are newly manufactured in the UK and charred before use.²³

Oak casks manufactured for the bourbon and sherry industries are both subjected to heat treatment during cooperage. This process is hugely important during cask construction, as it holds an important role in the cask's ability to mature the spirit that it contains.²⁹ Bourbon casks are heat treated by two methods to create a thermal gradient through the wood. Initially the cask is toasted, which is a milder form of heating achieved over a more prolonged time period. This is then followed by charring, which is a much faster process and involves heating the inside of the cask with a gas burner until it catches fire and becomes carbonised. This results in a layer of active carbon or char on top of the already toasted layer.^{29,30} Sherry butts are typically heat treated by placing them over an open fire at 200 °C, a procedure which also aids in making the cask more pliable for curving into shape.²⁹

Although different methods of heat treatment exist, the objectives of each are the same:²⁹⁻³¹

- To degrade wood polymers and so achieve the formation of many important colour and flavour related compounds.
- To eliminate components present in the wood that are known to transfer unpleasant aromas to the maturing spirit.
- To aid in the removal of undesirable characteristics present in the distillate, *via* the active carbon layer.

Once the new make spirit has been transferred into oak casks, the maturation process can begin. Most countries enforce a minimum timescale for maturation and for Scotch Whisky this is legally assigned as at least 3 years.¹⁰ During the time spent in the cask, major changes occur to the chemical composition of the spirit, both enhancing its flavour and introducing colour. There are a vast number of reactions occurring during the process which are responsible for these chemical changes and they can be divided into: additive, subtractive and interactive reactions.^{23,29,33}

- **Additive reactions** refer to the extraction of components from cask wood during maturation. The main constituents extracted from oak casks are thermal degradation products of the wood polymers cellulose, hemicellulose

and lignin, originating from the heat treatment stage of cask manufacture. Constituents such as vanillin, syringaldehyde, coniferaldehyde, furfural and sinapaldehyde originate from wood polymers and have all been identified as having sensory importance to the final spirit. Endogenous wood substances can also be extracted from the cask and include compounds such as: oak lactones, associated with a coconut aroma; eugenol, which imparts a clove like flavour; and tannic substances including gallic and ellagic acid. Another source of additive components can be from carryover of compounds from the previous use of a cask, for example it is possible to identify characteristics of sherry and bourbon in whisky matured in ex-sherry and ex-bourbon casks respectively.

- **Subtractive reactions** incorporate the evaporation of low boiling point compounds through the cask wood and can also involve the absorption of compounds onto the active carbon surface of the cask. The most common subtractive reactions facilitate the removal of undesirable sulphur related compounds by both of these methods.
- **Interactive reactions** take place as maturation starts to progress and incorporate components of the original distillate either reacting with each other or with components which have been extracted from the oak wood. Esterification reactions are very common, with any free acids interacting with the ethanol and many important whisky aromas are produced by this manner.

The final composition of the whisky is very complex due to the vast number of components introduced during maturation, meaning a wide variety of flavour and colour related compounds are formed.³¹ The exact make-up from one whisky to another is dependent on a number of cask variables, as different cask conditions will affect the extent to which components are extracted from the wood and consequently the reactions which occur to the spirit thereafter.^{31,33,34} The affects of these variables on whisky colour will be discussed in more detail in section 1.4.1.

1.3.6 Blending and Bottling

Blending was pioneered by Andrew Usher in Edinburgh during the early 1860s and describes the process of mixing single whiskies to produce a product of unique and recognizable flavour.²⁹ The individual grain and malt whiskies chosen for a blend all offer a specific flavour profile and are selected based on their ability to complement and enhance each others flavours. Malt whiskies consist of a greater quantity of flavour congeners and so their role in a blend is to provide the key flavours. The grain whiskies possess lighter flavours and so their addition imparts a more rounded character on the blend, toning down harsh notes whilst also revealing certain flavours of the malts.^{2,23}

Blending also enables a consistency of character to be achieved, as it reduces the differences which may be seen between the individual products due to the wide variety of manufacturing parameters. Blended whiskies can contain anything from about 20 to 50 different malts combined with 2 – 5 grain whiskies, the proportion of which depends entirely on the requirements set out by the blender, but typically more grain whisky is used than malt. Preparing a blend is a complex procedure and heavily relies on the expertise and knowledge of the blender. Combining the whiskies is not as simple as following step by step instructions and only the experience of the blender allows for mixing of the appropriate whiskies at adequate proportions to achieve the desired characteristics. Consistency is even harder to accomplish, with component whiskies varying in quality and on some occasions becoming unavailable. The blender therefore has to draw upon their knowledge to adapt the blend formula as required.^{23,29}

The first task in blending is to locate and retrieve the specific casks required for the blend formulation. The blender can quickly assess the sensory characteristics of each cask by drawing a small sample and testing the aromas by nose. Casks of satisfactory quality are then combined together in the correct proportions by draining into stainless steel vats where they are mixed thoroughly using mechanical agitators or compressed air. The resulting product is assessed again by the blender who can highlight any problems and recommend any further cask additions.^{29,35}

Once vating is complete, many blenders believe that ‘marrying’ is the next essential step for optimising the quality of the blend. This involves storing the vatted whisky in exhausted wooden casks for a period of time to allow the components of the blend to come together fully.²⁹ After marrying, there are only a few final steps to complete before bottling. The alcoholic strength of the whisky needs to be reduced, typically to 40% or 43%, and this is achieved by dilution with water.³⁵ Once diluted the product then requires filtration, roughly first to eliminate bits of particulate material and secondly, using chill filtration to remove any components that will cause a haze when the whisky is stored in the bottle.^{23,29} The final stage before bottling is the addition of food grade caramel. The caramel does not impart any flavour or taste on the whisky due to the low levels introduced, instead its primary purpose is to achieve consistency of colour from one batch to another.^{29,35} The influence of caramel on whisky colour will be discussed in section 1.4.2.

1.4 The Origins of Colour in Scotch Whisky

The colour of Scotch Whisky is known to originate from two sources: the natural maturation process; and *via* the addition of plain spirit caramel.^{2,29}

1.4.1 Natural Colour

The natural colour of Scotch Whisky is known to originate during maturation in oak casks, where the virtually colourless distillate changes into the golden brown associated with the final product. Colour related components are introduced to the spirit by their extraction from the cask wood, the three major constituents of which are lignin, cellulose and hemicellulose.^{29,36} Heat treatment of casks during manufacture promotes thermal degradation of these wood polymers and it is the breakdown of hemicellulose in particular that is thought to contribute to whisky colour during maturation. Certain tannic substances derived from lignin are also believed to contribute to whisky colour; however the degradation products of this wood polymer predominantly influence flavour.^{29,37}

Hemicelluloses are branched polymers comprising of several different sugar monomers, such as glucose, xylose, arabinose and galactose. On degradation, hemicellulose breaks down into its constituent sugars, which then degrade further into caramelisation products, such as furfural, hydroxymethyl furfural and maltol. These sugar condensation products then go on to become highly condensed structures and it is these complex materials that are thought to provide the brown colour of whisky.^{37,38}

The reactions involved in the formation of colour during maturation are very complex and as a consequence very little is known about the exact chemical structure of natural colour arising during maturation. The different colour intensities and hues associated with different whiskies however, are known to depend on a number of cask variables such as: cask history, fill strength and maturation age.^{23,29,33,34}

1.4.1.1 Cask history

Sherry vs. bourbon casks

As has been mentioned before, the majority of casks used for the maturation of Scotch Whisky have previously been used for the storage of either sherry or bourbon. This previous cask use will change the composition of colour extractives as certain compounds may have already been completely removed from the wood.³² The previous beverage may also have caused the direct or indirect formation of new colour related compounds in the wood and these will consequently be available for extraction during subsequent whisky maturation.³¹ Sherry casks, despite the milder use of heat treatment, are known to impart high levels of colour on a Scotch Whisky during maturation and these originate from the previously used sherry itself. Ex-bourbon casks on the other hand are known to pass on very slight amounts of colour from bourbon already absorbed in the oak wood.²⁹

Maturation in a newly charred cask, which has not been used previously with bourbon or sherry, imparts a high degree of colour to the maturing spirit. This is a direct result of the heat treatment which is undertaken in its manufacture, as research has shown that the level of colour components extracted generally increases with the intensity of toasting and charring.^{29,31} This is reasonable to suggest as the natural colour of Scotch has already been proposed as originating from the degradation of wood polymers.

First fill vs. refill casks

In the Scotch Whisky industry, casks are re-used several times for maturation, introducing a further variable affecting the profile of the final product. Repeated use of casks results in a decrease in the quantity of colour components present in the wood and this leads to changes in the characteristics of the maturing spirit. Comparison of first fill and refill casks do show that the majority of components remain present, however the levels observed are lower. The reduced amounts of cask extractives will also limit interactive reactions during maturation, therefore impacting on the final whisky composition.^{29,33,39}

Casks which no longer produce satisfactory maturation, due to depletion of cask extractions from continued re-use, can undergo regeneration. This process involves scraping away the original char to create a new wood surface and then re-charring the cask with a gas burner for a controlled period of time. This promotes the thermal degradation of wood polymers again to yield similar components as a newly charred cask.²⁹ It is however reported that re-charring does not restore the maturation potential of used barrels to the same extent of a new one, which is likely a result of certain oak constituents, such as lactones and hydrolysable tannins, being unable to regenerate.^{29,31,40} Re-charring is also a difficult process to control due to variable moisture and spirit contents in the wood of different casks. The level of colour produced from regenerated casks can therefore vary depending on the length of time employed for charring.²⁹

1.4.1.2 Other variables

A cask's history covers the factors responsible for the greatest degree of variation observed between whiskies after maturation. Other variables such as maturation time and fill strength however, will also influence the maturing spirit.^{29,37}

Maturation time

The time frame for maturation is variable and although a minimum of three years is the legal requirement, maturation periods of ten to twenty years are not uncommon.²⁹ Studies have shown that the extraction of colour during maturation generally occurs most rapidly over the first year of storage in oak casks. From this point onwards the extraction rate is reduced, however a steady increase in colour is still observed throughout maturation.^{33,40} A longer maturation time therefore allows for a greater change in chemical composition and so the longer maturation progresses for, the more colour will develop. Although colour is therefore known to be affected by maturation time, the important reactions involved in its generation remain unknown. The main restriction which has so far prevented this is that modelling of maturation in the laboratory does not allow appreciable observations within a practical timescale.²⁹

Cask fill strength

New make spirits from distillation are typically filled into casks at a constant strength; however variations in fill strength will alter the extent to which certain congeners are extracted from the oak wood. Lower fill strengths favour the extraction of components that are water soluble, while higher alcohol concentrations extract components which are more soluble in ethanol.^{29,40} This will consequently have an affect on the colour intensity obtained and certain studies have shown that increasing the fill strength will reduce the level of colour developed during maturation.^{37,41,42}

1.4.2 Caramel Colour

Colourants have played a vital role in the food and beverage industry for many years, being added to food to: make up for colour that may be lost during processing; add consumer appeal to an otherwise colourless product; to infer a taste by colour association; and to provide colour consistency from batch to batch.^{43,44} The SWR legally permit the use of plain spirit caramel (E150a) in Scotch Whisky with the purpose of achieving consistency of colour in the final product.^{10,29}

The use of caramel colourings in foodstuffs is very closely legislated by the European Union, which has adopted the four internationally recognised caramel classes as legal: E150a, E150b, E150c and E150d. These caramels are regulated by the European Union Directive 2008/128/EC and are described in Table 1.1.^{45,46}

Table 1.1: Descriptions of the four caramel classes recognised by the European Union Directive 2008/128/EC.^{45,46}

Caramel Class	Caramel name	Restrictions on Preparation	Colloidal charge
E150a	Plain Spirit Caramel	No ammonium or sulphite compounds can be used	Negative
E150b	Caustic Sulphite Caramel	In the presence of sulphites but no ammonium compounds	Negative
E150c	Ammonia Caramel	In the presence of ammonium compounds but no sulphite compounds	Positive
E150d	Sulphite Ammonia Caramel	In the presence of both sulphite and ammonium compounds	Negative

Caramel colourants are described by their legislation as dark brown to black liquids or solids and there are several means by which this colouring can be produced. The two most important reactions involved in the formation of colour components, also known as browning, are:⁴³

- **The Maillard reaction** – a series of reactions in which sugars, aldehydes and ketones react with nitrogen containing compounds in the presence of heat to form complex mixtures of colour and flavour related compounds.
- **Caramelisation reactions** – a series of reactions in which sugars undergo pyrolysis in the absence of nitrogen containing compounds.

E150 products are therefore produced by the carefully controlled heat treatment of carbohydrates, which are the monomers glucose and fructose, and polymers thereof (e.g. glucose syrups, sucrose, dextrose). This is typically done in the presence of food grade acids, alkalis and salts to promote the caramelisation process; however restrictions on preparation must be adhered to for different caramel classes as stated in Table 1.1.⁴³⁻⁴⁶ These different parameters of manufacture result in differences being observed in the final composition of these caramels; however the mechanisms of colour formation remain consistent.⁴⁶ During caramelisation reactions, sugars initially undergo dehydration on exposure to heat, which creates a range of low molecular weight (LMW) compounds providing only very light colour. Many of these LMW compounds then begin to undergo condensation or polymerisation reactions that result in the formation of strongly coloured high molecular weight (HMW) polymers. Caramel colourants are therefore a very complex mixture of components and as a result, there is currently very little known about their exact chemical natures. It has been suggested that the LMW fractions of caramel colourants comprise of compounds such as furan derivatives (e.g. 5-(hydroxymethyl)-2-furfural (a.k.a. HMF) and 2-hydroxyacetylfuran (HAF)), furanones (e.g. hydroxydimethyl furanone (HDF)), pyranones (e.g. maltol), a variety of saccharides and many other components.^{47,48} The HMW components on the other hand remain mostly uncharacterised and are suggested as being made up of caramelan ($C_{12}H_{18}O_9$), caramelen ($C_{36}H_{50}O_{25}$) and caramelin ($C_{96}H_{102}O_{51}$);

polymeric products that constitute a mixture of different compounds whose structures are currently unknown.^{44,47,49} Maillard reactions follow a similar scheme as described for caramelisation however only occur in the presence of nitrogen containing components; they are therefore typically observed during only the production of E150c and E150d caramels. Figure 1.7 has been included below to help demonstrate an example reaction scheme of the caramelisation process, representing the production of a few key LMW components from glucose.^{47,48}

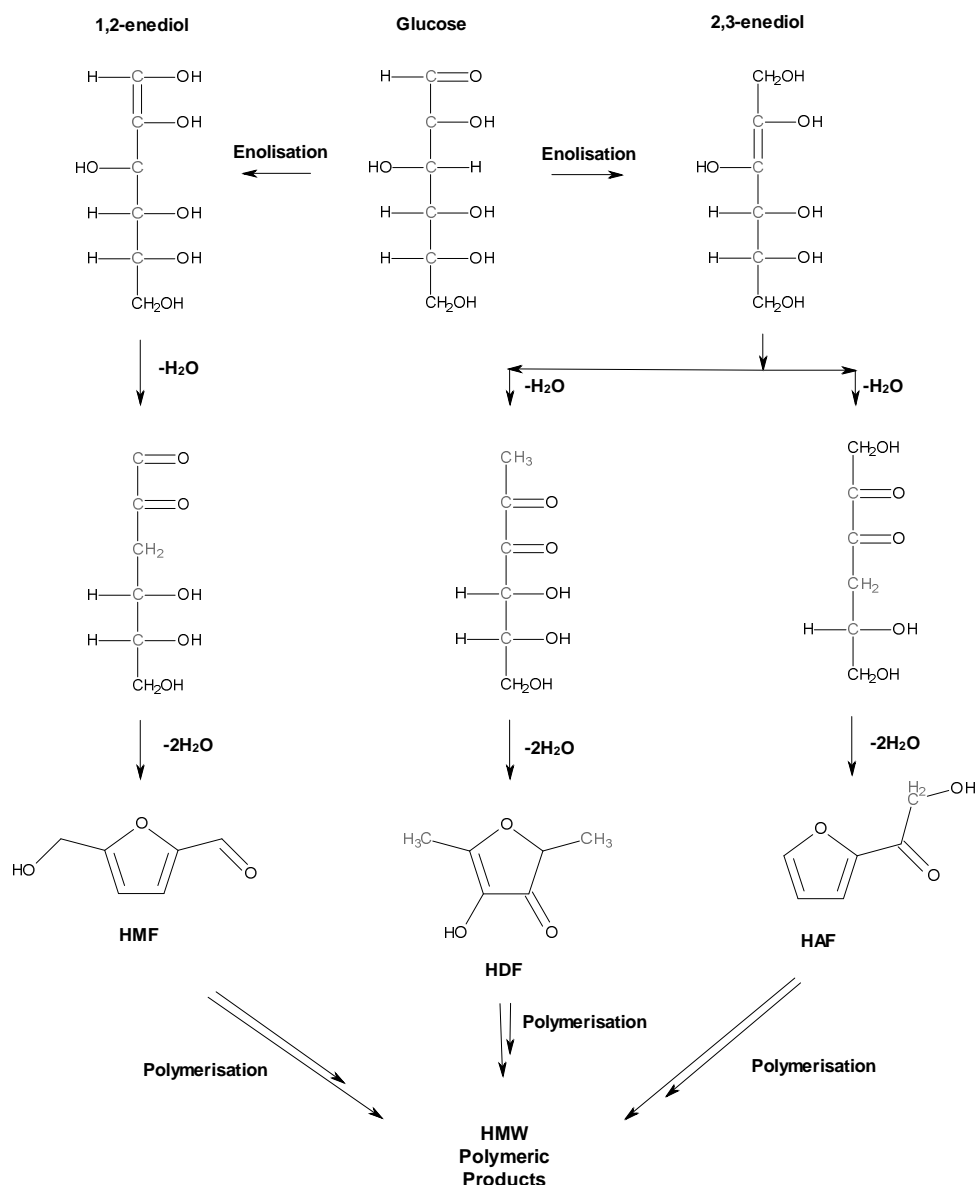


Figure 1.7: An example of reaction schemes that occur during the caramelisation process, demonstrating the formation of HMF, HDF and HAF (LMW components) from glucose, that subsequently undergo polymerisation reactions to form HMW polymeric products.⁴⁸

As described above, caramel colour is a complex mixture of components and some of the HMW polymers are known to form colloidal aggregates. These aggregates can be either positively or negatively charged depending upon the reactants used in their manufacture (see Table 1.1). This is an important feature of caramels, which often determines the most appropriate caramel for a particular application. The charge of the colourant must match that of the product it's being added to otherwise the particles of opposite charge may attract towards one another and form larger, insoluble particles. These will then settle out which would be an undesirable characteristic for any food or beverage.^{43,46}

The SWR state that only E150a can be legally added to Scotch Whisky and the slight negative charge of the caramel is compatible with the beverage. Another factor which affirms the use of E150a in Scotch Whisky is that it remains stable in solutions containing up to about 80% alcohol, the highest tolerance of all four caramels.⁵⁰

1.5 General Thesis Scope and Aims

The primary objective of this research was to investigate and develop analytical approaches that can be used to profile and understand more about Scotch Whisky colour, both originating from the addition of plain spirit caramel and also that derived naturally during maturation. Attenuated total reflectance mid-infrared (ATR-MIR) spectrometry and liquid chromatography – mass spectrometry (LC-MS) were the two primary techniques investigated for this purpose.

Initial research presented in Chapter 3 assessed the ability of ATR-MIR for profiling caramel colour and the main objectives were:

- To determine whether the technique could successfully acquire profiles of caramel materials.
- To identify if the technique could discriminate between different classes of caramel (E150a – E150d) and additional colourants prohibited in Scotch Whisky.
- To find out whether E150a caramels prepared using different conditions of manufacture could be differentiated between.
- To determine the influence of natural Scotch Whisky colour (and real scenarios affecting whisky colour) on ATR-MIR spectral profiles, when caramel is dissolved in this matrix.

As well as presenting a tool that can aid in understanding more about Scotch Whisky colour, the ability of ATR-MIR to profile caramel colourants in accordance with the above aims would be extremely useful to the Scotch Whisky industry in terms of product authenticity. For instance, being able to distinguish between different classes of caramel would help to identify whether a material other than the legally permitted E150a had been implemented to provide colour within a suspect whisky sample. In addition, the ability to distinguish between different formulations of E150a could introduce the potential for E150a manufacture to be manipulated in the future to create caramel materials with distinct signature profiles that could be added to

different products and so act as inherent markers for the positive identification of authentic whisky samples.

After a preliminary investigation of the above objectives in Chapter 3, the work was subsequently progressed within Chapter 4 to determine whether caramel identities (alone and in Scotch Whisky) could actually be predicted based on their characteristic spectral profiles acquired using ATR-MIR. PCA with GLSW preprocessing, HCA, PC-DFA and k -NN classification were the data analysis tools investigated for this purpose.

Chapters 5 and 6 investigate the capabilities of LC-MS as a tool for profiling Scotch Whisky, with the former focussing on profiling caramel colourants and the latter generally investigating the non-volatile compounds (which encompass colour related components) derived naturally during production. As with Chapter 3, the primary aim of Chapter 5 was to assess the ability of LC-MS for profiling caramel colour and the main objectives matched those described above. In contrast to ATR-MIR however, LC-MS systems can have the potential to allow structural elucidation to be investigated and so it was an additional aim of Chapter 5 to determine whether any of the components responsible for differentiation between samples could be picked out and their structures subsequently identified. Chapter 6 investigated the ability of LC-MS to assess naturally derived components in Scotch Whisky and was primarily used in this research to identify whether changes in production variables could be picked up and if the components responsible for these differences could be identified. The main objectives were therefore:

- To identify whether LC-MS could differentiate between samples that varied only by their maturation age.
- To determine if LC-MS could distinguish between samples taken from casks with different histories (i.e. first fill vs. refill and sherry casks vs. bourbon casks).
- To find out whether whiskies with authentic maturation profiles could be distinguished from those that have been artificially matured, using LC-MS.

- To identify differences between different whisky products on the market (i.e. different blends and malt whiskies).
- To determine whether any components responsible for variations in the LC-MS profiles of different whisky samples could be singled out.

The research presented within Chapters 5 and 6 would be extremely beneficial to the Scotch Whisky industry, as the ability to profile individual non-volatile components within the spirit would allow a greater understanding of the composition of colour within Scotch Whisky, a subject area where there is currently very little knowledge. LC-MS would also be a particularly useful tool for understanding more about the non-volatile fraction of Scotch Whisky in general, not only in relation to colour components.

1.6 References

1. D. Daiches, *Scotch Whisky Its Past and Present*, André Deutsch, London, 1969
2. M. S. Moss, J. R. Hume, *The Making of Scotch Whisky*, James & James, Edinburgh, 1981
3. B. Simpson, *Uisgebaugh*, in *Scotch Whisky*, Macmillan Leisure Books, Basingstoke, 1974
4. S. W. Sillett, *Illicit Scotch*, Beaver Books, Aberdeen, 1965
5. Scotch Whisky Association, *Scotch Whisky – Questions and Answers*, The Scotch Whisky Association, Edinburgh, 1972
6. *History of Scotch Whisky*, Scotch Whisky Association,
<http://www.scotch-whisky.org.uk/understanding-scotch/history-of-scotch-whisky/>, Accessed 15/08/2015
7. T. P. Lyons, *Production of Scotch and Irish whiskies: their history and evolution*, in *The Alcohol Textbook*, Nottingham University Press, Nottingham, 3rd Edition, 1999
8. G. N. Bathgate, *History of the development of whisky distillation*, in *Whisky: Technology, Production and Marketing*, (ed.) I. Russell, Elsevier Academic Press, London, 2003
9. F. P. Pacult, *A Double Scotch: How Chivas Regal and the Glenlivet Became Global Icons*, John Wiley & Sons, New Jersey, 2005
10. *The Scotch Whisky Regulations 2009*,
<http://www.legislation.gov.uk/ukxi/2009/2890/contents/made>, Accessed 15/08/2015
11. *Facts & Figures*, Scotch Whisky Association,
<http://www.scotch-whisky.org.uk/what-we-do/facts-figures/>, Accessed 15/08/2015
12. T. C. S. Dolan, *Malt whiskies: raw materials and processing*, in *Whisky: Technology, Production and Marketing*, (ed.) I. Russell, Elsevier Academic Press, London, 2003
13. G. N. Bathgate, R. Cook, *Malting of barley for Scotch Whiskies*, in *The Science and Technology of Whiskies*, (eds.) J. R. Piggott, R. Sharp, R. E. B Duncan, Longman Scientific & Technical, Harlow, 1989

14. B. M. Harrison, F. G. Priest, *J. Agric. Food Chem.*, 2009, **57(6)**, 2385–2391
15. G. D. Wilkin, *Milling, cooking and mashing*, in *The Science and Technology of Whiskies*, (eds.) J. R. Piggott, R. Sharp, R. E. B Duncan, Longman Scientific & Technical, Harlow, 1989
16. I. Campbell, *Yeast and fermentation*, in *Whisky: Technology, Production and Marketing*, (ed.) I. Russell, Elsevier Academic Press, London, 2003
17. H. Berbert de Amorim Neto, B. K. Yohannan, T. A. Bringhurst, J. M. Brosnan, S. Y. Pearson, J. W. Walker, G. M. Walker, *J. Inst. Brew.*, 2009, **115(3)**, 198-207
18. *Raoult's Law and Non-Volatile Solutes*,
<http://www.chemguide.co.uk/physical/phaseeqia/raoultnonvol.html>, Accessed 23/03/2016
19. M. Clugston, R. Flemming, *Advanced Chemistry*, Oxford University Press, Oxford, 2000
20. I. Campbell, *Grain whisky distillation*, in *Whisky: Technology, Production and Marketing*, (ed.) I. Russell, Elsevier Academic Press, London, 2003
21. R. J. Panek, A. R. Boucher, *Continuous distillation*, in *The Science and Technology of Whiskies*, (eds.) J. R. Piggott, R. Sharp, R. E. B Duncan, Longman Scientific & Technical, Harlow, 1989
22. B. Harrison, O. Fagnen, F. Jack, J. Brosnan, *J. Inst. Brew.*, 2011, **117(1)**, 106-112
23. J. R. Piggott, J. M. Conner, *Whiskies*, in *Fermented Beverage Production*, (eds.) A. G. H. Lea, J. R. Piggott, Blackie Academic & Professional, Glasgow, 1995
24. D. Nicol, *Batch distillation*, in *The Science and Technology of Whiskies*, (eds.) J. R. Piggott, R. Sharp, R. E. B Duncan, Longman Scientific & Technical, Harlow, 1989
25. D. Nicol, *Batch distillation*, in *Whisky: Technology, Production and Marketing*, (ed.) I. Russell, Elsevier Academic Press, London, 2003
26. The International Centre for Brewing and Distilling, *Unit 4: Batch distillation*, in *Distilling Module*, 2001
27. The International Centre for Brewing and Distilling, *Unit 5: Continuous distillation*, in *Distilling Module*, 2001

28. P. J. Hardy, J. H. Brown, *Process Control*, in *The Science and Technology of Whiskies*, (eds.) J. R. Piggott, R. Sharp, R. E. B Duncan, Longman Scientific & Technical, Harlow, 1989
29. J. Conner, K. Reid, F. Jack, *Maturation and blending*, in *Whisky: Technology, Production and Marketing*, (ed.) I. Russell, Elsevier Academic Press, London, 2003
30. J. Clyne, J. M. Conner, A. Paterson, J. R. Piggott, *Int. J. Food. Sci. Tech.*, 1993, **28**, 69-81
31. J. R. Mosedale, *Forestry*, 1995, **68**, 203-230
32. J. Lamond, R. Tucek, *The Malt Whisky File*, Canongate Books Limited, Edinburgh, 4th edition, 2007
33. K. Nishimura, R. Matsuyama, *Maturation and maturation chemistry*, in *The Science and Technology of Whiskies*, (eds.) J. R. Piggott, R. Sharp, R. E. B Duncan, Longman Scientific & Technical, Harlow, 1989
34. J. R. Piggott, J. M. Conner, A. Paterson, J. Clyne, *Int. J. Food. Sci. Tech.*, 1993, **28**, 303-318
35. M. Booth, W. Shaw, L. Morhalo, *Blending and bottling*, in *The Science and Technology of Whiskies*, (eds.) J. R. Piggott, R. Sharp, R. E. B Duncan, Longman Scientific & Technical, Harlow, 1989
36. J. R. Mosedale, J-L. Puech, *Trends. Food. Sci. Tech.*, 1998, **9**, 95-101
37. The International Centre for Brewing and Distilling, *Unit 6: Maturation*, in *Distilling Module*, 2001
38. *The Composition of Oak and an Overview of it's Influence on Maturation*, <http://homedistiller.org/oak.pdf>, Accessed 15/08/2015
39. R. Sharp, *Analytical techniques used in the study of whisky maturation*, in *Current Developments in Malting, Brewing and Distilling*, (eds.) F. G. Priest, I. Campbell, Institute of Brewing, London, 1983
40. G. H. Reazin, *Am. J. Enol. Viticult*, 1981, **32(4)**, 283-289
41. S. Baldwin, A. A. Andreason, *J. Assoc. Off. Ana. Chem.*, 1974, **57(4)**, 940-950
42. G. H. Reazin, *Chemical analysis of whisky maturation*, in *Flavour of Distilled Beverages: Origin and Development*, (ed.) J. R. Piggott, Ellis Horwood, Chichester, 1983

43. W. Kamuf, A. Nixon, O. Parker, G. C. Barnum, *Cereal Food World*, 2003, **48(2)**, 64-69
44. H. A. Sepe, O. D. Parker, A. R. Nixon, W. E. Kamuf, *Global color quality of beverages utilizing caramel color*, in *Color Quality of Fresh and Processed Foods*, (eds.) C. A. Culver, R. E. Wrolstad, American Chemical Society, Washington, 2008
45. *Commission Directive 2008/128/EC 'laying down specific purity criteria concerning colours for use in foodstuffs'*, <http://eur-lex.europa.eu/LexUriServ/LexUriServ.do?uri=OJ:L:2009:006:0020:0063:EN:PDF>, Accessed 15/08/2015
46. M. J. Scotter, *Food. Addit. Contam.*, 2011, **28(5)**, 527-596
47. P. Tomasik, *Caramel*, in *Encyclopaedia of Food Science, Food Technology, and Nutrition*, (eds.) R. Macrae, R. K. Robinson, M. J. Sadler, Academic Press, San Diego, 1993
48. L. W. Kroh, *Food Chem.*, 1994, **51**, 373-379
49. S. Kitaoka, K. Suzuki, *Agr. Biol. Chem.*, 1967, **31**, 753-755
50. J. Thornton, *J. Food. Sci. Tech.*, 1990, **4(1)**, 9-11

2.0 THEORY

Attenuated total reflectance mid-infrared (ATR-MIR) spectrometry and liquid chromatography – mass spectrometry (LC-MS) were the two primary techniques investigated within this research for profiling colour related components in Scotch Whisky. The theory behind them will therefore be discussed within this chapter. The data acquired from both of the above mentioned tools were compared using multivariate data analysis tools; principal component analysis (PCA) being the predominant tool implemented for preliminary assessments of trends and relationships between samples. In addition to PCA, a selection of other pattern recognition techniques were investigated when assessing the ATR-MIR data, being implemented to determine whether sample identities could be predicted based on characteristic spectral features. The background theory for the data analysis tools investigated within this research is therefore also discussed in the following text.

2.1 ATR-MIR Spectrometry

2.1.1 MIR Spectrometry

Spectroscopic measurements are commonly used to gather information relating to the structure of a compound and are based around the interaction of electromagnetic radiation with matter. The infrared portion of the electromagnetic spectrum covers a wavenumber range of approximately $10 - 14000 \text{ cm}^{-1}$ and can be subdivided into three main regions: near infrared (NIR), mid infrared (MIR) and far infrared (FIR). The frequency range defined by infra red radiation corresponds to the energy required to cause molecular vibrations in a compound. These vibrations are characteristically different for each bond type in the molecule and so infrared spectroscopy can be used to identify the functional groups present in a compound.^{1,2}

On irradiation by infrared light, a sample will absorb energy characteristic of its vibrational structure and the difference between the incident and detected energy will lead to the production of a spectrum with distinctive absorption bands. For a vibration to be detected with infra red spectroscopy it must be accompanied by a net change in dipole moment, which is defined as the product of the charge and the

distance of separation between two atoms.^{1,3} MIR spectroscopy, which encompasses the region between 400 and 4000 cm^{-1} , corresponds to the fundamental vibrations of virtually all the functional groups of organic molecules. These particular vibrations are the most strongly absorbed and provide sharp spectral lines, resulting in the MIR region of infrared being of greatest practical use for the characterisation of compounds.⁴

To better understand the molecular vibrations responsible for the characteristic bands of MIR spectroscopy, it is useful to consider a simple model derived from classical mechanics. A pair of atoms joined *via* a covalent bond can therefore be thought of as being like two masses (m_1 and m_2) attached by a spring, as shown in Figure 2.1.⁵



Figure 2.1: Schematic depicting a simple diatomic molecule as two masses (m_1 and m_2) attached by a spring.⁵

This is the typical construction of a simple harmonic oscillator and the system can vibrate with different amounts of energy at a frequency that depends on the masses of the two atoms and the strength of the bond. The frequency of vibration (ν) can be approximated by Hooke's Law, where μ defines the reduced mass of the diatomic molecule and k describes the force constant:^{1,6}

$$\nu = \frac{1}{2\pi} \sqrt{\frac{k}{\mu}} \quad \text{Where: } \mu = \frac{m_1 m_2}{m_1 + m_2} \quad \text{Equation: 2.1}$$

For the classic harmonic oscillation of a diatomic molecule, the potential energy (V) of the system (related to frequency by $V=h\nu$) is given by Equation 2.2, where x is the displacement of the spring and k still refers to the force constant.³

$$V = \frac{1}{2}kx^2$$

Equation: 2.2

A plot of the potential energy curve for the diatomic system as a function of the internuclear distance is thus a parabola that is symmetric about the equilibrium distance (x_e) (Figure 2.2a). Here, x_e occurs at the energy minimum and is established depending on the attractive and repulsive forces of the two atoms. The potential energy sharply increases to either side of x_e as the bond is compressed or stretched away from equilibrium.^{3,4}

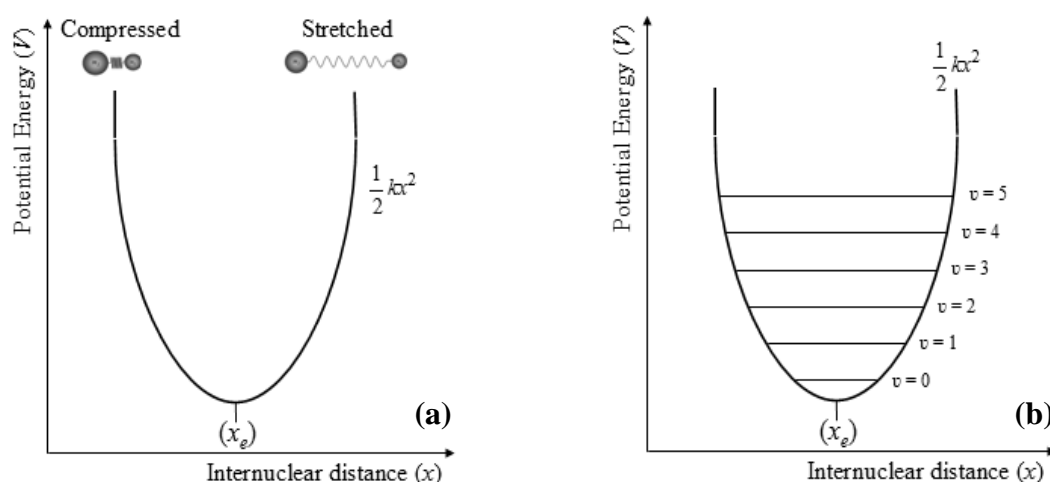


Figure 2.2: Potential energy curves for (a) a simple harmonic oscillator and (b) a diatomic molecule, constrained to the quantum mechanical model.⁷

The simple model shown in Figure 2.2a implies that a molecule could absorb energy at any frequency to result in deviation of the bond from equilibrium; however quantum mechanics dictates that molecules can only exist in quantized energy states of discrete values. These vibrational energy levels, illustrated in Figure 2.2b, are equidistant from each other and exist at energy values defined by Equation 2.3: where h is Planck's constant; ν is the frequency of vibration; and v defines the quantum number, which can have only positive integer values (0, 1, 2, ...).^{3,7}

$$E_{vib} = \left(v + \frac{1}{2} \right) h\nu$$

Equation: 2.3

Molecules can undergo transitions between vibrational energy levels on absorption of photons with corresponding energy. When considering a harmonic oscillator, these transitions can only occur across one energy level ($\Delta v = \pm 1$), for example $v = 0 \rightarrow v = 1$ and $v = 1 \rightarrow v = 2$ are allowed while $v = 0 \rightarrow v = 2$ is forbidden. The first transition from $v = 0 \rightarrow v = 1$ is the strongest of the allowed transitions, as the Boltzmann distribution dictates that at room temperature most molecules will exist in the ground vibrational state. These transitions result in what are termed fundamental vibrations. Transitions occurring from levels higher than $v = 0$ will be much weaker, as there will be a lower population of molecules occupying these energy states.^{4,5}

In reality molecules do not comply with simple harmonic motion and are classed instead as anharmonic oscillators. Anharmonicity results if the change in dipole moment is not linearly proportional to the nuclear displacement coordinate and there are two main reasons which cause this to happen with diatomic molecules. Firstly, as the molecule compresses, the electron clouds of the two atoms limit the approach of the nuclei due to the build up of repulsive forces. This results in the potential energy of the system rising rapidly when internuclear distances become smaller than the equilibrium distance (x_e). When the internuclear distance is increasing from equilibrium, the atoms are becoming further apart and the bond between them eventually breaks when the dissociation energy is reached. At this point the potential energy levels off. These deviations from harmonic oscillation are demonstrated in Figure 2.3.^{3-5,7}

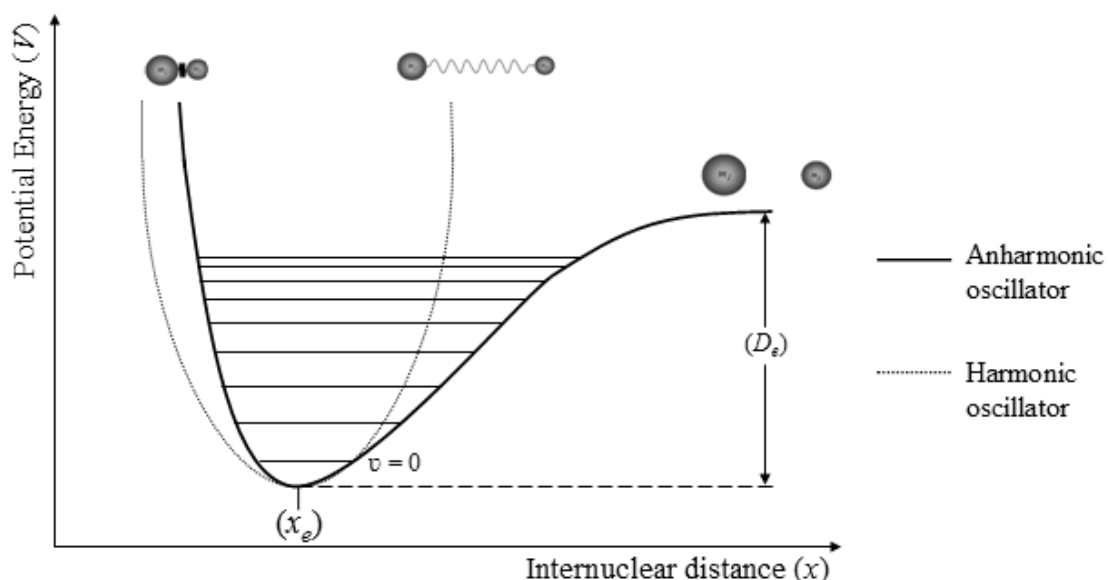


Figure 2.3: Potential energy diagram comparing harmonic and anharmonic oscillators. D_e is the energy of dissociation of the atoms and x_e indicates the equilibrium bond length.³

It can also be seen from the diagram that deviation from harmonic motion becomes greater as the vibrational quantum number increases: the separation between adjacent energy levels becomes smaller at higher vibrational levels until the dissociation limit is reached. The energy term corrected for anharmonicity can be expressed by Equation 2.4, where $x_e v_e$ defines the magnitude of the anharmonicity.^{3,5}

$$E_{vib} = h\nu_e \left(v + \frac{1}{2} \right) - hx_e v_e \left(v + \frac{1}{2} \right)^2 \quad \text{Equation: 2.4}$$

The transitions which are observed under anharmonic conditions are also seen to deviate from those that are allowed for a harmonic oscillator model. Experimentally, as well as the fundamental transitions (i.e., $\Delta v = \pm 1$) both overtones ($\Delta v = \pm 2$) and combination bands are seen. These transitions occurring to higher vibrational energy states are however far less probable than the fundamentals and so in practice they are seen at much lower intensities.³⁻⁵ When the frequency of a fundamental vibration for a particular functional group is quite low, then overtones may be observed in the MIR region. Combination bands and overtones however, are typically responsible for features in the NIR spectral region.

2.1.2 ATR-MIR Spectrometry

ATR-MIR spectrometry has rapidly grown in popularity in recent years, a feat which is mainly due to its ease of operation and the advantages it holds over more conventional approaches of MIR analysis.^{8,9} Traditionally, samples have been commonly analysed by means of transmitting radiation directly through the material, however for transmission to be possible it is often a requirement that sample thickness be restricted to the order of tens of microns. The main disadvantage of this approach is that sample preparation is generally quite time consuming and can often be relatively complex. For example solid samples would typically have to be ground to a fine powder and either: pressed into a disc after mixing with a matrix material (e.g. KBr); or suspended in the form of a mull between two MIR transparent windows. Liquid samples on the other hand would typically be analysed as thin films by transferring them into cells constructed with MIR transparent windows. An additional difficulty associated with these methods of sample preparation is the ability to attain samples of suitable concentration - a trial and error approach is commonly employed to prepare samples that allow the acquisition of adequate spectra.^{9,10}

ATR-MIR spectrometry is much simpler to operate and analyses can be undertaken of solid, liquid and gas samples as long as the material of interest is placed in direct contact with an element or crystal of high refractive index.⁸⁻¹¹ Rather than infrared radiation being transmitted through the sample, the technique operates by measuring changes that occur in an infrared beam, which is totally internally reflected within the crystal, when that beam comes into contact with the sample as shown in Figure 2.4. Interaction between the infrared beam and the sample is achieved *via* an evanescent wave that extends beyond the surface of the crystal of the order of microns – good contact between the sample and crystal is therefore vital.^{10,11}

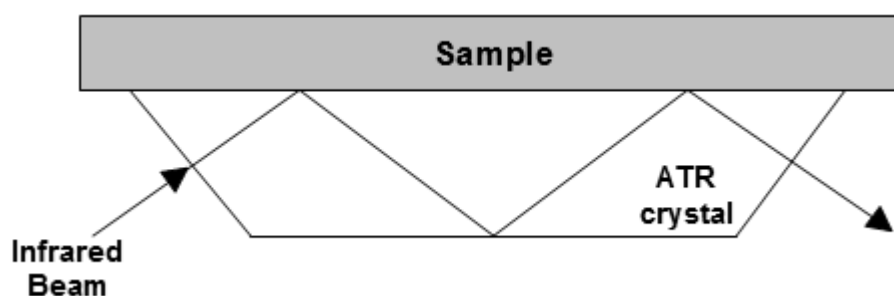


Figure 2.4: Schematic of a multi reflection ATR system to demonstrate contact between a sample and ATR crystal resulting from total internal reflection.

ATR-MIR spectrometry therefore allows a vast reduction in both sample preparation time and complexity and so the tool offers advantages over more traditional approaches in terms of faster sampling and spectral reproducibility.⁸⁻¹¹ The instrumentation used to complete this research incorporated an MIR spectrometer coupled to an ATR fibre optic probe and so the principles behind this particular technology are described in the following subsections in relation to this set up.

2.1.2.1 Optical fibres

The use of optical fibres has become invaluable for many techniques incorporating spectroscopic analysis, as they provide a means of transmitting light over long distances. Optical fibres remove the need for extractive sampling and can be used *in situ*. This has the advantage of facilitating the acquisition of data from otherwise inaccessible areas, as well as providing the option for the analyser to stay clear of hazardous areas.^{12,13}

An optical fibre typically consists of a cylindrical core of refractive index (η_1) which is enclosed by an annular cladding material of higher refractive index (η_2). Fibres constructed in such a way are known as step-index optical fibres, as both η_1 and η_2 are uniform throughout the core and cladding respectively. Light is transmitted along the fibre through the core material and is confined there by total internal reflection at the core-cladding interface.¹³⁻¹⁷ The propagation of light along an optical fibre is illustrated in Figure 2.5.

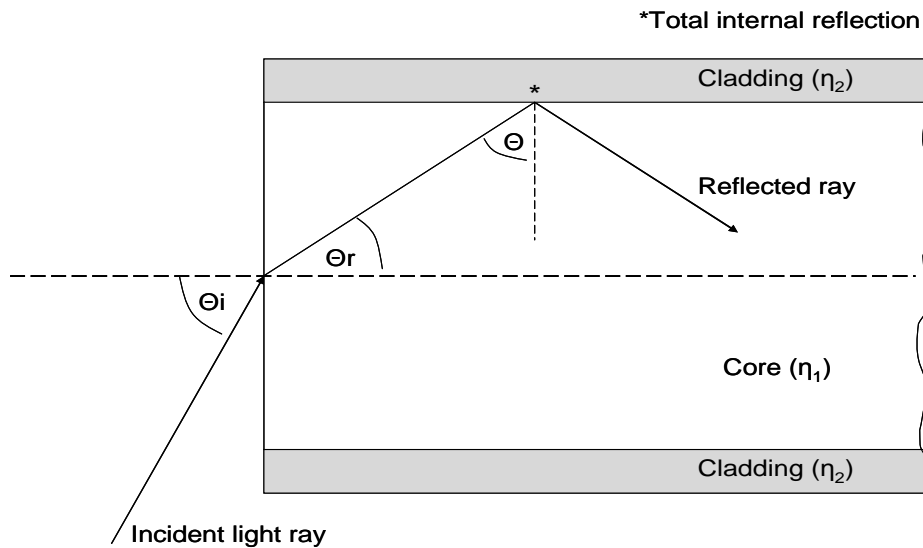


Figure 2.5: A cross section through a step index optical fibre, illustrating how light propagates along it by total internal reflection.¹⁴

When considering the propagation of light along an optical fibre, Snell's law can be used to relate angles of refraction to angles of incidence when the beam of light is passing through a boundary of two media with different refractive index.¹⁶ At the air-core interface, where light is introduced to the fibre, the angle of refraction (θ_r) of the incident ray can therefore be related to the angle of incidence (θ_i) as follows:¹³

$$\sin \theta_i = \eta_1 \sin \theta_r \quad \text{Equation: 2.5}$$

From this it can be deduced that the refracted ray will strike the core-cladding interface of the fibre at an angle of incidence (θ) equal to $(90^\circ - \theta_r)$. For total internal reflection to occur and so continue the transmission of light along the fibre, a minimum value of θ is required. This angle can be determined by the following equation:^{15,16}

$$\eta_1 \sin \theta_{\min} = \eta_2 \quad \text{Equation: 2.6}$$

As light propagates along an optical fibre, transmission losses will occur as a result of attenuation. Attenuation is the term used to describe the reduction in intensity of the propagating light beam due to scattering and absorbance by the core material.^{14-16,18} Different core materials will vary in their performance to transmit electromagnetic radiation and so are chosen depending on their ability to limit

attenuation and maximise the amount of transmitted light at the wavelengths required for a given technique.¹⁵

Optical fibres for MIR spectrometry have been challenging to develop, especially in comparison with NIR spectrometry and this is due to the limited choice of core materials available to provide adequate transmission of IR radiation. NIR typically uses fibres made of silica, which as well as having excellent transmission in this region is low in cost. Silica fibres can also transmit NIR light over distances greater than a thousand metres and as a result the technique has become well established for applications in process analysis. Unfortunately silica is not transparent in the MIR region and so the use of MIR spectrometry with optical fibres was initially limited whilst more specialised fibre materials were sought.¹⁵ The main fibre optic materials that have been developed for use with MIR spectrometry have been summarised in Table 2.1.^{13,15,19}

Table 2.1: Fibre optic materials for use with MIR and their properties.^{13,15,19}

Fibre Optic Material	Transmission range		Comments
	(cm ⁻¹)	(μm)	
Heavy Metal Fluoride (HMF) e.g ZrF ₄ based	1820 – 5000	2 – 5.5	<ul style="list-style-type: none"> • Higher laser power delivery capabilities • Low frequency cut off ~1820 cm⁻¹ • Brittle/fragile • Difficult to manufacture • Sensitive to moisture
Hollow Waveguides	400 – 10 000	1 – 25	<ul style="list-style-type: none"> • Cover a broad spectral range • Very robust • Demonstrate strong attenuation on bending • Length restricted to a few metres
Chalcogenide e.g. As ₂ S ₃	~ 1500 – 5000	2 – 6.5	<ul style="list-style-type: none"> • Expensive • Toxic & Fragile • Low frequency cut off ~1500 cm⁻¹ • Absorb at 2500 and 3300 cm⁻¹ • Non-hygroscopic
Silver halide	~ 600 – 3100	3.2 – 17	<ul style="list-style-type: none"> • Visible light sensitive • Non-toxic • Non-hygroscopic • Very flexible & robust

The first accounts of non-silica-based fibres for use with MIR radiation were reported in the 1960s. These newly developed fibres were being constructed from chalcogenide glass, a material that is still in use today. The applications of these fibres are however limited and this is due to their toxicity, fragility and a lack of transmission below ~1000 cm⁻¹. Alternative optical fibres have since been developed, including hollow waveguides, heavy metal fluoride fibres and silver

halide fibres - each offering a number of advantages as well as some of their own restrictions (see Table 2.1). Of these materials, silver halide fibres have proven increasingly popular and have greatly broadened the application prospects of MIR spectroscopy incorporating optical fibres. Silver halide fibres resolve many of the issues associated with those constructed from chalcogenide, being non-toxic, more flexible and allowing the transmission of a wider range of MIR light.^{15,19}

Although there have been many advancements in fibre optic technology for applications within spectroscopy, optical fibres still have certain limitations that need to be considered. One of the primary limitations is that all fibres will suffer losses of radiation as a result of attenuation; in other words, light will be lost due to absorbance and scattering by the core material, an occurrence that will reduce the overall signal reaching the detector. In addition, any fibre movement during transmission can influence final spectra due to changes in the angle of incidence influencing total internal reflection. A further consideration when implementing fibre optics is related to optimising the fibre diameter. Thin fibres will have much greater flexibility, less attenuation and smaller cost implications whereas larger diameter fibres can carry more light and so improve signal throughput. Larger diameter fibres are also considered easier to interface to spectrometers. The process of coupling fibres to a spectrometer can additionally affect the efficiency of a fibre. If the radiation beam is wider than that of the fibre core then over-filling will occur, resulting in much of the radiation being lost to the fibre cladding but if the fibre diameter is greater than that of the radiation beam then the core is not transmitting radiation to its full potential. Time also has to be taken to ensure optimum alignment of the radiation beam with the optical fibre so as to maximise signal throughput.^{13,15}

2.1.2.2 ATR-MIR probe technology

As eluded to in the previous subsection, MIR spectrometry was initially not as well established as NIR spectrometry in applications that required coupling to optical fibres. This was primarily due to the incompatibility of MIR with silica fibres but since the development of fibre optics constructed from silver halide materials, the popularity of MIR for these applications has greatly risen in recent years.²⁰ The tools

main advantage over NIR is that the MIR frequencies corresponding to fundamental vibrations are more strongly absorbed and give much narrower and more distinct spectral lines.^{5,21} As a consequence however, sample pathlengths typically have to be short when dealing with MIR spectrometry and so it is now common to find these fibres coupled with ATR probes.^{13,21}

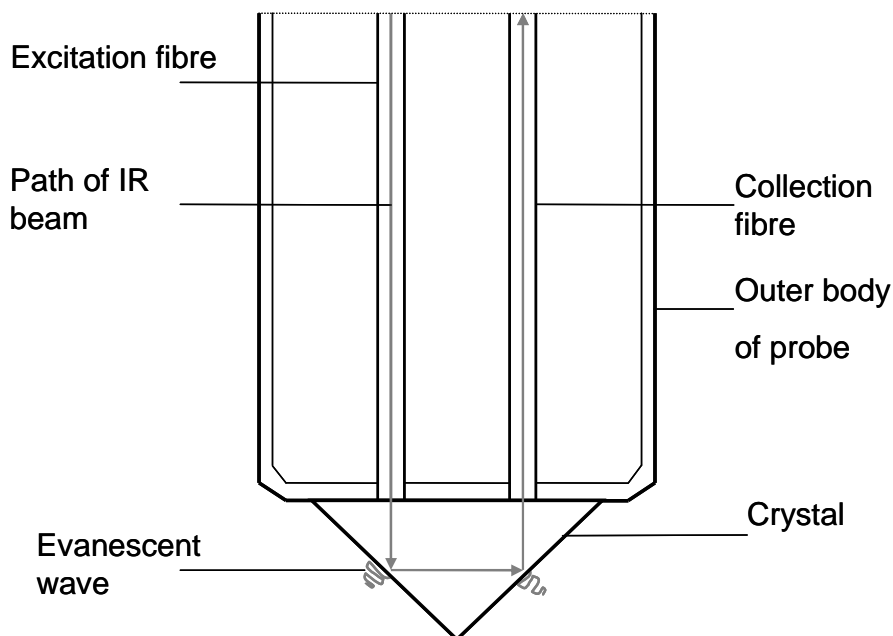


Figure 2.6: Schematic of an ATR probe head.^{13,22}

The typical construction of an ATR probe head is shown in Figure 2.6.^{13,22} The infrared radiation in an ATR probe is transmitted along the excitation fibre and directed to a crystal of high refractive index. This will result in total internal reflectance at the points of contact as long as the beam strikes the crystal at the critical angle (θ_c), governed by Equation 2.7, where η_1 is the refractive index of the crystal and η_2 is the refractive index of the medium that the crystal is in contact with.^{21,23}

$$\theta_c = \sin^{-1}\left(\frac{\eta_1}{\eta_2}\right) \quad \text{Equation: 2.7}$$

The IR beam interacts with the sample *via* an evanescent wave produced at the sample-crystal interface, which becomes altered in regions of the spectrum where the sample absorbs. This attenuated information is then directed along a collection fibre and carried to a detector where a spectrum of the sample is generated.^{21,24}

The penetration depth (d_p) of the evanescent wave for a single reflection is given by Equation 2.8, where θ is the angle of incidence and λ is the wavelength of the excitation radiation.^{21,23-25}

$$d_p = \frac{\lambda}{2\pi\eta_1 \left[\sin^2 \theta - (\eta_2/\eta_1)^2 \right]^{0.5}} \quad \text{Equation: 2.8}$$

The pathlength (b) can also be defined and relates to the number of reflections and the penetration depth as shown in Equation 2.9.²⁶

$$b = d_p * \text{No. of reflections at the crystal} \quad \text{Equation: 2.9}$$

ATR crystals therefore possess very short equivalent pathlengths, as the penetration depth of the evanescent wave into the sample is small at each reflection (of the order of microns). This is the main reasoning behind the effective use of ATR probes for the analysis of strongly absorbing compounds that are encountered when using MIR spectrometry.^{13,21,23}

2.1.2.3 ATR probe design^{20,27-30}

The ATR probe used for this research incorporated silver halide optical fibres and was supplied by Fibre Photonics. Due to their development being an ongoing process, probe designs differ slightly between manufacturers and the typical ATR probe currently adopted by Fibre Photonics is illustrated in Figure 2.7.

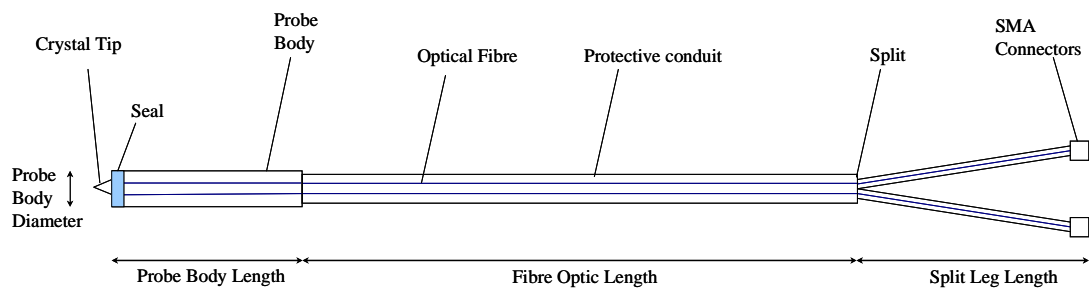


Figure 2.7: Schematic of the typical ATR probe design adopted by Fibre Photonics.

The Fibre Photonics ATR probe consists of two silver halide optical fibres running parallel to each other from the crystal tip to the split; the purpose of the split being to allow one of the fibres to be connected to the source and the other to the detector, which are attached to the spectrometer using SMA connectors. The whole assembly is encased to protect the fibres and this protective conduit is typically made using stainless steel (Figure 2.8a). Recent developments however have indicated that this allowed too much flexibility and so the fibres within became prone to breakage. The majority of probes now offered by Fibre Photonics, including the one used in this research, therefore incorporate liquid tight protection which makes use of an extra silicon coating to hold the fibres in place more rigidly (Figure 2.8b).

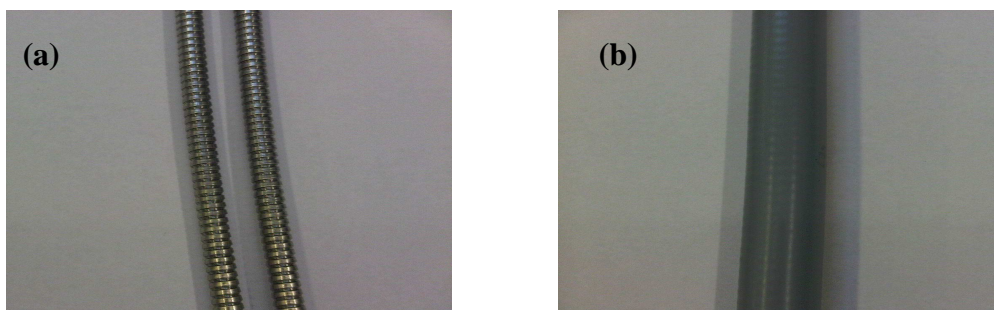


Figure 2.8: Pictures illustrating the protective conduit materials used by Fibre Photonics (a) stainless steel and (b) liquid tight protection.

The probe body can also be constructed from stainless steel, however hastelloy is generally more common. This part of the assembly protects the end of the fibres and allows them to be positioned at the edge of the crystal tip. The probe body is completely sealed around the crystal to prevent substances infiltrating the probe and damaging the fibres inside. The material used for this purpose was originally polytetrafluoroethylene (PTFE or Teflon), however this was often found to crack as a

result of the pressure exerted on it during probe manufacturing. The alternative seal material currently employed is polyether ketone (PEEK), which has been found to be much more robust.

ATR crystals can be constructed from a variety of materials, each having different properties. Crystals made from zinc selenide (ZnSe) or diamond are most commonly employed and though the former is relatively inexpensive the latter is generally favoured. This is related to the robust nature of diamond allowing it to withstand much harsher conditions than ZnSe; ZnSe can be prone to scratching and its use is restricted to a small pH range (between ~pH 5 - 9). The only major downfalls of diamond are its expense and that it absorbs IR radiation between about 1900 and 2200 cm^{-1} . Crystals constructed of germanium, silicon and thallium-bromiodide are also available but less frequently employed. Germanium has a very high refractive index which makes it well suited for the analysis of highly absorbing samples and due to the resulting low penetration depth it can be useful for the analysis of thin films. Silicon also has a high refractive index but is affected by strong acids and alkalis. Thallium-bromiodide crystals cover a very wide spectral range however they are very soft and can be easily damaged. Caution must also be taken due to the material being highly toxic.

The ATR probe used in this research incorporated a diamond crystal of 2.4 mm diameter and its geometry is illustrated in Figure 2.9. Different crystal geometries will influence the number of reflections at the crystal surface, which in turn will affect pathlength and consequently probe performance.

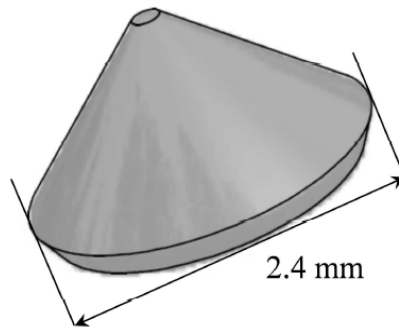


Figure 2.9: Schematic of the diamond crystal geometry as currently in use by Fibre Photonics.²⁰

2.1.3 Fourier Transform Infrared Spectrometry

The instrumentation utilised for infrared spectrometry typically implements either a dispersive or fourier transform infrared (FTIR) spectrometer. The original instruments that were developed for infrared spectrometry were of the dispersive type and these worked by sequentially measuring the individual frequencies of energy emitted from an infrared source. The typical set up of a dispersive spectrometer is provided within Figure 2.10, demonstrating the workings of this instrumental setup. Source energy is initially directed through a reference and a sample at the same time (so as to account for any instrument interferences specific to that analysis, such as differences in lamp brightness) before both beams are directed onto a rotating segmented mirror known as a ‘chopper’. The purpose of the chopper is to alternately focus each beam onto the detector *via* a monochromator. The monochromator – typically a prism or more commonly a diffraction grating – then separates the wavelengths of light in the spectral range so that each wavelength of radiation is passed one at a time through a slit to the detector, where the amount of energy at each frequency is measured sequentially to create a spectrum of intensity vs. frequency.³¹⁻³³

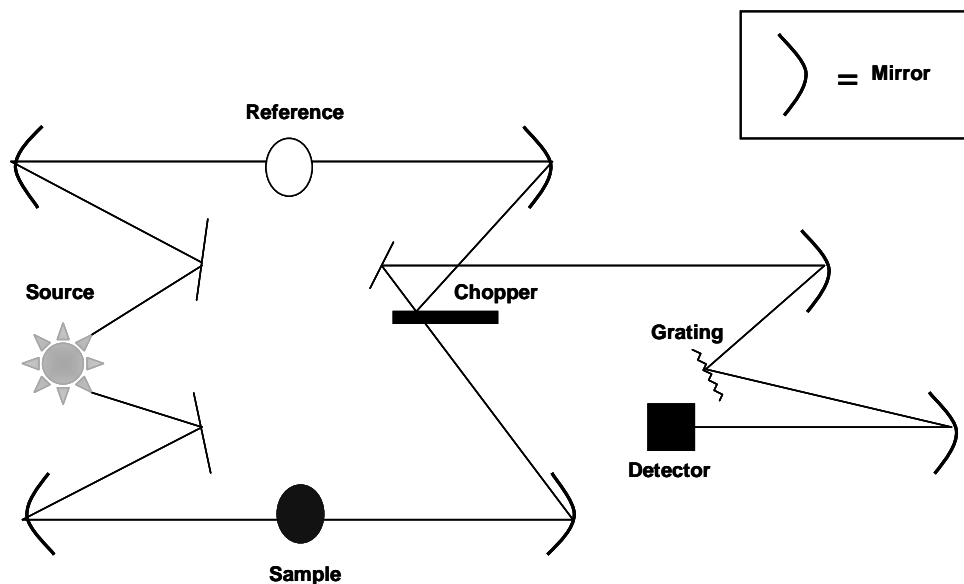


Figure 2.10: Diagram demonstrating the typical set up of a dispersive IR spectrometer.^{31,32}

FTIR spectrometers emerged later and were developed as a means to measure all IR frequencies simultaneously, a key advantage over dispersive spectrometry. An FTIR spectrometer uses a system known as an interferometer to achieve this type of spectral measurement and the typical setup of this instrument type has been depicted within Figure 2.11.³¹⁻³⁴

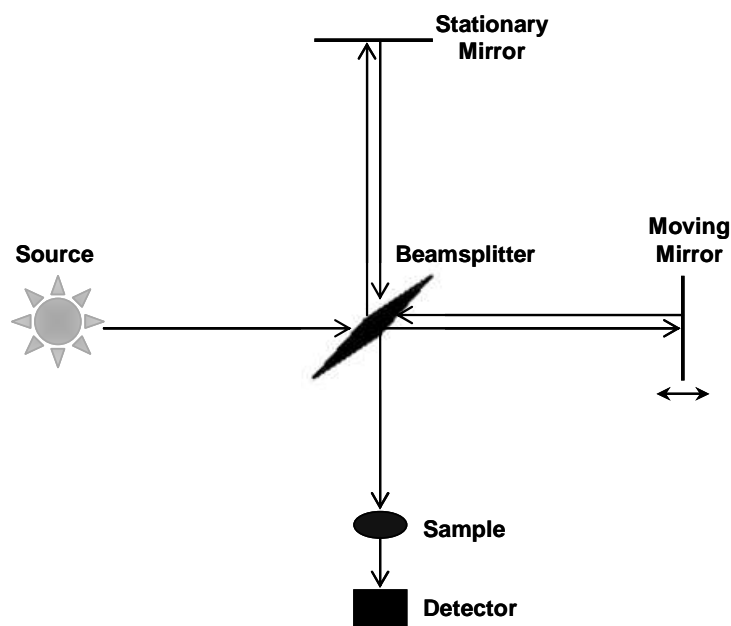


Figure 2.11: Diagram demonstrating the typical set up of an FTIR spectrometer.³¹

As depicted in Figure 2.11, source radiation is passed onto a beamsplitter which splits the energy beam into two parts: one being transmitted onto a stationary mirror whilst the other is reflected onto a mirror that moves back and forth with a constant velocity. Once reflected back by both mirrors, the beams are then recombined at the beamsplitter. If the two mirrors are at the same distance from the beamsplitter when this occurs, the distance travelled by the two beams will be equal and this situation is defined as the zero path difference (ZPD). As the movable mirror travels away from the beamsplitter however, the light beam striking this mirror will travel a longer distance compared to the radiation reflected from the stationary mirror. This results in wavelengths recombining at the beamsplitter with either constructive or destructive interference depending on the extra distance travelled by the moving mirror. The extra distance travelled is defined as the optical path difference (OPD) and is equal to two times the distance that the movable mirror travels away from the beamsplitter. When the OPD is the multiples of the wavelength (Equation 2.10, where $n = 0,1,2,3\dots$ and λ is the wavelength) constructive interference occurs and a maximum intensity signal is observed by the detector. When the OPD is in accordance with Equation 2.11 (where again $n = 0,1,2,3\dots$ and λ is the wavelength) destructive interference occurs and minimum intensity signals are instead observed.³¹⁻³⁴

$$OPD = n\lambda \qquad \text{Equation: 2.10}$$

$$OPD = \left(n + \frac{1}{2}\right)\lambda \qquad \text{Equation 2.11}$$

These two situations for OPD are the extreme scenarios and as the moving mirror travels back and forth from the beamsplitter, the intensity of the signal increases and decreases between them giving rise to a cosine wave known as the interferogram. When a broad band source is utilised as in FTIR, a peak is found at the ZPD of the interferogram and the signal decays quickly at other distances as the movable mirror travels back and forth. The interferogram then passes through the sample where some energy is absorbed and the remainder transmitted, the latter portion reaching the detector which reads information about every wavelength simultaneously. The interferogram collected by the detector is a function of time (relative intensity vs.

OPD) and to obtain the infrared spectrum, the interferogram is converted from the time domain to the frequency domain using an algorithm known as the Fourier transform. This decoded signal is also corrected using a background spectrum acquired with no sample present so as to remove features arising from the instrumentation in the resulting infrared spectrum. A single background can be used for many sample measurements.³¹⁻³⁴

As well as allowing spectral ranges to be measured simultaneously as opposed to sequentially, FTIR spectrometry has a variety of other advantages over the dispersive type that make the former preferred for infrared spectrometry in the present day. These have been summarised below:^{21,31}

- Data collection with an FTIR spectrometer is much quicker due to its ability to measure all frequencies simultaneously. A dispersive spectrometer has to measure each spectral wavelength individually – a much slower process.
- The signal-to-noise ratio measured on an FTIR spectrometer is higher than attained using a dispersive spectrometer, meaning sensitivity is greatly improved. A few reasons responsible for this are: the fast speed of scanning means that several scans can be averaged in order to reduce random measurement noise; and optical throughput is much higher as the absence of a slit and fewer mirror surfaces means that more energy reaches the detector.
- High resolution measurements are of a better quality when using an FTIR spectrometer as the instrument does not use a slit to limit individual frequencies reaching the sample and detector. A dispersive spectrometer does implement this setup however and so in order to measure wavelengths closer together (i.e. of higher resolution) the slit must severely limit the amount of energy transmitted, which results in poor quality spectra.
- The FTIR spectrometer uses a laser to control the velocity of the moving mirror and this can in addition be used as an internal wavelength calibration standard, making the device self-calibrating. Dispersive spectrometers on the other hand require external calibration standards and this can result in spectra being less comparable due to instrument unknowns during and between scans.

2.2 Liquid Chromatography – Mass Spectrometry

Liquid chromatography – mass spectrometry (LC-MS) is an analytical technique that combines the physical separation power of LC with the mass determining capabilities of mass spectrometry. It is therefore a very useful technique for concurrently obtaining the separation of components in complex mixtures and the identification of component masses.³⁵ LC-MS is also particularly well suited to the analysis of non-volatile components and so overall the tool is very appealing for the investigation of colour related constituents within Scotch whiskies and caramel materials, of which there is currently very little knowledge.

2.2.1 Liquid Chromatography

Chromatography is the collective term that describes a set of analytical techniques used for the separation of mixtures. The aspect that the majority of these systems have in common is that separation occurs due to the partitioning of sample components between a mobile and a stationary phase.³⁵ In liquid chromatography, a liquid mobile phase is incorporated and this carries analytes over a stationary phase that typically consists of a liquid medium bound to a solid support. An equilibrium arises between the two phases and component separation will be achieved if different analytes are distributed between the phases to different extents. Components with a higher affinity for the stationary phase material will interact more strongly and so be retained in the system for longer, whereas analytes with a lower attraction will interact less and so move more quickly to the detector, hence allowing component separation.³⁵⁻³⁷

The mobile phase employed for LC depends on the mode of chromatography being applied and reversed phase chromatography is typically the most popular.³⁸ This form of chromatography incorporates a mobile phase that is more polar than the stationary phase meaning that hydrophobic molecules tend to partition to a greater extent in the stationary phase. Mobile phases therefore tend to be aqueous based, although if the system incorporated only water then separation would be extremely time consuming due to strong component interactions with the stationary phase. Organic solvents are therefore implemented that reduce the affinity of hydrophobic

analytes to the stationary phase, therefore providing more practical retention times.^{35,36} The presence of organic solvents is also important for the up keep of stationary phases, which are known to collapse if stored in the wrong medium. The ratio of aqueous to organic, generally termed **A** and **B** respectively, can be altered during analysis to produce gradient conditions. The components of a mixture in this case are separated as a function of the affinity for the current mobile phase composition relative to the stationary phase. The more hydrophilic solutes will elute when the composition of the mobile phase is mainly aqueous, while the hydrophobic components will elute later in the run when the composition is mainly organic. Gradients can therefore be altered to suit the sample of interest and provide the best separation in the shortest amount of time possible.³⁵⁻³⁸

Stationary phases typically incorporate spherical particles of porous silica as the solid support to which many different chemical groups can be incorporated to allow interactions with the majority of compound types. Silica is an ideal support material due to its mechanical strength, the well established silane chemistry, its porous structure and the wide range of particle and pore dimensions that it can adopt.³⁵ A porous material such as silica allows analytes to diffuse into the pores and this is what permits an equilibrium to be established with the stationary phase surface.³⁸ In theory this can be achieved more quickly by reducing particle size and would result in a significant gain in the chromatographic efficiency below 2.5 μm . This is in accordance with the Van Deemter equation that infers such efficiency will not diminish even at increased flow rates or linear velocities. Equation 2.12 depicts the Van Deemter equation, the terms of which can be defined as follows: H is the plate height, μ is the linear flow rate; A depicts eddy diffusion; B represents longitudinal diffusion and C portrays mass transfer.

$$H = A + \frac{B}{\mu} + C\mu \quad \text{Equation: 2.12}$$

Plate height (H) is a measure of column efficiency and is inversely proportional to the number of theoretical plates (N) as depicted by Equation 2.13 (where L equates to column length).

$$H = \frac{L}{N}$$

Equation: 2.13

The number of theoretical plates (N) is defined as the number of independent equilibration events that occur between the stationary and mobile phases and so the greater the number of theoretical plates, the better the efficiency of the column. This in turn means that to obtain optimum column efficiency, plate height (H) needs to be minimised. This can be achieved by reducing terms A, B and C of the Van Deemter equation (Equation 2.12), all of which portray the main factors contributing to band broadening, a phenomenon that greatly reduces the efficiency of separation over a column. Band broadening in relation to eddy diffusion (A), longitudinal diffusion (B) and mass transfer (C) have been discussed below along with explanations of how the effects can be minimised.³⁹⁻⁴²

- Eddy diffusion:** Eddy diffusion describes the fact that the molecules of an analyte can take different paths through the particles of a column even if they start at the same position. Some analyte molecules will therefore take longer than others to elute from the column, the consequence being that the analyte band is broadened. Band broadening caused by eddy diffusion is independent of the linear flow rate of the mobile phase, it can however be reduced by decreasing the column particle size. Smaller stationary phase particles will cause the differences in analyte paths to be reduced resulting in much narrower analyte bands, a principle depicted within Figure 2.12.

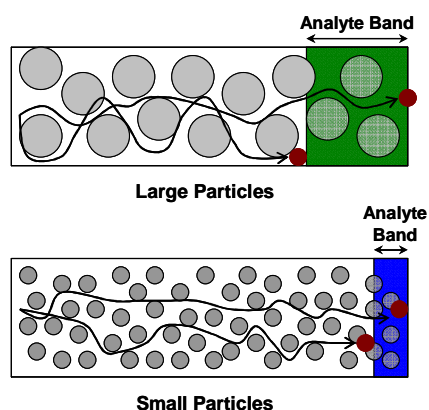


Figure 2.12: Illustration of the reduction of band broadening caused by eddy diffusion by the implementation of smaller stationary phase particles.^{39,41}

- **Longitudinal diffusion:** Longitudinal diffusion describes the process by which a band of analytes will disperse in every direction due to the concentration gradient at the outer edges of the band. The analyte molecules are effectively moving from an area of high concentration (the centre of the analyte band) to an area of lower concentration (the edges of the band) to achieve equilibrium and this results in band broadening. The extent of band broadening caused by longitudinal diffusion will increase the longer a component is present in the column; higher linear flow rates will therefore reduce the effects of band broadening caused by this parameter.
- **Mass Transfer:** Particles of the stationary phase consist of a porous material, utilised so that a very large surface area is available for separation to occur. Out with these pores the mobile phase flows at the stipulated rate, however inside the pores the mobile phase is stagnant or motionless. This means that analyte molecules that diffuse through the pores will take longer to elute than analyte molecules that don't enter the pores. Analyte molecules that diffuse to different depths within a pore will also be held up to different extents and as a result of these factors, band broadening will occur. One way to reduce the effect of band broadening caused by mass transfer is to reduce the linear flow rate, however a reduction in the size of stationary phase particles will also minimise these effects. Smaller particles result in pore sizes being reduced meaning that: the distance for analyte diffusion is less; diffusion time within the pores is minimised; and any differences in analyte diffusion caused by analytes travelling to different depths within the pores is reduced.

As alluded to in the preceding text, the two primary factors that influence the effects of band broadening (and so improve column efficiency by minimising H) are the linear flow rate of the mobile phase and the particle size of the stationary phase. The relationship between plate height (H) and linear flow rate in relation to terms A, B and C (both individually and cumulatively) has been depicted using a Van Deemter plot as shown in Figure 2.13a. This clearly demonstrates that optimum column efficiency occurs at the lowest plate height and is dependant on the linear flow rate.

Figure 2.13b then demonstrates how the Van Deemter plot is influenced by the use of stationary phase particles of different sizes and it is clearly shown that smaller particles yield better column efficiencies. It is also observed that the curve becomes flatter and less affected by higher flow rates in accordance with decreasing particle size, emphasising the point stated earlier that there is a significant gain in chromatographic efficiency below 2.5 μm which is not compromised by the use of faster linear velocities.³⁹⁻⁴²

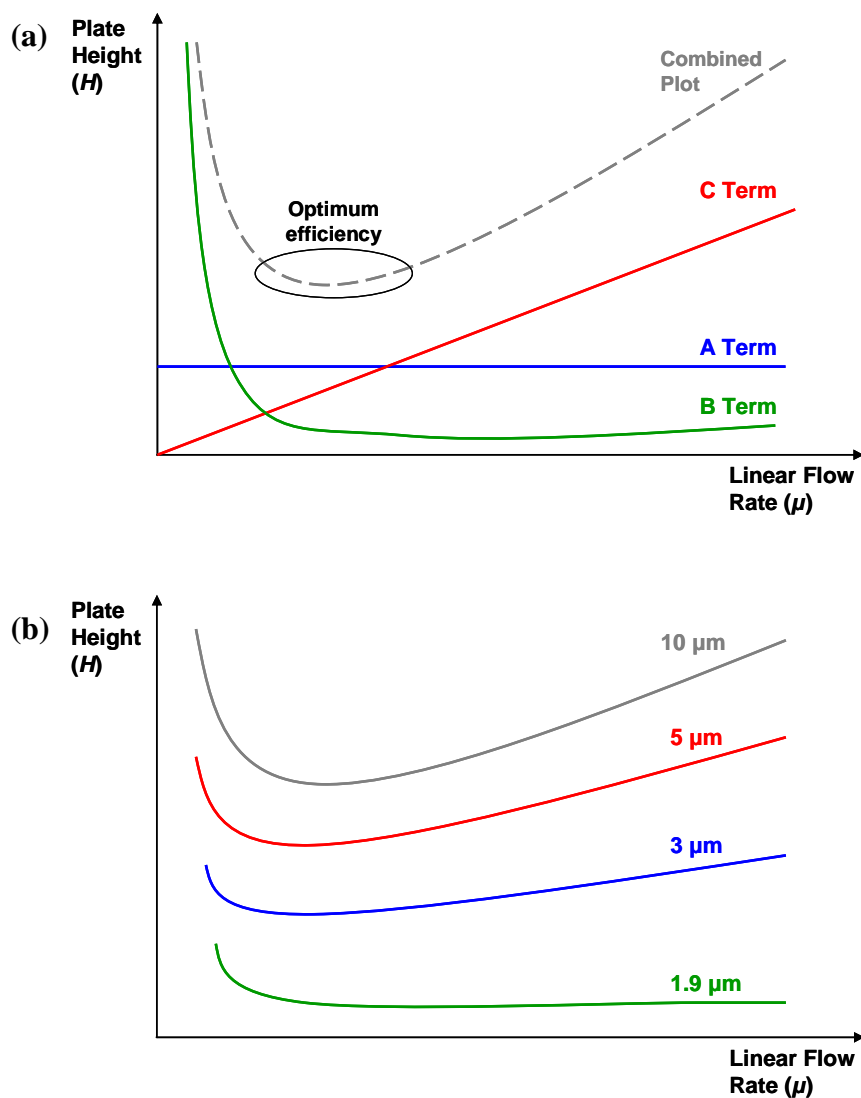


Figure 2.13: (a) Van Deemter plot illustrating the relationship between plate height and linear flow rate in relation to eddy diffusion, longitudinal diffusion and mass transfer. (b) Van Deemter plot illustrating the influence of stationary phase particle size on plate height as linear flow rate increases.

Although smaller particles are known to improve column efficiency, in practice the use of smaller particles creates resistance to the mobile phase stream and so very high pressures are required to drive the flow of molecules over the stationary phase. Standard high performance liquid chromatography (HPLC) typically uses columns containing particles with sizes from 3 to 5 μm , however the development of ultra performance liquid chromatography (UPLC) has allowed sizes down to 1.8 μm to be used. UPLC therefore offers the ability to run efficient separations at higher flow rates, allowing faster analysis speeds and does so with superior resolution and sensitivity.⁴³⁻⁴⁵

Analytes eluting from the LC column are typically detected using a UV detector, as the majority of organic compounds absorb in this region. These detectors generally fall into two categories allowing either fixed wavelength or multi-wavelength detection. The latter are most commonly favoured because they allow a wide choice of wavelengths to be covered during a single analysis. Diode array detectors are typically employed for this purpose.^{35,38}

Liquid chromatography with UV detection can be a very powerful tool for the identification of many compounds, as long as a suitable reference material is available for comparison or the relative amounts of each component are known. If however a complex mixture containing unknown components is being dealt with, then analyte identification may prove difficult by LC alone. Combining LC with a technique such as mass spectrometry can instead be used to determine the molecular masses of components and so aid in the confirmation of analyte identity.^{36,37}

2.2.2 Mass Spectrometry

Mass spectrometry is an analytical technique that is used to determine the molecular mass of components, which can in turn be helpful in terms of structural elucidation. The principle behind the technique consists of ionising chemical compounds to generate charged molecules or molecule fragments and then measuring these by their mass to charge (m/z) ratio. The typical instrumentation generally consists of three main modules: an ion source for the conversion of the sample into gas phase ions; a

mass analyser that sorts the ions according to their m/z ratio; and a detector, which measures and records the abundances of ions for each m/z value present.^{36,37}

2.2.2.1 Ion source

The ion source is the section of the mass spectrometer where sample components are ionised to provide gas phase ions that can then be accelerated towards the mass analyser. A number of ionisation methods exist (examples being electron ionisation, chemical ionisation, atmospheric pressure chemical ionisation) however the most common mode employed when coupled to LC instrumentation is electrospray ionisation, depicted by Figure 2.14.^{46,47}

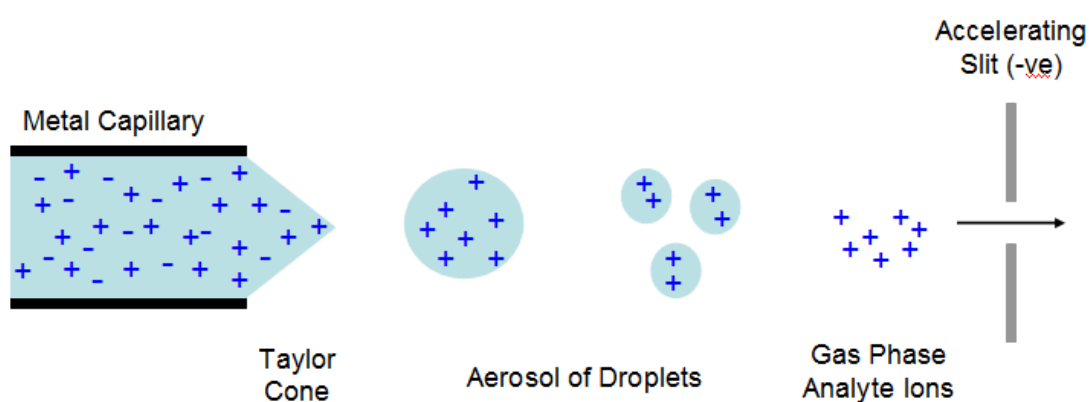


Figure 2.14: Illustration of electrospray ionisation. The light blue areas containing dark blue plus/minus signs indicate the solvated ions.^{46,47}

An electrospray consists of two main parts, a metal capillary and an accelerating slit positioned between approximately 0.3 – 2.0 cm away from the capillary tip. The analyte solution is drawn from the capillary into a Taylor cone due to the large potential difference with respect to the slit.^{46,48} When a threshold voltage is reached the solution is emitted from the tip as a jet of liquid that is progressively broken up into smaller droplets until all solvent has evaporated. It is generally considered that this occurs as the repulsive forces between positive ions in solution exceed surface tension and eventually leaves behind only gas phase analyte ions.^{36,46-48} These are then accelerated to the mass analyser to be sorted according to their m/z ratio. Electrospray ionisation is generally a very gentle type of ion formation and so the molecular structure of even large complicated molecules can be retained.⁴⁶

Ionisation can be employed in two different modes to obtain either positive ion spectra or negative ion spectra. Positive ionisation is generally used for analytes containing functional groups that readily accept a proton (H^+) and trace amounts of formic or acetic acid are commonly added to aid in this process. Negative ionisation on the other hand is typically used for components that will more readily lose a proton and ammonia solution is one additive that can be used to assist with this ionisation mode.⁴⁶

2.2.2.2 Mass analyser

Ions generated in the ion source are directed to the mass analyser, which sorts the ions depending on their m/z ratio. A variety of different mass analyser types are available and these can include magnetic sectors, quadrupoles, time of flight (TOF) mass analysers and ion traps.³⁶ The TOF is currently one of the most desirable mass analysers due to its quick speed of analysis and higher sensitivity (accurate to approximately 1 mDa) and as such it was required and utilised to facilitate the objectives set out within this research project. The construction of a typical TOF mass analyser is shown in Figure 2.15.^{36,39}

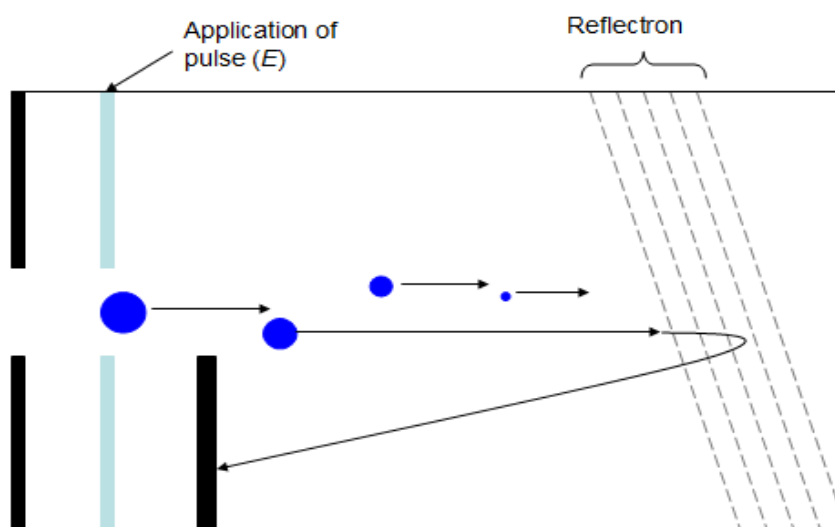


Figure 2.15: Illustration of a time of flight mass analyser. Ions are represented by the blue circles, in order of descending mass from left to right.

In a TOF mass analyser, ions simply drift along a field free vacuum at velocities dictated by their mass. This is in accordance with the equation of motion (Equation

2.14) which dictates that an ion's velocity (v) will decrease with ascending mass (m).⁴⁷ Consequently if energy (E) remains constant, lighter ions will travel faster than heavier ones, resulting in ions arriving at the detector in order of increasing mass. This set up allows the detection of all ions as they arrive at the detector and so accounts for the technique's high sensitivity.^{46,47}

$$E = \frac{1}{2}mv^2 \qquad \text{Equation 2.14}$$

Ions are introduced into the analyser as a pulse and so all receive the same initial kinetic energy (E). An issue that may arise from this is that in practice the pulse may not be experienced by all ions to the same intensity, resulting in a slight kinetic energy distribution for each m/z ion and so lower resolution. This is typically corrected by the application of a reflectron at the end of the drift zone, consisting of a series of electric fields (usually at a displaced angle). This allows ions to be re-pulsed back along the flight tube to be refocused with the same m/z value on the reflectron detector.^{36,46-48}

The TOF mass analyser (as with all mass analysers) can be used independently to gain information about component masses, however for structural information to be obtained (as required within this project), a molecule must be fragmented to yield a combination of ions that are generally characteristic of that analyte. Fragmentation of components can typically be achieved using tandem mass spectrometry where two mass analysers, separated by a collision cell, are used in combination with each other.⁴⁹ There are four different ways that data can be acquired using this instrumental set up but the most useful for providing structural information of individual components is the product ion experiment. In this case the first mass analyser is used to select an ion of interest (a parent ion), which is then passed on to the collision chamber where an inert gas is admitted to collide with the selected ion and bring about its fragmentation. These fragment ions are then passed onto the second mass analyser which separates them according to their m/z ratio, before directing them to the detector. All of the fragment ions detected arise directly from the initially selected parent ion and so a fingerprint pattern specific to the parent ion

singled out by the first mass analyser is provided. This information can therefore be extremely useful for the structural elucidation of analytes however is typically restricted to the investigation of a single parent ion at a time.^{39,49,50}

Waters has patented an analysis mode, termed MS^E (where E represents collision energy), which can overcome the abovementioned limitation of traditional tandem mass spectrometry and instead can allow the fragmentation patterns of all parent ions to be catalogued from a single injection.^{51,52} This offers a significant advantage when complex mixtures with very little compositional knowledge are to be assessed. MS^E technology has been utilised within this research and an orthogonal acceleration time of flight (oa-TOF) mass analyser was used to facilitate the analysis. A schematic of the oa-TOF instrumentation has been provided in Figure 2.16 to help visualise how it works.³⁹

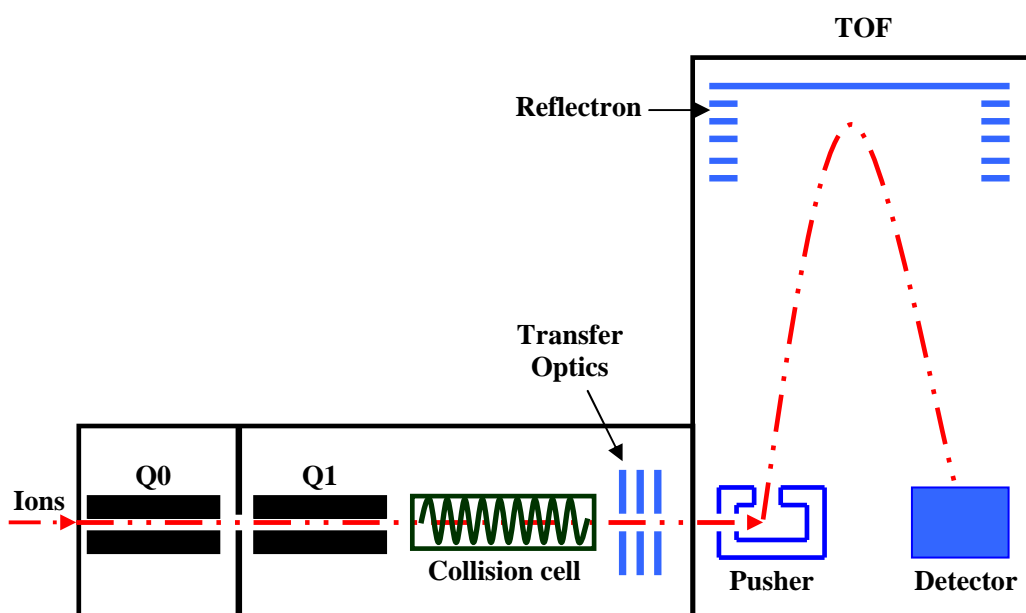


Figure 2.16: Schematic depicting the workings of an oa-TOF mass analyser.

Once generated at the ion source, ions are directed into the oa-TOF mass analyser where they are focussed by an RF only quadrupole (Q0), which facilitates the initial transmission of parent ions along the mass analyser and allows all parent ions to pass through. The ions then pass through a second quadrupole (Q1), which if required can be set to select a specific parent ion for targeted analysis.³⁹ The analysis undertaken

within this research however was untargeted and so did not utilise this function; the quadrupole was instead set to allow the passage of all ions straight to the collision cell. MS^E data collection is then implemented and works by rapidly alternating the collision cell between two scanning functions for data acquisition. The first scanning function uses a low collision energy over the selected mass range, which allows spectra to be generated relating to all parent ions present in the sample, whilst the second scanning function uses an elevated energy, ramped up to the extent where the fragmentation of the parent ions can occur. This latter function therefore allows spectra to be acquired that provide information about the fragmentation patterns of all analyte ions that were found in the preceding scan.⁵¹⁻⁵³ Ions passing through or generated within the collision cell are transmitted (*via* transfer optics) to the TOF and on entering this section of the mass analyser are orthogonally ‘pushed’ by an accelerating voltage. This creates a discrete packet or pulse of ions which travel through the TOF mass analyser and are separated as described earlier in this section, before reaching the detector in order of ascending mass.³⁹

2.2.2.3 Detector

Once ions leave the mass analyser they are collected by the detector (in modern mass spectrometers this is typically an electron multiplier or a photomultiplier) and their relative abundances measured.³⁹ Typically the MS detector monitors the ion current, amplifies it and then transmits the signal to the data system where it is recorded in the form of a mass spectrum.⁴⁶ A mass spectrum is usually presented as a vertical bar graph in which each bar represents an ion of a specific m/z ratio and the height of the bar indicates the relative abundance of the ion. Most ions formed in the mass spectrometer have a single charge and so the m/z value is actually equivalent to the mass of the ion itself.^{48,54}

When working with LC-MS, data are normally presented as a mass chromatogram, which is a representation of signal intensity versus retention time. The mass spectra acquired at a particular retention time can then be extracted and interpreted using data collection software to allow the identification of any components present at that point.⁵⁴

2.2.3 MarkerLynx XSTM Software⁵⁵⁻⁵⁸

MS^E mass spectrometry generates a vast amount of high dimensionality data and so sophisticated software is required that can extract the appropriate information and also allow its interpretation. MarkerLynx XSTM is a one such package that can make sense of MS^E data and was utilised for the interpretation of data within this research. The software is able to extract *m/z* values from the mass spectra and aligns these data (or mass peaks) according to their retention time. This process is done using an algorithm known as ‘ApexPeakTrack’, however the details of this are not publically revealed. The mass peaks extracted in this way, known as exact mass retention time (EMRT) pairs, are then populated into a browser where multivariate data analysis can be completed to compare samples based on the EMRT pairs (or in other words components) they are found to contain.

PCA is one of the main statistical approaches used within MarkerLynx XSTM to compare samples based on the EMRT pairs they contain, a tool that is described in more detail in Section 2.3.1. PCA displays data in the form of a scores plot to assess any patterns between samples; samples falling in similar regions of the plot having similarities in their composition and *vice versa*. The variables (i.e. the EMRT markers) responsible for particular groupings in a scores plot can then be determined from corresponding loadings data and passed back in to the MarkerLynx XSTM browser where elemental composition can be assessed based on the masses (accurate to ~1 mDa) obtained *via* UPLC-MS. A direct link from the software to online databases then has the potential to allow the assignment of chemical structures, if a suitable match can be determined.

To aid in the determination of component structures the MarkerLynx XSTM software has a useful feature termed ‘MassFragment’, which can be used as an aid for structural elucidation. As well as MarkerLynx XSTM aligning mass peaks with their associated retention times, the software can also align the precursor information from the low energy scanning with the corresponding fragmentation spectra acquired during high energy scans. The MassFragment tool generates a list of the of the most likely fragment ions that would result from a proposed structure by undertaking

calculations based on a series of algorithms representing the most likely bond disconnections. The tool then allows the exact mass fragment ions (obtained from the high energy data of the MS^E acquisition mode) associated with the parent ion of interest to be evaluated against those from the proposed structure.

2.3 Data Analysis

ATR-MIR spectrometry and UPLC-MS both generate vast quantities of high dimensionality data: MIR spectra consisting of a large number of data points that depict absorbance values over a range of wavenumbers, whilst LC-MS data typically cover a variety of analyte masses over a range of retention times. Samples analysed using these techniques are therefore described by a large number of variables and manual interpretation of trends is therefore very difficult (as four or more variables cannot be represented graphically). Multivariate data analysis tools can therefore be implemented to help identify patterns or groupings within such high dimensionality datasets.⁵⁹⁻⁶¹ A range of multivariate data analysis tools have been utilised within this research and the theory behind each has been described within the following subsections.

2.3.1 Principal Component Analysis (PCA)

PCA is an exploratory data analysis tool that involves the visualisation of relationships between samples and also between variables, without prior knowledge of those samples. The basic function of PCA is to reduce the dimensionality of a large complex dataset by compressing it into a smaller number of abstract variables, termed 'latent variables' or 'principal components (PCs)'. For the statistical analysis to be successful however, the PCs acquired from the original data must retain the underlying structure of the dataset, both in terms of associated samples and any variable correlations.^{60,62}

A few rules exist for computing PCs, the first of which being that the primary PC must account for the greatest amount of variation in the data and successive PCs then describe the maximum amount of variation that has not already been accounted for by the preceding PC. The first PC is therefore drawn as a line through the centroid of the data (assuming the data has been mean centred), in the direction of maximum variation (Figure 2.17a). Another important condition that must be followed is that the second and any subsequent PCs must always be orthogonal to the previous PC and be drawn through the direction denoting the next most variation in the data (Figure 2.17b).⁵⁹⁻⁶³

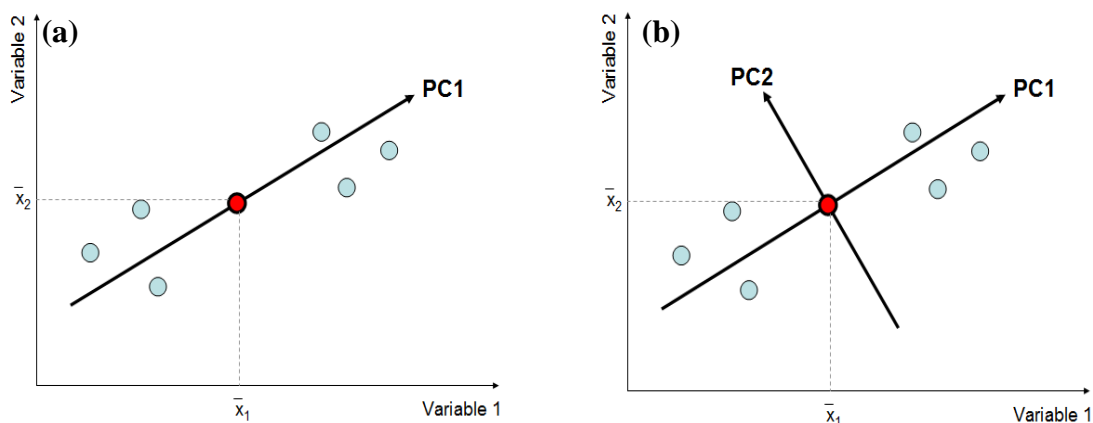


Figure 2.17: *Simplistic plots constructed to represent the data from 6 samples (blue dots) and two measured variables to demonstrate (a) PC1 being drawn through the centroid of the data in the direction of maximum variation and (b) PC2 as being orthogonal to PC1 in the direction of next most variation. The centroid is illustrated by a red dot.*⁶²

When undertaking multivariate data analysis, a spectral dataset can be represented as a matrix \mathbf{X} , where rows describe the spectra of different samples and each column represents the variables (different wavenumbers). The data matrix is considered as being composed of two separate components: the underlying structure or model of the data (\mathbf{M}); and random fluctuations known as ‘noise’ (\mathbf{E}), due to the measurement process. It can therefore be described as shown in Equation 2.15.⁶²

$$\mathbf{X} = \mathbf{M} + \mathbf{E} \qquad \text{Equation: 2.15}$$

Successful PCA results in the model matrix (\mathbf{M}) being broken down into two smaller matrices, \mathbf{T} and \mathbf{P} , such that:⁶¹⁻⁶⁴

$$\mathbf{X} = \mathbf{TP} + \mathbf{E} \qquad \text{Equation: 2.16}$$

\mathbf{T} is known as the scores matrix and it indicates whether any relationships exist between *samples*. A PC score for a particular sample is defined as the point at which that data point is projected onto the PC axis (Figure 2.18a).^{59,62,63} Thus samples related to each other will be found in the same area of multidimensional space and so possess similar scores.

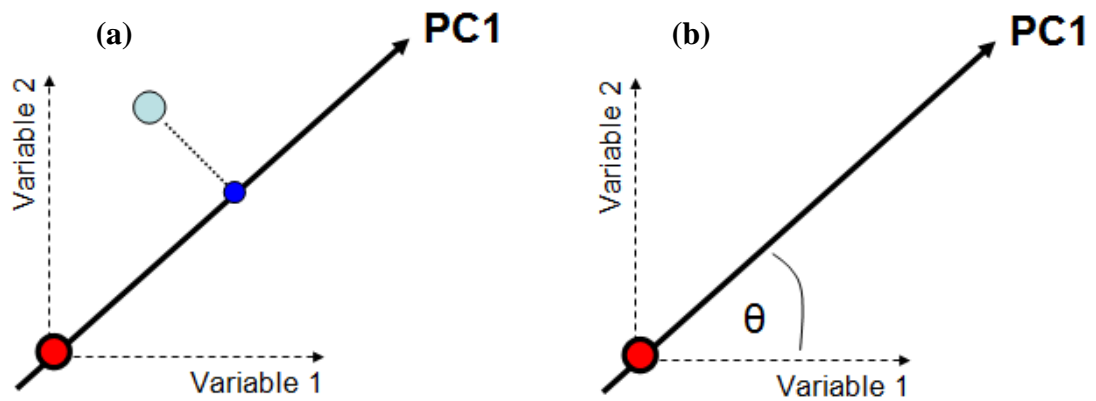


Figure 2.18: Plots demonstrating (a) the projection of a data point onto a PC1 axis to obtain a score and (b) the angle that would be used to determine the loading value relating to PC1 and variable 1.⁶²

P describes the loadings matrix and indicates any relationships between individual measurement *variables*, which in the case of this work are the different wavenumbers at which measurements have been taken. The loadings also help to explain any clustering or separation between samples in the scores plots. Loadings are determined for a given PC by calculating the cosines of the angles between the individual variable axis and the direction of the PC, as illustrated in Figure 2.18b. The smaller the angle, the closer the loading value becomes to 1, which indicates that the PC is closely associated or correlated to that particular variable (or in this case wavenumber). Conversely, if a variable has very little influence on the PC then the loading will be close to 0 and results from an angle close to 90 degrees. Variables can also be anti-correlated to a PC, which occurs if the angle is near to 180 degrees, giving loading values close to -1.^{59,62,64}

Mathematically, PCA relies upon an eigenvector decomposition of the covariance matrix of the process variables. Covariance is a measure of how much each of the dimensions being assessed (e.g. the different process variables) vary from the mean with respect to each other and is measured between variables to determine if there is a relationship between those parameters. When more than two variables are being considered, covariance can be represented as a matrix and so for a given data matrix (**X**) with m rows (samples) and n columns (variables), the covariance matrix ($\text{cov}(\mathbf{X})$) would be defined as shown in Equation 2.17, provided that the data have been mean centred.⁶⁵

$$\text{cov}(\mathbf{X}) = \frac{\mathbf{X}^T \mathbf{X}}{m-1}$$

Equation: 2.17

The covariance matrix is then decomposed into eigenvectors and eigenvalues, the former denoting the direction of a PC whilst the latter describes how much variance there is in the data in that direction (the largest eigenvalues corresponding to the strongest correlation in the dataset). The eigenvector with the highest eigenvalue therefore signifies the primary PC and subsequent PCs are in order of decreasing eigenvalue (i.e. in order of significance from highest to lowest). When the eigenvalue becomes so low that it no longer describes any additional variance in the data there is said to be a sufficient number of PCs to describe the measurement data. In other words the dimensionality of the original data matrix is reduced and can be described by a smaller number of latent variables (PCs) that maintain the underlying structure of the data.^{62,65}

2.3.2 Clustering and Classification Tools

Data sets often consist of samples that belong to a number of different groups or ‘classes’ and the ability to classify samples into their associated categories based on measured responses is a common requirement. There are a variety of methods that have been developed to achieve this and most of them can be split into being either unsupervised pattern recognition or supervised pattern recognition techniques. Unsupervised pattern recognition, also termed cluster analysis, attempts to identify groupings (or ‘clusters’) without the use of pre-established class information. This is also true of exploratory data analysis (EDA) tools such as PCA, however the main difference between the two approaches is that unsupervised pattern recognition aims to detect similarities between samples and so search for groupings, whereas EDA has no particular prejudice as to whether any groups (or how many groups) will be found. In the case of supervised pattern recognition (also called classification) knowledge of the class membership is required in advance for a set of training samples and the main aim of such a tool is to use this information to try and allocate new samples of unknown identity into the correct class. The classification of unknown samples can also be achieved using cluster analysis; however in this case it

would have to be done manually and so would also rely on the judgement of the analyst.^{59,65,66} Details of the specific pattern recognition techniques that have been investigated within this research have been described in the following subsections.

2.3.2.1 Hierarchical cluster analysis (unsupervised)

There are a variety of clustering methods encompassed by the term ‘hierarchical cluster analysis’ (HCA) and the majority of these are based on the assumption that samples close together on a measurement space are likely to belong to the same class.⁶⁵ The first step taken as part of HCA is therefore to define the distance between samples and there are a variety of ways to achieve this. The most common approach used is to measure Euclidean distance and this is depicted by Equation 2.18, which defines the Euclidean distance (d) between samples k and l , where there are j measurements and x_{kj} is the j^{th} measurement on sample k .^{64,67}

$$d_{kl} = \sqrt{\sum_{j=1}^J (x_{kj} - x_{lj})^2} \quad \text{Equation: 2.18}$$

Another popular distance measure is Mahalanobis distance and although this is similar to Euclidean distance, it takes into account that some variables may be correlated and so considers the possibility that variation in some directions is much larger than in others. It should also be noted here that distance measures can be determined based on either the raw data or on PCA scores. The latter can provide colinearity and noise reduction benefits, however additionally requires the selection of an appropriate number of PCs.^{64,65}

Once the distance between samples has been defined, the next step of HCA is to link samples together to form clusters. There are many clustering techniques encompassed by HCA, however these methods can be classified into two main categories: partitional clustering, which starts with all samples being considered as a single cluster and progresses by dividing existing clusters into smaller ones; and agglomerative clustering, whereby all samples are initially considered as lone clusters before gradually being connected to each other in groups.^{64,67} Agglomerative

clustering is the most frequently employed of the two techniques and was the approach utilised within this research.

In general an agglomerative clustering method begins by finding the samples with the smallest distance between them (calculated using one of the measures described above e.g. Euclidean distance) and linking them together to form a new set of clusters. The distances between the newly formed groups are then compared once more and the two nearest clusters are again combined; a process which is repeated until a stopping criterion is met.^{64,67} It is important to note here that although Euclidean or Mahalanobis distance measures are used to define distances between individual samples, they cannot be used to measure the distance between groups of samples.⁶⁸ In the case of agglomerative clustering, linkage between groups of samples can instead be determined by a variety of methods, such as: nearest neighbour, furthest neighbour, centroid, and Ward linkage. The nearest neighbour method (also known as single-linkage clustering) is generally considered as the simplest approach and defines the distance between any two clusters as the minimum of all possible pair-wise distances of samples between the two clusters.^{64,65}

To help visualise the steps followed during agglomerative clustering, an example has been depicted in Figure 2.19 for five samples (A-E) that have two associated measured responses (X_1 and X_2). Figure 2.19a shows the beginning of the process, where each of the five samples is considered as an individual cluster and in the first step of agglomerative clustering the distance between each of these samples would be determined – typically using the Euclidean distance measure. The next step then links together the samples that are closest to each other in distance and in this example the closest samples are clearly B and C, which are therefore shown to form a new cluster in Figure 2.19b. The method is then repeated so that the next closest clusters are grouped together and in this example samples D and E are next closest in distance to each other (now shown grouped together in Figure 2.19c). In the next repetition of the clustering technique, sample A is linked to the group containing B and C to form the two clusters illustrated within Figure 2.19d. This is the next closest distance between clusters and has been defined by the nearest neighbour linkage method as groups of samples are now being considered. The final step of the

clustering process, illustrated by moving from Figure 2.19d to 2.19e, links together the cluster containing samples A – C with the cluster of samples D and E. This again used the nearest neighbour linkage method and so the value defining the distance between the two clusters was the distance between samples C and D – this distance representing the minimum of all possible pair-wise distances for all sample combinations between the two clusters depicted in Figure 2.19d.

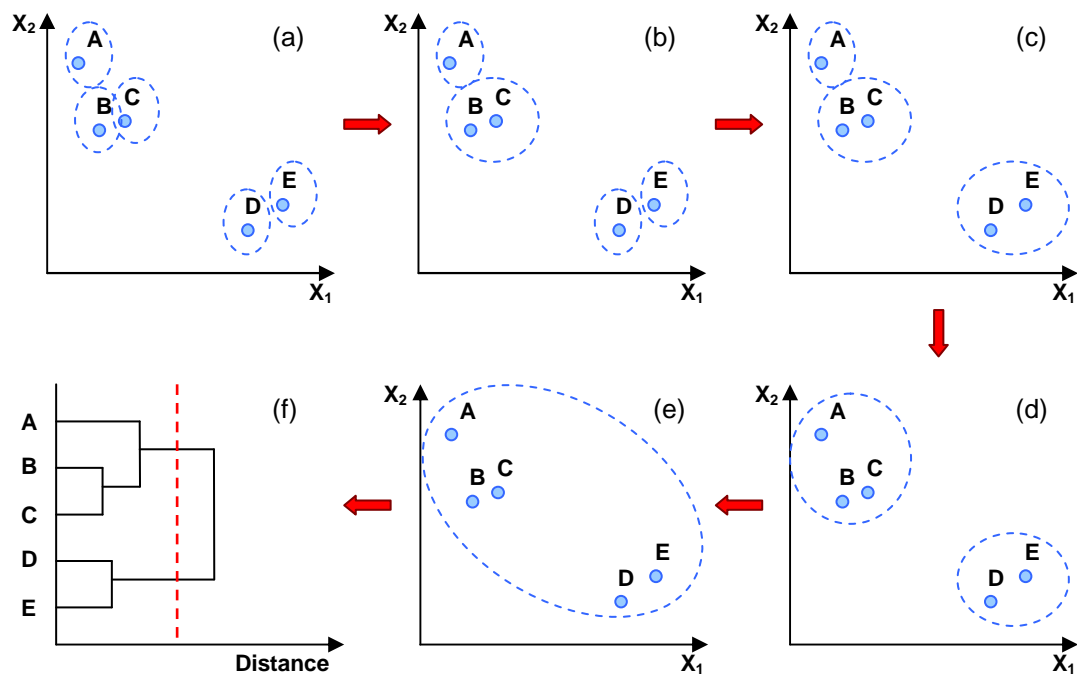


Figure 2.19: An example of agglomerative clustering analysis involving five samples (A-E) and two measured responses (x_1 and x_2). Plots (a) - (e) illustrate the steps taken during the clustering process whilst plot (f) shows the resulting dendrogram. The dashed blue circles in each plot represent the clusters formed at each repetition of the method.

The results of HCA are often represented in the form of a dendrogram and the dendrogram generated from the above example has been provided in Figure 2.19f. The vertical bars in the dendrogram indicate which samples (or groups of samples) are linked together, while the horizontal bars denote the distance between the linked samples or groups. When interpreting a dendrogram, it can be broken at different levels to yield different clustering of the data.^{65,67} In the example above (Figure 2.19f), the clusters would be defined by placing a vertical line across it and moving it up and down the distance axis; for any given distance, the number of clusters would then be signified by the number of horizontal lines that intersect the vertical line. In

Figure 2.19f, the red dashed line that has been inserted would therefore indicate the presence of two clusters in the example dataset.

2.3.2.2 *k*-nearest neighbour (*k*-NN) classification

The *k*-NN classification method is a supervised pattern recognition technique and so can be used to automatically predict the identity of an unknown sample as long as a training set is available where the class membership of each sample is already known. Once the class of each training sample has been assigned, the unknown sample can then be projected into the measurement space and its identity predicted based on the pre-established class information of the training set. The *k*-NN classification method works by calculating the distance of the unknown sample to all members of the training set; typically achieved using the Euclidean distance measure (see 2.3.2.1) although other approaches can be used if required. The *k* smallest distances are then identified to determine which training samples the unknown sample is closest to and the unknown sample is then allocated to the class that the majority of the *k* samples belong to.^{59,66} If no majority is found (which can occur if more than two classes are being considered) then the unknown sample is assigned to the class of the closest training sample.⁶⁹ It is typical for *k* to take on the value of a small odd number such as 3; however it is often useful to test a few additional values (e.g. 5 and 7) to see if classification changes.^{59,66}

An example of *k*-NN classification has been depicted by Figure 2.20, which represents the measurement space describing two variables (X_1 and X_2) and was generated from a training set of samples incorporating three classes (Classes 1 – 3). The unknown sample projected on to the measurement space has been depicted by a black cross and a value of $k = 5$ has been utilised to predict its identity. It is clear from the figure that the majority of the five nearest neighbours (encircled by a grey dashed line) are members of Class 1 and so the identity of the unknown sample in this case would be assigned as Class 1.

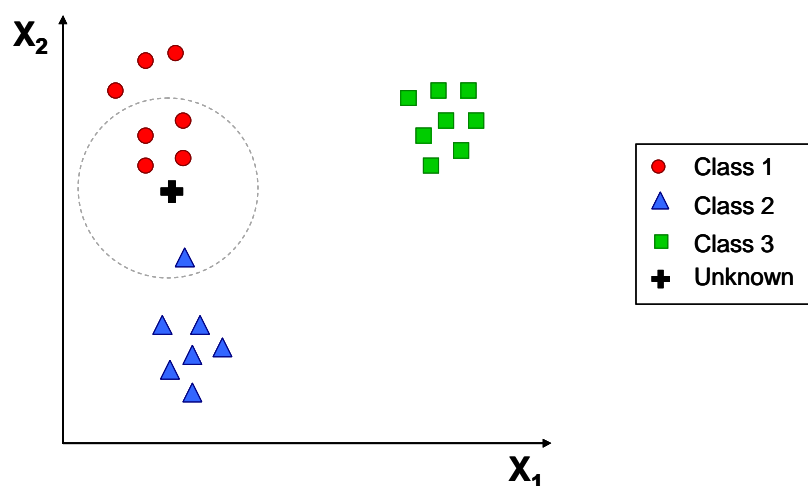


Figure 2.20: An example of the k -NN classification method being applied to predict the identity of an unknown sample (represented by a black cross), where $k=5$. The dashed grey line encompasses the 5 closest samples to the unknown and the majority of these are clearly from Class 1. The identity of the unknown sample would therefore be predicted as belonging to Class 1.

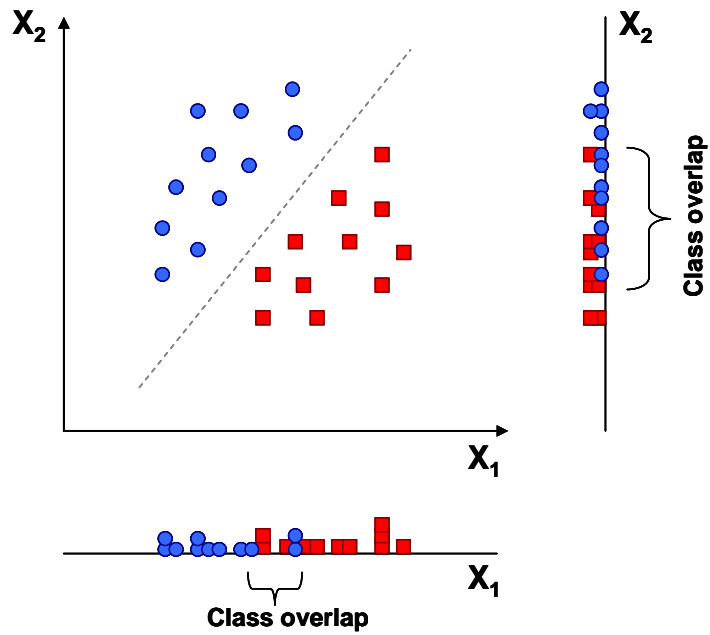
The simplicity of the k -NN method has made it extremely popular for the classification of scientific data and it can easily be applied to data sets recording many more than two measured responses; only two measurement variables were used in the example above however, for ease of visualisation. Another appealing feature of k -NN classification is that it can prove extremely useful when the groups in a training set cannot be separated by a plane.⁵⁹ Despite these advantageous characteristics, k -NN classification does have a number of potential limitations that are important to consider prior to its application.^{59,66,69} Firstly, it is important that the numbers of samples within each class of the training set are approximately equal, as this prevents there being a bias towards the class with the most representatives. It is also important that no outliers or ambiguous samples are contained within the training data, as such samples could wrongly influence classification. Another potential issue arises when samples have been characterised by many variables that possess different degrees of significance (e.g. when spectroscopic data is being considered). In such a case, it might be necessary to select a smaller number of variables prior to classification or to investigate alternative means to measure distances between samples. It is also important to keep in mind that k -NN classification does not take into account the spread or variance in a class and so in some cases it might be appropriate to use more sophisticated versions of the methodology that can employ voting schemes other than a majority vote.⁵⁹

2.3.2.3 Principal components – discriminant function analysis (PC-DFA)

PC-DFA is another supervised pattern recognition technique and so aims to classify new, unknown samples based on the identity of previously classified samples from a training (or calibration) dataset.⁷⁰ DFA (also known as canonical variate analysis (CVA)) is based on linear discriminant analysis (LDA) and so attempts to find linear combinations of the originally measured variables which best separate two or more classes (termed canonical variates).^{68,70-73} This procedure has been depicted within Figure 2.21 for the simplest scenario, where there are two classes (A and B) and two measurement variables (X_1 and X_2). In Figure 2.21a it is clear that both of the classes are clearly distinct from each other when the measurement variables are plotted against each other; however when each sample is projected onto the individual X_1 and X_2 axes (as shown in the figure), it is clear that if used alone neither of the two measurement variables would be able to discriminate between the two classes. Both measurement variables are therefore crucial for classification and Figure 2.21b demonstrates how a canonical variate can be implemented to enable class separation using information from both measurement variables but based on only a single dimension. Figure 2.21b shows that a line (dotted grey in this example) can be drawn between Classes A and B that allows them to be clearly distinguished from each other. All samples can then be projected onto a single line at right angles to this discriminating line (the new line being the canonical variate) that allows clear visualisation of the distinction between the two classes based on a new single variable.^{59,64,66} The identity of unknown samples can then be predicted based on their value when projected onto the canonical variate; canonical variates (Y) typically being described by the function given in Equation 2.19, where a_n is the coefficient for measurement variable X_n .⁵⁹

$$Y = a_1X_1 + a_2X_2 + \dots + a_nX_n \qquad \text{Equation 2.19}$$

(a)



(b)

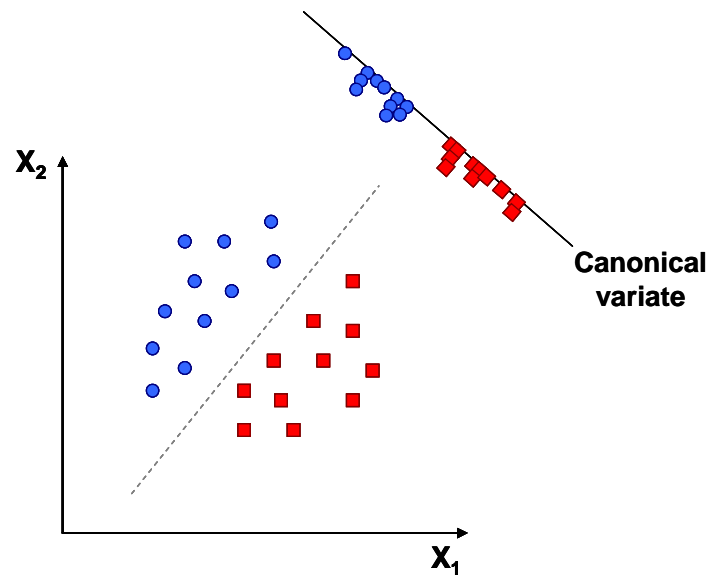


Figure 2.21: Plots of X_1 vs. X_2 for samples covering two classes (blue circles depict Class A and red squares denote Class B). Plot (a) demonstrates that when samples are projected onto the individual axes, class discrimination cannot be achieved when using only one of the measurement variables. Plot (b) then illustrates the use of a canonical variate to allow class discrimination by the creation of a new single measurement variable that is a linear combination of the original measurement variables (X_1 and X_2).

Although the above example only depicts how DFA would separate between two classes (with two associated measurement variables) it is commonly used in much more complex situations and seeks out canonical variates that will maximise between group distances whilst reducing within group variation.⁷⁰⁻⁷² The main advantages of DFA are that it is fast and simple to implement and it will also give good classification when samples are linearly separable.⁷¹ Despite this however, DFA does suffer when data are highly collinear and also when the number of features (wavenumbers in the case of this research) are higher than the number of samples.^{68,70,72-73} The condition described by Equation 2.20 typically has to be met; where N_s corresponds to the number of samples, N_g depicts the number of groups and N_v reflects the number of features.⁶⁸

$$(N_s - N_g - 1) > N_v \quad \text{Equation 2.20}$$

To overcome the above mentioned limitations, PCA can be performed on the data prior to DFA, hence the term PC-DFA. PCA is able to reduce the dimensionality of the data whilst preserving its underlying structure and does so without using prior knowledge of the sample groupings. This means that after PCA has been applied to the original dataset, only a small number of new uncorrelated latent variables remain to be employed during DFA. This therefore removes the effect of collinearity and also reduces the number of variables to satisfy the condition depicted within Equation 2.15.^{68,70,72-73}

2.3.3 Data Preprocessing Tools

2.3.3.1 Derivatisation

Derivatives can be applied to data prior to multivariate (or univariate) analysis and are commonly used to pre-process spectral data to remove the effects of baseline offset or to remove sloping baseline offsets, achieved using 1st and 2nd derivatives respectively. In simple terms the 1st derivative shows the rate of change of a tangent drawn at each point of the untreated data, a principle illustrated by Figure 2.22 for the transformation of data with a baseline offset by the 1st derivative. Figure 2.22 demonstrates that: when the tangent slope is increasing to the greatest extent a

maximum is observed in the 1st derivative spectrum; when the slope is decreasing to the largest degree a minimum is observed in the 1st derivative plot; and when the slope is flat (such as at the top of a peak within the untreated data) the value of the 1st derivative becomes zero. If the 2nd derivative were sought after this would be acquired in the same manner as for the 1st derivative but taking the rate of change of the 1st derivative spectrum as opposed to the untreated data.⁶⁴

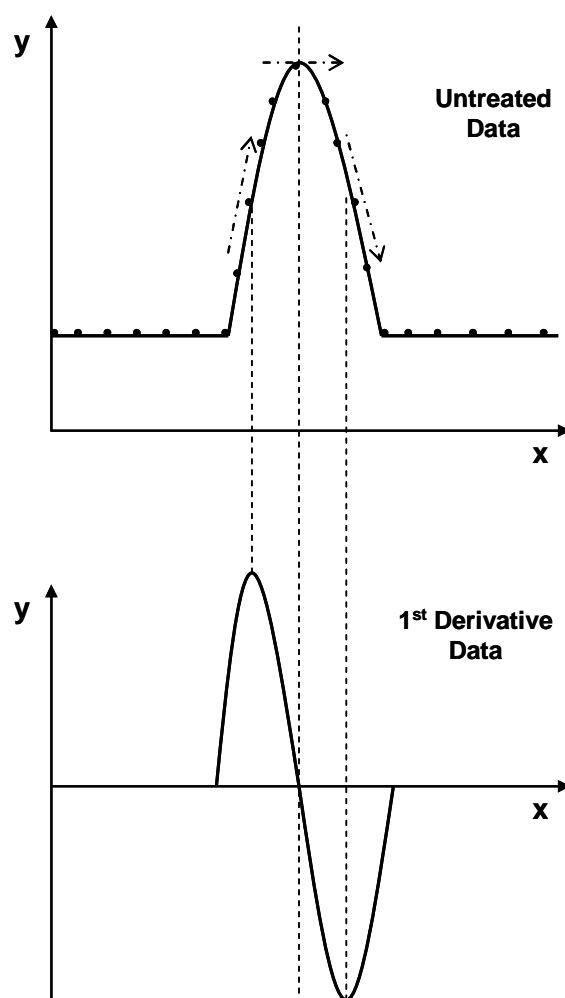


Figure 2.22: Schematic depicting the transformation of untreated data to the 1st derivative.

Transforming data to the 1st or 2nd derivative can be done using the Savitzky-Golay filter, which in addition to applying derivatisation will simultaneously smooth the data. This typically allows noise reduction without any significant loss of the signal of interest.⁶⁴ The Savitzky-Golay algorithm works by fitting a polynomial to windows around each point in a spectrum and requires the selection of the window size (filter width), the order of the polynomial and the order of the derivative. In

general, the larger the window and the lower the polynomial, the more smoothing will be applied and so these settings have to be carefully selected depending on the data being assessed. If the filter width is too large then distortion of the derivative curve may occur but if the chosen window size is too small, unwanted noise can be introduced.⁶⁵

2.3.3.2 Normalisation⁶⁵

Normalisation preprocessing methods are typically used to correct for scaling/gain effects in data that have caused the variables measured for a given sample to be increased or decreased from their true value by a multiplicative factor. Scaling effects can be caused by a variety of reasons, for example they might arise from instrumental sensitivity effects (e.g. source/detector variations and pathlength effects) or alternatively could arise from physical and chemical effects such as the physical positioning of a sample relative to a sensor. A normalisation preprocessing method attempts to correct for these types of effects by identifying an aspect of each sample that should remain virtually constant from one sample to another and then amends the scaling of all variables based on that feature.

When being applied as a preprocessing tool prior to the application of multivariate data analysis, normalisation can also help to give all samples an equal impact on the model being created. This is typically required if the relationship between variables – and not the magnitude of the response – is the aspect of the data most crucial for identifying a species. This would be the case for instance, if simply the presence of a material is important for identification and not the concentration at which it is there. If normalisation were not applied in this case, certain samples with large multiplicative scaling effects might not be considered by many multivariate tools due to not significantly contributing to variance.

A number of different normalisation preprocessing methods are available and simple normalisation will calculate one of several different metrics using all of the variables of each sample. Common normalisation methods include: dividing each variable by the sum of the absolute value of all variables for the given sample; normalising to the sum of the squared value of all variables for a given sample (which is a form of

weighted normalisation where larger values are weighted more heavily in the scaling); and normalising to the maximum value observed for all variables for a given sample (also weighted, where only the largest value is considered in the scaling).

Normalisation should typically be applied after the removal of any baseline offset (e.g. by derivatisation) and prior to any centring of the data. The presence of baseline offset when normalisation is applied can impede the correction of multiplicative scaling effects (unless the baseline is very consistent from one sample to another, in which case it would provide a useful reference for normalisation).

2.3.3.3 Generalised least squares weighting preprocessing

Generalised least squares weighting (GLSW) is a data preprocessing tool that has been implemented within this research (primarily prior to PCA) as a means to improve the prediction of test samples when data analysis tools for classification have been investigated (work undertaken within Chapter 4). GLSW incorporates an algorithm that calculates a filter matrix from the differences between samples which should otherwise be similar and subsequently attempts to down weight these differences which it considers ‘clutter’ or interference. In the case of classification, similar samples would be the members of a given class and so in this case, the main goal of GLSW is to reduce any within class variation without bringing the individual groupings any closer together (i.e. whilst maintaining between category variance). Such an objective thus enables better discrimination of classes. In more detail, GLSW works by centring the data from pre-assigned categories to their own class means and uses this ‘class-centred’ data to calculate the filter matrix. The algorithm itself contains only a single adjustable parameter, the weighting parameter (α), which dictates the degree to which the GLSW filter matrix down weights any clutter. Adjusting α towards higher values would decrease the effects of the filter, whilst lower values would apply a higher degree of filtering. The α value therefore needs to be optimised for any individual dataset and those values implemented within this research will be quoted where appropriate in later chapters.^{65,74-75}

2.4 References

1. D. L. Pavia, G. M. Lampman, G. S. Kriz, J. R. Vyvyan, *Introduction to Spectroscopy*, 4th Edition, Brooks/Cole, London, 2009
2. J. H. Van Der Maas, *Basic Infrared Spectroscopy*, 2nd Edition, Heyden & Son, London, 1972
3. P. J. Larkin, *Infrared and Raman Spectroscopy: Principles and Spectral Interpretation*, Elsevier, Oxford, 2011
4. P. R. Griffiths, *Introduction to Vibrational Spectroscopy*, in Handbook of Vibrational Spectroscopy: Volume 1, (eds) J. M. Chalmers; P. R. Griffiths, J. Wiley, New York, 2002
5. D. N. Sathyanarayana, *Vibrational Spectroscopy: Theory and Applications*, New Age International, New Delhi, 2004
6. H. W. Siesler, *Introduction*, in Near-infrared Spectroscopy: Principles, Instruments, Applications, (eds.) H. W. Siesler; Y. Ozaki; S. Kawata; H. M. Heise, Wiley-VCH, Weinheim, 2002
7. *Chapter 15 – Infrared Spectroscopy: Theory*, <http://orgchem.colorado.edu/Spectroscopy/irtutor/IRtheory.pdf>, Accessed 10/08/2015
8. F. M. Mirabella, *Introduction*, in Modern techniques in Applied Molecular Spectroscopy, (ed.) F. M. Mirabella, John Wiley & Sons, New York, 1998
9. P. R. Griffiths, J. A. De Haseth, *Fourier Transform Infrared Spectrometry*, John Wiley & Sons, Hoboken, 2007
10. *FT-IR Spectroscopy: Attenuated Total Reflectance*, Technical Note, Perkin Elmer, 2005
11. V. Sablinskas, G. Steiner, M. Hof, *Applications*, in Handbook of Spectroscopy, (eds.) G. Gauglitz; T. Vo-Dinh, Wiley-VCH, Weinheim, 2003
12. S. M. Khopkar, *Basic Concepts of Analytical Chemistry*, New Age International, New Delhi, 2nd Edition, 1998
13. D. Littlejohn, *Chapter 5: Optical Fibres*, in Process Analysis Module, University of Strathclyde, 2007

14. I. R. Lewis, S. S. Rosenblum, *General Introduction to Fibre Optics*, in Handbook of Vibrational Spectroscopy: Volume 2, (eds) J. M. Chalmers; P. R. Griffiths, J. Wiley, New York, 2002
15. C. W. Brown, *Fibre Optics in Molecular Spectroscopy*, in Modern Techniques in Applied Molecular Spectroscopy, (ed.) F. M. Mirabella, John Wiley & Sons, New York, 1998
16. R. Hui, M. O'Sullivan, *Fibre Optic Measurement Techniques*, Elsevier, Amsterdam, 2009
17. W. B. Allan, *Fibre Optics: Theory and Practice*, Plenum Press, London, 1973
18. W. B. Allan, *Fibre Optics*, Oxford University Press, Oxford, 1980
19. B. Lendl, B. Mizaikoff, *Optical Fibres for Mid-Infrared Spectrometry*, in Handbook of Vibrational Spectroscopy: Volume 2, (eds) J. M. Chalmers; P. R. Griffiths, J. Wiley, New York, 2002
20. A. C. McIntyre, Ph.D Thesis, *Extending the scope of mid-infrared spectrometry for in situ process analysis through ATR immersion probes*, University of Strathclyde, 2011
21. D. Littlejohn, *Chapter 6: Molecular Spectrometry*, in Process Analysis Module, University of Strathclyde, 2007
22. G. McMahon, *Analytical Instrumentation: A guide to laboratory, portable and miniaturised instruments*, John Wiley & Sons, Chichester, 2007
23. Y. Raichlin, A. Katzir, *Appl. Spectrosc.*, 2008, **62**, 55A-72A
24. P. J. Melling, M. Thomson, *Fibre-optic Probes for Mid-infrared Spectrometry*, in Handbook of Vibrational Spectroscopy: Volume 2, (eds.) J. M. Chalmers; P. R. Griffiths, J. Wiley, New York, 2002
25. F. M. Mirabella, *Attenuated Total Reflectance Spectroscopy*, in Modern techniques in Applied Molecular Spectroscopy, (ed.) F. M. Mirabella, John Wiley & Sons, New York, 1998
26. P. Fredericks, L. Rintoul, J. Coates, *Vibrational Spectroscopy: Instrumentation for Infrared and Raman Spectroscopy*, in Analytical Instrumentation Handbook, (ed.) J. Cazes, Marcel Dekker, New York, 3rd Edition, 2005
27. G. Colquhoun, Fibre Photonics, Livingston, *Personal Communication*, June 2012
28. *Fibre Photonics Webpage*, <http://www.fibrephotonics.com>, Accessed 28/06/2014

29. *ATR accessories: An overview*, Technical Note, Perkin Elmer, 2004
30. *ATR – Theory and Applications*, Application Note, Pike Technologies, 2011
31. *FT-IR vs. Dispersive Infrared*, Technical Note, Thermo Nicolet, 2002
32. D. L. Pavia, G. M. Lampman, G. S. Kriz, J. A. Vyvyan, *Introduction to Spectroscopy*, Cengage Learning, Stamford, 5th Edition, 2015
33. B. H. Stuart, *Infrared Spectroscopy: Fundamentals and Applications*, John Wiley & Sons, Chichester, 2004
34. B. C. Smith, *Fundamentals of Fourier Transform Infrared Spectroscopy*, CRC Press, Boca Raton, 2nd Edition, 2011
35. S. Moldoveanu, V. David, *Essentials in Modern HPLC Separations*, Elsevier, Waltham, 2013
36. R. E. Ardrey, *Liquid Chromatography – Mass Spectrometry: An Introduction*, John Wiley & Sons, Chichester, 2003
37. W. M. A. Niessen, *Liquid Chromatography – Mass Spectrometry*, CRC Press, Boca Raton, 2006
38. L. R. Snyder, J. J. Kirkland, J. W. Dolan, *Introduction to Modern Liquid Chromatography*, John Wiley & Sons, New Jersey, 3rd Edition, 2010
39. S. Cubbon, Ph.D Thesis, *LC-MS for the metabonomic study of human urine samples*, University of York, 2007
40. M. W. Dong, *Modern HPLC for Practicing Scientists*, John Wiley & Sons, New Jersey, 2006
41. A. Braithwaite, J. F. Smith, *Chromatographic Methods*, Springer Science, London, 5th Edition, 1996
42. *The Theory of HPLC Band Broadening*,
http://www.chromacademy.com/lms/sco3/Theory_Of_HPLC_Band_Broadening.pdf, Accessed 25/03/16
43. M. E. Swartz, *J. Liq. Chromatogr. R. T.*, 2005, **28**, 1253-1263
44. A. de Villiers, F. Lestremau, R. Szucs, S. Gelebart, F. David, P. Sandra, *J. Chromatogr. A.*, 2006, **1127**, 60-69
45. C. C. Leandro, P. Hancock, R. J. Fussell, B. J. Keely, *J. Chromatogr. A.*, 2006, **1103**, 94-101

46. A. M. Westman-Brinkmalm, G. Brinkmalm, *A Mass Spectrometers Building Blocks*, in *Mass Spectrometry: Instrumentation, Interpretation, and Applications*, (eds.) R. Ekman, J. Silberring, A. M. Westman-Brinkmalm, A. Kraj, John Wiley & Sons, New Jersey, 2009
47. E. de Hoffman, V. Stroobant, *Mass Spectrometry: Principles and Applications*, John Wiley & Sons, Chichester, 2nd Edition, 2001
48. J. Barker, *Mass Spectrometry*, (ed.) D. J. Ando, John Wiley & Sons, Chichester, 2nd Edition, 1999
49. A. M. Westman-Brinkmalm, G. Brinkmalm, *Tandem Mass Spectrometry*, in *Mass Spectrometry: Instrumentation, Interpretation, and Applications*, (eds.) R. Ekman, J. Silberring, A. M. Westman-Brinkmalm, A. Kraj, John Wiley & Sons, New Jersey, 2009
50. *An Introduction to Mass Spectrometry*,
<http://www.astbury.leeds.ac.uk/facil/MStut/mstutorial.htm>, Accessed 10/08/2015
51. R. S. Plumb, K. A. Johnson, P. Rainville, B. W. Smith, I. D. Wilson, J. M. Castro-Perez, J. K. Nicholson, *Rapid Commun.*, 2006, **20**, 1989-1994
52. *Waters Website: MS^E Technology*,
<http://www.waters.com/waters/promotionDetail.htm?id=10205700>, Accessed 07/08/2015
53. D. Pezo, M. Fedeli, O. Bosetti, C. Nerin, *Anal. Chim. Acta.*, 2012, **756**, 49-59
54. C. G. Herbert, R. A. W. Johnstone, *Mass Spectrometry Basics*, CRC Press, Boca Raton, 2003
55. *Waters website: MarkerLynx*,
http://www.waters.com/waters/en_GB/MarkerLynx-/nav.htm?cid=513801, Accessed 07/08/2015
56. S. Cubbon, Waters, Manchester, *Personal Communication*, September 2012
57. W. Zhou, S. Su, J. Duan, J. Guo, D. Qian, E. Shang, J. Zhang, *Molecules*, 2010, **15**, 6217-6230
58. R. S. Plumb, J. H. Granger, C. L. Stumpf, K. A. Johnson, B. W. Smith, S. Gaulitz, I. D. Wilson, J. Castro-Perez, *Analyst*, 2005, **130**, 844-849
59. J. N. Miller, J. C. Miller, *Statistics and Chemometrics for Analytical Chemistry*, 6th Edition, Pearson Education Limited, Harlow, 2010

60. M. J. Adams, *Chemometrics in Analytical Spectroscopy*, 2nd Edition, The Royal Society of Chemistry, Cambridge, 2004
61. R. G. Brereton, *Chemometrics for Pattern Recognition*, John Wiley & Sons, Chichester, 2009
62. A. Nordon, *Multivariate Analysis*, in Radioanalytical Chemistry and Multivariate Analysis Module, University of Strathclyde, 2012
63. L. Eriksson, E. Johansson, N. Kettaneh-Wold, J. Trygg, C. Wikström, S. Wold, *Multi- and Megavariate Data Analysis: Part 1 Basic Principles and Applications*, 2nd Edition, Umetrics, Umeå, 2006
64. R. G. Brereton, *Chemometrics: Data Analysis for the Laboratory and Chemical Plant*, John Wiley & Sons, Chichester, 2003
65. B. M. Wise, N. B. Gallagher, R. Bro, J. M. Shaver, W. Windig, R. S. Koch, *Chemometrics Tutorial for PLS_Toolbox and Solo*, Eigenvector Research, Inc., Wenatchee, 2006
66. R. G. Brereton, *Applied Chemometrics for Scientists*, John Wiley & Sons Ltd., Chichester, 2007
67. A. K. Jain, M. N. Murty, P. J. Flynn, *ACM Comput. Surv.*, 1999, **31**, 264-323
68. P. S. Gromski, Y. Xu, H. L. Kotze, E. Correa, D. I. Ellis, E. G. Armatige, M. L. Turner, R. Goodacre, *Metabolites*, 2014, **4**, 433-452
69. G. Dougherty, *Pattern Recognition and Classification: An Introduction*, Springer, New York, 2013
70. P. S. Gromski, H. Muhamadali, D. I. Ellis, Y. Xu, E. Correa, M. L. Turner, R. Goodacre, *Anal. Chim. Acta.*, 2015, **879**, 10-23
71. P. S. Gromski, Y. Xu, E. Correa, D. I. Ellis, M. L. Turner, R. Goodacre, *Anal. Chim. Acta.*, 2014, **829**, 1-8
72. P. S. Gromski, Y. Xu, K. A. Hollywood, M. L. Turner, R. Goodacre, *Metabolomics*, 2015, **11**, 684-695
73. S. Serranti, D. Cesare, F. Marini, G. Bonifazi, *Talanta*, 2013, **103**, 276-284
74. P. S. Gromski, E. Correa, A. A. Vaughan, D. C. Wedge, M. L. Turner, R. Goodacre, *Anal. Bioanal. Chem.*, 2014, **406**, 7581-7590
75. H. Martens, M. Høy, B. M. Wise, R. Bro, P. B. Brockhoff, *J. Chemometr.*, 2003, **17**, 153-165

3.0 ATR-MIR SPECTROMETRY FOR PROFILING CARAMEL COLOUR IN SCOTCH WHISKY

3.1 Introduction

3.1.1 Basis of this Study

As discussed previously, there are four classes of caramel recognised by the European Union for use in foodstuffs (E150a, E150b, E150c and E150d) and the research presented in this study has attempted to profile these materials. Particular emphasis has been given to the study of E150a caramels as these are the only class legally permitted for use in Scotch Whisky.¹ Understanding the profiles provided by these caramel colourants and their behaviour in Scotch Whisky would therefore be extremely useful to the industry in terms of product authenticity.

A wide variety of E150a products are available on the market as the manufacturing process can incorporate a number of variable parameters, such as: the starting carbohydrate substrate implemented; the reactants added to aid with caramelisation; the concentration of added reactants; and the temperature and pressure profiles of the reaction vessel.^{2,3} Changing any of these conditions has the potential to affect the final product composition and so the main purpose of this work was to determine whether any spectral differences could be identified between E150a caramels prepared in different ways. The ability to do this could indicate whether there is the potential to manipulate E150a manufacture in the future and create distinct signature profiles. These could then be spiked into different whisky products to act as inherent markers for the positive identification of authentic samples. The ability to distinguish the profiles of E150a caramels from other sources of colour that would be prohibited in Scotch Whisky (e.g. alternative caramel classes or any other sources that provides the characteristic yellow/brown colour of a Scotch) would also be important for achieving this aim - it would potentially allow suspect samples to be screened based on their colour profile. To enable these concepts to be implemented, it would also be crucial to assess the affect of the Scotch Whisky matrix on the ability to identify the presence of particular caramels. This was additionally considered when completing the research presented in this chapter.

This chapter investigates the use of mid infrared spectrometry (MIR) combined with an attenuated total reflection (ATR) probe for the analysis of caramel colourants. The literature review that follows explores how caramels have been characterised in the past and consequently summarises why ATR-MIR has been chosen for use in this research.

3.1.2 Profiling Caramel Colourants in Foodstuffs – A Literature Review

Caramel colourants are extremely difficult to characterise, which is directly related to the complexity of their chemical composition. As previously discussed in Chapter 1, the process of caramelisation involves a complex series of reactions and results in a dense mixture of low molecular weight (LMW) compounds and high molecular weight (HMW) polymers in the form of colloidal aggregates.² The majority of studies in the literature have therefore attempted to simplify caramel characterisation by the analysis of separate fractions rather than the caramel colourant as a whole.⁴⁻¹³

There are a few studies in the literature that have attempted to characterise the HMW fractions of caramels and these have used techniques such as gel permeation chromatography, ultrafiltration and size-exclusion high performance liquid chromatography.^{4-8,11-12} Although some knowledge has been acquired about the overall characteristics of these HMW fractions for different caramel materials, little information has actually been acquired about their chemical composition. Considerable issues were also identified when using these tools to assess the presence of caramels in food products.^{4,5} The application of high performance liquid chromatography (HPLC) and gas chromatography (GC) for the analysis of LMW compounds has therefore proven much more popular, although the case remains that relatively few compounds have actually been structurally identified. Most analytical studies relating to the analysis of caramel colourants have consequently centred on the acquisition of characteristic or ‘fingerprint’ profiles. This was an approach taken by A. Patey *et al.*, who used a chloroform/ethanol mixture to extract LMW components from a selection of E150a, E150b and E150c classed caramels.⁹ Analysis of the silylated extracts using GC revealed distinct traces for caramels of different class and also allowed the manufacturer of UK produced E150c caramels to

be identified. Consistency of marker components specific to all caramels in a class could not however be determined; neither could individual caramel types within a class.

Subsequent studies by Litch *et al.* have progressed caramel characterisation further, HPLC being particularly useful for the identification of LMW components.^{11,12} Multiple samples from each of the four caramel classes were analysed in this work and similar chromatographic profiles were obtained for all caramels within a particular class, regardless of differences in the conditions of manufacture. This indicated compositional uniformity within each class. Clearly distinct profiles were also identified for caramels belonging to separate classes, highlighting the potential of HPLC for caramel differentiation. Further work by Litch *et al.* took these results, along with additional information relating to the physical and compositional properties of caramels, to develop specifications that would clearly define the four classes of caramel colour.¹⁴ They presented a series of simple and practical tests that when combined, could ensure both the class of caramel and conformity of that caramel to the outlined specifications.

Despite these advances in caramel characterisation, transferring such methods to allow the detection of caramel materials in foods and beverages has proven very complex.¹⁵ When incorporated into food matrices it becomes much more difficult to identify components that are characteristic of a particular caramel, which is largely due to difficulties in distinguishing between components present as a result of caramel addition and those that have been formed naturally during the manufacture and cooking of foodstuffs. Rather than attempting to identify specific caramel components, the literature demonstrates that the presence of caramel in foods and beverages has taken on a more empirical approach.¹⁶⁻¹⁹ In other words, most studies have relied on the detection of unknown marker components that have been identified as unique to the caramel and can be measured without interference from the features of food and beverage matrices. Coffey and Castle for instance, report the use of ion-pair HPLC for the detection of a distinct peak in the chromatographic trace of E150c caramels that was absent from the profiles of E150a and E150d classes.¹⁶ This methodology was then successfully applied for the detection of E150c

caramel in a variety of food products, with no significant interference being found at the retention time for the marker peak.¹⁸ L. Ciolino also demonstrated the use of HPLC to identify caramel components in foodstuffs, confirming the adulteration of acerola juice with a specific E150d formulation.¹⁹ This analysis was based on the detection of four distinct peaks in the chromatographic trace, matched with a reference caramel already identified as the adulterant. Although this demonstrates the potential of HPLC for caramel analysis, the particular methodology would be difficult to apply to caramels of unknown origin.

Although the literature surrounding caramel characterisation has been found to centre largely on HPLC, research into the application of capillary electrophoresis (CE) has also been investigated.^{13,16-17} CE separates sample analytes based on differences in ionic mobility and so is suited to the analysis of caramels, which are generally charged as a result of the reactants used during manufacture. L. Royle *et al.* undertook a study using CE for the assessment of E150d caramels and developed a method that could clearly separate five different caramels within this class – the migration time of peaks was found to be related to the sulphur content of each material.¹⁷ They were then able to implement this methodology for the identification and quantification of E150d caramels in a range of soft drinks.^{17,20} Further work by the same group has also assessed the possibility to distinguish between caramel classes E150a, E150c and E150d using CE and characteristic profiles have been obtained.¹³ This latter study however has not assessed the affect of food matrices on peak detection and so this would need to be considered if the methodology were to be applied for the identification of these caramels in foodstuffs.

Whilst the preceding studies demonstrate the success of unknown marker components to confirm the presence of caramel materials in foodstuffs, some headway has been made in the identification of specific marker compounds. For instance, a number of studies over the last two decades have indicated that a family of compounds known as difructose dianhydrides (DFAs) form during the process of caramelisation and so could be indicative of the presence of caramel colourants in foodstuffs.²¹⁻²⁶ A study by A. Montilla *et al.* has made use of this information and demonstrated that honey samples adulterated by the addition of caramel could be

successfully identified by GC-MS analysis to confirm the presence of DFAs.²⁷ The main limitation of this approach to confirm the presence of caramels in foodstuffs would arise if the food (or beverage) product itself involved a caramelisation process during manufacture. In this case, DFAs would already be present even without the addition of caramel – A. Montilla *et al.* for instance were able to identify the process used for roasting coffee beans by assessing DFA profiles.²⁷ Analysing for the presence of DFAs might therefore be restricted for the assessment of caramel colourants in Scotch whiskies as natural colour in the product results from a caramelisation process (see Chapter 1). Monitoring DFA levels might therefore be a more appropriate alternative to confirm the presence of caramels in Scotch whiskies, however it is currently unclear from a search of the literature whether profiles acquired of DFAs would allow caramels from different classes and of varying formulation to be distinguished.

The majority of literature highlighted so far in this review has indicated that the characterisation of caramel colourants has been most successful using chromatographic based techniques and also with capillary electrophoresis. These analytical tools could be investigated for the analysis of caramels in Scotch Whisky however they generally require quite sophisticated equipment and often employ quite complex and time consuming methods. These techniques would therefore be impractical for use on a routine basis, however there is currently a drive in the Scotch Whisky industry for tools that can provide quick and simple screening of samples.²⁸⁻³⁵ The potential for miniaturisation is also a desirable characteristic to the industry, as such tools could allow screening of suspect samples in the field to allow an initial assessment of authenticity before more comprehensive investigations can be undertaken in the laboratory.^{28-32,36-37} After reviewing the literature it appears as though techniques based on optical spectroscopy are being commonly assessed with this purpose in mind.²⁹⁻³² A publication by W. Mckenzie *et al.* for example demonstrates the use of a hand held UV-Visible spectrophotometer for the analysis of Scotch whiskies, allowing brand authenticity to be confirmed in the field based on the absorbance spectra of samples.²⁹ Suspect samples were assigned based on their absorbance spectra falling out with limits predetermined for the genuine brand.

Analysis time was reported to take less than one minute per sample and only those that failed were passed on for confirmatory analysis in the laboratory. GC would typically be used for this purpose and in this case the analysis of a single sample could take at least 20 minutes. Using the portable UV-Visible spectrophotometer as a screening tool therefore offers advantages in terms of mobility and speed, as well as lowering analysis costs.

Only one example could be found in the literature where UV-Visible spectrophotometry has been used as a tool to specifically assess caramel colourants and it was implemented to identify both the presence and quantity of caramel in spirits aged in oak casks.³⁸ The work made use of the ratio between absorbance values at two wavelengths (210 and 282 nm) to achieve this finding however there was no indication as to whether it would be possible to distinguish between different caramel materials using this methodology.

Further assessment of the literature indicated that MIR spectrometry might be better suited for the analysis of caramel colourants in Scotch Whisky. In addition to the tool providing more comprehensive spectral features, A. McIntyre *et al.* have demonstrated its potential for profiling caramels in whisky products.³² Using MIR spectrometry combined with an ATR probe, this group were able to characterise 17 samples as either authentic or counterfeit based on a combination of 2 methods: the determination of ethanol concentration; and an assessment of the colourant added. The latter was achieved by analysing the dried residues of whisky samples and comparing the resulting profiles to those obtained from the dried residues of caramels dissolved in 40% ethanol. Distinction between one type of caramel from each of the four classes recognised by the European Union was clearly achieved in this study. The research presented in this chapter builds upon the methodology developed by A. McIntyre *et al.* for profiling caramels by dried sample residue analysis and has particular emphasis on the assessment of E150a products.

A few other examples have been found in the literature where colour profiles of liquid samples have been assessed by the analysis of dried residues using MIR.^{39,40} Picque *et al.* for instance used transmission MIR to successfully distinguish cognacs

from other distilled spirits by the analysis of dried sample extracts – these extracts being described as containing carbohydrates, caramel and extractable material from oak wood.³⁹ Another example published by N. Naik *et al.* shows how it was possible to use MIR analysis of spentwash residues to monitor melanoidin and caramel degradation.⁴⁰

3.1.3 Study Objectives

This chapter has investigated the use of ATR-MIR spectrometry for the analysis of caramel colourants and highlights the potential benefits for Scotch Whisky authentication. The main objectives of the work were:

- To determine whether ATR-MIR can differentiate between E150a caramels prepared using different conditions of manufacture.
- To identify whether differentiation is also achieved between E150a colourants and the three remaining caramel classes recognised by the European Union.
- To determine whether burnt sugar profiles can be distinguished from those acquired of E150a caramels.
- To examine the influence of natural colour on ATR-MIR spectra when caramels are dissolved in the more complex matrix of a Scotch Whisky; would features characteristic of the added colourant still be observed and/or dominate dried residue profiles?
- To find out whether the background matrix of different blends would influence ATR-MIR spectra to different extents.
- To explore how ATR-MIR spectra might be affected by scenarios that influence actual Scotch Whisky products such as variation in caramel concentration and colour fading over time.

After the exploration of these initial aims and based on the information gathered, an additional investigation was undertaken to assess the ability of ATR-MIR to

differentiate between the dried residue profiles of Scotch Whisky blends already on the market.

3.2 Experimental

3.2.1 Samples and Materials

3.2.1.1 Caramels and colourant materials

Fifteen E150a caramels were provided for this study by the Scotch Whisky Research Institute (Riccarton, Edinburgh, UK), including eight different formulations covering three manufacturers. Multiple batches of some of these caramels were analysed to compare batch to batch variability with variation between E150a caramels prepared using different conditions of manufacture. At least one type of each of the other caramels recognised by the European Union (E150b, E150c and E150d) were also analysed in this work to allow a comparison of E150a profiles with those acquired from caramels not legally permitted for use in Scotch Whisky. Three burnt sugar (BS) materials were also included in this sample set, such products being produced in the same way as caramel colourants but without the aid of reactants to promote caramelisation. All samples have been summarised in Table 3.1 and have been denoted with a code for future referral.

Table 3.1: Summary of the main colourant samples analysed within this study.

<u>Colourant Class</u>	<u>Manufacturer</u>	<u>Formulation</u>	<u>Number of Batches</u>	<u>Starting substrate</u>	<u>Reference Code</u>
E150a	X	1	3	Maize	E150A_X1
		2	3	Maize	E150A_X2
	Y	3	2	Wheat	E150A_Y3
		4	2	Maize	E150A_Y4
		5	2	Sucrose	E150A_Y5
	Z	6	1	Maize	E150A_Z6
		7	1	Wheat and Maize	E150A_Z7
		8	1	Wheat and Maize	E150A_Z8
E150b	X	9	1	-	E150B_X9
E150c	X	10	2	-	E150C_X10
E150d	X	11	2	-	E150D_X11
BS	X	12	1	-	BS_X12
	Z	13	1	-	BS_Z13
		14	1	-	BS_Z14

All colourant samples were either dissolved in 40% ethanol or a Scotch Whisky blend prior to analysis using ATR-MIR. Absolute ethanol was acquired from Sigma Aldrich and prepared to the required concentration by diluting with distilled water, whilst the whisky blends were provided by the SWRI. Two blends were acquired for this research, each of which was devoid of any previous caramel addition. The first blend (**Blend Whisky A**) represented a typical blend whisky that would be found on the market, whilst the second blend (**Blend Whisky B**) represented a much higher level of colour that would be developed naturally for a Scotch Whisky product.

3.2.1.2 Blends for discrimination study

Four whisky blends that are available on the market were analysed in this study to assess whether any differences could be observed in the colourant profiles of different blends (all known to contain caramel). Twenty samples were analysed in total, including five batches of each whisky. All blends were supplied by the Scotch Whisky Research Institute (Riccarton, Edinburgh, UK).

3.2.2 Mid-infrared Spectrometry

MIR spectra were acquired using an ABB MB3000 FTIR spectrometer (Clairet Scientific, Northampton, UK) coupled with polycrystalline silver halide optical fibres to a 25 cm long, 12 mm diameter hastelloy bodied ATR probe containing a diamond cone (Fibre Photonics Ltd., Livingston, UK). The total fibre-probe length was approximately 1.8 m. All measurements were obtained using 51 scans per spectrum with a resolution of 16 cm^{-1} in the $400 - 4000\text{ cm}^{-1}$ region. Spectra were acquired using GRAMS AI software version 7.00 and exported as SPC files into MATLAB for further interpretation. An air background was always obtained prior to any analysis.

3.2.3 UV-Visible Spectrometry

UV-Visible spectra were obtained using a Model 440 UV-Visible Spectrometer (S.I. Photonics, Tucson, Arizona) fitted with a tungsten lamp. Samples were analysed using a Dip-Probe of 1 cm pathlength (S.I. Photonics, Tucson, Arizona) and absorbance data were collected from 390 to 700 nm with a 1.1 nm spectral

bandwidth. Triplicate measurements were taken for all samples (removing the probe head between each acquisition) and the average absorbance used for any subsequent work. Spectra were referenced against 40% ethanol in water (prepared by volume).

3.2.4 Methods of Analysis

3.2.4.1 Samples spiked in 40% ethanol

All caramel and burnt sugar samples described within Table 3.1 were analysed in this part of the study and solutions of these materials were prepared at approximately 2.2 g per 100 mL in 40% ethanol (by volume). For MIR analysis, the ATR probe was set up in an inverted position and an air background obtained. A 10 μL aliquot of sample solution was then injected onto the probe tip so as to completely cover the diamond crystal. The sample deposition was next dried with the use of a heat lamp for about 5.5 min to leave a thin film over the crystal for analysis. The maximum temperature at the probe tip was kept between 60 – 70°C and checks were performed to ensure that samples were not being degraded by the heat (discussed in more detail in section 3.3.1.1). Spectra were then acquired of the dried residues once the probe had been allowed to cool back to ambient temperature. This was repeated in triplicate for each sample and six repeat spectra were acquired and averaged for each deposition. When six replicate spectra were compared from a single deposition of a typical E150a caramel, the average %RSD based on the absorbance of the five most prominent peaks (in the range 1000 – 1800 cm^{-1}) was 0.33%. When the first derivative spectra (normalised to the largest peak) from three separate depositions of the same caramel were measured, the average %RSD acquired from the six most intense peaks was found to be 4.11%.

3.2.4.2 Samples spiked in blended Scotch Whisky

Only a selection of the samples described within Table 3.1 were utilised in this part of the study and those that were assessed are described where relevant in the results and discussion section (section 3.3). All samples analysed were added to either Blend Whisky A or Blend Whisky B (the particular whisky used being described where relevant in the results and discussion section) until the final colour level became similar to that of a typical blend available on the market. To allow consistent colour

levels to be achieved, all sample solutions were monitored using UV-Visible spectrometry to ensure that the absorbance at 430 nm was close to 0.55 (the level predetermined for a typical blend). The mass of caramel required to reach this level was much lower (~0.08 g per 100 mL) than that added to 40% ethanol and so all sample solutions required preconcentration prior to analysis by MIR to allow spectra of adequate absorbance to be acquired. This was done with the use of a hairdryer, reducing 6 mL of sample down to dryness before reconstituting the resulting residue in 300 μ L of distilled water. The concentrated sample solutions were then analysed using ATR-MIR as described for the samples dissolved in 40% ethanol. In this case, when the first derivative spectra (normalised to the largest peak) from three separate depositions of a typical sample solution were compared, the average %RSD acquired from the six most intense peaks was found to be 2.52%. As this methodology also incorporated an additional sample preparation step, the spectra acquired from preparing and analysing one sample three times were also compared. The %RSD in this case was calculated as 2.04%.

3.2.4.3 Caramel concentration study

Control samples

Four glass vials were each filled with approximately 15 mL of 40% ethanol and an E150A_X1 type caramel was added to each vial to obtain four different solutions with the following absorbance levels at 430 nm: 0.2, 0.4, 0.6 and 0.8. All absorbance levels were monitored using UV-Visible spectrometry and the above absorbance range was chosen as it represented the range of colour associated with blends on the market. To acquire spectra of adequate absorbance, all sample solutions required concentrating prior to analysis by ATR-MIR. This was achieved as described in section 3.2.4.2; solutions were reduced from 6 mL to 300 μ L with the use of a hairdryer. The resulting sample solutions were then analysed by ATR-MIR using the methodology as described in section 3.2.4.1.

Study samples

Eight caramel solutions were prepared in this part of the study (all using the same E150A_X1 type caramel as the above control samples); four dissolved caramel in

40% ethanol, whilst the remaining four had caramel dissolved in Blend Whisky A. For each different solution medium, the four solutions were prepared to possess absorbance levels of 0.2, 0.4, 0.6 and 0.8 at 430 nm. Blend Whisky A alone had an absorbance of approximately 0.07 at 430 nm and all absorbance levels were again monitored using UV-Visible spectrometry. Prior to analysis by ATR-MIR, each sample solution required pre-concentrating and this was achieved by reducing 6 mL of solution down to dryness before reconstituting the resulting residues in specific volumes (109, 218, 327 and 436 μL respectively) depending on their original absorbance. The purpose of this adapted concentration step was to ensure that all solutions were prepared to equivalent absorbance levels prior to ATR-MIR analysis – results from the control samples had indicated that the ATR-MIR methodology did not provide consistent profiles when solution concentrations varied (described in more detail in section 3.3.2.1). The procedure used to determine appropriate volumes is described in Appendix 8.1.

3.2.4.4 Caramel fade study

In this part of the study one E150A_X1, a single E150A_X2 and one E150D_X11 caramel were examined. Stock caramel solutions were prepared for each caramel type by the addition of caramel to 40% ethanol (about 90 mL) until an absorbance of approximately 0.80 at 430 nm was reached (monitored using UV-Visible spectrometry). This absorbance level was chosen as it represented the higher end of colour that would be associated with blends on the market. Once prepared, the stock solutions were then split, using 10 mL aliquots, into eight separate clear glass vials all of equal dimensions. Five of these vials were then placed in a UV light box and one removed after each of the following time points: 1 day, 2 days, 3 days, 4 days, and 7 days. The absorbance of each sample at 430 nm was measured again after its removal from the light box and subsequently recorded. Each sample was then concentrated prior to ATR-MIR analysis so that spectra of adequate intensity could be acquired. Sample volumes were reduced using a hairdryer as described in section 3.2.4.2 but in this case the volume to which each residue was reconstituted was adjusted so that the final absorbance of all samples was equivalent (see Appendix 8.1 for example calculation). Once concentrated to the required level, each sample was

analysed using ATR-MIR as described for caramels dissolved in 40% ethanol (section 3.2.4.1).

The three remaining sample vials for each caramel type, each containing 10 mL of stock solution, were used as controls. Control Sample 1 was analysed by ATR-MIR on the same day that other samples were placed in the UV light box (Day Zero). Control Sample 2 was kept under ambient conditions in the lab and its absorbance at 430 nm monitored from day zero to day seven, prior to analysis using ATR-MIR spectrometry on day seven. Control Sample 3 was fully wrapped in aluminium foil and stored in the UV light box for the 7 day duration of the experiment. This latter control sample was then analysed by ATR-MIR after its removal from the UV light box. Prior to the analysis of these controls using ATR-MIR, each sample was concentrated to the required level as described for the other five samples included in this study.

3.2.4.5 Blend discrimination study

This study was undertaken using the whisky samples described in section 3.2.1.2. The absorbance of each sample at 430 nm was initially assessed using UV-Visible spectrometry. Samples were then concentrated prior to further analysis so that ATR-MIR spectra of adequate absorbance could be acquired. A hairdryer was used for this purpose and the reduction in volume for each sample was undertaken according to the procedure described in Appendix 8.1. Once concentrated to the required level, the blend samples were analysed using ATR-MIR spectrometry as described for the samples dissolved in 40% ethanol (section 3.2.4.1).

3.2.5 Data Analysis

All ATR-MIR data were imported for analysis into MATLAB version 7.13.0.564 (R2011b) (Mathworks Inc., Natick, MA, USA) with PLS_Toolbox version 6.7 (Eigenvector Research Inc., WA, USA) incorporated. Before the application of multivariate data analysis, all data were processed using a Savitsky-Golay first derivative filter, which employed a width of 7 data points and a second order polynomial. PCA was then carried out using 155 variables in the 625 – 1813 cm^{-1}

range of the derivatised spectra, hence removing regions that only contributed noise to the measurements. Multiple PCA models were constructed during this study and the samples included in each model are stated where appropriate in section 3.3. All data were normalised to the largest peak (consistently found between 950 and 1050 cm^{-1}) and mean centred before PCA was performed.

3.3 Results and Discussion

3.3.1 ATR-MIR for Profiling Caramel Colourants

3.3.1.1 Assessment of the ATR-MIR method

Rational behind methods

In this research, caramel colourants were profiled after being dissolved in one of two media: in 40% ethanol, to allow an initial assessment of profiles in a form similar to that of a Scotch Whisky but without any interference from natural whisky colour or; in a Scotch Whisky blend devoid of previous caramel addition, to subsequently investigate whether caramel profiles could still be identified when inherent whisky components might interfere. Sample preparation was slightly different for these two media and this was due to differences in the masses of caramel being added to each solution medium. When in 40% ethanol, caramel was dissolved at a concentration much higher than would typically be found in a Scotch Whisky product (2.2 g vs. ~0.08 g per 100 mL). This was so that spectra of adequate absorbance could be acquired without the need for any sample pre-treatment. When caramels were dissolved in blend whisky however, they were added to a colour level that matched that of a typical product and as a result, all solutions required preconcentration prior to analysis with the ATR-MIR method.

Although sample preparation of caramel solutions in the two media used different approaches, the actual methodology for ATR-MIR analysis was exactly the same; spectra were obtained from dried residues acquired by drying 10 uL of a sample directly onto the ATR crystal with the use of a heat lamp. This procedure was used as it allowed features relating to the underlying colour constituents to be observed; something that was not possible using a conventional approach. When implementing MIR spectrometry with an ATR probe, the analysis of liquid samples such as those considered in this research would traditionally be undertaken by immersion of the probe head directly into each sample. When this approach was implemented for the analysis of caramel solutions (in 40% ethanol or in a blend whisky) however, spectra were completely dominated by the features of ethanol and water. This is demonstrated *via* Figure 3.1a which shows the liquid spectrum of an E150A_X1

caramel dissolved in 40% ethanol. The spectral features were accounted for as follows: the broad band around 1640 cm^{-1} was caused by the H-O-H bending mode of water; the features between 1200 and 1500 cm^{-1} have been attributed to the H-C-H bending of ethanol; the peaks at 1085 and 1045 cm^{-1} were caused by the C-O stretch and C-C-O bending modes of ethanol; and the band found at $\sim 875\text{ cm}^{-1}$ has arisen from the C-C ethanol stretch.^{41,42} Identical features were observed for all other caramel solutions (whether dissolved in 40% ethanol or a whisky blend) analysed by immersion of the probe head directly into each liquid.

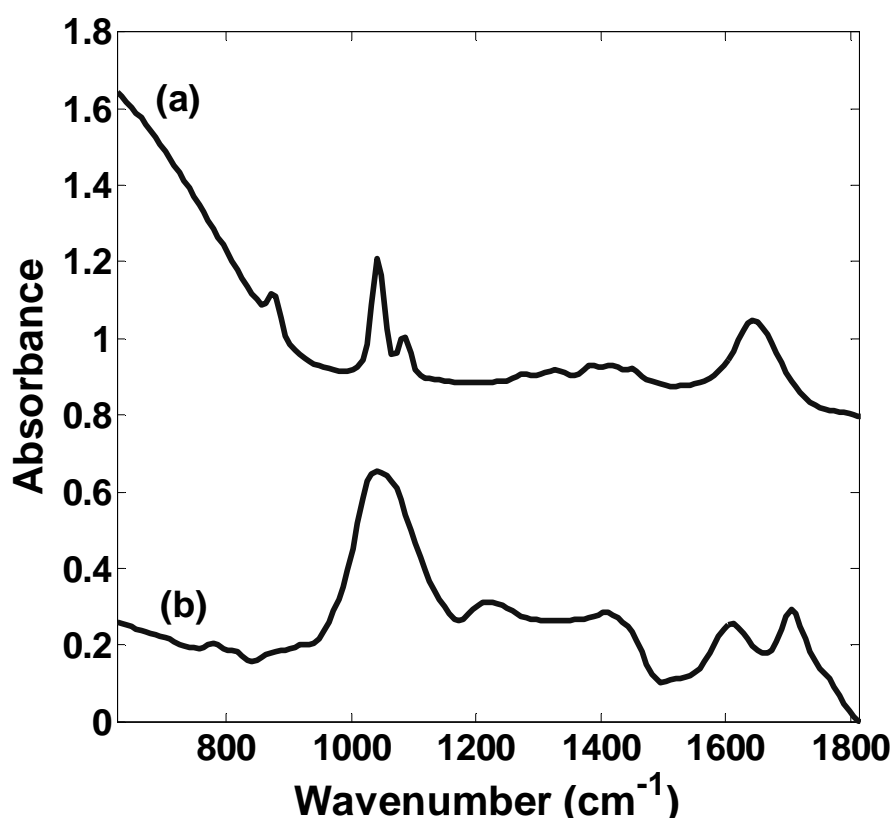


Figure 3.1: (a) The ATR-MIR spectrum of an E150A_X1 caramel dissolved in 40% ethanol, acquired by immersing the probe head directly into the sample solution and (b) the ATR-MIR spectrum of the same caramel sample, acquired by drying the solution directly onto the ATR crystal. The absorbance of spectrum (a) has been offset (by 0.8) with respect to spectrum (b).

As it was not possible to observe features relating to colour components by conventional ATR-MIR analysis, a methodology was developed that involved inverting the fibre optic probe head so that sample solutions could be dried directly onto the ATR crystal. This allowed ethanol, water and any other volatile congeners (the latter being present when caramels were dissolved in Scotch Whisky) to be

evaporated, leaving behind a residue that was found to be dominated by colour components. The dried residue profile of an E150A_X1 caramel dissolved in 40% ethanol has been provided in Figure 3.1b to allow a comparison of the features obtained with those acquired from the equivalent sample analysed in the traditional manner (Figure 3.1a). As caramel colourants encompass a complex mixture of both LMW compounds and HMW polymers it was difficult at this point to assign the resulting spectral features to specific components or functional groups. It is likely that the spectral contributions have resulted from a combination of the typical functional groups associated with a range of organic molecules.

Method repeatability

To gain a greater understanding of the ATR-MIR methodology applied in this research a number of experiments were undertaken to assess method repeatability and also to investigate whether any parameters of the method could be affecting the precision of spectral measurements.

Repeatability of the ATR-MIR methodology was assessed by comparing the spectra obtained from three replicate depositions of E150A_X1 caramel solutions. The average %RSD values, based on the absorbances acquired from the six most intense peaks in the first derivative spectra (normalised to the largest peak), were found to be 4.11% and 2.52% respectively when this caramel was dissolved in 40% ethanol and then in Blend Whisky A. Although this assessment of repeatability only accounted for one type of caramel colourant, it provided a good indication that the acquisition of repeat measurements resulted in consistent spectra. Measurements of all other sample solutions however were analysed in triplicate, to verify that this level of repeatability was maintained throughout.

When caramels were dissolved in a blend whisky, samples required concentrating prior to ATR-MIR analysis; an extra step that was not needed when caramels were incorporated in 40% ethanol. To assess the repeatability of measurements that required this additional sample preparation, three solutions of an E150_X1 caramel in Blend Whisky A were prepared and separately concentrated before each was analysed by the ATR-MIR method. In this case the %RSD (acquired in the same

manner as above but for the three replicate samples) was determined as being 2.04%. This value is comparable with those quoted previously and so indicates that the additional sample preparation step for caramels dissolved in a blend whisky did not compromise the repeatability of spectra.

The methodology used in this research has been developed from an approach originally implemented by McIntyre *et al.*, who used the analysis of dried residues by ATR-MIR to compare the colourant profile of a Scotch Whisky product with that provided by different caramel colourants.³² In their work, all solutions had a colour level similar to that of a typical blend whisky and so spectra of adequate absorbance were acquired by building up dried residues from 10 – 60 μL directly onto the ATR crystal (in 10 μL aliquots). This highlights the main difference between the two methods: McIntyre *et al.* concentrating samples for analysis by building up depositions directly on the ATR crystal, whilst the methodology presented in this research concentrated samples prior to injection, meaning that only a single deposition of sample solution onto the probe tip was required. When three separately built up residues of an E150a caramel were compared by McIntyre *et al.*, the %RSD value was cited as being 4.5%. The values reported in this work were therefore comparable if not slightly improved. The reason behind this improved repeatability could be explained by the reduction in the number of sample injections being deposited on the ATR crystal. Concentrating samples prior to deposition on the ATR-MIR crystal also greatly improved the timescale of analysis, reducing the full measurement of one sample to approximately 30 minutes from over 3 hours.

The %RSD values quoted above indicated that the ATR-MIR methodology employed in this research allowed the acquisition of reasonably consistent spectra. Despite this, a few additional investigations were undertaken to assess whether certain factors of the methodology were influencing spectral measurements. For example an investigation was undertaken to examine whether caramel materials might be affected by thermal degradation as a result of their exposure to a heat lamp for drying. To examine this, three additional spectra were acquired of the E150A_X1 caramel in 40% ethanol where the solution was left to dry naturally rather than with the use of a heat lamp. Figure 3.2 shows the triplicate normalised first derivative

spectra acquired for the two different drying scenarios (with and without the use of a heat lamp). From a visual comparison of the spectra provided in Figure 3.2 it was observed that the positioning of spectral features was consistent when the E150A_X1 solution was dried by the two different approaches. This indicated that thermal degradation had not affected the sample residue to an extent where its composition was significantly altered. The break down of caramel components into degradation products would have resulted in a reduction of corresponding peak absorbances and the formation of new peaks. Although there was little to no variation in spectral features, it did appear as though there were slight differences in the peak absorbances between 1550 and 1800 cm^{-1} , when a heat lamp had been implemented rather than natural drying. Although this might indicate a small change in composition, it was found that the repeatability of triplicate spectra was actually comparable for both drying procedures. The %RSD values based on the six peak maxima or minima indicated in Figure 3.2 were 4.11% for the use of a heat lamp and 2.97% for the case of natural drying. Although these findings indicated that the repeatability of spectra was slightly better when natural drying was employed, the use of a heat lamp was maintained as part of the methodology. The slight compromise in repeatability meant that each sample could be analysed in less than half the time (20-25 minutes rather than ~55 minutes).

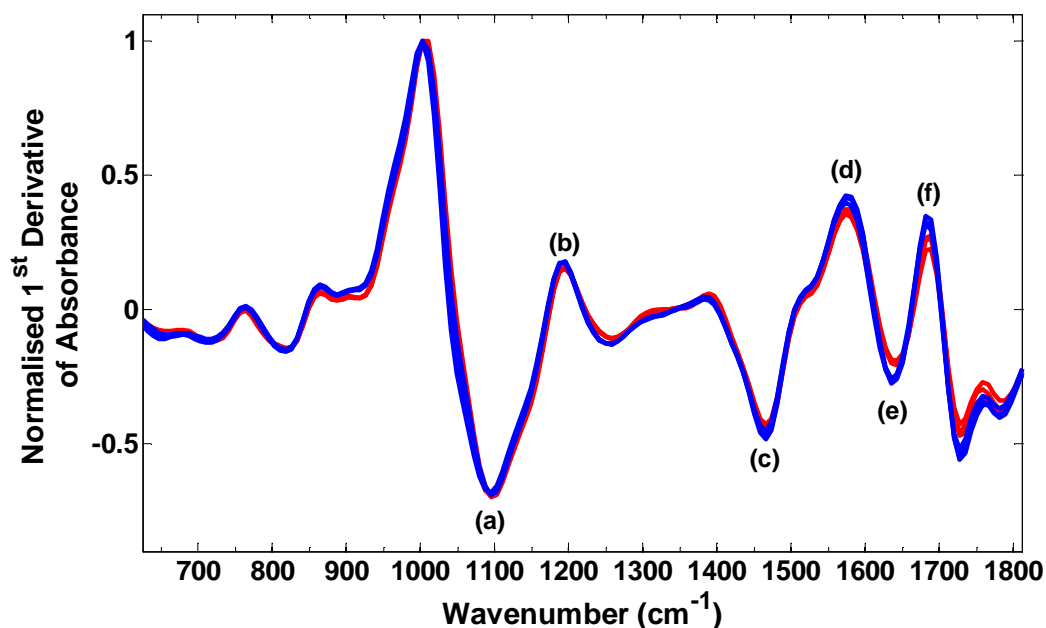


Figure 3.2: Overlay of the normalised first derivative spectra acquired from the dried residue of an E150A_X1 solution, firstly dried using a heat lamp (red) and then left to dry naturally (blue). The six peak maxima/minima used to assess spectral repeatability are labelled as (a)-(f).

As well as the heat lamp potentially causing thermal degradation, it was considered that the slight change in spectra and the small drop in repeatability could have been an affect of the heat lamp on the probe itself rather than on the residue components. As the background reference spectra for this method were always acquired in air prior to the use of the heat lamp, measurements taken after drying could have been affected by a consequent change to the probe. This was examined by running through the methodology without any sample being deposited on the probe head and spectra were acquired throughout the analysis. Figure 3.3 shows the spectra acquired at various time points through the method and it was clear that the spectral features deviated slightly from the original air spectrum as heat was applied to the probe head. Once the heat lamp was turned off and left to cool back to room temperature however, the features were then seen to revert back towards the original air spectrum. These findings indicated that the application of a heat lamp could potentially affect sample spectra and Figure 3.4 demonstrated that the spectra of the caramel residue from E150A_X1 (dissolved in 40% ethanol) were clearly different when acquired just after the heat lamp was switched off (temperature between 60-70°C) and after the probe head had cooled back to room temperature. All measurements of dried caramel solutions were therefore only acquired once the probe head had cooled back

to room temperature, to try and reduce any issues with repeatability that might be caused by the influence of the heat lamp on the probe.

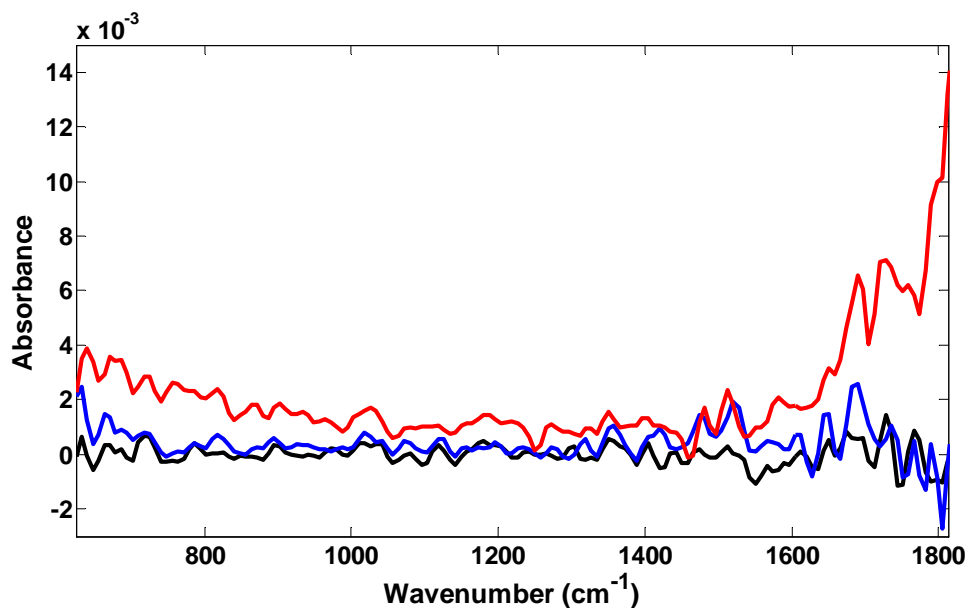


Figure 3.3: Overlay of the air spectra acquired at different time points when the ATR-MIR method was applied without any sample on the probe head. The black spectrum was acquired prior to the application of the heat lamp; the red spectrum was taken after the probe head had been exposed to the heat lamp for 5 minutes; and the blue spectrum was obtained once the probe head had cooled back to room temperature.

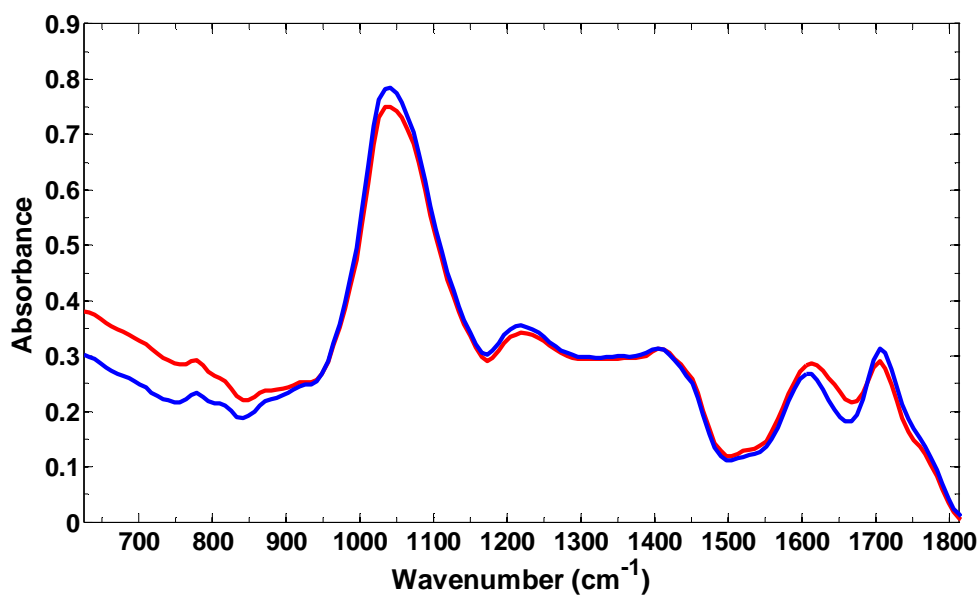


Figure 3.4: Overlay of two ATR-MIR spectra acquired from the dried residue of the E150A_X1 solution (in 40% ethanol). The blue spectrum was acquired just after the heat lamp was switched off, whilst the red spectrum was acquired when the probe had cooled back to room temperature.

Another aspect of the ATR-MIR methodology that could have been affecting measurement repeatability was related to the solution drying process, which would likely be influenced by the coffee ring effect. The coffee ring effect is the term describing the formation of a more concentrated deposit of suspended particles around the outer perimeter of a dried residue due to capillary flow induced by differential evaporation rates across the drop – in other words, liquid evaporating from the edges of the droplet is replenished by liquid from the interior of the droplet hence concentrating dispersed material to the outer edge of the dried residue.^{43,44} This process could potentially result in heterogeneity in the composition of the dried residue covering the ATR crystal and the heterogeneity would likely differ from one deposition to another, creating variation between the spectra of duplicate measurements. An interesting publication by L. Lovergne *et al.* discusses the coffee ring effect in relation to dried blood serum samples and has used spectral imaging to visualise the heterogeneity of their sample residues prior to analysis using FTIR.⁴⁵ Using this approach they were able to clearly demonstrate that certain components had a tendency to migrate towards the periphery of the sample residues (monitored by assessing characteristic wavelengths for protein bands). They also noted that the effect was more visible when serum samples were diluted before drying, a process that actually resulted in a better homogeneity over the residue surface. Neat samples on the other hand were shown to contain cracks across their surface and it was suggested that these could also contribute to spectral distortion. The group therefore suggested that improved reproducibility could be obtained by using more dilute samples and also smaller sample depositions. In addition they noted that when dried directly onto an ATR crystal (as has been done in this research when assessing caramel solutions) spectra were more representative of the whole serum sample as an averaged spectrum is acquired over the whole surface. It would be extremely interesting to use a similar approach within this research to investigate the influence of the coffee ring effect on dried caramel residues. Time and resources however were not available to assess this in greater detail and the reproducibility of replicate spectra was deemed suitable to move forward with preliminary studies.

In addition to the occurrence of the coffee ring effect, another factor that might have influenced the reproducibility of replicate sample measurements was that such thin films of sample are being dealt with. The dried residues could therefore be of a similar thickness to the penetration depth of the evanescent wave, meaning full measurements might not be obtained for each sample deposition. This was not a factor that could easily be controlled with the current instrumental set up and so again was not considered further at this point, as sample repeatability was adequate for the purpose of preliminary investigations.

3.3.1.2 Profiling caramels in 40% ethanol

Dried residues of 8 different E150a formulations (dissolved in 40% ethanol) were analysed to determine whether differences in spectral features could be identified as a result of differences in the manufacturing conditions of different sample types. The dried residues of at least one caramel from each of the other EU recognised classes (1 x E150b, 2 x E150cs and 2 x E150ds) were also analysed to determine whether the profiles of different classes could also be distinguished when multiple types of E150a were included in the dataset. In addition to these caramel samples, three burnt sugar materials were assessed so as to include an additional colourant material that is known to provide the golden brown colour associated with Scotch whiskies. The ATR-MIR absorbance spectra acquired from the dried residues of selected samples are provided in Figure 3.5, illustrating one E150a caramel from each manufacturer and a spectrum from each of the remaining colourant classes described in Table 3.1. Clear differences were visible between colourants of different class and although the three chosen E150a caramels possessed similar spectral features, variation was still observed between their relative peak ratios. It also appeared as though there were slight differences in the shape of the peak at approximately 1050 cm^{-1} in the E150a spectra.

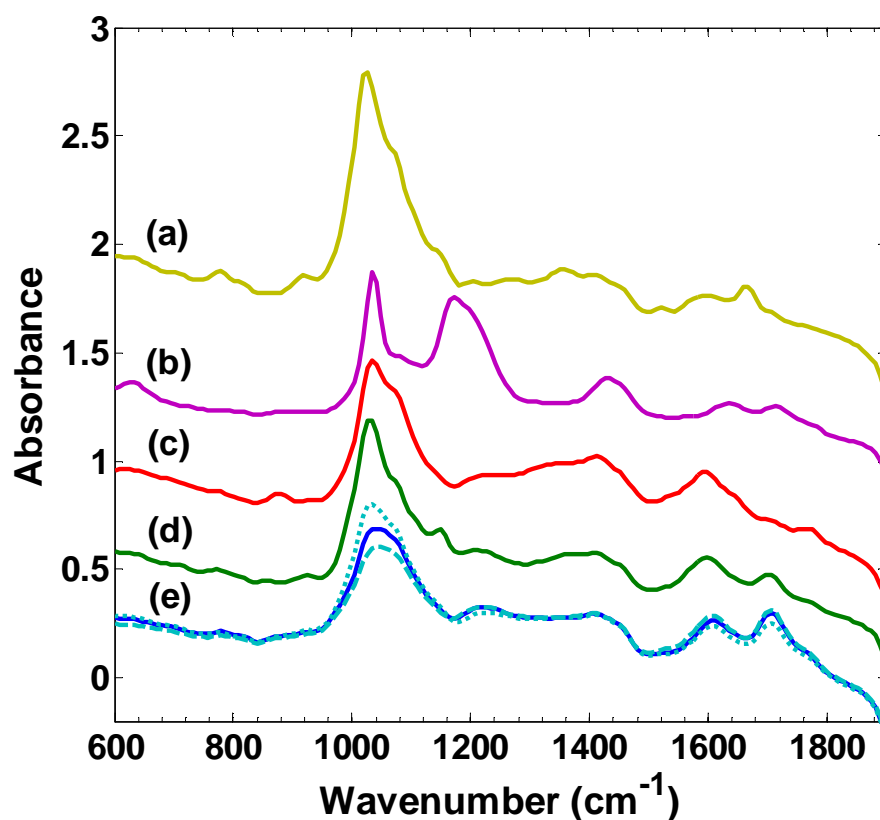


Figure 3.5: ATR-MIR absorbance spectra acquired from the dried residues of a batch each of (a) BS_X12, (b) E150D_X11, (c) E150C_X10, (d) E150B_X9 and (e) E150A_X1 (solid line), E150A_Z6 (dashed line), E150A_Y3 (dotted line). The spectra of all samples have been offset with respect to the three E150A profiles.

Once the dried residues of all 20 caramels and the 3 burnt sugar materials had been analysed using ATR-MIR, PCA was carried out on all of these samples to allow a comparison of their spectral profiles. The resulting PC1 vs. PC2 scores plot is provided in Figure 3.6 and clear separation is demonstrated between the four caramel classes, even though multiple types of E150a have been considered in the model. This is an advancement on the work completed by McIntyre *et al.*, who obtained this same distinction but when only a single type of each caramel class was considered.³² Figure 3.6 also showed that burnt sugar materials can be clearly distinguished from all types of caramel in the dataset, the between type variability of the burnt sugars being visibly much smaller than the spectral differences between burnt sugars and caramel colourants.

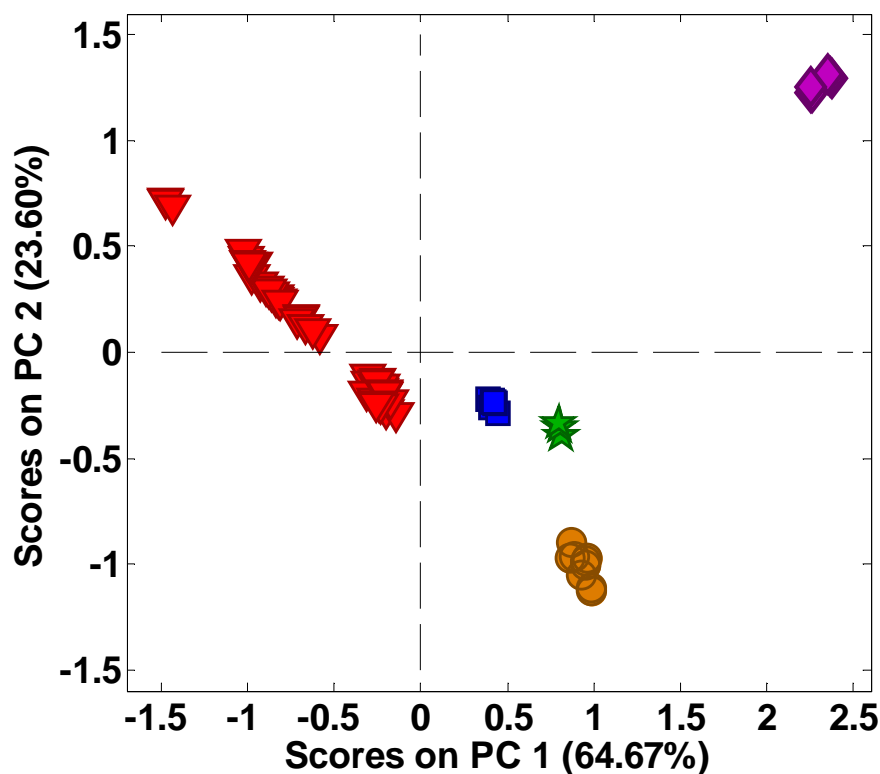


Figure 3.6: PC1 vs. PC2 scores plot obtained from PCA of the ATR-MIR spectra acquired from all fifteen E150A caramels (red triangles), one batch of E150B_X9 (green stars), two batches of E150C_10 (blue squares), two batches of E150D_11 (purple diamonds) and the three burnt sugar materials (orange circles). Each sample had been dissolved in 40% ethanol and was analysed in triplicate.

The spectral regions responsible for the above observations were investigated by looking at the loadings data corresponding to PCs 1 and 2. These loadings plots are provided in Figure 3.7 alongside the normalised first derivative spectra of all samples incorporated in this PCA model. Differentiation between the four caramel classes was clearly observed along PC1 and the corresponding loadings plot indicated that spectral variation was present throughout the region covering 1000 to 1800 cm^{-1} . Within this range, the spectral region between about 1050 and 1200 cm^{-1} was seen to have the largest influence on separation along PC1, an observation that was supported by a visual comparison of the spectra in Figure 3.7a. There is a feature in the PC1 loadings just above 1050 cm^{-1} that indicated PC1 was anti-correlated with this wavenumber and in the normalised first derivative spectra the absorbance at this point were seen to clearly decrease as the PC1 score increased (which occurs in the order of E150a→E150c→E150b→E150d). The region immediately surrounding approximately 1150 cm^{-1} was also seen to be correlated with PC1 scores and

absorbance at this variable could be seen to clearly increase along with PC1 scores. Distinction between caramel colourants and burnt sugar materials was achieved along the PC2 axis and loadings data again indicated that spectral variation was present over a large range (between approximately 950 and 1800 cm^{-1}).

Although it was possible to separate out all five of the colourant categories based on PCs 1 and 2, these latent variables only accounted for 88.27% of the variation in the data. PC3 and PC4 (accounting for 7.66% and 2.49% variation in that order) were also assessed and allowed further distinction of E150c and E150b classed caramels respectively. The scores plots and loadings data corresponding to these additional PCs can be found in Appendix 8.2.

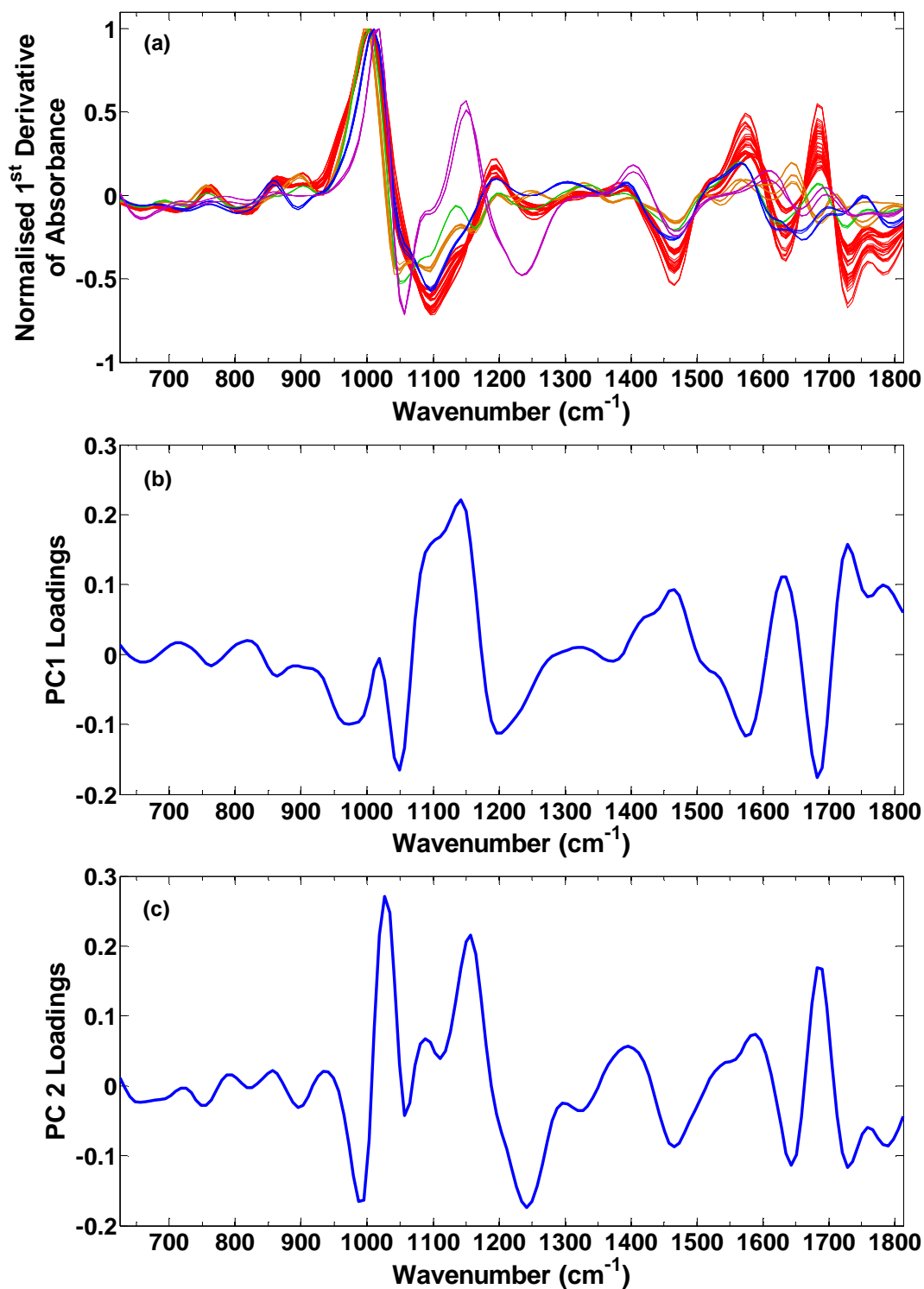


Figure 3.7: (a) Normalised ATR-MIR spectra of all caramels dissolved in 40% ethanol: fifteen E150a caramels (red); one E150B_X9 caramel (green); two E150C_10 caramels (blue); two E150D_11 caramels (purple); and the three burnt sugar materials (orange). All spectra have been acquired from the 1st derivative spectra and each sample has been analysed in triplicate. Shown alongside the loadings plots for (b) PC1 and (c) PC2 obtained from PCA of all caramel samples.

An additional observation from the scores plot provided in Figure 3.6 was that within the E150a classed caramels, a few distinct clusters could be observed. On closer inspection it was found that although some types of E150a were overlaying with others, multiple batches of the same type of E150a were all clustering in the same region of space. Distinction between different types of E150a was also found to be slightly more pronounced when additional PCs up to PC4 were considered (see Appendix 2.2). These findings therefore indicated that differences in spectral profiles were being detected between different E150a caramels as a result of variation in the manufacturing conditions used to produce these samples. Further PCA was therefore carried out to incorporate only the fifteen E150a caramels to determine whether the use of a more focused model could allow each type of E150a caramel to be clearly distinguished. The resulting PC1 vs. PC2 scores plot (in total accounting for 93.7% of the variation in the data) is shown in Figure 3.8 and clear differentiation has been demonstrated between the different types of E150a caramel. Only caramels E150A_Y3 and E150A_Y4 from this dataset were found to have profiles that overlapped, indicating that their spectral features were very similar. This was confirmed when their normalised first derivative spectra were shown to overlay very closely (Figure 3.9) and when the assessment of additional PCs could not allow any further separation. An additional finding drawn from the scores plot depicted by Figure 3.8 was that when multiple batches of an E150a caramel were considered they were found to cluster tightly together; indicating that the spectral variation between different caramel formulations was much more significant than batch to batch variability.

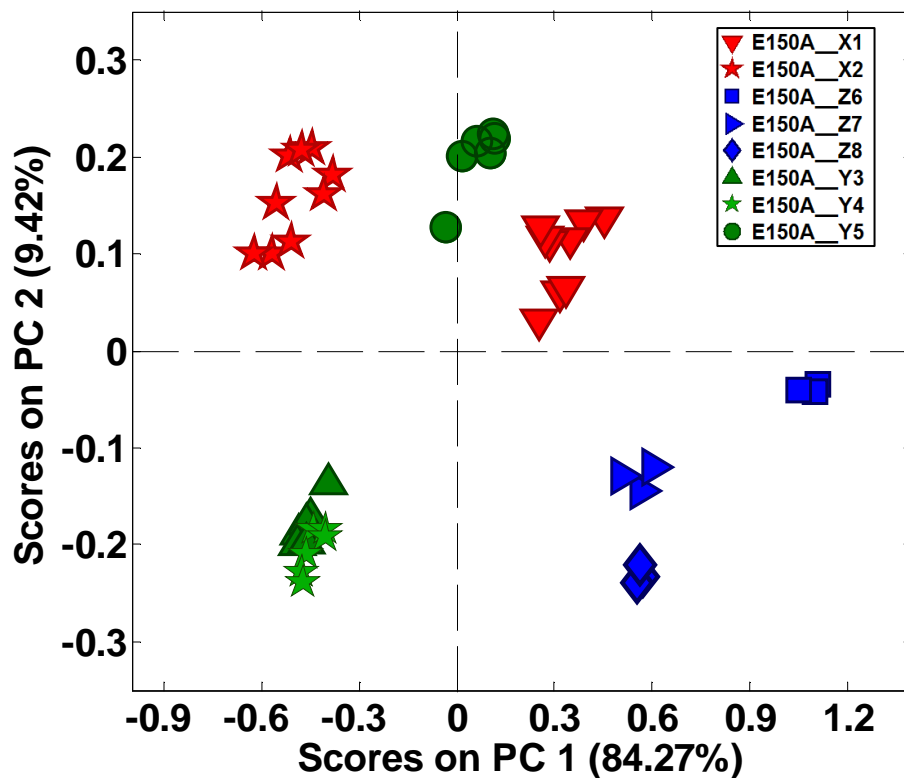


Figure 3.8: PC1 vs. PC2 scores plot obtained from PCA of the ATR-MIR spectra acquired from all fifteen E150a caramels (eight different formulations) dissolved in 40% ethanol. Caramels from the same manufacturer are colour coordinated whilst different types within these manufacturers have been given different symbols.

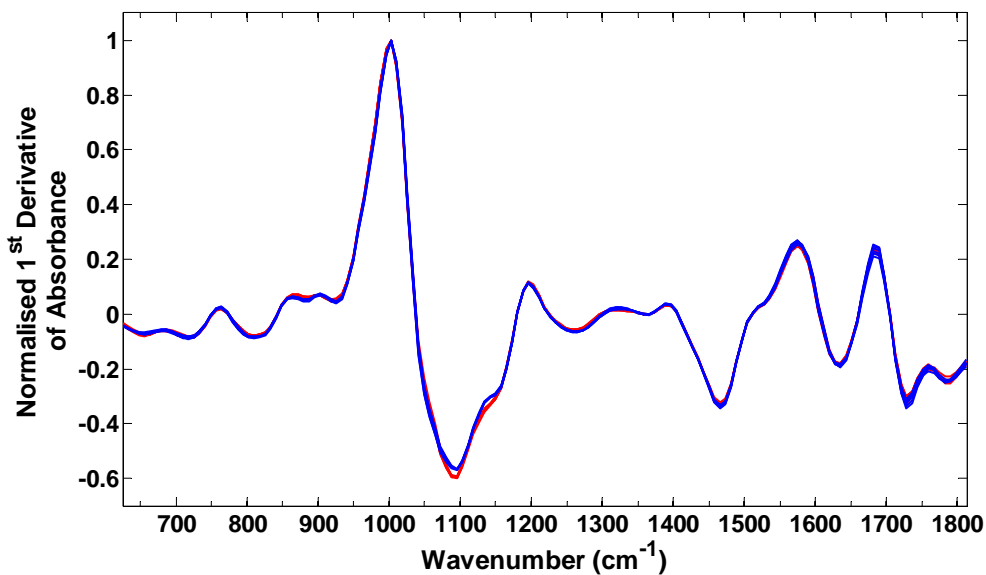


Figure 3.9: Overlay of the normalised first derivative spectra acquired from two batches of E150A_Y3 (red) and E150A_Y4 (blue). Samples were analysed in triplicate and all repeat spectra are shown.

The PC1 and PC2 loadings data corresponding to the PCA model created using only E150a caramels have been provided in Figure 3.10 alongside the normalised first derivative spectra of all fifteen E150a caramels. Although the spectral features were shown to occur at very similar positions for all E150a caramels, the loadings for PC1 and PC2 indicated that separation in the corresponding scores plot (Figure 3.8) was influenced primarily by features in the region between 1500 and 1750 cm^{-1} . The ratios of peaks in this region were observed as being distinctly different for each E150a caramel formulation and the ratios remained consistent when multiple batches of the same caramel were considered. The PC1 and PC2 loadings also indicated that spectral features close to 1050 cm^{-1} and just above 1100 cm^{-1} respectively influenced separation along these axes, a finding which complements the earlier observation made when comparing the raw spectra of three different E150a caramels (Figure 3.5). The peak observed in the raw spectra in the region encompassing these wavenumbers appeared to differ slightly in shape when different types of E150a caramel were considered.

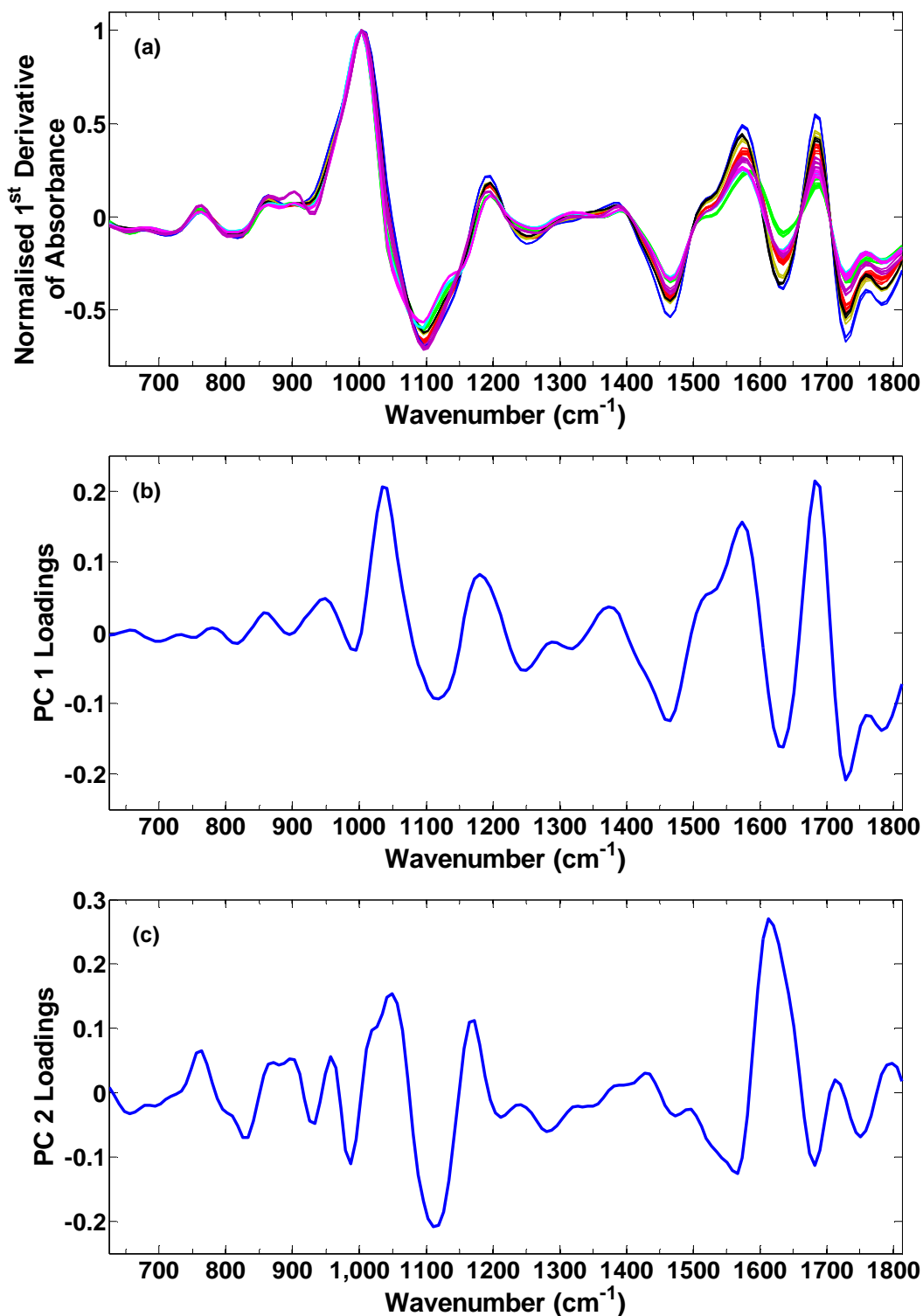


Figure 3.10: (a) Normalised ATR-MIR spectra of all fifteen E150a caramels in 40% ethanol: three batches of E150A_X1 (red); three batches of E150A_X2 (green); two batches of E150A_Y3 (cyan); two batches of E150A_Y4 (pink); two batches of E150A_Y5 (purple); one batch of E150A_Z6 (dark blue); one batch of E150A_Z7 (dark yellow); and one batch of E150A_Z8 (black). All spectra have been acquired from 1st derivative spectra and each sample was analysed in triplicate. Shown alongside the loadings plots for (b) PC1 and (c) PC2 obtained from PCA of all E150a caramels.

At this point in the research it was difficult to determine exactly what manufacturing conditions were responsible for the spectral variation observed between different E150a caramels. The reason behind this was that specific details relating to production conditions were confidential and could not be released by each manufacturer. The only information provided to aid with the interpretation of data, described what starting substrate had been used during production. It was also confirmed that each of the eight formulations had been produced by a different combination of production conditions (apart from E150A_Z6 and E150A_Z7, which only differed by their starting substrate). Caramel samples E150A_X1 and E150A_X2 are from the same manufacturer and have been prepared using the same starting substrate (maize). The ability to separate these materials along the PC1 axis therefore demonstrated that variation in production parameters can provide spectrally different caramels. Comparison of caramel samples E150A_Z6 and E150A_Z7 then demonstrated that changing the starting substrate (from maize to a combination of wheat and maize respectively) could also provide caramels with distinct spectral profiles, as they were clearly separated along the PC1 axis. In this case, the production parameters of the two caramels were known to be the same. In contrast to this finding, the two caramels that overlaid on the scores plot (E150A_Y3 and E150A_Y4) were both prepared using different starting substrates (wheat and maize respectively) but their profiles could not be separated. This indicated that changing the starting substrate may not influence caramel composition in all situations.

These initial findings have clearly demonstrated that in certain cases it is possible to differentiate between E150a caramels produced using different starting substrates and different combinations of production conditions. An interesting next step would be to determine exactly what influence individual production parameters have on caramel profiles, as a greater understanding of how the process conditions affect caramel composition could allow E150a manufacture to be manipulated in the future to create caramels with distinct signature profiles. These materials could then potentially be added to different blend whiskies to result in products with unique colourant profiles, an action that could aid with authenticity testing and counterfeit detection.

3.3.1.3 Profiling caramels in blended Scotch Whisky

The results to this point demonstrated that it was possible to differentiate between caramels of different class and also between E150a products of different formulation, based on the ATR-MIR spectra acquired from dried residues of sample solutions (in 40% ethanol). This next section of the study has been undertaken to build on these initial observations and assess whether the profiles of different caramels could still be distinguished when spiked in the more complex matrix of a Scotch Whisky. In this case, dried residue spectra may also be influenced by natural whisky colour components that have been imparted on the spirit during maturation. It was therefore important to assess whether colour from this source would mask the unique spectral features that have so far allowed distinction between different caramel materials.

Fifteen samples were dissolved in Blend Whisky A for this purpose including: twelve E150a caramels (incorporating at least one batch from each of the eight different formulations); one batch of E150B_X9; a single batch of E150C_X10; and one batch of E150D_X11. Once the dried residues of these sample solutions were analysed using ATR-MIR (following preconcentration as described in section 3.2.4.2), two PCA models were constructed using the resulting spectral profiles. The first model was created using all samples dissolved in Blend Whisky A, whilst the second contained data from only the twelve E150a caramels in this solution medium. The PC1 vs. PC2 scores plots for these models are provided in Figures 3.11 and 3.12 respectively. Figure 3.11 highlighted that separation between the four classes of caramel was maintained when samples were dissolved in a typical Scotch Whisky and Figure 3.12 showed that it was still possible to distinguish between profiles of different types of E150a when added to this typical blend. These findings therefore indicated that the spectral features responsible for variation between different caramel materials were not all masked by contributions from natural whisky colour. It should also be noted here that the scores plots obtained for these models were very similar to those acquired when the same caramel types were dissolved in 40% ethanol, as were all loadings plots (not shown). This observation indicated that spectral features in the same regions were effectively responsible for separation in this case, supporting the proposal that the characteristic features of caramels

dominate spectra and have not been masked by the natural colour matrix of a typical blend.

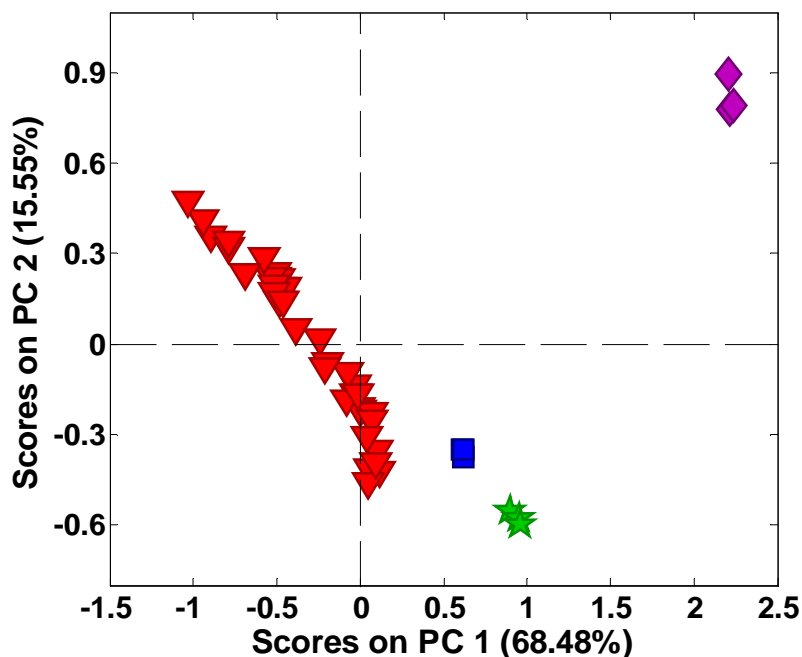


Figure 3.11: PC1 vs. PC2 scores plot obtained from PCA of the ATR-MIR spectra acquired from a selection of caramel colourants dissolved in Blend Whisky A. Samples have been colour coded according to their caramel class: E150a (red triangles), E150b (green stars), E150c (blue squares) and E150d (purple diamonds). Each sample was analysed in triplicate.

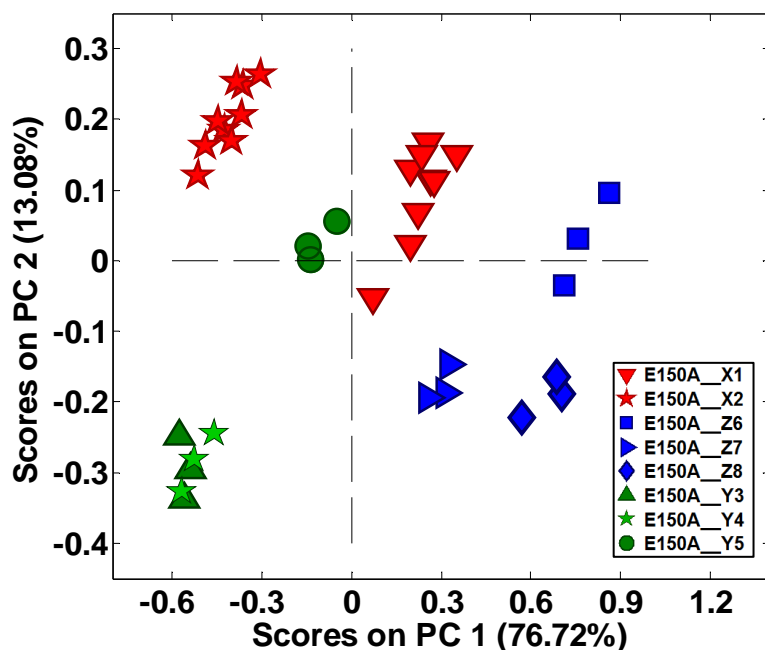


Figure 3.12: PC1 vs. PC2 scores plot obtained from PCA of the ATR-MIR spectra acquired from twelve different E150a caramels (incorporating eight different formulations) dissolved in Blend Whisky A. Caramels from the same manufacturer are colour coordinated whilst different types within these manufacturers have been given different symbols.

Although the above findings demonstrated that caramel features dominated the ATR-MIR spectra of dried residues when dissolved in a typical blend whisky, at this point the contributions from natural colour were not known. To investigate this further, two additional sample solutions were prepared of an E150A_X2 caramel: the first sample dissolved this caramel in 40% ethanol, to identify whether spectral differences were present when compared to the equivalent sample added to Blend Whisky A; whilst the second solution dissolved the caramel in a different whisky matrix (Blend Whisky B), to identify whether the influence of natural colour components varied for different blends. Blend Whisky B contained only malt whisky products and so represented the higher level of natural colour found for real products on the market. Thus as well as allowing a comparison of the effects of different blend matrices, it was thought that this solution medium would provide a good indication as to whether characteristic caramel features might be masked by natural colour even in more extreme cases. Both solutions described above were prepared and analysed as described in section 3.2.4.2 so that they could be compared directly with the caramels dissolved in Blend Whisky A.

Once the two additional E150A_X2 samples were analysed, the resulting normalised first derivative spectra were projected into the PCA model previously constructed for all twelve E150a caramels dissolved in Blend Whisky A so as to obtain their PC1 and PC2 scores. The resulting PC1 vs. PC2 scores plot is shown in Figure 3.13. It was clearly demonstrated by this figure that the E150A_X2 caramel dissolved in 40% ethanol did not overlay with the equivalent sample dissolved in Blend Whisky A. This highlighted that features originating from natural whisky colour were influencing spectra in the regions where characteristic caramel features occurred; although as previously demonstrated this was not to the extent where the characteristic nature of the latter features were being masked. It was also shown by Figure 3.13 that the E150A_X2 sample in Blend Whisky B was clearly separated from the E150A_X2 sample dissolved in Blend Whisky A. This showed that as well as natural colour influencing the ATR-MIR profiles of dried solution residues, the extent of natural colour contributions differed for the two blend whiskies assessed in this study.

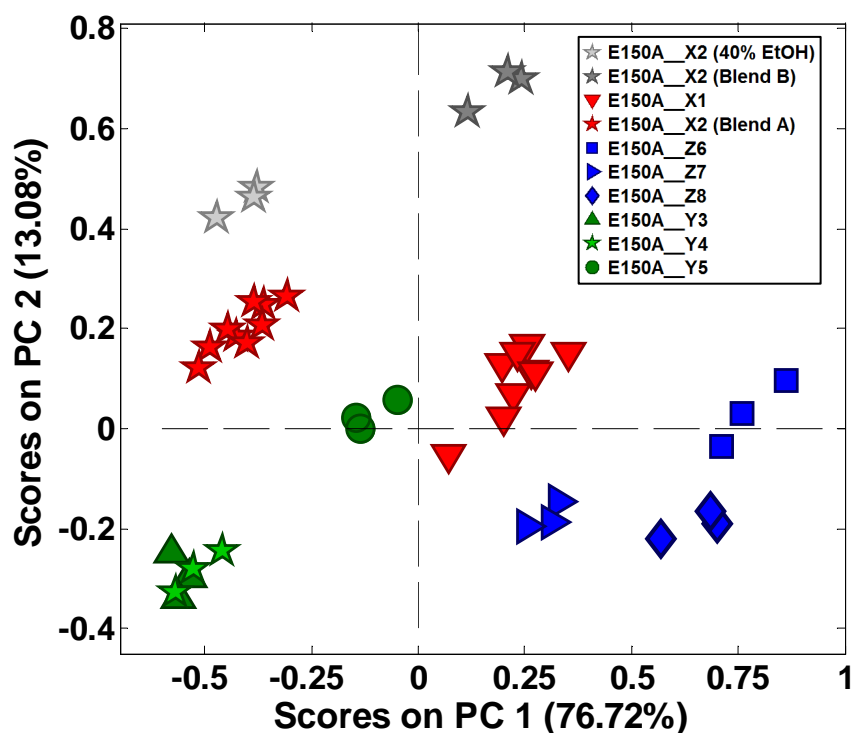


Figure 3.13: Projection of the PC1 and PC2 scores values for two solutions of E150A_X2 – in 40% ethanol (light grey star) and in Blend Whisky B (dark grey star) – into the subspace defined by the PCA model acquired from the twelve E150a caramels dissolved in Blend Whisky A. Triplicate data for all samples have been included.

The raw spectra acquired from each solution of E150A_X2 have been overlaid in Figure 3.14 to allow a comparison of their spectral features and to help visualise why the profiles of this caramel dissolved in the three different media did not overlap on the scores plot provided in Figure 3.13. When the spectrum acquired from E150A_X2 dissolved in Blend Whisky A was assessed, additional peaks were clearly visible in the region between 1150 and 1550 cm^{-1} that were not observed in the spectrum acquired for the same caramel dissolved in 40% ethanol. In addition to this, the relative absorbance levels of the two peaks between 1550 and 1750 cm^{-1} appeared to differ between the spectra of these two samples. When the profiles of E150a caramels were originally assessed when dissolved in 40% ethanol (section 3.3.1.2), loadings data indicated that characteristic caramel features were found throughout the region covering 1000 to 1800 cm^{-1} , primarily being attributed to features between 1500 and 1750 cm^{-1} . The above observation from Figure 3.14 therefore explained why separation was observed in Figure 3.13 between E150A_X2 caramel profiles in 40% ethanol and Blend Whisky A, as natural colour components

were clearly influencing spectra within the regions where characteristic caramel features have previously been found.

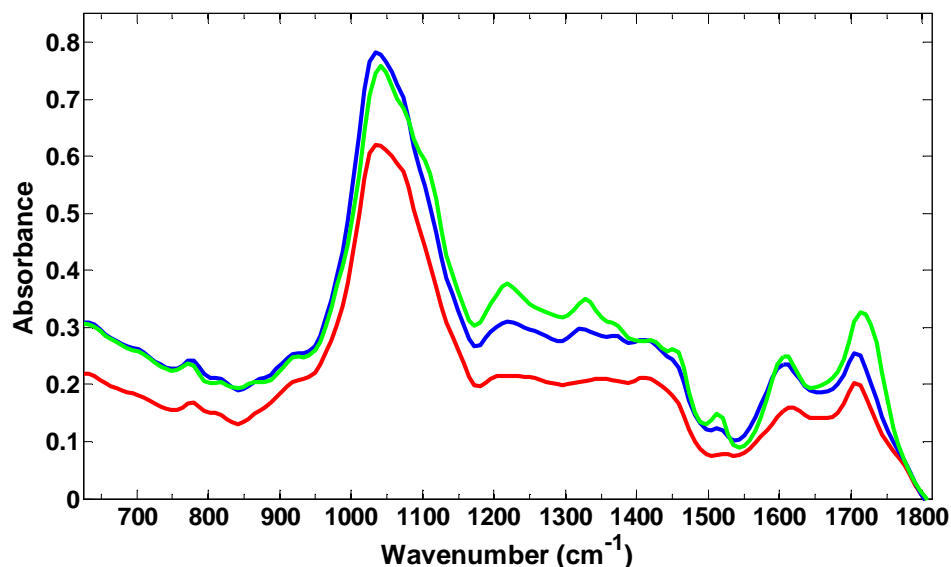


Figure 3.14: Overlay of the ATR-MIR spectra acquired from the dried residues of three different caramel solutions: E150A_X2 in 40% ethanol (red spectrum); E150A_X2 in Blend Whisky A (blue spectrum); and E150A_X2 in Blend Whisky B (green spectrum). Each spectrum has been averaged from triplicate results.

When the raw spectra of caramel E150A_X2 in the two different blend matrices were compared, peaks caused by natural colour were generally shown to appear at consistent positions for both samples. The main differences between the two spectra were instead related to variations in peak intensities; the natural colour features were clearly more prominent when the caramel was dissolved in Blend Whisky B. This could potentially be explained by the fact that Blend Whisky B represented the high end of natural colour that would be associated with blends on the market, whereas Blend Whisky A possessed a much lower, more typical colour level (absorbances of approximately 0.26 and 0.07 respectively at 430 nm before caramel addition).

As natural colour from Blend Whisky B clearly influenced spectra to a different extent than Blend Whisky A, this raised the question as to whether natural colour features might actually mask characteristic caramel features when different whisky matrices are considered. Solutions of three different types of E150a caramel were therefore prepared in Blend Whisky B to assess whether differentiation was maintained when a whisky matrix with a high level of natural colour was considered

as opposed to a typical whisky blend (Blend Whisky A). Caramels E150A_X1, E150A_X2 and E150A_Y5 were chosen for this purpose as their profiles were already quite close together when compared in Blend Whisky A and so their differentiation might be affected to a greater extent by an increased influence from natural whisky colour. Once the dried residues of these sample solutions had been analysed using ATR-MIR, PCA was undertaken to compare their spectral profiles. Also included in the model was the previously analysed E150A_X2 caramel in 40% ethanol and the dried residue profile of Blend Whisky B devoid of any caramel addition. The resulting PC1 vs. PC2 scores plot is provided in Figure 3.15.

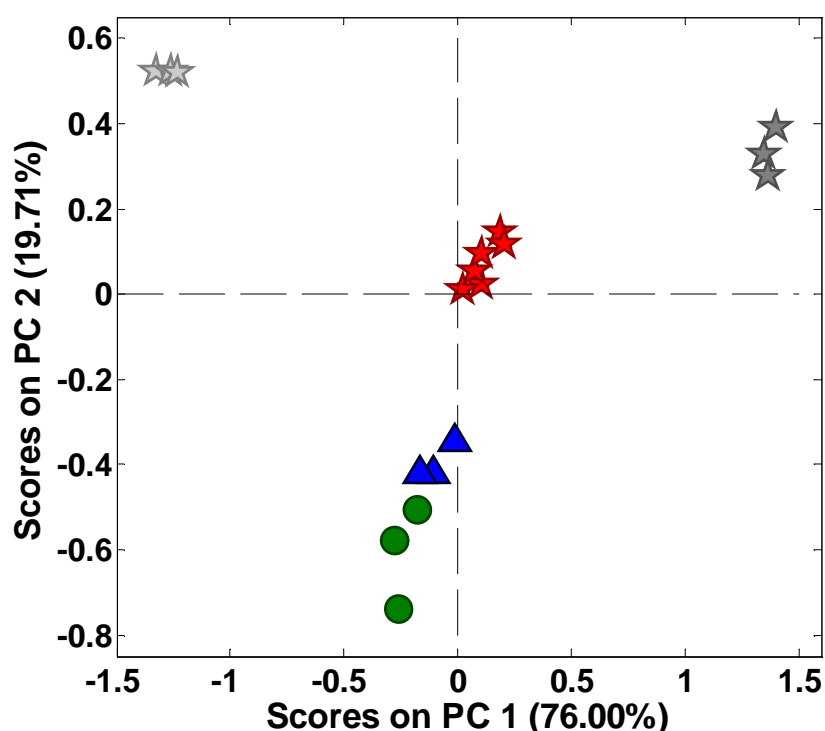


Figure 3.15: PC1 vs. PC2 scores plot obtained from PCA of the ATR-MIR spectra acquired from a selection of caramel solutions in Blend Whisky B: an E150A_X1 caramel (blue triangles); two batches of E150A_X2 caramel (red stars); and one E150A_Y5 caramel (green circles). Also included in the model were the dried residue spectra acquired from a sample of E150A_X2 dissolved in 40% ethanol (dark grey stars) and a sample of Blend Whisky B devoid of caramel addition (light grey stars). All samples were analysed in triplicate.

Figure 3.15 showed that E150A_X2 in Blend Whisky B was clearly separated from the equivalent caramel dissolved in 40% ethanol, which reiterated that natural colour components from Blend Whisky B influenced the spectra of dried solution residues. When the same sample was compared to the profile of Blend Whisky B containing

no caramel however, the profiles were again clearly distinct, indicating that caramel features were not completely masked by a high level of natural colour in the case of E150A_X2. The other caramel solutions included in the model were also clearly separated from the blend whisky matrix alone and distinction was still achieved between the three different types of E150a caramel when dissolved in Blend Whisky B. These findings therefore indicated that even when the level of natural colour is at a high level, features characteristic to different caramel materials can still potentially be observed.

The spectral regions responsible for the above observations were investigated by looking at the loadings data corresponding to PCs 1 and 2. These loadings plots have been provided in Figure 3.16 alongside the averaged normalised first derivative spectra acquired for each type of solution incorporated in the PCA model. Solutions of the E150A_X2 type caramel dissolved in the dark blend were clearly differentiated from the dark blend alone and the equivalent caramel dissolved in 40% ethanol along the PC1 axis. The corresponding loadings plot indicated that spectral variation in this case was present throughout the range covering 950 to 1800 cm^{-1} . Within this range, a few notable regions that were clearly influencing separation along PC1 were identified as 1095, 1190, 1580 and 1750 cm^{-1} . Distinction between the three different E150a caramels when dissolved in Blend Whisky B was observed along the PC2 axis and the corresponding loadings data indicated that variables in the regions surrounding 900, 1120 and 1750 cm^{-1} were primarily responsible for the observed separation. Comparison of the normalised first derivative spectra at these wavenumbers supported these findings, showing clear differences between the three E150a caramel solutions at these points.

As natural colour in this case has been shown to influence spectra throughout the spectral range it cannot definitively be said that all caramels could still be distinguished when dissolved in a blend with high levels of colour; or in fact in any other blend matrices. It has however been shown that characteristic caramel features still influenced dried residue spectra and so the potential exists to create distinct product profiles even when caramels are spiked into darker blends.

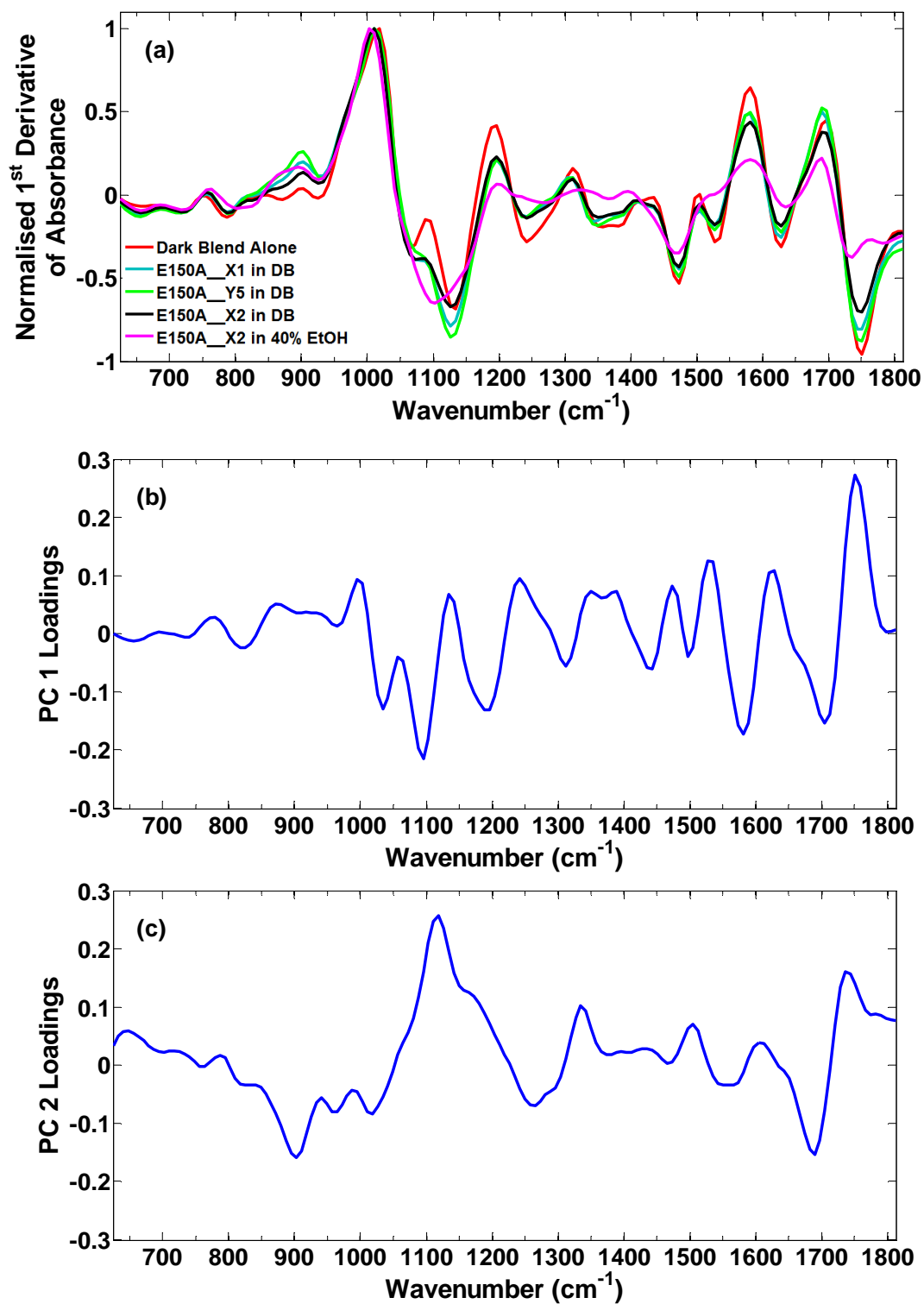


Figure 3.16: (a) Normalised ATR-MIR spectra showing the average profiles acquired from three different types of E150a caramel dissolved in Blend Whisky B. The average spectrum acquired from an E150A_X2 caramel dissolved in 40% ethanol and also from a sample of Blend Whisky B devoid of caramel addition have also been included. All spectra have been acquired from 1st derivative spectra, each sample being analysed in triplicate. Shown alongside the loadings plots for (b) PC1 and (c) PC2 obtained from PCA of these selected samples in Blend Whisky B.

3.3.2 Scenarios Relevant to ‘Real’ Whisky Products

3.3.2.1 Caramel concentration study

In all initial experiments involving the addition of caramel to a blend whisky, the affect of changing the amount of caramel present was not considered. In reality however, the amount of E150a caramel added to a particular Scotch Whisky will vary from one batch to another. This is because the level of natural colour is not typically consistent from one batch to another – the development of natural colour being dependant on the individual casks implemented during the maturation step of production. The amount of E150a caramel required to achieve consistent colouring for a Scotch Whisky product will therefore vary from one batch to another. The following study was therefore undertaken to identify whether spectral features are affected by changing the ratio of caramel colour to natural colour in the case of Blend Whisky A. It was considered a possibility that when less caramel was present, natural colour features might begin to influence spectra to a greater extent and potentially mask certain caramel features (and *vice versa* if more caramel were present).

Control samples

Prior to assessing how changing the level of caramel in a blend would affect spectral profiles, it was important to assess whether the ATR-MIR methodology itself was robust to changes in caramel concentration. To assess this, four caramel solutions ranging in their level of absorbance from 0.2 – 0.8 (in increments of 0.2) were prepared using an E150A_X1 type caramel in 40% ethanol. Each sample solution was initially concentrated using the methodology described in section 3.2.4.2 and subsequently analysed using the ATR-MIR methodology outlined in the same section.

Once all four sample solutions were analysed, the resulting normalised first derivative spectra were projected into the PCA model previously constructed for all fifteen E150a caramels when dissolved in 40% ethanol (see section 3.3.1.2 (Figure 3.8) for original model) so as to obtain their PC1 and PC2 scores. The resulting PC1 vs. PC2 scores plot is shown in Figure 3.17 and demonstrated that although all four

samples of variable caramel concentration were found in a similar region to the original E150A_X1 sample, both the PC1 and PC2 scores for these samples clearly decreased as caramel concentration increased.

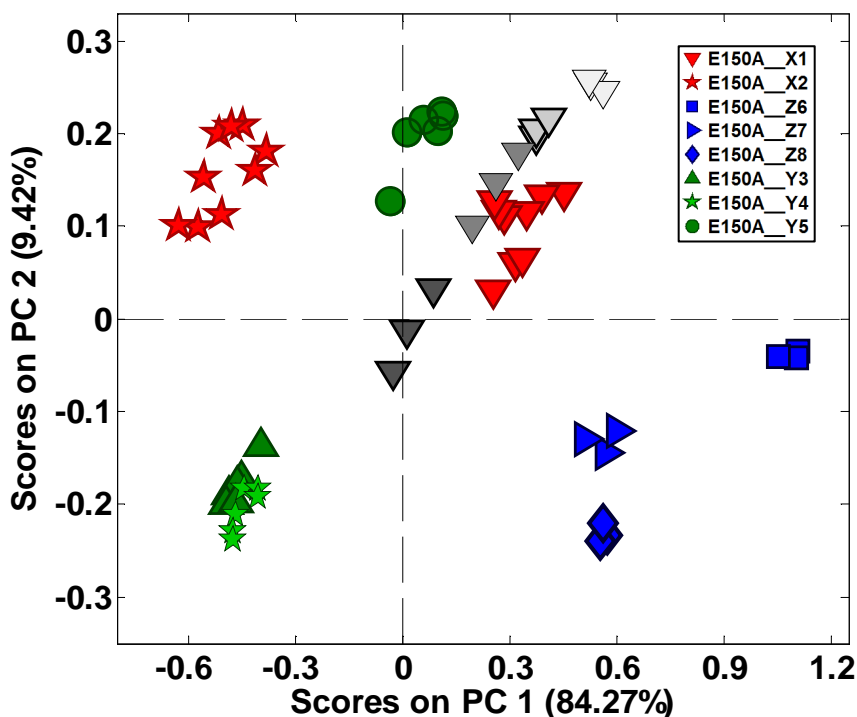


Figure 3.17: Projection of the PC1 and PC2 score values, for four solutions of E150A_X1 at various concentrations, into the subspace defined by the PCA model acquired from fifteen E150a caramels dissolved in 40% ethanol. The E150A_X1 samples of different concentration are all represented by grey triangles, becoming darker as the absorbance values increased from 0.2 to 0.8 in increments of 0.2. Triplicate depositions have been included for all samples.

The above findings therefore demonstrated that when implementing the current ATR-MIR methodology, changes in caramel concentration resulted in spectral variation, even though all spectral measurements had been normalised. This had not been a problem for previous analyses as all samples had been prepared to the same concentration; however it was now indicated that something about the ATR-MIR method was sensitive to concentration changes. This could possibly be explained by the fact that all solution residues being dried onto the ATR crystal were very thin films and so the sample thickness would be on a similar scale to the evanescent wave. This was discussed previously in section 3.3.1.1 as a parameter that could influence spectral repeatability as a result of full measurements not being attained. When solutions that gradually increased in caramel concentration were being

analysed, it could therefore be the case that certain features were being picked up as increasing whilst others were not. No other examples could be found in the literature that assessed ATR-MIR analysis of samples at a similar thickness to the evanescent wave and so further investigation would be required to assess this further. This was not something that could be studied further within the timescale of this project but would be important to factor into the design of any future work and instrument development.

Study samples

After analysis of the control samples as described above, it was determined that if the current ATR-MIR methodology were to be employed to assess the effect of adding different amounts of caramel to a blend, then any spectral variation could be caused by the methodology rather than real differences from changing the caramel:natural colour ratio. A change was therefore made to the methodology to determine if the variation in spectral features resulting from concentration differences in the control samples could be reduced or removed. To do this an alteration was made to the concentration step involved with sample preparation prior to analysis by ATR-MIR. Rather than all samples being concentrated by the same factor (from 6 mL to 300 μ L), they were instead concentrated so that the final absorbance level of all samples was always equivalent. This was achieved by reducing 6 mL of sample to dryness as normal but reconstituting in a volume that depended on the original absorbance of each sample at 430 nm.

The developed methodology was initially tested using the four solutions of E150A_X1 caramel dissolved at different absorbance levels in 40% ethanol (absorbances of 0.2 – 0.8 in increments of 0.2). Once concentrated using the new approach and analysed using ATR-MIR, the PC1 and PC2 scores for these samples were acquired by projecting their normalised first derivative spectra into the PCA model constructed for all fifteen caramels when dissolved in 40% ethanol. The resulting PC1 vs. PC2 scores plot is shown in Figure 3.18 and it was demonstrated that a trend between initial concentration and PC scores was no longer observed;

samples instead clustered together in the same region of space as the original E150A_X1 samples.

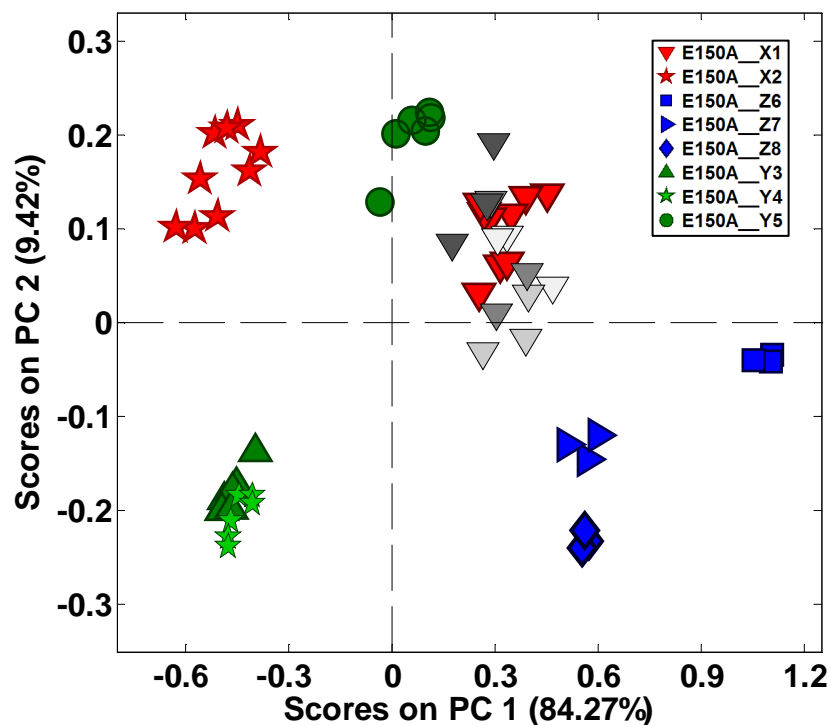


Figure 3.18: Projection of the PC1 and PC2 score values, for the four solutions of E150A_X1 at various concentrations and analysed by the adapted ATR-MIR methodology, into the subspace defined by the PCA model acquired from fifteen E150a caramels dissolved in 40% ethanol. The E150A_X1 samples of different concentration are all represented by grey triangles, becoming darker as the absorbance values increased from 0.2 to 0.8 in increments of 0.2. Triplicate depositions have been included for all samples.

These findings therefore indicated that the adapted methodology could allow spectra to be acquired that were unaffected by concentration dependent variation introduced via the application of the original ATR-MIR methodology. The adapted methodology was therefore taken forward and used to compare sample solutions containing different levels of caramel in Blend Whisky A; any spectral differences should now only be related to a change in the caramel:natural colour ratios.

To assess this, four sample solutions were prepared by dissolving different amounts of an E150A_X1 caramel in Blend Whisky A. The four solutions had absorbance levels of 0.2, 0.4, 0.6 and 0.8 at 430 nm, meaning that both the level of caramel added and hence the ratio of caramel:natural colour was increasing respectively. Once each sample was pre-concentrated and analysed using ATR-MIR, the PC1 and

PC2 scores were again obtained by projecting the normalised first derivative spectra into the PCA model constructed previously from the twelve E150a caramels when dissolved in Blend Whisky A at an absorbance of approximately 0.55 (see section 3.3.1.3 (Figure 3.12) for original model). The resulting PC1 vs. PC2 scores plot is shown in Figure 3.19 and it was demonstrated that all samples from this study clustered tightly together in the same region occupied by the E150A_X1 type caramels previously analysed. This indicated that in the case of Blend Whisky A, no significant difference was observed between spectra that contained different ratios of caramel:natural colour, within the range investigated. These data therefore implied that if different amounts of caramel have been added to a typical blend whisky, both the characteristic caramel features and the colour profile should not be influenced to a significant extent. Further work would be needed to determine whether this finding was maintained for other blend matrices but could not be completed within the timescale of this project.

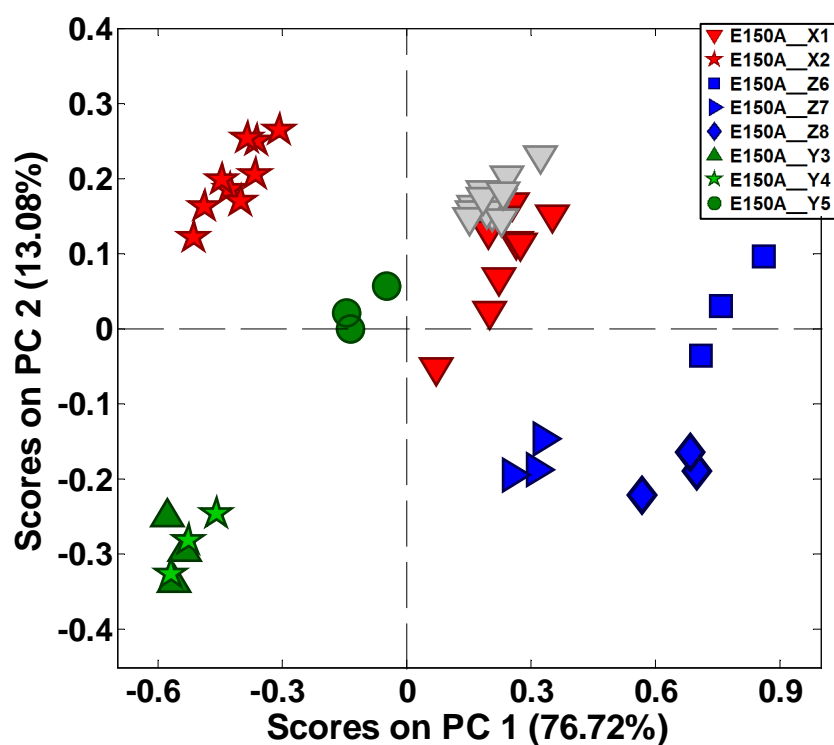


Figure 3.19: Projection of the PC1 and PC2 scores values, for the four solutions of E150A_X1 at various concentrations in Blend Whisky A, into the subspace defined by the PCA model acquired from twelve E150a caramels dissolved in Blend Whisky A. The E150A_X1 sample solutions of different concentration are represented by grey triangles. Triplicate depositions have been included for all samples.

3.3.2.2 *Caramel fade study*

All preliminary experiments undertaken in this research have used caramel solutions that have been prepared freshly from raw caramel prior to analysis (both when in 40% ethanol or in a blend whisky). Alcoholic beverages containing caramel however are known to fade in the bottle over time, a factor that occurs at a significantly increased rate when products are left in direct sunlight.⁴⁶ The process of caramel fade over time indicates that certain components within the caramel are being degraded and so the caramel composition will be changing. A study was therefore undertaken by Gemma Gardiner as part of her undergraduate thesis project to identify whether the caramel fading process would affect the ATR-MIR profiles of dried caramel solution residues.⁴⁷

Stock solutions of an E150A_X1, an E150A_X2 and an E150D_X11 were prepared in glass vials and forcibly faded as described in section 3.2.4.4. To summarise, each caramel solution was split into eight portions, five of which were placed in a UV light box to simulate the fading process but on an accelerated timescale. One sample was removed from the light box after each of the following time points: 1 day, 2 days, 3 days, 4 days and 7 days. The remaining three aliquots of each solution were used as control samples: one being analysed on day 0 (i.e. not faded); the next being stored under ambient conditions in the lab and analysed on day 7; and the final sample being wrapped in aluminium foil and stored in the UV light box for the 7 day duration of the experiment.

The colour levels of all solutions within this study were monitored using UV-Visible spectrometry, prior to any analysis by ATR-MIR. Figure 3.20 has plotted the absorbance values (at 430 nm) for each sample solution and a clear decrease in colour was demonstrated as time within the UV light box increased. It could also be seen that the two E150a caramels faded to a greater extent than the E150d classed caramel. The absorbance levels of all control samples were consistent, indicating that natural fade had not influenced samples over the timescale of this experiment.

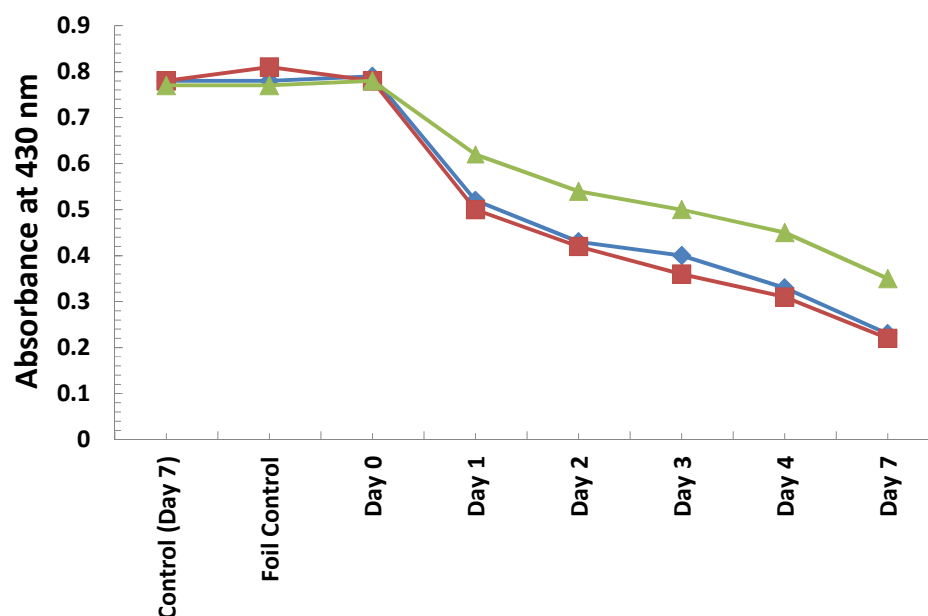


Figure 3.20: Plot of absorbance at 430 nm versus sample solutions for each caramel type assessed in this study: E150A_X1 (blue trendline), E150A_X2 (red trendline) and E150D_X11 (green trendline).

The percentage of original colour remaining after each time point was determined from the absorbance values at 430 nm and the resulting values were summarised in Table 3.2. For the E150a caramels, these values demonstrated that the level of colour had reduced to just below 30% of the original value, which represented an extreme level of fade as might be encountered with real samples in the industry.⁴⁸

Table 3.2: Percentage values demonstrating the level of colour remaining for each caramel solution after being stored in the UV light box for various time points over a 7 day period.

	Percentage of colour remaining at 430 nm (%)		
	E150A_X1	E150A_X2	E150D_X11
After 'Day 1'	66.4	63.3	80.2
After 'Day 2'	54.9	53.2	69.8
After 'Day 3'	51.1	45.6	64.7
After 'Day 4'	42.1	39.2	58.2
After 'Day 7'	29.4	27.8	45.3

On completion of the fading experiment, each sample was prepared for and analysed using ATR-MIR as described in section 3.2.4.4. PCA was then used to compare the resulting spectral profiles for each of the three caramel types individually. When a model was constructed using the eight solutions of E150A_X1, PC1 was found to account for 93.38% of the spectral variation. The resulting PC1 scores for each E150A_X1 solution have been plotted in Figure 3.21 and in general were shown to decrease as time spent in the UV light box (and hence the level of fade) increased. The PC1 scores for all control samples were again consistent and subsequent principal components did not indicate any further trends between samples.

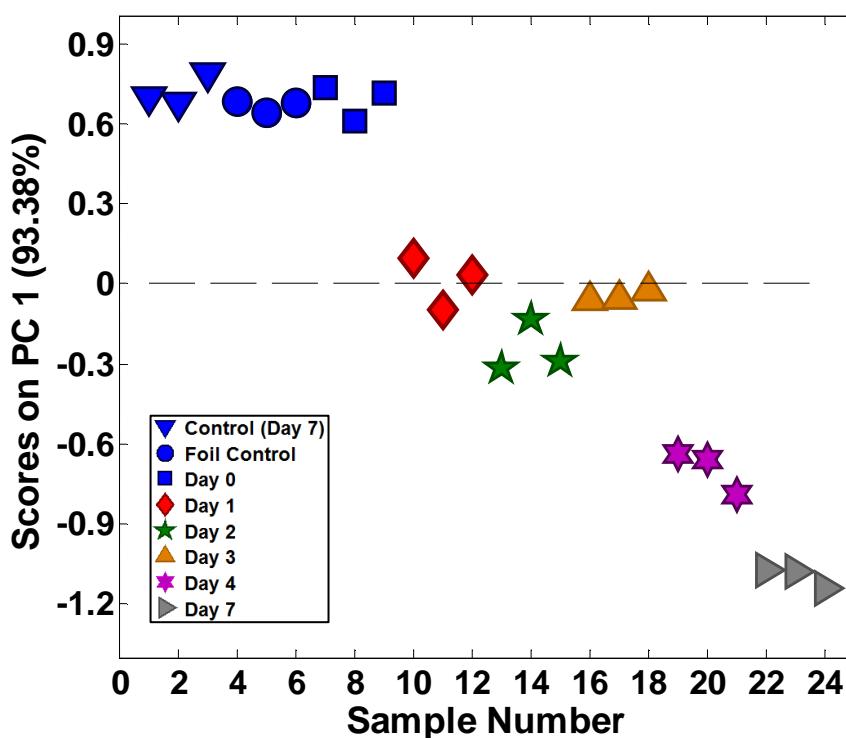


Figure 3.21: Plot showing the PC1 scores acquired from PCA of the eight E150A_X1 sample solutions included in this study. ATR-MIR analysis was undertaken in triplicate for all samples.

The above findings indicated that the ATR-MIR profiles of E150A_X1 type caramels were affected by the process of fading. To help visualise which spectral features were responsible, the normalised first derivative spectra acquired for the eight E150A_X1 solutions have been provided in Figure 3.22 alongside the PC1 loadings.

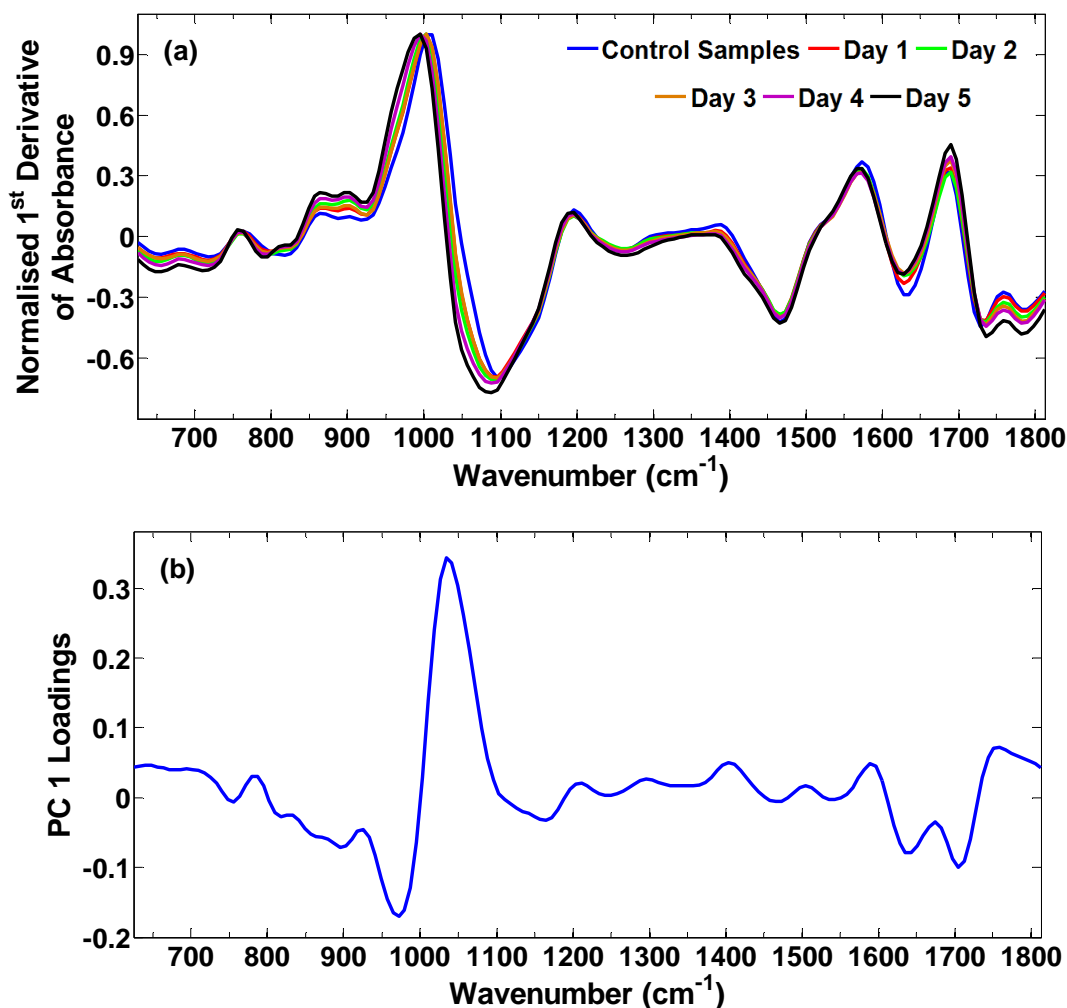


Figure 3.22: (a) Normalised ATR-MIR spectra showing the average profiles acquired from the control samples and five faded samples of an E150A_X1 caramel dissolved in 40% ethanol. All spectra have been acquired from 1st derivative spectra and each sample was analysed in triplicate. Shown alongside (b) the PC1 loadings plot acquired from PCA of all eight E150A_X1 solutions.

The PC1 loadings plot shown in Figure 3.22b indicated that caramel fade primarily affected the normalised first derivative spectra of E150A_X1 at approximately 1040 cm⁻¹. This variable was clearly correlated to PC1 and on inspection of the corresponding region in Figure 3.22a, spectra were seen to clearly decrease in absorbance in accordance with their PC1 scores (provided in Figure 3.21). The loadings data also indicated a few variables that were clearly anti-correlated with PC1; these being found at 970, 1640 and 1710 cm⁻¹. Absorbance values were clearly seen to increase in these regions in a manner that corresponded with PC1 scores.

Two additional PCA models were constructed to assess the affect of caramel fade on the other caramel types assessed in this study: a different type of E150a caramel

(E150A_X2) and a caramel of different class (E150D_X11). In both cases, PC1 scores were generally found to decrease the longer sample solutions were kept in the UV light box, as was found previously for the E150A_X1 caramel solutions. These findings have been demonstrated in Figures 3.23 and 3.24 respectively for the E150A_X2 and E150D_X11 caramel solutions. When the PC1 loadings data were assessed for each of these additional PCA models (data not shown), those acquired from the E150A_X2 caramel model were very similar to those already acquired for E150A_X1. These data therefore indicated that similar spectral regions (and potentially similar components) were being affected by the fading process for this other E150a caramel. Loadings data obtained for the E150D_X11 model indicated that different spectral regions were being affected by the fading process (primarily from 1000 to 1300 cm^{-1} and at approximately 1680 cm^{-1}). Subsequent principal components did not indicate the presence of any further trends resulting from caramel fade for these two additional caramel types.

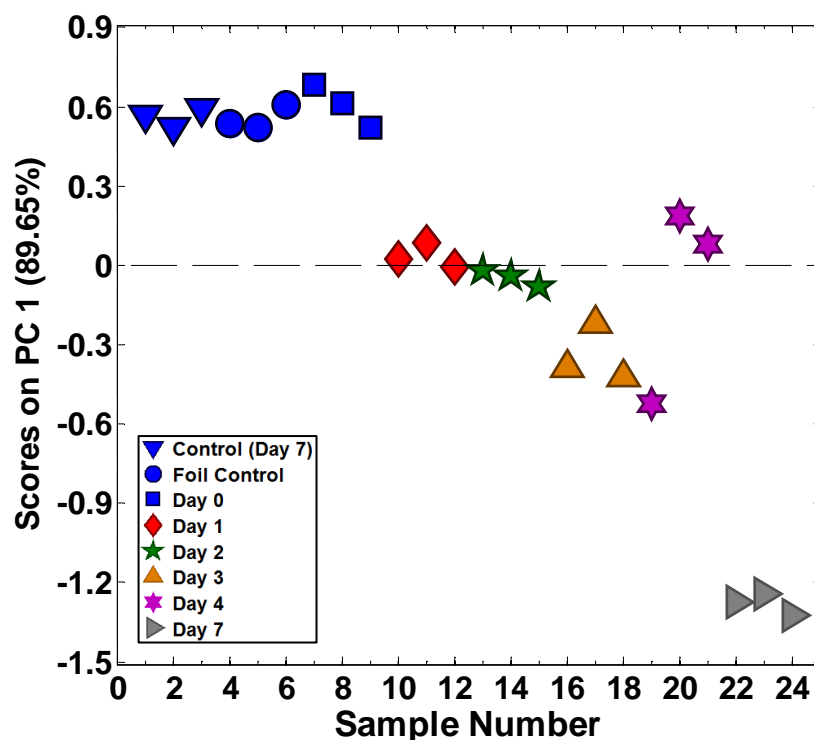


Figure 3.23: Plot showing the PC1 scores acquired from PCA of the eight E150A_X2 sample solutions included in this study. ATR-MIR analysis was undertaken in triplicate for all samples.

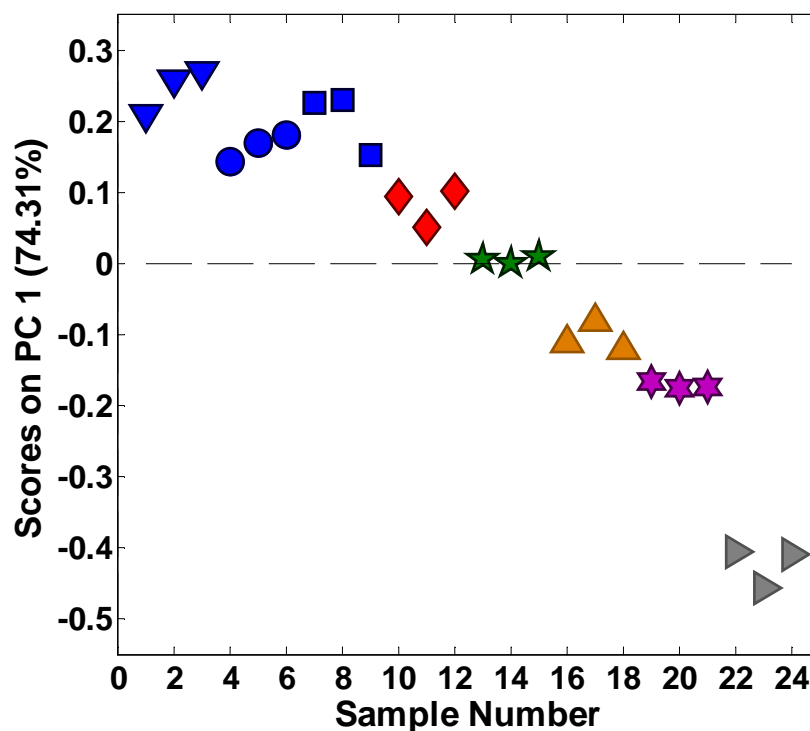


Figure 3.24: Plot showing the PC1 scores acquired from PCA of the eight E150D_X11 sample solutions included in this study. ATR-MIR analysis was undertaken in triplicate for all samples.

Overall this study has demonstrated that caramel fade would potentially influence the ATR-MIR spectra of dried Scotch Whisky residues. At this point however, it had not been identified whether the extent of spectral variation would make a particular caramel profile unrecognisable. This will be considered in more detail in Chapter 4 when the influence of caramel fade on the ability to predict caramel profiles is investigated.

3.3.3 Blend Discrimination Study

Prior to the commencement of this project, literature indicated that the ATR-MIR spectral features acquired from the residues of Scotch whiskies containing caramel were dominated by the features of this added colourant rather than those from natural colour components.³² It has been demonstrated within this research however, that natural colour does influence residue spectra and can do so to different extents for different blend matrices (see section 3.3.1.3). These findings therefore indicated that the dried residues of different blends containing caramel could already have distinct profiles based on the potentially unique natural colour contributions. An investigation was therefore undertaken to determine whether it was possible to

discriminate between different blend products (containing caramel) by the assessment of dried residue profiles using ATR-MIR.

Five batches each of four different Scotch Whisky blends were prepared and analysed using ATR-MIR as described in section 3.2.4.5. The spectral profiles that were attained were then compared using PCA and the resulting PC1 vs. PC2 scores plot has been provided in Figure 3.25. It was clear from this plot that some differentiation was possible between different blend products; Blend 1 being clearly separated from all others along the PC2 axis. The remaining three blends however could not be distinguished in this plot. These findings therefore indicated that the natural colour contributions from Blend 1 were significant to the extent that a distinct profile could be obtained, whilst the contributions from natural colour from the other blends were not significant enough to allow them to be distinguished using these PCs. The fact that Blends 2-4 overlaid in Figure 3.25, whilst Blend 1 separated out, could be due to the fact that the former three blends all originated from the same brand.

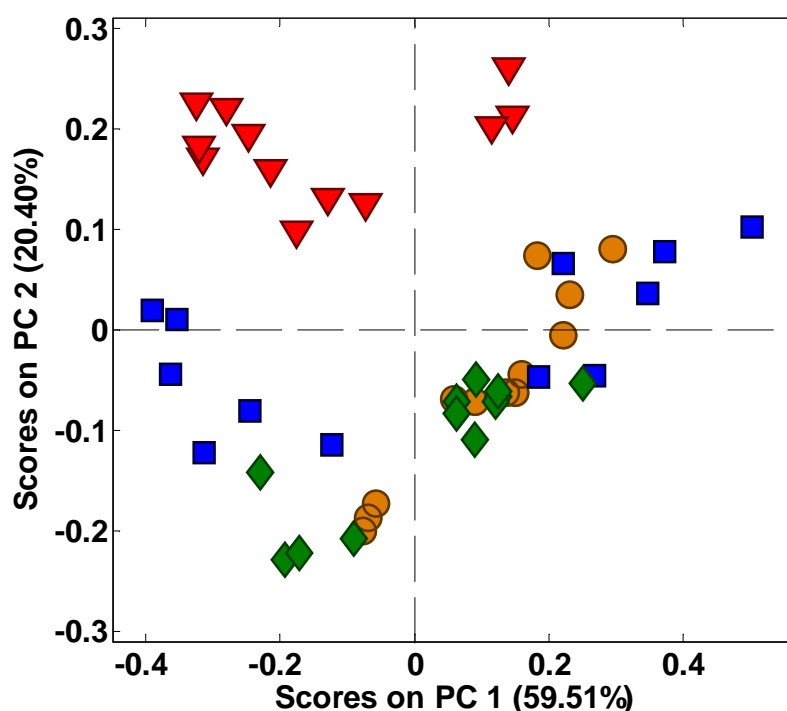


Figure 3.25: PC1 vs. PC2 scores plot acquired from PCA of the normalised first derivative spectra acquired from ATR-MIR analysis of the dried residues of five batches each of four blend whiskies: Blend 1 (red triangles), Blend 2 (orange circles), Blend 3 (blue squares) and Blend 4 (green diamonds). Each sample has been analysed in triplicate.

PCs 1 and 2 only accounted for 79.91% of variation in the data and so PC3, describing an additional 11.89% of the spectral variation, was also considered to see whether further differentiation between the blends could be achieved. The PC1 vs. PC3 scores plot has been provided in Figure 3.26 and it was clearly demonstrated that Blend 3 could also be separated from all others along the PC3 axis. The triplicate repeats of a single batch of Blend 4 however, were found to have similar PC3 scores to Blend 3. The only difference associated with this particular batch was that it was a few years older than the others and so it was considered a possibility that degradation over time may have altered certain spectral features of this blend (mainly those associated with PC3).

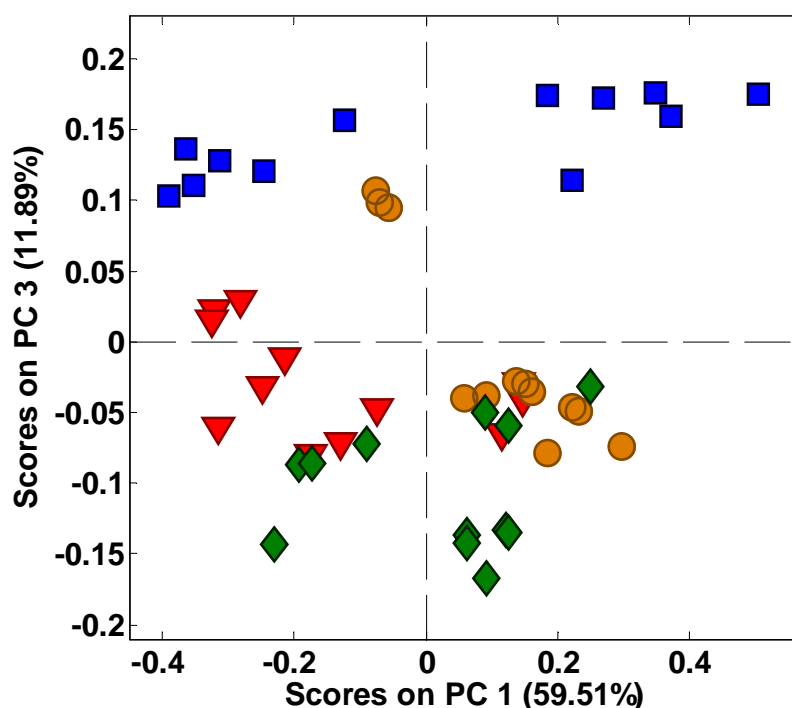


Figure 3.26: PC1 vs. PC3 scores plot acquired from PCA of the normalised first derivative spectra acquired from ATR-MIR analysis of the dried residues of five batches each of four blend whiskies: Blend 1 (red triangles), Blend 2 (orange circles), Blend 3 (blue squares) and Blend 4 (green diamonds). Each sample has been analysed in triplicate.

Overall, this particular study has demonstrated that it was possible to differentiate between some blends on the market containing caramel, based on spectral contributions from natural colour that are distinct to different products (it was assumed that the same E150a caramel was used in each blend). Although it was not possible to distinguish between all of the blends assessed in this study, it is a

possibility that alternative data analysis tools could allow differentiation to be improved – this is discussed in more detail in Chapter 4. A more extensive study incorporating a wider range of blends would also be required to determine whether these findings are true for the majority of products available on the market. It would also be interesting to see whether Scotch Whisky products containing no caramel could be distinguished based on their natural colour features alone.

3.4 Conclusions

ATR-MIR spectrometry has been successfully implemented in this research for profiling caramel colourants and was achieved by the analysis of dried solution residues when the caramel samples were dissolved in either 40% ethanol or a blend whisky matrix. Characteristic profiles were attained for different E150a caramel products and the implementation of PCA demonstrated clear differentiation between all but two of the E150a materials analysed in this study. PCA also demonstrated that it was possible to clearly distinguish between the four caramel classes recognised by the EU (and burnt sugar materials), even with the non uniformity of profiles for different product formulations within the E150a class. Separation between different caramel products was also shown to be maintained when these materials were dissolved in a standard blend whisky, indicating that dried residues of this spirit would typically be dominated by the colourant added. These data therefore highlighted an appealing attribute of this methodology for characterising caramel colourants in foodstuffs over other procedures described in the literature, as the latter are often limited by interference from components already present in food and beverage products.^{15,17,19}

The ability to identify characteristic caramel profiles in Scotch Whisky products, as demonstrated in this study, could be greatly beneficial to the industry in terms of counterfeit detection; authentic products could potentially be identified based on the confirmation of a specific colourant profile. The main advantage of the ATR-MIR methodology over other tools that are currently implemented for authenticity testing is that the ATR-MIR technology (and hence methodology) could be developed into a portable instrument. This would therefore permit simple screening of suspect samples in the field and there is currently a growing requirement for such techniques in the Scotch Whisky industry.

This study has also investigated how the ATR-MIR dried residue profiles of caramel solutions might be affected by different scenarios relevant to real Scotch Whisky products. Firstly, it was shown that even though characteristic caramel features dominate the dried residue spectra of a typical whisky, natural colour components

will also influence the profile. It was also found that the contributions from natural colour will potentially vary for different blend matrices. Despite the latter finding however, distinction between different caramel materials was shown to be maintained even when a blend matrix possessing a high level of natural colour was assessed. Additional experiments have assessed how spectral profiles might be affected by varying the concentration of caramel present in a blend and also how they might be influenced by the process of caramel fade. When the ratio of caramel:natural colour was varied for a typical blend whisky, there did not seem to be any affect on spectral profiles; caramel fade however, was found to influence spectral profiles. Each of these findings have been explored in greater detail in Chapter 4, which is based around the use of data analysis tools to predict caramel identities when dissolved in either 40% ethanol or blend whisky. Part of that work therefore assessed whether each of the above mentioned scenarios would affect dried residue profiles to the extent where the type of caramel present would no longer be recognisable.

3.5 References

1. The Scotch Whisky Regulations 2009, UK Government, www.legislation.gov.uk, 2009
2. D. V. Myres, J. C. Howell, *Food Chem. Toxicol.*, 1992, **30(5)**, 359-363
3. J. Calland, D. D. Williamson, Manchester, *Personal Communication*, June 2014
4. E. Hellwig, E. Gombocz, S. Frischenschlager, F. Petuely, *Deut. Lebensm. Rundsch.*, 1981, **77**, 165-174
5. S. Frischenschlager, E. Hellwig, F. Petuely, *Deut. Lebensm. Rundsch.*, 1982, **78**, 385-389
6. Y. S. Lee, S. Homma, K. Aida, *J. Jpn. Soc. Food Sci.*, 1987, **34**, 313-319
7. S. Kishihara, S. Fujii, M. Komoto, *J. Jpn. Soc. Food Sci.*, 1980, **27**, 479-482
8. A. L. Patey, G. Shearer, M. E. Knowles, W. H. B. Denner, *Food Addit. Contam.*, 1985, **2(2)**, 107-112
9. A. L. Patey, G. Shearer, M. E. Knowles, W. H. B. Denner, *Food Addit. Contam.*, 1985, **2(4)**, 237-246
10. A. L. Patey, J. R. Startin, P. M. Rowbottom, G. Shearer, *Food Addit. Contam.*, 1987, **4(1)**, 9-15
11. B. H. Licht, K. Shaw, C. Smith, M. Mendoza, J. Orr, D. V. Myres, *Food Chem. Toxicol.*, 1992, **30(5)**, 365-374
12. B. H. Licht, Shaw, C. Smith, M. Mendoza, J. Orr, D. V. Myres, *Food Chem. Toxicol.*, 1992, **30(5)**, 375-382
13. L. Royle, C. M. Radcliffe, *J. Sci. Food Agric.*, 1999, **79**, 1709-1714
14. B. H. Licht, K. Shaw, C. Smith, M. Mendoza, J. Orr, D. V. Myres, *Food Chem. Toxicol.*, 1992, **30(5)**, 383-387
15. M. J. Scotter, *Food Addit. Contam.*, 2011, **28(5)**, 527-596
16. J. S. Coffey, L. Castle, *Food Chem.*, 1994, **51**, 413-416
17. L. Royle, J. M. Ames, L. Castle, H. E. Nursten, C. M. Radcliffe, *J. Sci. Food Agric.*, 1998, **76**, 579-587
18. J. S. Coffey, H. E. Nursten, J. M. Ames, L. Castle, *Food Chem.*, 1997, **58(3)**, 259-267
19. L. Ciolino, *J. Agric. Food Chem.*, 1998, **46**, 1746-1753

20. R. A. Frazier, E. L. Inns, N. Dossi, J. M. Ames, H. E. Nursten, *J. Chromatogr. A*, 2000, **876**, 213-220
21. M. Manley-Harris, G. N. Richards, *Adv. Carbohydr. Chem. Bi.*, 1997, **52**, 207-266
22. J. Defaye, J. M. García Fernández, *Carbohydr. Res.*, 1994, **256**, C1-C4
23. J. Defaye, J. M. García Fernández, *Zuckerindustrie*, 1995, **120**, 700-704
24. M. Manley-Harris, G. N. Richards, *Carbohydr. Res.*, 1996, **287**, 183-202
25. V. Ratsimba, J. M. García Fernández, J. Defaye, H. Nigay, A. Voilley, *J. Chromatogr. A*, 1999, **844**, 283-293
26. J. Defaye, J. M. García Fernández, V. Ratsimba, *L'Actualité Chimique*, 2000, **236**, 24-27
27. A. Montilla, A. I. Ruiz-Matute, M. L. Sanz, I. Martínez-Castro, M. D. del Castillo, *Food Res. Int.*, 2006, **39**, 801-806
28. W. Meier-Augenstein, H. F. Kemp, S. M. L. Hardie, *Food Chem.*, 2012, **133**, 1070-1074
29. W. M. MacKenzie, R. I. Aylott, *Analyst*, 2004, **129**, 607-612
30. P. C. Ashok, B. B. Praveen, K. Dholakia, *Opt. Express*, 2011, **19(23)**, 22982-22992
31. A. G. Mignani, L. Ciaccheri, B. Gordillo, A. A. Mencaglia, M. L. González-Miret, F. J. Heredia, B. Culshaw, *Sensor. Actuat. B-Chem.*, 2012, **171-172**, 458-462
32. A. McIntyre, M. L. Bilyk, A. Nordon, G. Colquhoun, D. Littlejohn, *Anal. Chim. Acta.*, 2011, **690(2)**, 228-233
33. J. K. S. Møller, R. R. Catharino, M. N. Eberlin, *Analyst*, 2005, **130**, 890-897
34. M. Heller, L. Vitali, M. A. L. Oliveira, A. C. O. Costa, G. A. Micke, *J. Agr. Food Chem.*, 2011, **59**, 6882-6888
35. J. S. Garcia, B. G. Vaz, Y. E. Corilo, C. F. Ramires, S. A. Saraiva, G. B. Sanvido, E. M. Schmidt, D. R. J. Maia, R. G. Cosso, J. J. Acca, M. N. Eberlin, *Food Res. Int.*, 2013, **51**, 98-106
36. Y. S. Kim, S. Ha, Y. Yang, Y. J. Kim, S. M. Cho, H. Yang, Y. T. Kim, *Sensor. Actuat. B-Chem.*, 2005, **108**, 285-291
37. C. Wongchoosuk, A. Wisitsoraat, A. Tuantranont, T. Kerdcharoen, *Sensor. Actuat. B-Chem.*, 2010, **147**, 392-399

38. M. Boscolo, L. G. Andrade-Sobrinho, B. S. Lima-Neto, D. W. Franco, M. M. Ferreira, *J. AOAC Int.*, 2002, **85**, 744-750
39. D. Picque, P. Lieben, G. Corrieu, R. Cantagrel, O. Lablanquie, G. Snakkers, *J. Agr. Food Chem.*, 2006, **54**, 5220-5226
40. N. Naik, K. S. Jagadeesh, M. N. Noolvi, *Iranica J. Ener. Environ. I*, 2010, **4**, 347-351
41. B. C. Smith, *Infrared Spectral Interpretation: A Systematic Approach*, CRC Press, Boca Raton, 1999
42. J. Moore, C. Stanitski, P. Jurs, *Chemistry: The Molecular Science, Volume 2*, 3rd Edition, Thomas Brooks/Cole, Belmont, 2008
43. R. D. Deegan, O. Bakajin, T. F. Dupont, G. Huber, S. R. Nagel, T. A. Witten, *Nature*, 1997, **389**, 827-829
44. J. T. Wen, C. Ho, P. B. Lillehoj, *Langmuir*, 2013, **29**, 8440-8446
45. L. Lovergne, G. Clemens, V. Untereiner, R. A. Lukaszewski, G. D. Sockalingum, M. J. Baker, *Anal. Methods*, 2015, **7**, 7140-7149
46. *DDW: The Color House Webpage*, <http://www.ddwcolor.com/the-basics-of-caramel-colors>, Accessed 05/09/2014
47. G. Gardiner, BSc. Thesis, *An investigation of an attenuated total reflectance mid infrared spectrometry approach in the analysis of faded whisky*, University of Strathclyde, 2014
48. I. Goodall, S. Glancy, Scotch Whisky Research Institute, Edinburgh, *Personal Communication*, February 2014

4.0 THE APPLICATION OF CLASSIFICATION TOOLS FOR THE PREDICTION OF CARAMEL IDENTITIES

4.1 Introduction

4.1.1 Basis of this Study

The research presented previously in Chapter 3 assessed the potential of ATR-MIR spectrometry as a tool for profiling caramel colourants and it was clearly demonstrated that different caramel products possessed uniquely different spectral features. It was therefore possible to distinguish between caramels of different class (E150a – E150d) and also to differentiate between E150a caramels that had been produced using different conditions of manufacture. These findings were initially obtained from the assessment of caramels within 40% ethanol but were subsequently maintained when the same caramel materials were dissolved in the matrix of a typical Scotch Whisky blend. The work completed within this next chapter aimed to progress these findings further and determine whether it would actually be possible to predict the identity of test or ‘unknown’ caramels dissolved in Scotch Whisky, based on the characteristic ATR-MIR spectral features obtained. The ability to achieve this would be extremely beneficial to the Scotch Whisky industry, as the potential to confirm the presence (or absence) of a legally permitted caramel within a suspect product would aid in the determination of authenticity.

The research completed within this chapter therefore undertook preliminary studies to investigate and compare a selection of data analysis tools for the classification of a variety of test caramel solutions. It should be noted here that all test data were compared to calibration models constructed using caramels dissolved in 40% ethanol (i.e. pure caramel profiles). The test solutions initially investigated covered caramels dissolved at a typical concentration in 40% ethanol and in a typical Scotch Whisky blend and the main objectives were to determine firstly whether the caramel class could be correctly assigned and secondly whether the formulation of any E150a solutions could be subsequently predicted. Additional studies were then undertaken to investigate test solutions that represented non-typical situations: caramels dissolved in a blend matrix more heavily influenced by natural colour; caramel

solutions subjected to fade; and caramel solutions prepared at varied concentrations. Initial work presented within Chapter 3 indicated that such factors could influence the ATR-MIR spectral features acquired from caramel solutions.

4.1.2 Classification Tools for Profile Prediction – A Literature Review

From an assessment of the literature it was not possible to find any examples of data analysis tools being applied to the classification of caramel colourants, a finding that emphasised the novel nature of this research. A range of different classification tools were therefore compared within this chapter to determine the most appropriate approach. Those that provided the most useful information were: PCA with GLSW preprocessing, HCA, *k*-NN classification and PC-DFA. The literature review that follows explores how these data analysis tools have been implemented previously for classification and also describes some of the advantages and disadvantages that have been encountered.

4.1.2.1 GLSW preprocessing

As discussed previously in Chapter 2 (section 2.3.1.1), GLSW preprocessing creates a filter matrix that down weights differences between samples that should otherwise be similar and so its main goal is to eliminate or reduce the affects of extraneous variation, so that variation related to the task of interest can be more easily observed. GLSW has therefore proven extremely useful for a variety of applications within the literature and some of the most common uses found were: to remove interferences arising from background chemical species;^{1,2} to reduce variation caused by systematic sampling errors;^{3,4} to simplify calibration transfer problems by reducing variation caused by switching between instruments;^{5,6} and to compensate for scenarios that may cause measurement differences on a single instrument (e.g. temperature correction or system drift).⁷⁻⁹ The most relevant application of GLSW to this research however, was its implementation as a preprocessing tool for data being assessed using classification techniques.¹⁰⁻¹⁷ Within these publications, the implementation of GLSW was shown to maximise variation between classes whilst reducing the variability within classes, which gave better class discrimination and as a result typically improved classification accuracy. O. Rozenstein *et al.* for example

showed that the classification of different soil samples was significantly improved when GLSW was employed prior to the application of both partial least squares discriminant analysis (PLS-DA) and random forests (RF).¹⁰ In another example, J. H. da Silva Taveira *et al.* demonstrated that the addition of GLSW preprocessing was extremely beneficial when applied prior to PLS-DA, for the classification of coffee samples belonging to the same species but from different geographical origins.¹¹ These publications (along with a selection of others)¹²⁻¹⁵ clearly demonstrated that in certain situations, GLSW preprocessing can be a useful preprocessing tool when used prior to classification; its affect on each of the classification tools investigated within this chapter has therefore been investigated in cases where it was thought that prediction accuracy could be improved.

As well as being implemented prior to typical classification tools, examples were found in the literature of GLSW being used in combination with PCA, a more simplistic data analysis technique. Although PCA is normally considered as being an exploratory data analysis tool, literature indicated that the application of GLSW prior to PCA could potentially facilitate its use for classification due to its ability to improve distinction between sample classes.¹³⁻¹⁷ S. Serranti *et al.* for instance used GLSW preprocessing in combination with PCA to obtain better discrimination between oat and goat profiles based on NIR hyperspectral imaging data and in another publication, the same group demonstrated more distinct separation between different wheat kernels when GLSW was implemented prior to PCA (spectral data being utilised in this case). Although these two papers went on to assess different tools for the classification of test samples, some research by Eigenvector Research Inc. demonstrated that it is possible to use PCA with GLSW for classification and indicated that such an approach may be simpler than other classification tools.^{16,17} Researchers at Eigenvector Research Inc. used PCA in combination with GLSW to classify different types of food grade oil and as well as obtaining improved separation between sample groups, they were able to introduce T^2 confidence ellipses around each of the assigned classes within the calibration data.^{16,17} When test data were then projected onto the calibration model, 100% of test oil samples accurately fell within the corresponding confidence ellipses. It was also possible to clearly

identify when oil samples had been adulterated by the addition of a cheaper oil at a level greater than 5%. An approach similar to that employed by Eigenvector Research has therefore been investigated within this research to determine whether the same procedure (PCA with GLSW preprocessing) could be implemented for the classification of unknown caramel colourants based on characteristic differences in their ATR-MIR spectral profiles. The only potential limitation found in relation to the implementation of GLSW preprocessing prior to the application of a classification tool was that any potential sources of extraneous variation within samples would typically have to be accounted for within the calibration data to allow for accurate predictions to be obtained.¹⁸

4.1.2.2 HCA

As discussed previously in Chapter 2 (section 2.3.2) HCA is an unsupervised pattern recognition tool and so aims to search for groupings between samples without the use of pre-established class information. If samples of different categories can therefore be distinguished between using HCA, it can be a very useful tool for classification; the prediction of test data would however have to be manually interpreted. Examples of HCA being implemented for a wide variety of applications were observed in the literature and these included fields such as: metabonomics/metabolomics;¹⁹⁻²⁵ market research/analysis;²⁶⁻³⁰ studies relating to the food and drinks industries;³¹⁻³⁵ and also for medical applications (e.g. for disease diagnosis and psychiatry).³⁶⁻⁴²

In all of the publications identified above, it was found that HCA was most useful as an exploratory tool. In other words it was implemented simply to determine whether samples could be classified into distinct groupings but not to actually predict the identities of unknown/test data; this was instead completed using an additional multivariate data analysis tool, if completed at all. Y. Tikunov *et al.* for instance used HCA to distinguish between different types of tomatoes using GC-MS data of the volatile tomato constituents; the authors however, did not go on to predict test sample identities.²⁰ In a different publication, O. Beckonert *et al.* implemented HCA as a means to provide an impression of how well sample groups could be separated prior to applying a subsequent classification tool.¹⁹ The authors were testing urine

taken from mice dosed with different toxins to determine whether similarities were present in the response of the animals to four classes of toxin (control, liver, kidney and other). It was shown that HCA had the ability to discriminate between these four classes (based on ^1H NMR spectral data) and subsequent data analysis using k -NN classification demonstrated very good prediction rates when applied to test data. In another example, C. Yu *et al.* successfully utilised HCA based on HPLC data to clearly distinguish between three different species of the ginseng plant (often used for medicinal purposes but only one of the three species is considered as appropriate for a wider range of patients).⁴² The authors were then able to successfully predict the identity of test samples using LDA and so their findings demonstrated the possibility to screen ginseng for medicinal purposes to ensure that it has originated from the correct source/species.

A similar approach as those described above was therefore undertaken within this research project; HCA was used as an exploratory data analysis tool to investigate whether samples could be clearly classified into distinct groupings, before additional classification tools were investigated for predicting the identities of test data. No examples of HCA being applied to differentiate between caramel colourants could be found in the literature (indicating the novelty of attempting this) however there were publications demonstrating its successful application using infrared data (the type being implemented within this research). M. De Luca *et al.* for example implemented HCA for the classification of Moroccan olive oils that had been analysed using fourier transform infrared (FTIR) spectrometry.³² The authors successfully demonstrated that HCA was able to separate olive oils produced from four different regions into four corresponding groupings, the separation between each class being extremely distinct. This was described as being related to the good sensitivity of FTIR and its ability to obtain unique fingerprints of compounds (in this case picking up on differences in samples of the same variety of olive oil that differ only in production locations). In another publication, S. Gok *et al.* have also demonstrated the successful application of HCA to IR data.³¹ S Gok *et al.* utilised ATR-FTIR to analyse honey samples from different botanical origins to determine whether their profiles could be distinguished between. Twelve different sample types were

included in the study: five classes originated from flowers, three were from trees, three were fake honey (commonly known adulterants) and one was maple syrup (used as a non honey control). When HCA was applied to the data, clear cut clusters were obtained, in the first instance splitting the samples into four groupings: those originated from flowers; those sourced from trees; those that were fake; and those that were maple syrup. It was also demonstrated that all samples had as their nearest neighbour samples from the same class, indicating that in general the data could also be split further into the twelve individual sample types using HCA. This publication in particular indicated that HCA could be well suited for allowing different types of caramel colourants to be separated into clusters according to their class or E150a formulation. The publication by S Gok *et al.* includes figures of the ATR-FTIR spectra of the different honeys and many of the features shown are similar to those observed in Chapter 3 for caramel materials, carbohydrates being responsible for the majority of peaks in both cases.³¹ The success observed in this piece of literature based on small compositional differences between honey types could therefore be indicative of the same success being observed with caramel substances that vary only due to slight changes in manufacturing conditions.

4.1.2.3 *k*-NN classification

As described beforehand in Chapter 2 (see section 2.3.2.2), *k*-NN classification is a supervised pattern recognition technique and so can be used to predict the identities of test samples by their comparison to a training set (where the class membership of samples has already been established). The *k*-NN tool can therefore be implemented for classification in a wide range of applications and a review of the literature demonstrated examples of its use in medical/biological fields,⁴³⁻⁴⁹ within the fuel industry,⁵⁰⁻⁵² for metabonomic/metabolomic studies,^{19,53} and most relevant to this research, frequent references were found relating to the application of *k*-NN for classification in the food and beverage industry.⁵⁴⁻⁶² Many of the publications listed above also demonstrated *k*-NN being applied successfully for the classification of spectroscopic data.^{43-45,50,51,54-56,58-60} This therefore indicated that *k*-NN classification could have potential for classifying caramel colourants within this research, which were analysed using ATR-MIR spectrometry.

Some of the most notable examples found within the literature were published by the following authors: M. Kansiz *et al.*, who demonstrated the use of *k*-NN for the classification of 6 different cyanobacterial strains analysed using FTIR spectrometry - test data being predicted with an accuracy level of 98% or above when the wavelength range (and data preprocessing conditions) utilised to build the *k*-NN model was optimised;⁴³ R. M. Balabin *et al.*, who showed that *k*-NN could successfully classify both gasoline (by its type) and 10 different types of biodiesel samples when analysed using NIR spectrometry, obtaining prediction accuracies typically greater than 96% and 93% respectively;^{50,51} E. Sikorska *et al.*, who illustrated that *k*-NN classification could be used to predict the identity of 8 different types of edible oils with a prediction accuracy of approximately 98% – the oil samples being analysed using fluorescence spectroscopy;⁵⁴ and H. B. Ding *et al.*, who analysed beef hamburgers using NIR spectrometry and demonstrated that *k*-NN classification could be used to classify test samples as being authentic or adulterated with other meats/ingredients with a prediction accuracy of up to ~93%.

A common consensus identified between the papers demonstrating applications of *k*-NN classification, was that the main advantage of this tool is related to its simplicity and ease of implementation – persons who are not experts in analytical chemistry and/or chemometrics could still easily interpret the data produced by this technique.^{45,50-51} In addition, the *k*-NN models themselves can be quickly constructed with only basic programming skills.⁵⁰⁻⁵¹ A few of the publications also indicated a further advantage of the *k*-NN technique over other classification tools being related to the fact that it is free from statistical assumptions about class distributions.^{55,61} One potential limitation identified in relation to *k*-NN classification was that it typically requires a large training set of samples to improve performance.⁶¹

4.1.2.4 PC-DFA

As described previously in Chapter 2 (section 2.3.2.3) PC-DFA is a supervised pattern recognition technique and so like *k*-NN classification, it can be used to classify test/unknown samples based on the identity of previously classified samples in a training dataset. PC-DFA is generally considered as being equivalent to the

classification tool LDA but in the case of the former, PCA is performed prior to LDA so as to reduce the dimensionality of data. This additional step prior to LDA can be a common requirement when being implemented for classification, as LDA becomes restricted when the number of variables being assessed is higher than the number of samples (commonly seen with spectroscopic/chromatographic data).^{53,55,63} Many examples of LDA and PC-DFA being implemented for classification were observed within the literature and these examples were found to assess samples covering a wide range of fields (as was the case for previously described multivariate data analysis tools): medicinal/biological studies;^{44,46,64,65} engineering applications;⁵⁰ metabolomic research;^{53,63,66-68} and investigations within the food and drinks industry.^{54-56, 59-62,69-70}

As was the case for *k*-NN classification, examples of LDA/PC-DFA being applied to spectroscopic data were observed amongst those listed above, highlighting that it may have potential for the classification of caramel colourants analysed using ATR-MIR spectrometry. Some of the papers demonstrating successful classification using spectroscopic data were published by the following authors: P. Ritthiruangdej *et al.*, who demonstrated the use of LDA to classify three types of fish sauce (analysed using NIR spectrometry) into groupings with a classification rate above 82%;⁵⁵ E. Sikorska *et al.*, who showed the implementation of LDA to successfully classify beers according to their duration of storage, analysed *via* fluorescence spectroscopy;⁶⁰ R. M. Jarvis *et al.*, who successfully implemented PC-DFA to discriminate between and classify different strains of bacteria according to their surface-enhanced Raman scattering spectra;⁶⁴ and R. Goodacre *et al.*, who demonstrated the use of PC-DFA to classify authentic cocoa butters *vs.* those that had been adulterated with other vegetable fats, the data being acquired using FTIR spectrometry.⁷⁰

One of the main advantages of LDA/PC-DFA that was highlighted *via* the literature was that it is typically considered fast and simple to implement and will give good classification when samples are linearly separable.^{63,71} Although few limitations of this tool were identified, a few publications highlighted that model performance will suffer when data are highly collinear.^{44,53,63} G. Kos *et al.* for example experienced

this limitation of LDA when attempting to classify healthy corn samples *vs.* those afflicted with a fungal infection.⁴⁴

One of the overall observations highlighted when reviewing literature relating to classification tools was that they each have their own associated advantages and disadvantages and so one is not always better than another. In other words, the performance of different classification tools will typically depend on the data being examined. Many publications identified throughout this literature review were therefore found to contain comparisons of multiple classification tools rather than just a single data analysis technique being presented. This became particularly evident early on in the literature review, as many of the publications previously identified as showing examples of *k*-NN classification were also found to assess their datasets using LDA or PC-DFA (as well as other classification tools not assessed within this research).^{44,46,50,53-56,59-61} It was for this reason that not just a single data analysis tool was selected to assess the prediction of caramel colourants within this research; so that the most effective and appropriate approach could be determined for this case.

4.1.3 Study Objectives

This chapter aimed to compare different multivariate data analysis tools for the prediction of caramel identities based on a comparison of their dried residue profiles (obtained via ATR-MIR spectrometry) to those obtained from pure caramel spectra. PCA with GLSW, HCA, *k*-NN classification and PC-DFA were all investigated for this purpose and the work aimed to assess their abilities firstly to predict the caramel class of test data and secondly to determine whether individual E150a formulations could be identified. A variety of test datasets were constructed to examine the capabilities of each data analysis tool for caramel prediction and the main objectives that they covered were:

- To assess the ability of each classification tool to predict caramel profiles when dissolved in 40% ethanol (the same solution medium as the calibration samples).

- To determine whether prediction of caramel identities is still possible when caramels are dissolved in a typical Scotch Whisky matrix.
- To identify whether high levels of natural colour within the background whisky matrix would mask the ability of data analysis tool to predict caramel identities.
- To determine whether variation in caramel concentration would affect the ability of classification tools to predict the identity of profiles.
- To find out what effect caramel fade would have on profile predictions.

After the exploration of these initial aims, an additional study was undertaken within this section of the research to assess whether any of the classification tools could also be used to predict the identity of blends already on the market. Four blends were used to construct the calibration model in this case and test data consisting of additional examples of these blends were projected onto the model to assess the prediction of their identities.

4.2 Experimental

4.2.1 Samples

To allow a comparison of data analysis tools for the prediction of caramel identities, this research attempted to classify a selection of different test samples based on the identity of previously classified calibration samples. The samples incorporated within both the calibration and test datasets are described over the following subsections.

4.2.1.1 Calibration samples/data

Two calibration datasets were compiled as part of this research: Dataset 1, which contained a range of caramel and burnt sugar materials and classified the calibration samples according to the identity of their caramel class; and Dataset 2, which contained only E150a caramels and classified samples according to their E150a formulation. The former aimed to assess the ability of the chosen classification techniques to predict the caramel class of test samples, whilst the objective of the latter was to assess the prediction of different E150a formulations. The calibration data used within this section of the research was that already acquired using ATR-MIR spectrometry within Chapter 3 for the samples described in section 3.2.1.1 (Table 3.1) when caramels/burnt sugars were dissolved in 40% ethanol. All samples had been analysed in triplicate as per the methodology described in section 3.2.4.1 and the resulting spectra (utilised for calibration models in this part of the research) have been summarised within Table 4.1, which also illustrates what sample spectra were incorporated within each of the two calibration datasets (and the calibration categories associated with each).

In general, all spectra incorporated within each calibration dataset were utilised for the construction of calibration models, however during the use of certain classification techniques the models required optimisation/validation. In these cases the calibration datasets were split into calibration spectra and validation spectra. The samples chosen for the latter grouping have been highlighted within Table 4.1 for both calibration datasets. The data analysis tools that required this to be undertaken have been highlighted where relevant in the results and discussion (section 4.3),

otherwise it should be assumed that all calibration samples for each dataset were utilised for the construction of calibration models.

Table 4.1: Summary of the ATR-MIR sample spectra utilised for the construction of calibration models within this chapter of the research.

	Dataset 1 Calibration Categories	Dataset 2 Calibration Categories				
Spectrum No.	Caramel Class	Caramel Identity	Batch No.	Replicate No.		
1 ^{1,2}	E150A	E150A_X1	1	1	Calibration Dataset 1	Calibration Dataset 2
2				2		
3 ^{1,2}				3		
4			1			
5			2	2		
6 ^{1,2}				3		
7 ^{1,2}				1		
8			3	2		
9 ^{1,2}				3		
10 ^{1,2}		1				
11 ¹		E150A_X2	1	2		
12				3		
13 ^{1,2}				1		
14			2	2		
15 ^{1,2}				3		
16				1		
17 ^{1,2}			3	2		
18 ^{1,2}				3		
19 ^{1,2}				1		
20 ¹		E150A_Y3	1	2		
21				3		
22 ^{1,2}				1		
23 ¹			2	2		
24				3		
25 ¹		E150A_Y4	1	1		
26 ¹				2		
27 ^{1,2}				3		
28			2	1		
29 ^{1,2}				2		
30		3				
31		E150A_Y5	1	1		
32				2		
33 ¹				3		
34 ^{1,2}			2	1		
35				2		
36 ^{1,2}		3				
37		E150A_Z6	1	1		
38				2		
39				3		
40 ^{1,2}		E150A_Z7	1	1		
41				2		
42 ^{1,2}				3		
43		E150A_Z8	1	1		
44 ^{1,2}				2		
45				3		
46	E150B	E150B_X9	1	1		
47				2		
48 ¹				3		

¹ Denotes the spectra utilised as validation samples (in certain cases) for Calibration Dataset 1.

² Denotes the spectra utilised as validation samples (in certain cases) for Calibration Dataset 2.

Table 4.1 cont.: Summary of the ATR-MIR sample spectra utilised for the construction of calibration models within this chapter of the research.

	Dataset 1 Calibration Categories	Dataset 2 Calibration Categories			
Spectrum No.	Caramel Class	Caramel Identity	Batch No.	Replicate No.	
49 ¹	E150C	E150C_X10	1	1	Calibration Dataset 1
50				2	
51 ¹				3	
52			2	1	
53				2	
54				3	
55	E150D	E150D_X11	1	1	
56 ¹				2	
57 ¹				3	
58			2	1	
59 ¹				2	
60				3	
61	Burnt Sugars	BS_X12	1	1	
62				2	
63 ¹				3	
64		BS_X13	1	1	
65				2	
66 ¹				3	
67		BS_X14	1	1	
68 ¹				2	
69 ¹				3	

4.2.1.2 Test samples/data

Five different test datasets were put together for this section of the research to examine the ability of different classification tools to predict caramel identities. Each test dataset was compiled to assess the prediction of caramel solutions representing different scenarios, all of which have been summarised below.

Test Set 1

Test Set 1 consisted of a selection of caramels dissolved in 40% ethanol (the same solution medium as the calibration samples) to allow an initial examination of the classification tools for predicting caramel profiles without any interference from other background sources. The samples included in Test Set 1 have been summarised within Table 4.2, where they have been split into four groups representing four different scenarios (as described in the table). All of these samples were analysed using ATR-MIR spectrometry as per the methodology described in Chapter 3 (section 3.2.4.1), triplicate spectra being acquired for each of the 10 samples.

Table 4.2: Summary of the test samples included within Test Set 1

Group Number	Test Sample Description	Category for Caramel Class	Category for E150a Formulation	No. of batches
1	E150A_X1 caramels re-prepared and re-analysed (Batches 1 and 2 from Table 4.1)	E150A	E150A_X1	2
2	New E150A_X1 caramels (i.e. fresh caramel samples not analysed before)		E150A_X1	2
3	New E150A_X2 caramels (i.e. fresh caramel samples not analysed before)		E150A_X2	2
4	E150A_X1 caramels passed their expiry date (newly acquired)		E150A_X1	4
			Total Samples	10

Test Set 2

Test Set 2 comprised of a selection of caramel materials dissolved in a typical blend whisky (Blend Whisky A as described in Chapter 3, section 3.2.1.1). Fifteen caramels were included in total and incorporated: twelve E150a caramels (at least one batch from each of the eight different formulations assigned in the calibration dataset); one batch of E150B_X9; a single batch of E150C_X10; and one batch of E150D_X11. These samples had been analysed previously as part of the preliminary studies within Chapter 3 (see section 3.3.1.3) and so their spectral data were taken forward to this section of the research to assess how the background matrix of typical whiskies might influence the prediction capabilities of classification tools. All samples were analysed as per the methodology described within section 3.2.4.2, each being analysed in triplicate.

Test Set 3

Test Set 3 was made up of five caramel samples dissolved in Blend Whisky B, a blend representing high levels of colour that would be developed naturally for a Scotch Whisky product. The caramels included within Test Set 3 comprised of one batch of E150A_X1, three batches of E150A_X2 and a single batch of E150A_Y5.

These samples were again analysed in triplicate as per the methodology previously depicted within section 3.2.4.2 and were included to determine whether the prediction of caramel identities using classification tools would be influenced by extremely high levels of natural whisky colour in the background matrix.

Test Set 4

Test Set 4 comprised of data acquired from caramel samples previously analysed as part of preliminary research within Chapter 3 (section 3.3.2.1) and was included as part of this subsequent study to examine whether/how changes in caramel concentration might influence profile predictions. A total of eight caramel solutions were included as part of Test Set 4 and encompassed the E150A_X1 caramel solutions dissolved in 40% ethanol previously described in section 3.2.4.3 (the samples from the study of concentration that were dissolved in Blend Whisky A were not included at this point). To summarise, these sample solutions were split into two subsets each containing four initially identical solutions ranging in absorbances from 0.2 – 0.8 (at 430 nm) in increments of 0.2. The Subset 1 samples were then prepared for analysis by pre-concentrating through reduction of the volume from 6000 μ L to 300 μ L, in other words maintaining the variation in caramel concentration. The Subset 2 samples were prepared for analysis by pre-concentrating from 6 mL to a volume that resulted in each caramel sample possessing the same final concentration prior to analysis using ATR-MIR spectrometry. More details relating to the preparation and ATR-MIR analysis of these samples can be found in Chapter 3, section 3.2.4.3.

Test Set 5

Test Set 5 was put together to investigate whether caramel fade would influence the prediction of caramel profiles using classification tools and it comprised of the samples previously investigated during preliminary studies within Chapter 3 (section 3.3.2.2). This test set therefore included eight samples each for an E150A_X1, an E150A_X2 and an E150D_X11 caramel, in each case covering 3 control samples (not faded) and 5 solutions subjected to different degrees of fade up to a final level representing the extreme case likely to be observed in a real Scotch Whisky product.

Additional details relating to the preparation and analysis of these samples can be found previously in section 3.2.4.4. Triplicate ATR-MIR spectra were acquired of all sample solutions and subsequently utilised for data analysis.

4.2.2 Data Analysis

4.2.2.1 Data preparation/pre-treatment

All ATR-MIR data were initially imported into MATLAB version 7.13.0.564 (R2011b) (Mathworks Inc., WA, USA) with PLS_Toolbox version 6.7 (Eigenvector Research Inc., WA, USA) incorporated. Prior to the application of any multivariate data analysis however, all raw data were processed using a Savitsky-Golay first derivative filter, which employed a width of 7 data points and a second order polynomial. All data analysis tools were then carried out using 155 variables in the 625 – 1813 cm^{-1} range of the derivatised spectra, so as to remove regions contributing only noise to the measurements. All data were normalised to the largest peak (consistently found between 950 and 1050 cm^{-1}) and mean centred before any classification tools were implemented.

4.2.2.2 PCA with GLSW preprocessing

PCA with GLSW preprocessing was undertaken using MATLAB software incorporating the PLS_Toolbox (the details of which have already been described above). The theory behind this technique has been described previously in Chapter 2 (section 2.3.1.1) and to briefly summarise it aims to enable optimal discrimination between classes by the implementation of a filter matrix that ultimately allows the reduction of within class variation whilst maximising between category variation. Two calibration models were constructed using PCA with GLSW preprocessing in this part of the research: one using the spectra of Calibration Dataset 1 and the other using the Calibration Dataset 2 spectra (details contained in Table 4.1). Only a single parameter had to be set for the construction of these calibration models (the weighting parameter (α)) and this was assigned a value of 0.06 for Calibration Dataset 1 and 0.03 for Calibration Dataset 2. These values were optimised using a trial and error approach by splitting each calibration dataset into calibration and

validation samples; the validation samples used for each of the calibration datasets have been indicated in Table 4.1.

4.2.2.3 HCA

HCA was undertaken using MATLAB software incorporating the PLS_Toolbox (the details of which have already been described above). The background theory for this data analysis tool has been described previously in section 2.3.2.1 and to quickly recap, this technique aims to detect similarities between samples and so search for groupings, without the use of pre-established class information. Two HCA models were initially constructed for this research, using Calibration Dataset 1 in the first instance and in the second using Calibration Dataset 2. In both cases the raw data (after data pre-treatment) were implemented for HCA, the distances between samples were defined using the Euclidean distance and the distances between groups of samples were measured using the nearest neighbour method. All 69 calibration spectra shown in Table 4.1 were utilised during the construction of the HCA calibration model for Dataset 1, whilst all of the relevant 45 spectra were utilised for the calibration model corresponding to Dataset 2. A third HCA model was additionally constructed using the same parameters as stated above and all of the Dataset 2 spectra. This however implemented the use of GLSW preprocessing using an α value of 0.03 to allow an improvement in class discrimination in this case.

4.2.2.4 *k*-NN classification

The technique of *k*-NN classification was undertaken using MATLAB software incorporating the PLS_Toolbox (the details of which have already been described above). The theory behind this classification tool can be found previously in section 2.3.2.2 and to briefly summarise, this tool allows the prediction of test samples based on the majority identity of the *k* nearest calibration samples (whose class memberships are already known). Two calibration models were constructed when utilising *k*-NN classification, one using all spectra from Calibration Dataset 1 and the other using all spectra from Calibration Dataset 2. In both cases a *k* value of 3 was implemented and GLSW preprocessing was utilised for the construction of the

Dataset 2 calibration model (using an α value of 0.03) to improve differentiation between categories.

4.2.2.5 PC-DFA

Data analysis utilising PC-DFA was completed by Piotr Gromski (a postdoctoral scholar within the same group at the University of Strathclyde at the time this research was undertaken) and conducted in R version 3.1.0. The background theory for PC-DFA has been described previously in 2.3.2.3 and its main objective is to seek out canonical variates that will maximise between group distances whilst reducing within category variation. Classification is generally very good when samples are linearly separable. As has generally been the case for the other classification tools, two PC-DFA calibration models were constructed within this work, for both calibration dataset 1 and 2. It should be noted however, that although all of the relevant 45 spectra were used in the construction of the latter model, the calibration model built for Calibration Dataset 1 was prepared using only the 34 spectra not marked as validation spectra. This was for ease of visualisation in the measurement space.

4.3 Results and Discussion

4.3.1 PCA with GLSW Preprocessing

Chapter 3 demonstrated good discrimination between different caramel classes using PCA, however as an unsupervised technique, PCA alone cannot be used for the prediction and classification of test samples. The additional implementation of GLSW as a preprocessing tool however, requires that the PCA model be provided with information about the category of all samples included, so that variation between samples of the same category can be minimised whilst between category variation is maximised or maintained. Prior knowledge of the category of calibration samples therefore also means that the potential exists to determine the identity of test or ‘unknown’ samples based on whether they fall within any of the confidence ellipses associated with the pre-assigned calibration groupings. The ability of PCA with GLSW preprocessing to determine the identity of test caramel samples is consequently discussed within the following sections. Two calibration datasets were investigated: Dataset 1, which assessed prediction of the unknown caramel class (i.e. can a sample profile be predicted as E150a as opposed to a different caramel class or burnt sugar); and Dataset 2, which assessed whether a particular E150a formulation could subsequently be predicted. Prior to the investigation of either dataset however, the GLSW parameters required optimisation and so this is discussed initially in section 4.3.1.1 below.

4.3.1.1 Optimisation of the weighting parameter (and model validation)

As described previously in section 2.3.1.1, GLSW utilises an algorithm that calculates a filter matrix from the differences between samples which should otherwise be similar. The filter matrix is then used to down weigh these differences which it considers interference or ‘clutter’ and so in the case of classification this can enable better discrimination of classes to be obtained. The degree to which the filter matrix down weighs clutter is dictated by the weighting parameter (α), the only adjustable parameter within the GLSW algorithm; adjusting α towards higher values decreases the effects of the filter, whilst lower values would apply a higher degree of filtering. The α value has to be optimised for any individual dataset and this was done manually within this research by splitting the calibration samples into a

‘calibration’ set and a ‘validation’ set (see Table 4.1 for details). The α parameter was then optimised based on classification error for the validation dataset, where a range of different α values were applied to construct different PCA with GLSW calibration models and the most appropriate model was selected based on how well the validation data was predicted onto each calibration model. An α value of 0.02 was used as a starting point for this process, as this was the value recommended by the software tutorial.² Additional values above and below this were then compared (0.005 – 0.09) to assess which would provide the optimum value. It was found that α values of 0.06 and 0.03 were the most appropriate for use with calibration Dataset 1 and calibration Dataset 2 respectively. Figure 4.1a shows the PC1 vs. PC2 scores plot obtained from the optimum PCA with GLSW calibration model chosen for Dataset 1, whilst Figure 4.2a illustrates the PC1 vs. PC2 scores plot acquired from the optimum PCA with GLSW calibration model chosen for Dataset 2. Figures 4.1b and 4.2b have also been included to show the PCA data without GLSW preprocessing and correspond to Datasets 1 and 2 respectively. These have been included to demonstrate that for both datasets, the implementation of the GLSW preprocessing tool has clearly enabled within category variation to be reduced whilst maintaining or maximising the between category variation.

From Figure 4.1a, differentiation is clearly visible between all of the calibration categories of Dataset 1 apart from the E150a and burnt sugar groupings. This can instead be seen more clearly in Figure 4.1c, which shows an enlargement of the subspace surrounding the E150a and burnt sugar clusters. Although there is still a slight amount of overlap visible between the confidence ellipses for these two categories, improved distinction could be obtained along the PC3 axis. The relevant PC1 vs. PC3 scores plot has been provided in Figure 4.3 to demonstrate this finding.

Figure 4.2a demonstrates clear differentiation between all of the calibration categories of Dataset 2, apart from the E150A_X3 and E150A_X4 caramels, whose confidence ellipses overlap (Figure 4.2c). This however can be related to the findings of Chapter 3 that indicated these two caramels possessed similar compositions due to similarities in their production conditions.

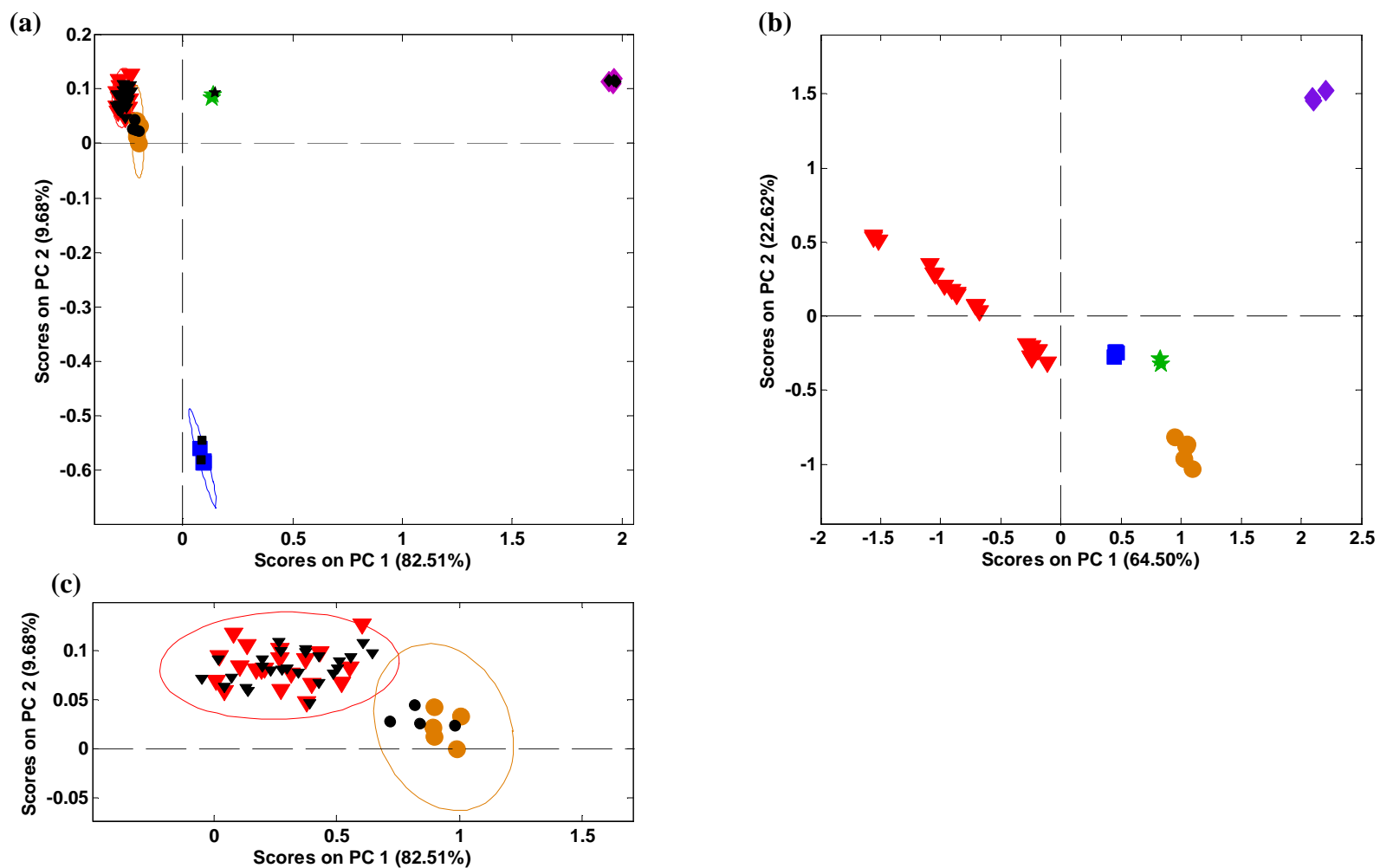


Figure 4.1: (a) *PC1 vs. PC2 scores plot obtained from PCA with GLSW ($\alpha=0.06$) of the ATR-MIR spectra acquired for the calibration samples of Dataset 1. The Dataset 1 validation samples are projected onto this calibration subspace.* (b) *Corresponding PC1 vs. PC2 scores plot obtained from PCA without GLSW preprocessing.* (c) *Shows an enlargement of the region surrounding the two clusters assigned as E150a caramels and burnt sugars. All relevant sets of calibration samples are enclosed by 95% confidence ellipses. KEY: E150a calibration caramels (red triangles), E150b calibration caramels (green stars), E150c calibration caramels (blue squares), E150d calibration caramels (purple diamonds), Burnt Sugar calibration caramels (orange circles), E150a validation caramels (black triangles), E150b validation caramels (black stars), E150c validation caramels (black squares), E150d validation caramels (black diamonds), Burnt Sugar validation caramels (black circles).*

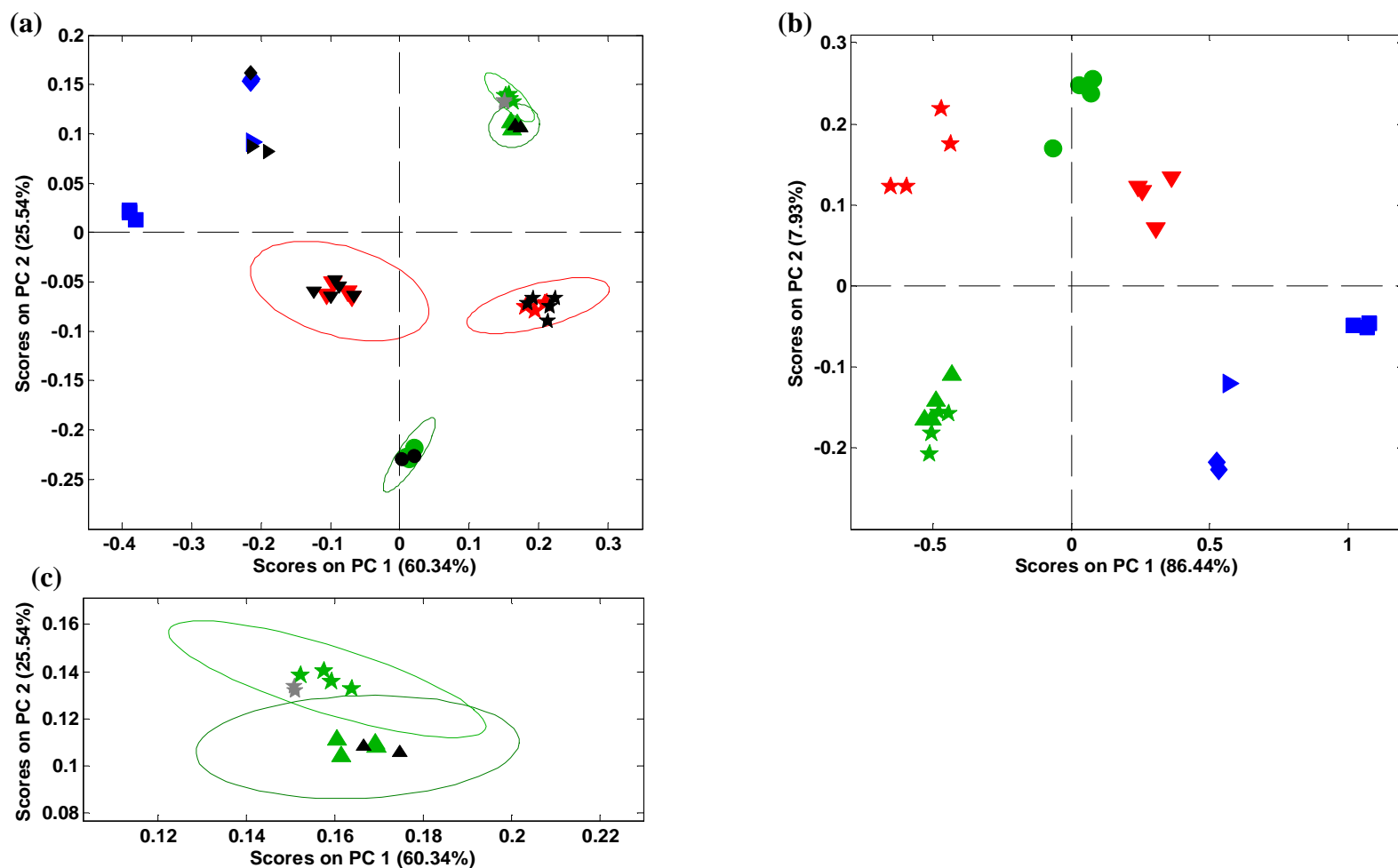


Figure 4.2: (a) PC1 vs. PC2 scores plot obtained from PCA with GLSW preprocessing ($\alpha=0.03$) of the ATR-MIR spectra acquired for the calibration samples of Dataset 2. The Dataset 2 validation samples are projected onto this calibration subspace. (b) Corresponding PC1 vs. PC2 scores plot obtained from PCA without GLSW preprocessing. (c) Shows an enlargement of the region surrounding the two clusters assigned as E150a_Y3 and E150a_Y4 caramels, both sets of calibration samples including 95% confidence ellipses. KEY: E150a_X1 calibration caramels (red triangles), E150a_X2 calibration caramels (red stars), E150a_Y3 calibration caramels (green triangles), E150a_Y4 calibration caramels (green stars), E150a_Y5 calibration caramels (green circles), E150a_Z6 calibration caramels (blue squares), E150a_Z7 calibration caramels (blue triangles), E150a_Z8 calibration caramels (blue diamonds). The symbols for the E150a validation samples match those of their corresponding calibration category but they are all coloured black (E150a_Y4 validation samples are grey stars to differentiate from E150a_X2 validation samples).

Figures 4.1a and 4.1c clearly demonstrated that when using an α value of 0.06 for PCA with GLSW, the validation samples for Dataset 1 overlaid extremely well with the samples of corresponding category in the calibration data. All validation samples were found within the 95% confidence ellipses of their corresponding calibration category where relevant. These findings were not as pronounced when α values lower than 0.06 were examined and when values higher than 0.06 were assessed, the between category variation began to significantly increase. This therefore indicated that an α value of 0.06 was optimum when PCA with GLSW preprocessing was undertaken for Dataset 1.

In the case of Dataset 2, Figures 4.2a and 4.2c clearly demonstrated that all validation samples overlaid very well with the samples of corresponding category in the calibration data, when an α value of 0.03 was used for PCA with GLSW preprocessing. All validation samples were found within the 95% confidence ellipses of their corresponding calibration category where relevant. When α values lower than 0.03 were examined the validation samples did not overlay sufficiently with their corresponding calibration data and when α values higher than 0.03 were assessed the reduction of between category variation was compromised.

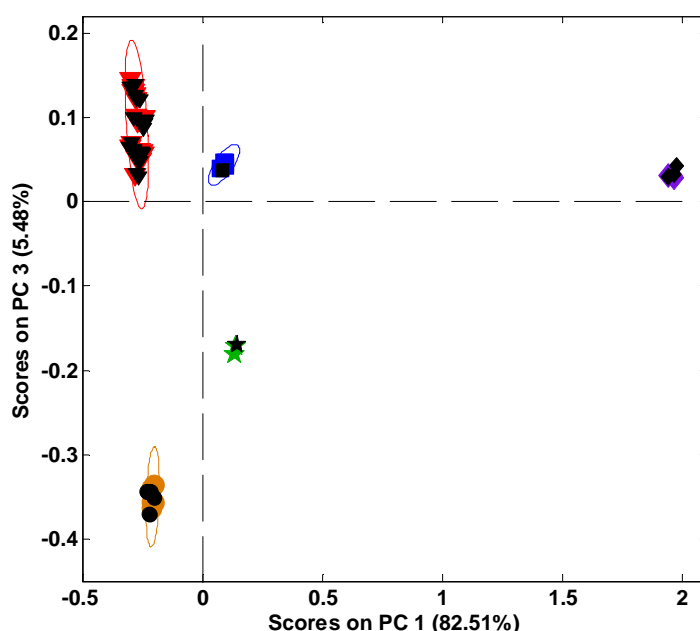


Figure 4.3: PC1 vs. PC3 scores plot obtained from PCA with GLSW preprocessing ($\alpha=0.06$) of the ATR-MIR spectra acquired for the calibration samples of Dataset 1. The Dataset 1 validation samples are projected onto this calibration subspace.

4.3.1.2 Predicting the caramel class and E150a formulation of test data

Test Set 1 – Caramels in 40% ethanol

Test Set 1 consisted of 10 caramel samples split into four groups (see Table 4.2). The four different groups have been summarised below along with an explanation as to their purpose as part of this test dataset:

- (1) 2 x batches of E150A_X1 re-prepared and re-analysed; to assess whether the PCA model (with GLSW preprocessing) is robust for the prediction of samples already incorporated within the calibration data.
- (2) 2 x batches of E150A_X1 freshly acquired and analysed; to determine whether the PCA model (with GLSW preprocessing) is robust for the prediction of fresh caramel samples, not previously found in the calibration data.
- (3) 2 x batches of E150A_X2 freshly acquired and analysed; included for the same reason as (2) but to investigate the prediction of a different E150a formulation.
- (4) 4 x batches of E150A_X1 passed their date of expiry; to ascertain whether prediction of caramel class and E150a formulation would be affected by the degradation of caramels over their likely time of use in industry.

It should also be noted here that all of the above samples were dissolved in 40% ethanol prior to analysis so as to match the medium of the calibration samples. This was done for Test Set 1 so that predictions could initially be undertaken without any interference from other background sources (e.g. the Scotch Whisky matrix).

Once ATR-MIR spectra had been acquired for all 10 of the test samples in Test Set 1 (analysed in triplicate), the spectra were first projected into the PCA with GLSW calibration model for calibration Dataset 1 to obtain scores and see whether their caramel class could be correctly predicted as E150a. Figure 4.4a illustrates the resulting PC1 vs. PC2 scores plot and it was clearly demonstrated that all of the test data points overlaid very closely with the E150a classed calibration samples. This can be seen more clearly in Figure 4.4b which shows an enlargement of the subspace

surrounding the E150a and burnt sugar calibration clusters. All of the test samples are clearly demonstrated to fall within the 95% confidence ellipse defined by the E150a calibration samples. To emphasise the prediction of these test caramels as being E150a classed caramels further, the PC1 vs. PC3 scores plot has been provided (Figure 4.5) and clearly shows all of the test samples overlaying with the E150a class, separated more obviously from the burnt sugars along the PC3 axis.

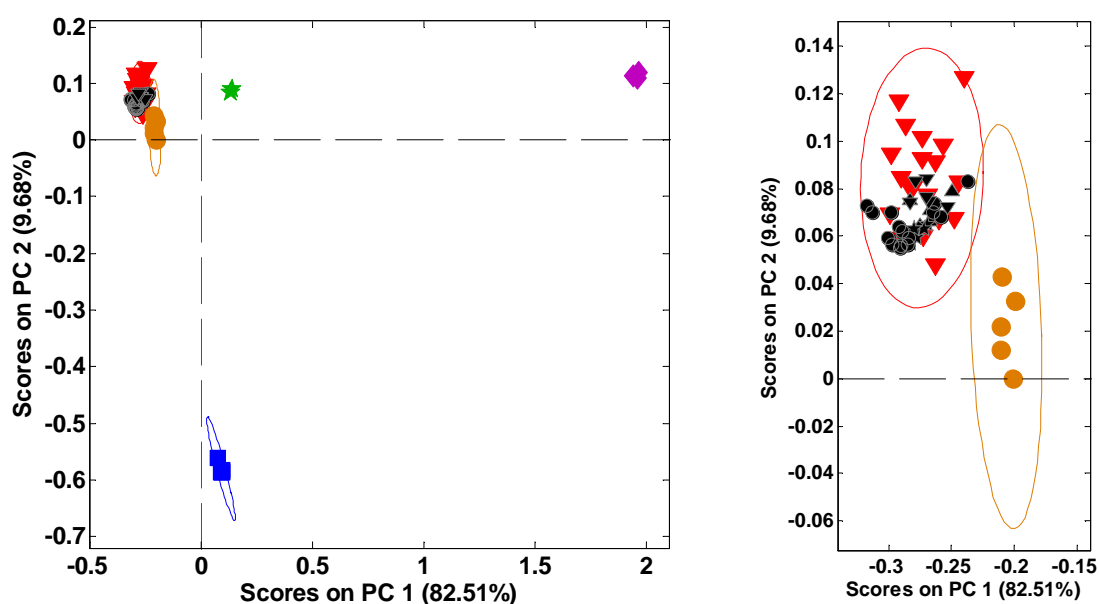


Figure 4.4: (A) Projection of the PC1 vs. PC2 scores for the Test Set 1 samples onto the subspace defined by the PCA with GLSW calibration model obtained for Calibration Dataset 1. (B) Shows an enlargement of the region surrounding the two calibration clusters assigned as E150a caramels and burnt sugars. KEY: E150a calibration caramels (red triangles), E150b calibration caramels (green stars), E150c calibration caramels (blue squares), E150d calibration caramels (purple diamonds), Burnt Sugar calibration caramels (orange circles), E150a Test Set 1 samples (black symbols with grey borders).

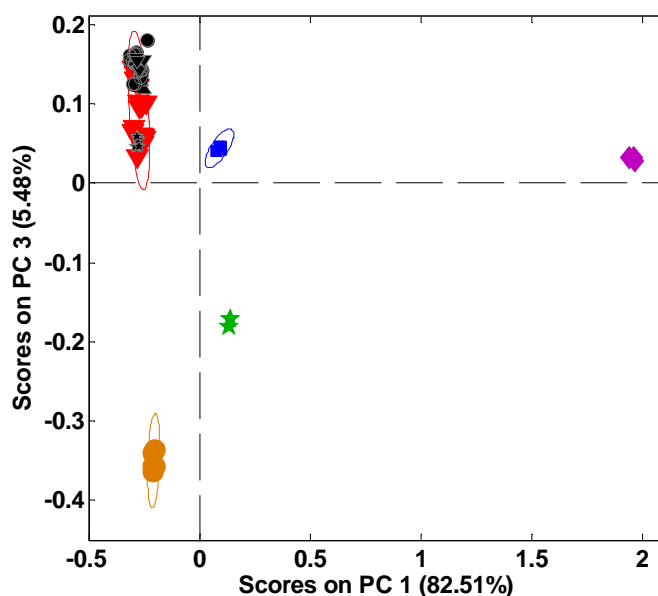


Figure 4.5: Projection of the PC1 vs. PC3 scores for the Test Set 1 samples onto the subspace defined by the corresponding PCA with GLSW calibration model obtained for Calibration Dataset 1. KEY: E150a calibration caramels (red triangles), E150b calibration caramels (green stars), E150c calibration caramels (blue squares), E150d calibration caramels (purple diamonds), Burnt Sugar calibration caramels (orange circles), E150a Test Set 1 samples (black symbols with grey borders).

After successfully utilising PCA with GLSW to predict the caramel class of the test samples within Test Set 1, the ATR-MIR spectra were subsequently projected into the PCA with GLSW calibration model for calibration Dataset 2 (to obtain scores). This was to determine whether the classification tool could also predict the E150a formulation of the test samples. The resulting PC1 vs. PC2 scores plot has been provided in Figure 4.6a and clearly demonstrates that all test samples known as being E150A_X1 were correctly classified within the E150A_X1 category of the calibration data whilst the test samples known as being E150A_X2 were correctly classified within the E150A_X2 calibration category. This can be observed more clearly in Figure 4.6b, which shows an enlargement of the subspace surrounding the E150A_X1 and E150A_X2 calibration clusters. All of the test samples are clearly demonstrated to fall within the 95% confidence ellipses defined by their corresponding calibration groupings.

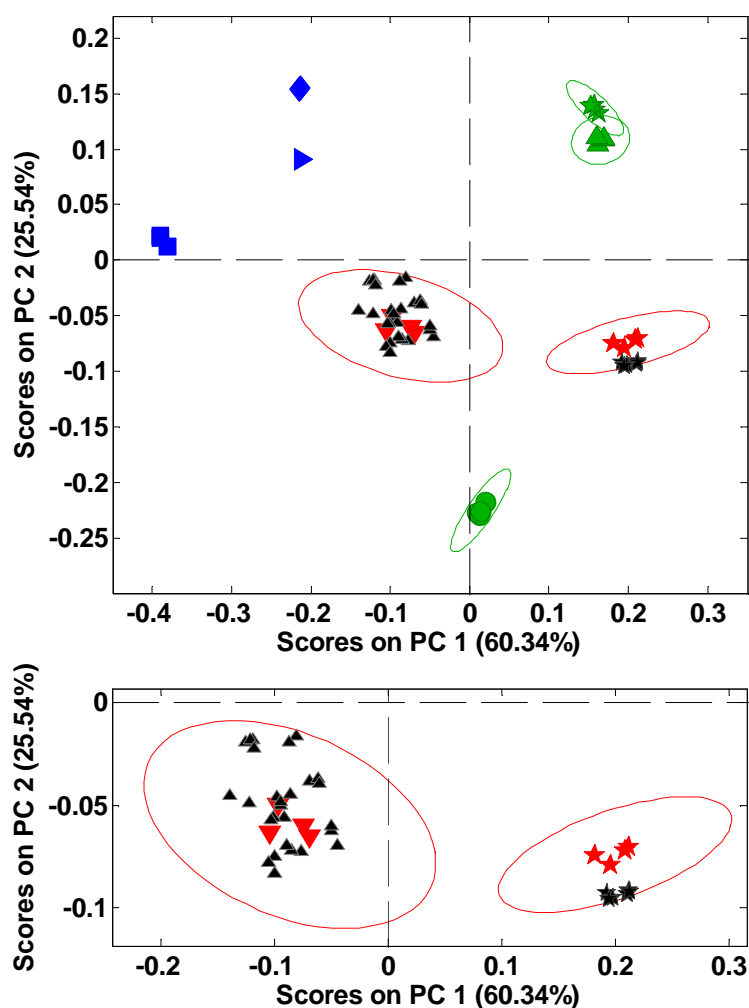


Figure 4.6: (A) Projection of the PC1 vs. PC2 scores for the Test Set 1 samples onto the subspace defined by the PCA with GLSW calibration model obtained for Calibration Dataset 2. (B) Shows an enlargement of the region surrounding the two calibration clusters assigned as E150A_X1 and E150A_X2. KEY: E150a_X1 calibration caramels (red triangles), E150a_X2 calibration caramels (red stars), E150a_Y3 calibration caramels (green triangles), E150a_Y4 calibration caramels (green stars), E150a_Y5 calibration caramels (green circles), E150a_Z6 calibration caramels (blue squares), E150a_Z7 calibration caramels (blue triangles), E150a_Z8 calibration caramels (blue diamonds), ‘E150A_X1’ samples from Test Set 1 (black triangles), ‘E150A_X2’ samples from Test Set 1 (black stars).

Overall, this assessment of Test Set 1 has indicated that PCA with GLSW has the potential to predict the identity of test E150a caramels when dissolved in 40% ethanol (the same medium as for the calibration samples). Both the caramel class and E150a formulations were correctly predicted for 100% of the samples incorporated by Test Set 1. This demonstrated that the classification tool was robust for the prediction of samples that had been re-prepared/reanalysed and also for those that had been freshly acquired. This can only be said however for the types of E150a included within this preliminary study (E150A_X1 and E150A_X2). Additional

samples would be required to confirm this finding for other E150a formulations and samples of other caramel classes. In addition to the above, the PCA with GLSW technique also correctly predicted the class and formulation of E150a caramels that had passed their date of expiry, indicating that this classification tool would not be affected by the introduction of ATR-MIR spectra acquired from caramel samples that are at different stages of their shelf life. This can only be stated in relation to E150A_X1 caramels however and so further samples would be required to determine whether this was always the case for different E150a formulations and also for classes of caramel other than E150a.

Test Sets 2-3 – Caramels in Scotch Whisky

After the initial success of PCA with GLSW preprocessing to predict the identity of Test Set 1 samples (dissolved in the same background matrix as the calibration samples), a subsequent study was undertaken using the same calibration models to investigate the prediction capabilities for caramels dissolved in Scotch Whisky. Two data sets were examined in this part of the research and included: Test Set 2; caramels dissolved in a typical blend matrix (Blend Whisky A) and Test Set 3; a selection of the same caramel materials dissolved in a blend representing the high levels of colour that would be developed naturally for a Scotch Whisky product (Blend Whisky B) (see section 4.2.1.2 for more details).

After the acquisition of ATR-MIR spectra for the samples included within Test Sets 2 and 3 (analysed in triplicate), the spectra were projected into the PCA with GLSW calibration model optimised for calibration Dataset 1, to assess whether caramel class could be correctly predicted. Figure 4.7 shows the resulting PC1 vs. PC2 scores plot and it was clearly demonstrated that although all of the E150a classed test samples (from both Test Sets 2 and 3) were close to the E150a cluster, they did not fall within the associated 95% confidence ellipse. This can be seen most clearly in Figure 4.7b which shows an enlargement of the subspace surrounding the E150a calibration samples and the test samples. The same finding was also observed for the remaining test samples of Test Set 2; none of the E150b, E150c and E150d test samples overlaying with their corresponding calibration clusters. These data therefore

indicated that the prediction of caramel class using PCA with GLSW is affected by a change in the background matrix from that of the calibration data. Although time and resources did not permit in this project, it would be interesting to create a new calibration model consisting of caramels in Blend Whisky A and B to confirm whether the prediction of caramels within this matrix is actually possible when the background matrix is accounted for during calibration. The success of Test Set 1 predicting caramels in 40% ethanol where the calibration samples were also in 40% ethanol indicates that this would be the case.

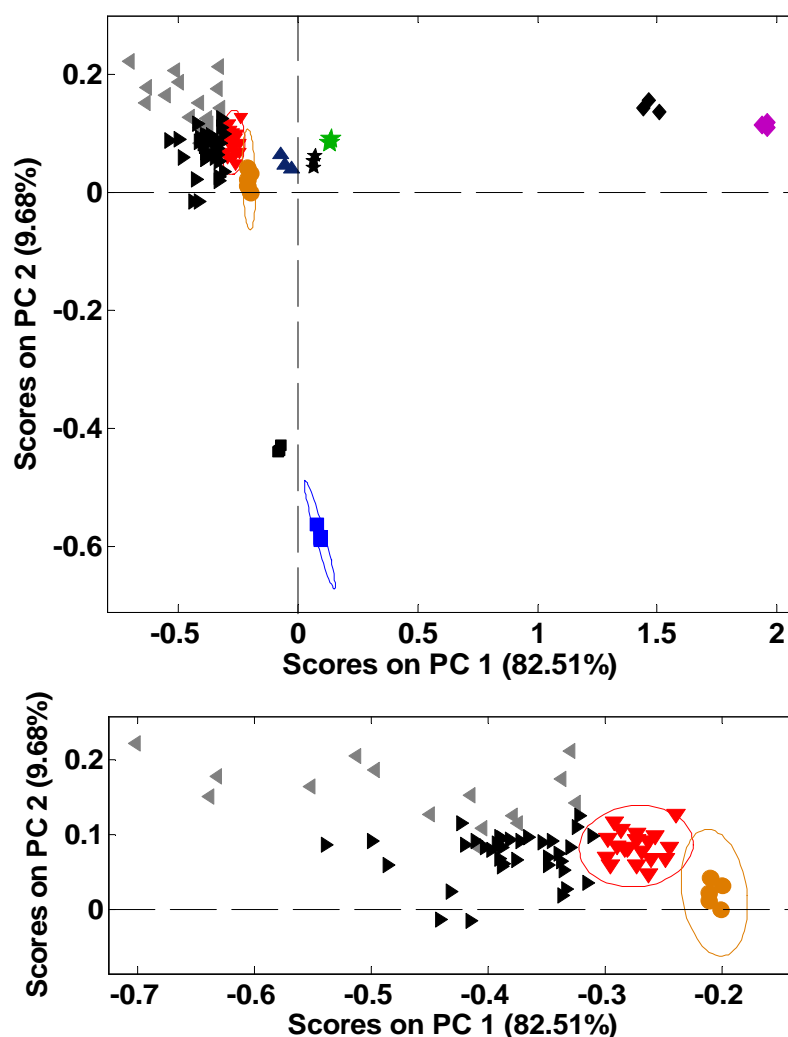


Figure 4.7: (A) Projection of the PC1 vs. PC2 scores for the Test Set 2 and 3 samples onto the subspace defined by the PCA with GLSW calibration model obtained for Calibration Dataset 1. (B) Shows an enlargement of the region surrounding the E150a calibration cluster and the test samples. KEY: E150a calibration caramels (red triangles), E150b calibration caramels (green stars), E150c calibration caramels (blue squares), E150d calibration caramels (purple diamonds), Burnt Sugar calibration caramels (orange circles), Test Set 2 E150a samples (black triangles), Test Set 3 E150a samples (grey triangles), Set 2 E150b samples (black stars), Set 2 E150c samples (black squares), Set 2 E150d samples (black diamonds), Blend Whisky B without caramel (blue triangles).

An additional sample analysed as part of Test Set 3 incorporated Blend Whisky B without the addition of any caramel and was included to see whether natural colour alone would be correctly predicted out with the confidence ellipses of all of the caramel calibration classes. This was demonstrated as being the case in Figure 4.7; the Blend Whisky B sample falling far from all of the caramel samples dissolved in Blend Whisky B (remaining Test Set 3 samples – grey triangles) and away from all of the calibration clusters. This would however need to be repeated for future calibration models created to account for caramels being dissolved in that particular background matrix, to confirm that the whisky without caramel can be successfully distinguished from the whisky with caramels present.

After the assessment of PCA with GLSW for the prediction of caramel class for Test Set 2 and 3 samples, the ATR-MIR spectra were projected into the calibration model optimised for calibration Dataset 2, to assess the ability of the classification tool for the prediction of E150a formulation when dissolved in blends. The resulting PC1 vs. PC2 scores plot, initially showing only the Test Set 2 data, has been provided in Figure 4.8 and demonstrated similarities to the findings observed for the prediction of caramel class. Although each type of E150a formulation from each of the test sets sat closest to its corresponding calibration cluster, only the E150A_X1 type test caramels were found to lie fully within the relevant 95% confidence ellipses (suggesting prediction of this caramel type was not affected by the matrix of a typical blend whisky). The other samples however, typically appeared to shift away from their equivalent calibration caramel groupings. This again could have been caused by the fact that the background matrix of the test samples did not match that of the calibration samples. It would therefore be interesting in future work to determine whether the prediction of E150a formulation using PCA with GLWS preprocessing is improved for test samples dissolved in a typical blend whisky by utilising a calibration model where samples are dissolved in the sample whisky matrix.

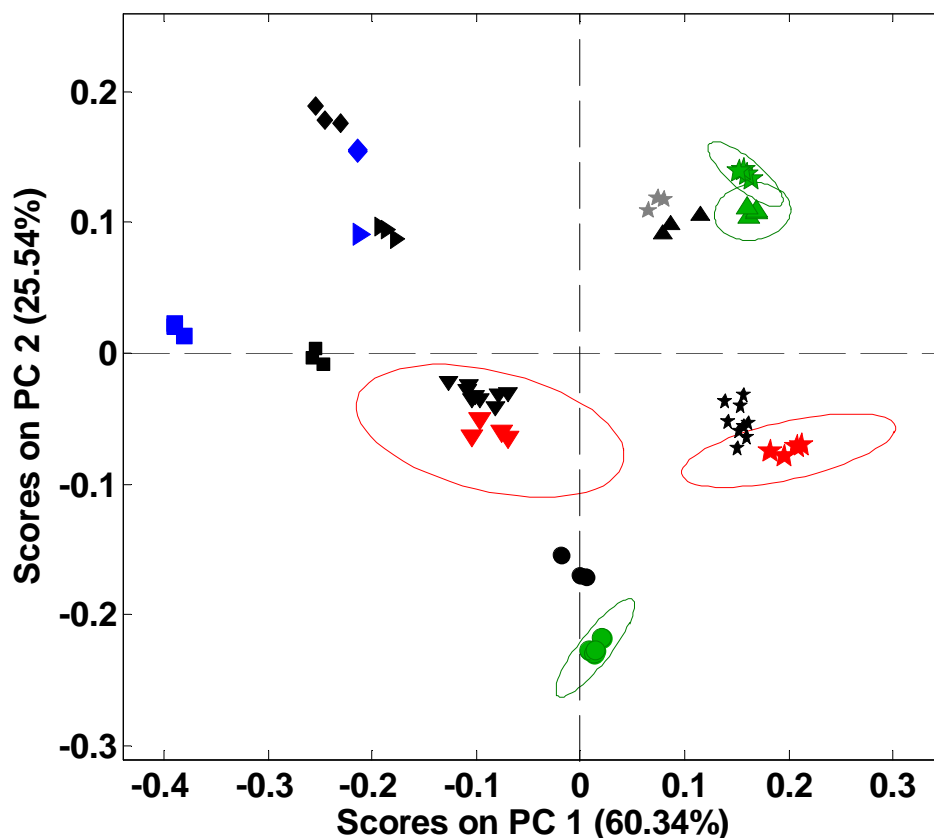


Figure 4.8: Projection of the PC1 vs. PC2 scores for the Test Set 2 samples onto the subspace defined by the PCA with GLSW calibration model obtained for Calibration Dataset 2. KEY: E150A_X1 calibration caramels (red triangles), E150A_X2 calibration caramels (red stars), E150A_Y3 calibration caramels (green triangles), E150A_Y4 calibration caramels (green stars), E150A_Y5 calibration caramels (green circles), E150A_Z6 calibration caramels (blue squares), E150A_Z7 calibration caramels (blue triangles), E150A_Z8 calibration caramels (blue diamonds), The symbols for the E150a formulation of the test samples match those of their corresponding calibration category but are all coloured black (E150A_Y4 test samples are grey stars to differentiate from E150A_X2 test samples).

Figure 4.9 illustrates the PC1 vs. PC2 scores plot that contains the Test Set 3 samples projected onto the calibration dataset for the prediction of E150a formulation (calibration Dataset 2). The sample of Blend Whisky B alone has been excluded at this point as in an ideal situation it should be discounted as an E150a caramel during the initial prediction to identify the caramel class. An E150A_X1 caramel is included within Test Set 3 and Figure 4.9 demonstrated that its formulation was correctly predicted even when dissolved within Blend Whisky B, the sample found within the 95% confidence ellipse for the E150A_X1 calibration samples. The other E150a caramels included within Test Set 3 however were not correctly predicted: an E150A_Y5 sample and 3 samples of E150A_X2. The scores obtained for these samples were closer to those of the E150A_X1 calibration samples than the

calibration groupings for their own corresponding E150a formulations. It was also the case that the Test Set 3 samples were much closer to each other than the test samples of Test Set 2 were (Figure 4.8) corresponding with the fact that more natural colour is present and affecting the characteristic caramel features of spectra. These data therefore again indicated that the prediction of E150a formulation using PCA with GLSW preprocessing will be influenced by the background matrix of a sample if this has not been accounted for in the calibration data. Future work to create a calibration model where caramels are dissolved within Blend Whisky B would be extremely interesting to undertake to determine whether E150a formulation could be predicted even when dissolved in a whisky matrix representing an extremely high case of natural colour. Previous findings within Chapter 3 (section 3.3.1.3) indicated that the ATR-MIR spectral features of these different E150a caramels could still be distinguished in this matrix.

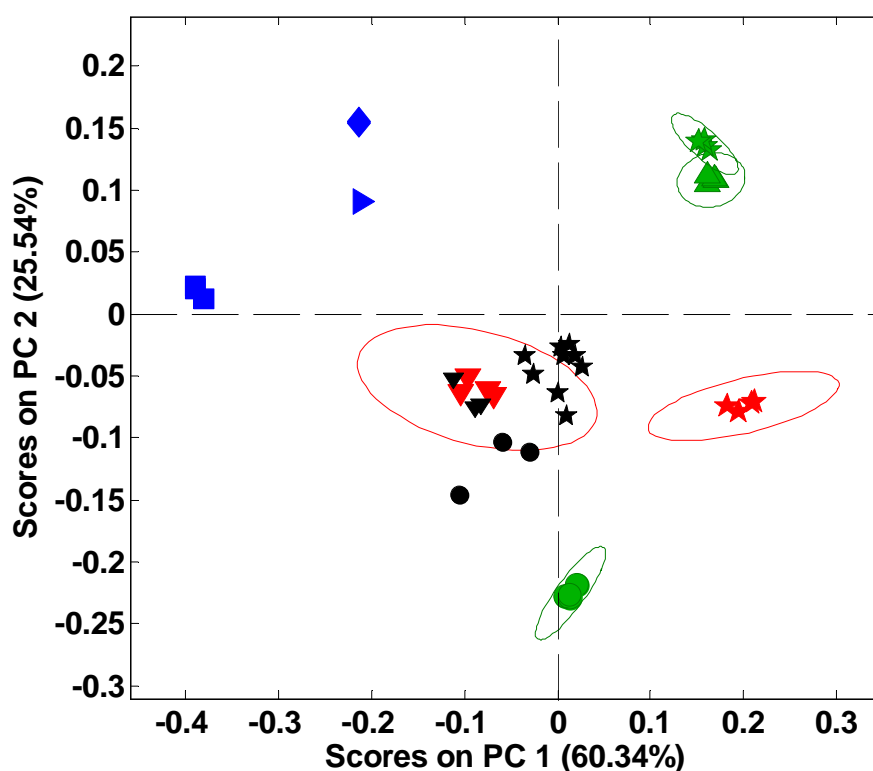


Figure 4.9: Projection of the PC1 vs. PC2 scores for Test Set 3 samples onto the subspace defined by the PCA with GLSW calibration model obtained for Calibration Dataset 2. KEY: E150A_X1 calibration caramels (red triangles), E150A_X2 calibration caramels (red stars), E150A_Y3 calibration caramels (green triangles), E150A_Y4 calibration caramels (green stars), E150A_Y5 calibration caramels (green circles), E150A_Z6 calibration caramels (blue squares), E150A_Z7 calibration caramels (blue triangles), E150A_Z8 calibration caramels (blue diamonds). The symbols for the E150a formulation of the test samples match those of their corresponding calibration category but are all coloured black (the black stars are test E150A_X2 samples).

It should also be noted at this point that in addition to variation in the background matrix affecting the prediction of the samples within Test Sets 2 and 3, it is also possible that the change in the preparation of the test samples in comparison with the preparation of the calibration samples (see experimental section 4.2) could have influenced spectra and so subsequently affected prediction. This relates back to findings previously presented within Chapter 3 (see section 3.3.2.1), which demonstrated that even when data have been normalised, changing the caramel concentration resulted in spectral variation. The following subsection (which discusses Test Set 4) examines this proposal in more detail to determine whether the change in concentration due to variation in sample preparation will influence spectra to the extent where prediction is affected.

Test Set 4 – Variation in caramel concentration

Test Set 4 incorporated samples put together to assess whether changes in caramel concentration (and also changes to the methodology in relation to the addition of a preconcentration step) would affect the prediction of caramel class and E150a formulation using PCA with GLSW preprocessing. The samples included within Test Set 4 have already been analysed by ATR-MIR within Chapter 3 (see sections 3.2.4.3 and 3.3.2.1) and can be split into two subsets which have been summarised below along with an explanation as to their purpose as part of Test Set 4 in this section of the research:

- (1) ‘Subset 1’: Four samples of a batch of E150A_X1 ranging in their colour level (and hence concentration) from an absorbance of 0.2 – 0.8 (at 430 nm) and dissolved in 40% ethanol. Sample preparation for these samples prior to ATR-MIR involved concentrating each sample up to the same final volume and so the variation in concentration was not accounted for during sample preparation. The samples were however prepared in the same sample medium as for the samples in calibration Datasets 1 and 2 and so investigating the prediction of these samples using these calibration models would identify if classification using PCA with GLSW can allow the correct prediction of caramels despite the influence that changing caramel concentration has already been found to have on ATR-MIR spectra.

(2) ‘Subset 2’: Four samples of a batch of E150A_X1 ranging in their colour level (and hence concentration) from an absorbance of 0.2 – 0.8 (at 430 nm) and dissolved in 40% ethanol. Preparation of these samples prior to ATR-MIR involved increasing the concentration of each sample up to the same final concentration (the same approach used for samples within Test Sets 2 and 3). Each sample was therefore prepared in the same sample medium as for the samples used in calibration Datasets 1 and 2 but any variation in concentration was accounted for during sample preparation. The only difference of these test samples compared to the calibration samples would therefore be in the sample preparation methodology: the test samples being pre-concentrated whilst the calibration samples were not. Investigating the ability of PCA with GLSW preprocessing to predict the identities of these four samples would therefore determine whether prediction is affected by the changes made to the ATR-MIR methodology between calibration and test samples.

The ATR-MIR spectra acquired from the E150a samples within Test Set 4 (both Subset 1 and Subset 2 samples) were initially projected into the PCA with GLSW calibration model optimised for calibration Dataset 1, to assess the prediction of caramel class. The resulting PC1 vs. PC2 scores plot has been given in Figure 4.10 and it could be seen from Figure 4.10a that all of the test samples were situated in a similar region of space as the E150a calibration grouping however they did not overlay with this cluster. Figure 4.10b has consequently been included to investigate this more closely and shows a zoomed in area around the E150a calibration samples and the Test Set 4 samples (the burnt sugar cluster is also visible).

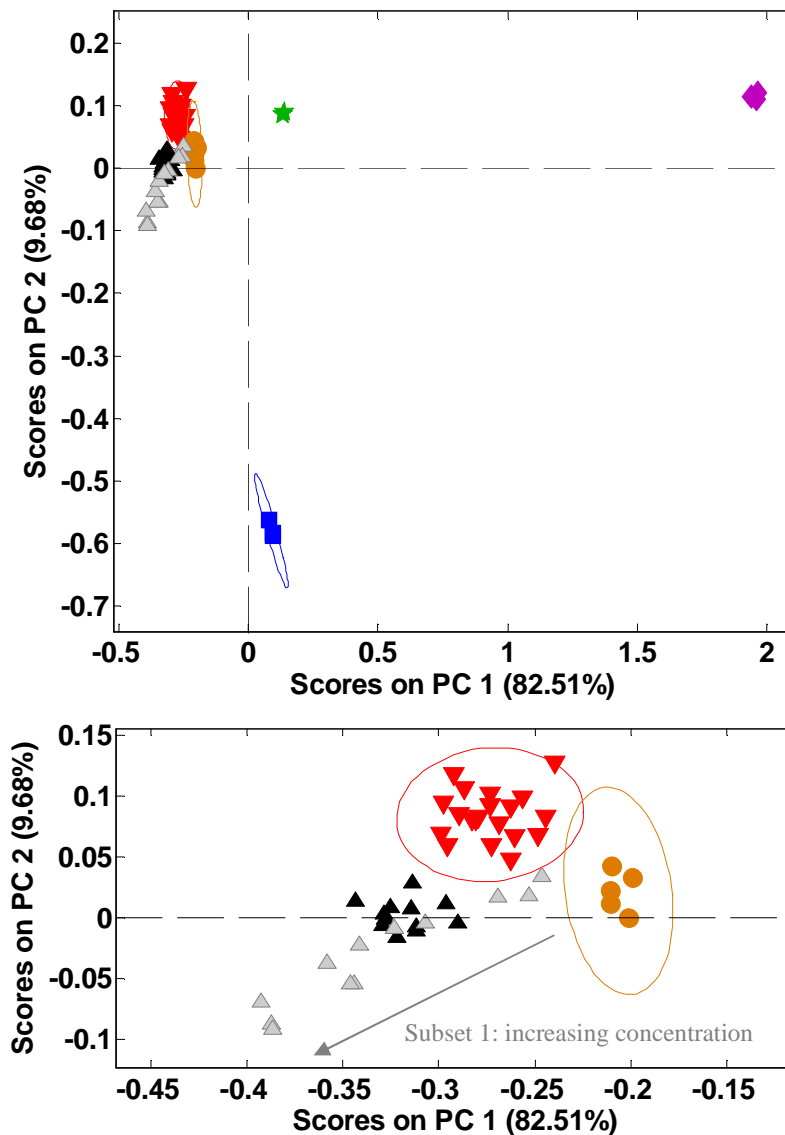


Figure 4.10: (A) Projection of the PC1 vs. PC2 scores for the Test Set 4 samples onto the subspace defined by the PCA with GLSW calibration model obtained for Calibration Dataset 1. (B) Shows an enlargement of the region surrounding the E150a calibration cluster and the test samples. **KEY:** E150a calibration caramels (red triangles), E150b calibration caramels (green stars), E150c calibration caramels (blue squares), E150d calibration caramels (purple diamonds), Burnt Sugar calibration caramels (orange circles), Test Set 4 'Subset 1' E150a samples (grey triangles), Test Set 4 'Subset 2' E150a samples (black triangles).

Considering Subset 1 first, it can be seen from Figure 4.10b that these samples spread out away from the E150a cluster with both the PC1 and PC2 scores decreasing in accordance with increasing sample concentration. This finding therefore indicates that the implementation of PCA with GLSW preprocessing does not filter out the ATR-MIR spectral regions that are affected by variation in caramel concentration and so classification with this tool is consequently affected by this

parameter. The test samples incorporated by Subset 2 on the other hand, are shown to cluster tightly together, which corresponds well to the fact that the changes in sample concentrations have been accounted for within sample preparation. The fact that these samples do not overlay with the E150a calibration cluster can therefore be attributed to the additional preconcentration step applied to these test samples in comparison with how the calibration samples were prepared for analysis. This also consequently helps to confirm that the separation observed previously between the samples of Test Sets 2/3 and their corresponding calibration categories could be related to the variation in sample preparation as well as the change in sample matrix.

Similar findings as above were subsequently observed when the samples from Test Set 4 were projected into the PCA with GLSW calibration model optimised for calibration Dataset 2, to assess the prediction of E150a formulation. This is illustrated within Figure 4.11, where it is clear that all test samples do not completely overlay with their corresponding E150a formulation (E150A_X1). This offset is likely a result of the additional preconcentration step applied for the preparation of these test samples but not for the preparation of the calibration samples. Figure 4.11 shows that the scores for the Subset 1 samples stretch further away from the E150A_X1 calibration grouping and possess a trend of increasing PC2 score in accordance with increasing caramel concentration. This again indicated that PCA with GLSW preprocessing does not filter out the ATR-MIR spectral regions that are affected by variation in caramel concentration and so classification of E150a formulation with this tool is consequently affected by this parameter. The Subset 2 samples however cluster together in no particular pattern, which corresponds to the fact that spectral variation resulting from changes in caramel concentration has been accounted for.

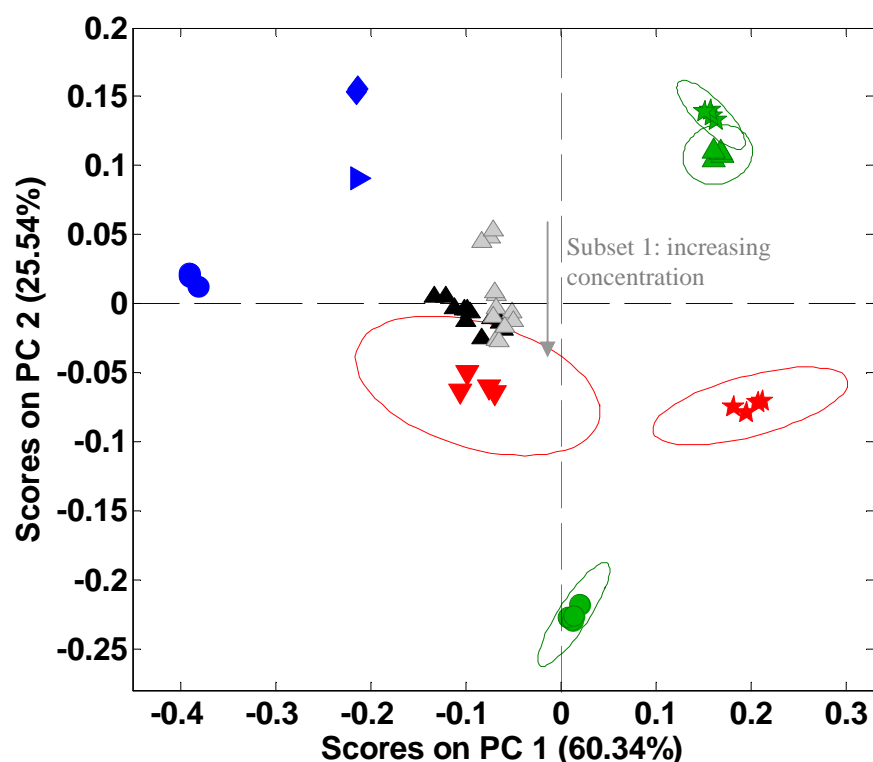


Figure 4.11: Projection of the PC1 vs. PC2 scores for Test Set 4 samples onto the subspace defined by the PCA with GLSW calibration model obtained for Calibration Dataset 2. **KEY:** E150A_X1 calibration caramels (red triangles), E150A_X2 calibration caramels (red stars), E150A_Y3 calibration caramels (green triangles), E150A_Y4 calibration caramels (green stars), E150A_Y5 calibration caramels (green circles), E150A_Z6 calibration caramels (blue squares), E150A_Z7 calibration caramels (blue triangles), E150A_Z8 calibration caramels (blue diamonds), Test Set 4 ‘Subset 1’ E150_X1 samples (grey triangles), Test Set 4 ‘Subset 2’ E150A_X1 samples (black triangles).

Test Set 5 – Caramels subjected to fade

Results obtained previously in Chapter 3 (section 3.3.2.2) demonstrated that the ATR-MIR spectral features of caramel materials can be affected by the process of fade. An E150A_X1, an E150A_X2 and an E150D_X11 caramel were examined in the previous work and all were shown to be affected by this parameter. Test Set 5 in this section of the research has therefore been made up using the data from these same caramel substances, incorporating eight samples for each material: 3 control samples and 5 samples faded for 1, 2, 3, 4 and 7 days under extreme conditions (see sections 3.2.4.4 and 3.3.2.2 for more details) that vary in their degree of fade from approximately 66% to 30% for the E150a caramels and 80% to 45% for the E150d caramel (see Table 3.2). The purpose of this was to determine whether the effect of fade on ATR-MIR spectral features was enough to influence prediction using the PCA with GLSW preprocessing classification tool. All of the samples were prepared

in 40% ethanol and so matched the background matrix of those making up calibration Datasets 1 and 2. In addition samples were all pre-concentrated to the same final concentration to eliminate/reduce variation in concentration as a factor influencing spectra. The preconcentration however was an additional sample preparation step in comparison to the calibration samples, which from earlier findings in this chapter indicated that a slight shift in data with respect to the calibration samples could be observed when implementing PCA with GLSW preprocessing.

The ATR-MIR spectra obtained from the caramel samples of Test Set 5 (acquired in triplicate for each sample) were initially projected into the PCA with GLSW calibration model optimised for calibration Dataset 1, to assess how the prediction of caramel class might be affected by the fading process. The resulting PC1 vs. PC2 scores plot has been provided in Figure 4.12. It was clear from the figure that neither of the E150A classed caramels overlaid well with their corresponding calibration category (emphasised in Figure 4.12b) and this was tentatively assigned to the difference in sample preparation between the test and calibration samples (the former being pre-concentrated whilst the latter was not). This made it quite difficult to determine the extent to which fade affects prediction using PCA with GLSW, however a few trends could be picked out from the data. For instance for both types of E150a it can be seen that all samples faded for up to 3 days (inclusive) cluster in a similar region of space as the control samples (not faded) and have PC2 scores quite close to the E150a calibration grouping. Fade then seems to have a more significant influence on samples after this point, i.e. the samples faded for a time period of 4 and 7 days move further away from the E150a calibration samples (the PC1 scores decreasing whilst the PC2 scores clearly increase). It could therefore be the case that fading of caramel up until a certain level will not extensively influence ATR-MIR spectra to the extent where prediction using PCA with GLSW preprocessing is affected, however further work would be needed to confirm this. The test samples would need to be compared to a calibration dataset incorporating the exact same sample preparation procedures as used for the test samples, so as to remove this factor already identified previously as being responsible for shifting PCA scores.

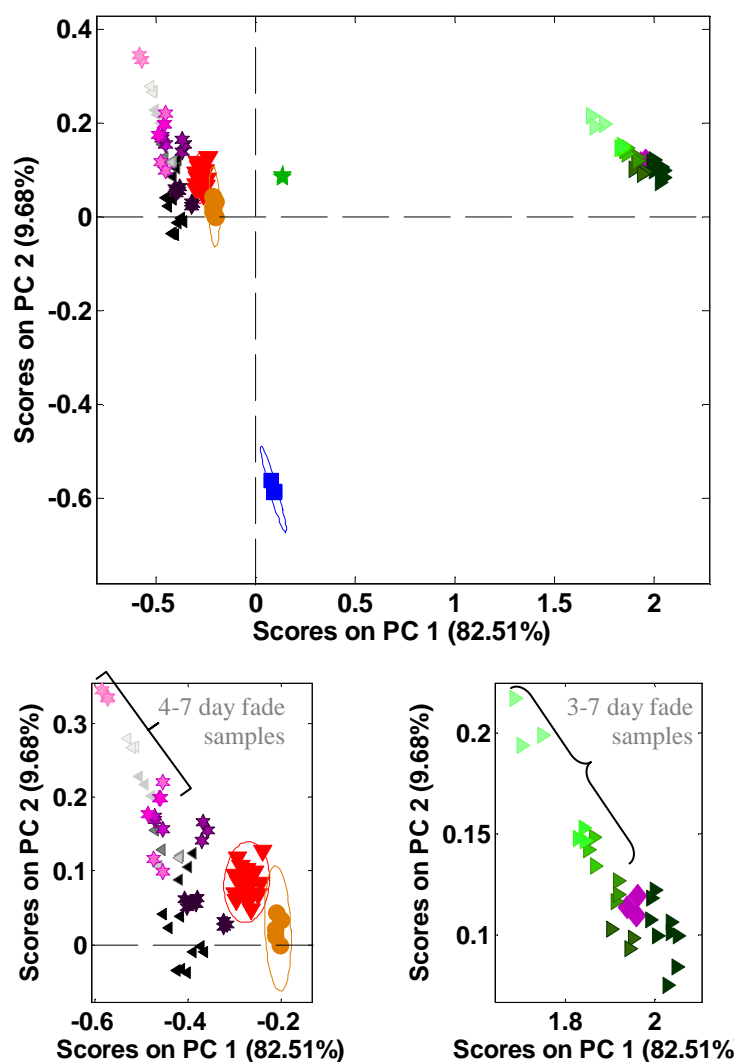


Figure 4.12: (A) Projection of the PC1 vs. PC2 scores for the Test Set 5 samples onto the subspace defined by the PCA with GLSW calibration model obtained for Calibration Dataset 1. (B) Shows an enlargement of the region surrounding the E150a calibration cluster and the test samples, whilst (C) has zoomed on the region surrounding the E150d calibration and test samples. KEY: E150a calibration caramels (red triangles), E150b calibration caramels (green stars), E150c calibration caramels (blue squares), E150d calibration caramels (purple diamonds), Burnt Sugar calibration caramels (orange circles), E150A_X1 test samples (black-grey triangles), E150A_X2 test samples (purple-pink stars), E150D_X10 test samples (green triangles). The colour of each test sample set decreases in shade as the degree of fade increases.

The E150D_X11 caramel samples showed a slightly different trend to the E150a caramels (Figure 4.12c). The E150D caramels faded for up to 2 days (inclusive) along with the control samples (not faded) overlaid very well with the E150D calibration samples, indicating that fade did not significantly affect spectra up to this level. After this point however, the PC2 scores of samples began to increase in accordance with increasing level of fade, implying that fade of this caramel type will also influence the prediction of its identity when using PCA with GLSW

preprocessing. Again, further work that involves matching the sample preparation of the calibration and test samples would be required to confirm these findings.

Similar findings to those observed above were subsequently seen when the E150a samples from Test Set 5 were projected into the PCA with GLSW calibration model optimised for calibration Dataset 2, to assess how fade might affect the prediction of E150a formulation when using this classification tool. This is demonstrated *via* Figure 4.13, where it is clearly seen (for both E150a formulations) that the three samples faded for 1, 2 and 3 days cluster quite closely together and are closest in their vicinity to the control samples; in the case of the E150A_X2 samples, the samples faded for 4 days are also found to have similar scores to these samples. It can then be clearly seen that the caramel samples faded for 4 and 7 days in the case of E150A_X1 and the sample faded for only the latter in the case of E150A_X2 begin to vary in their positioning on the scores plot; in both cases moving away from the remaining samples by a decrease in both their PC1 and PC2 scores. These findings therefore reiterated that caramel fade (after a certain degree) is likely to affect the prediction of caramel identities when using PCA with GLSW preprocessing. It would be extremely interesting to undertake further work in this area with a calibration dataset that matches exactly the conditions used to analyse the test samples and so determine exactly what level of fade would affect prediction using PCA with GLSW preprocessing.

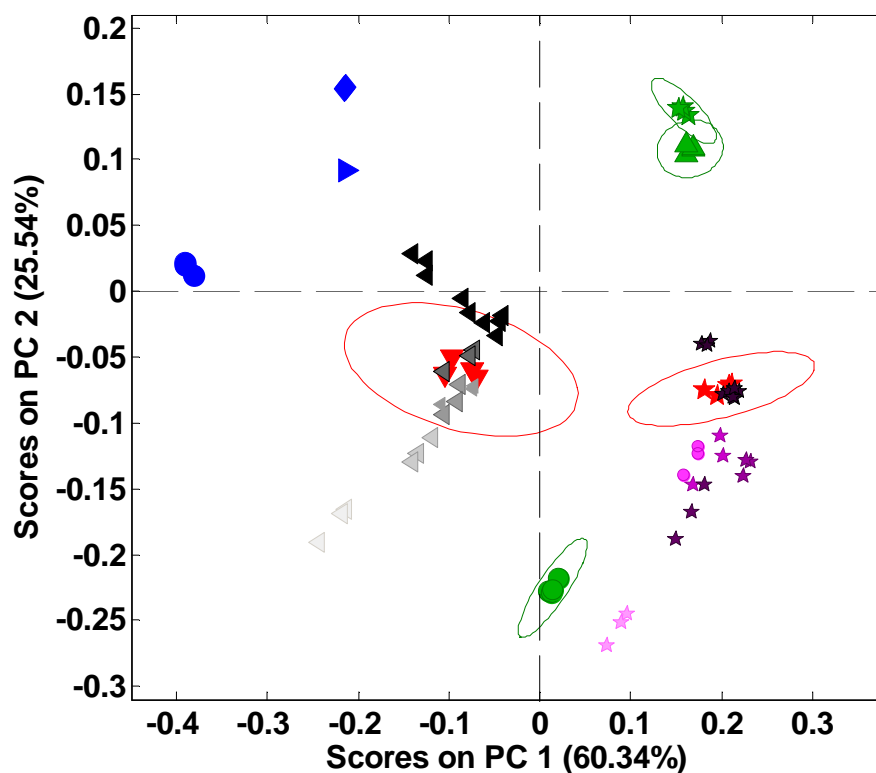


Figure 4.13: Projection of the PC1 vs. PC2 scores for Test Set 4 samples onto the subspace defined by the PCA with GLSW calibration model obtained for Calibration Dataset 2. KEY: E150A_X1 calibration caramels (red triangles), E150A_X2 calibration caramels (red stars), E150A_Y3 calibration caramels (green triangles), E150A_Y4 calibration caramels (green stars), E150A_Y5 calibration caramels (green circles), E150A_Z6 calibration caramels (blue squares), E150A_Z7 calibration caramels (blue triangles), E150A_Z8 calibration caramels (blue diamonds), E150A_X1 test samples (black-grey triangles), E150A_X2 test samples (purple-pink stars). The colour of each test sample set decreases in shade as the degree of fade increases.

4.3.1.3 Summary

Overall, the preliminary data presented in the above section of the research have demonstrated that PCA with GLSW has good potential as a classification tool for the prediction of caramel identities in Scotch Whisky. One key finding however, was that to be successful, the technique would have to account for the constituents of the background matrix in the calibration model. Different calibration models would therefore be required for all different brands of whisky, which could present a potential drawback. This study also indicated that profile prediction using PCA with GLSW would be affected by changes to sample preparation that vary between the calibration and test samples, in this case the inclusion of an additional preconcentration step implemented for test samples clearly influenced prediction. In addition, factors such as variation in caramel concentration and also the process of

caramel fade were found to present potential issues when utilising PCA with GLSW for the prediction of caramel identities. A selection of other data analysis tools was consequently investigated as part of this research to allow a comparison of their applicability for the prediction of caramel identities in Scotch Whisky. The resulting findings are presented within the subsequent sections.

4.3.2 HCA

As discussed previously (see theory section 2.3.2) HCA is an unsupervised pattern recognition technique and so attempts to detect similarities between samples with the aim of searching for groupings. In addition, as an unsupervised technique, it attempts to achieve this without the use of pre-established class information. HCA was therefore investigated in this work as the first progressive step after PCA as a means to determine whether sample clusters could be deliberately picked up within the calibration data; PCA on its own being an EDA technique and so not intentionally looking for groupings between samples. This was a logical progression as Chapter 3 had already demonstrated that similar samples grouped closely together using PCA. This part of the research has been included here as it provided a useful starting point for the selection of a potential alternative classification tool for the prediction of caramel identities within this project.

HCA was initially utilised to search for groupings in calibration Dataset 1 which in this case incorporated all 69 spectra described by the samples within Table 4.1. As a starting point, the most simplistic input parameters available in the data analysis software were used to perform HCA and so distances between samples were defined using Euclidean distance; the raw data (and not PCA scores were utilised) as data points; and the nearest neighbour method was implemented to measure the distances between groups of samples. Figure 4.14 shows the dendrogram resulting from HCA analysis for Calibration Dataset 1 using these conditions. The data has been colour coded according to caramel class in this figure however it should be noted that information on the classes was not used to help assign groupings during HCA.

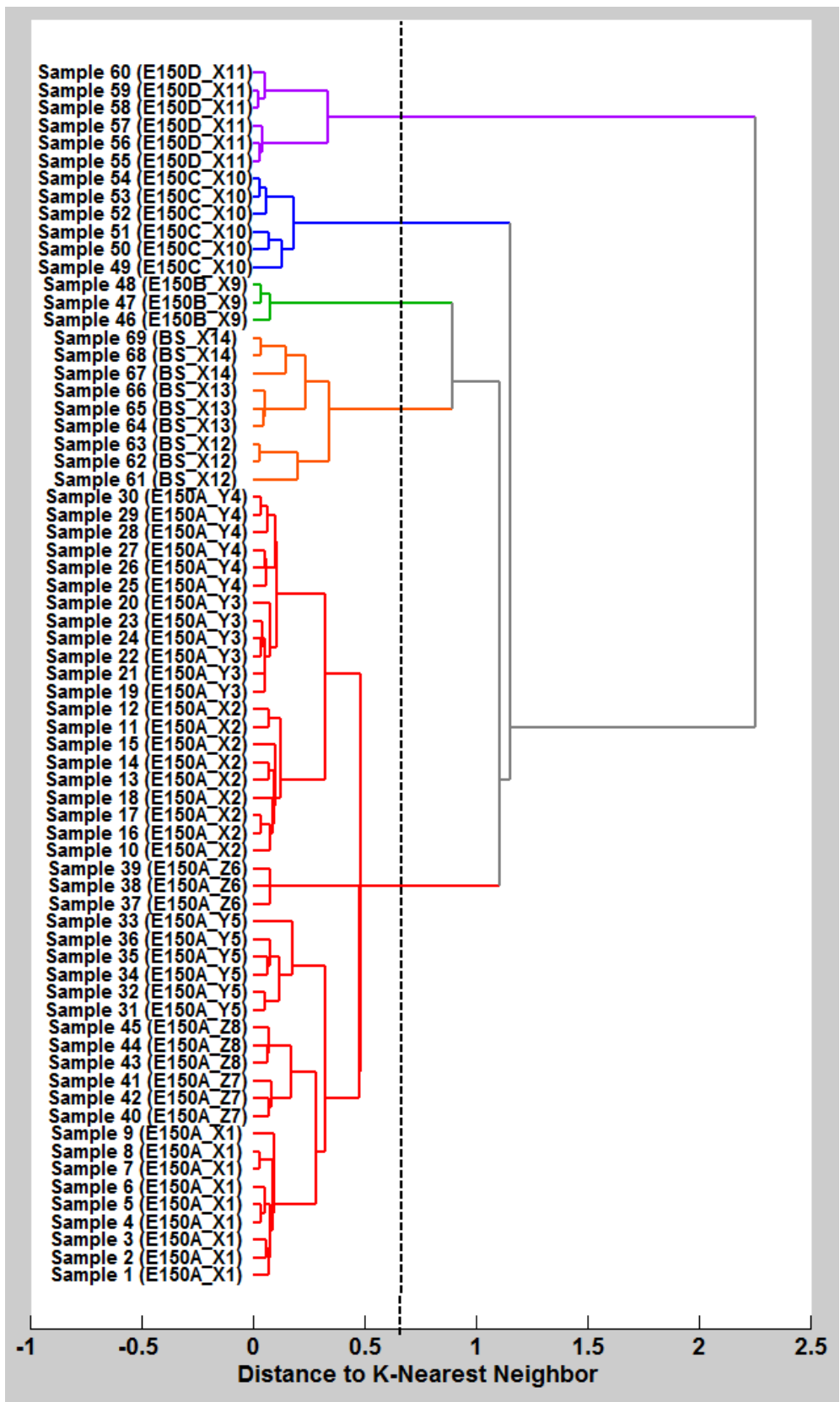


Figure 4.14: Dendrogram acquired from HCA of all 69 spectra obtained from ATR-MIR analysis of the Calibration Dataset 1 samples (all samples described within Table 4.1).

The dendrogram depicted within Figure 4.14 clearly demonstrated that all samples of the five different classes of interest in this case (E150a, E150b, E150c, E150d and Burnt Sugars) have as their nearest neighbour samples from the same class. By inserting a vertical line at a distance of approximately 0.7, the presence of five clear clusters has been demonstrated, with all calibration samples being found within the correct grouping (i.e. all E150a caramels were found in the E150a grouping, all E150b caramels were found in the E150b cluster, etc...). Another interesting observation from Figure 4.14 was that the different E150a formulations were also shown to be closest in distance to samples of equivalent formulation. Clear clusters for the different E150a formulation however, could not be demonstrated in this particular HCA model by the insertion of a vertical line. HCA was therefore next undertaken to include only the E150a calibration samples (Calibration Dataset 2, see Table 4.1) to investigate whether the different E150a formulations could also be assigned into individual clusters using this technique when only these samples were included within the calibration model. The resulting dendrogram has been provided within Figure 4.15.

The dendrogram provided within Figure 4.15 demonstrates that almost all samples of the eight different E150a formulations have as their nearest neighbour samples of equivalent formulation. If a vertical line were to be placed at a distance of approximately 0.25, the presence of five clusters would be indicated; the E150A_Y3 and E150A_Y4 caramels being considered part of the same grouping and also the E150A_Z7 and E150A_Z8 being deemed as part of the same cluster. The former of these observations can be linked back to PCA undertaken in Chapter 3 (see section 3.3.1.2) which indicated that E150A_Y3 and E150A_Y4 had very similar ATR-MIR profiles due to similarities in their manufacturing conditions. The close distance between the E150A_Z7 and E150A_Z8 caramels in this HCA model could also be linked to similar manufacturing conditions, being made from the same starting substrates and coming from the same manufacturer (see Table 3.1). It is clearly shown within Figure 4.15 however, that the latter two caramels can be split into separate clusters in this HCA model; looking at a shorter distance of ~0.15 allows distinction between these two caramel types. Additional work completed in an

attempt to improve HCA for Calibration Dataset 2 found that it was actually possible to clearly split the samples of this dataset into the eight clusters corresponding to the eight different E150a formulations. This could be achieved only after the implementation of GLSW preprocessing (using an α value of 0.03) and the resulting dendrogram has been provided in Figure 4.16. GLSW preprocessing utilises prior knowledge of sample categories during analysis and aims to reduce within category variation whilst maximising between category variation. This would therefore explain the improvement observed during HCA in this case.

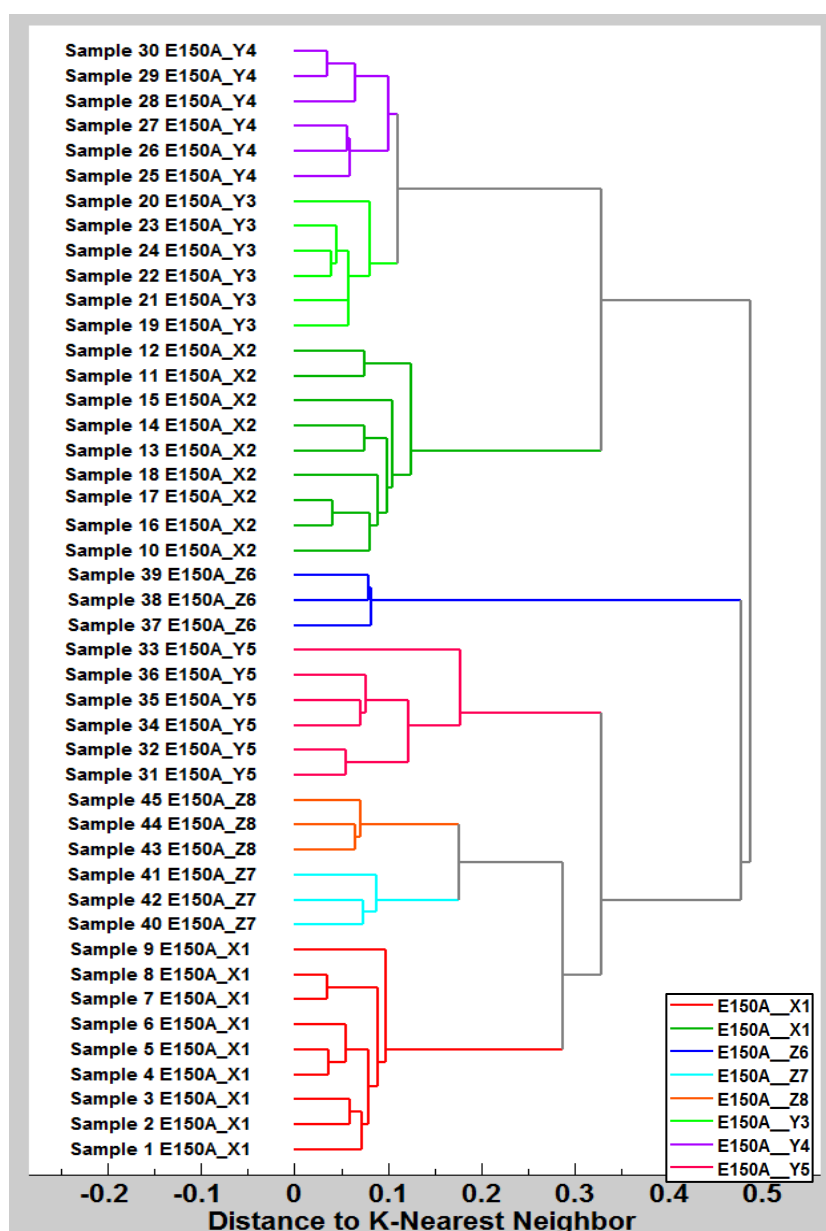
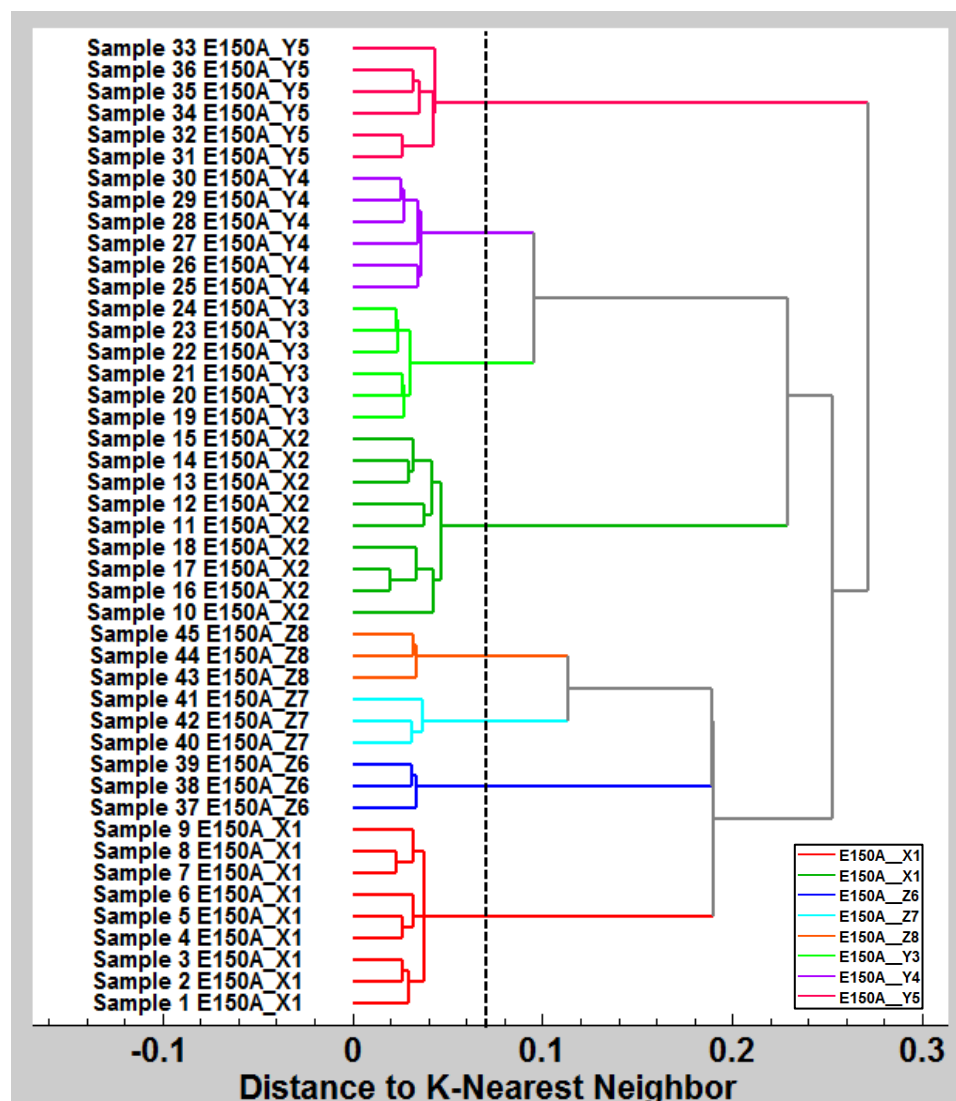


Figure 4.15: Dendrogram acquired from HCA of the 45 spectra obtained from ATR-MIR analysis of the Calibration Dataset 2 samples (samples described within Table 4.1).



4.16: Dendrogram acquired from HCA with GLSW preprocessing ($\alpha=0.03$) of the 45 spectra obtained from ATR-MIR analysis of the Calibration Dataset 2 samples (samples described within Table 4.1). The vertical line at a distance of ~ 0.7 indicates the presence of eight clusters.

As previously discussed in section 2.3.2, the classification of unknown or test samples using HCA would have to be done by manually including data into the model (due to the technique utilising no prior knowledge of samples). As well as this being extremely time consuming, classification would rely on the judgement of the analyst and so could easily result in misclassifications. As the nearest neighbour method for assigning distances between clusters allows very clear and accurate groupings of samples to be identified during HCA, this part of the research instead indicated that k -NN classification could be a useful supervised pattern recognition

tool for the automated prediction of caramel profiles. The technique of k -NN classification was subsequently investigated and the findings discussed below.

4.3.3 k -NN Classification

As previously described in the theory section 2.3.2.2, k -NN is a supervised classification technique and so can be used to automatically predict the identity of test (or unknown) samples provided that a training/calibration set is available where the class membership of each sample is already known. Test data can be projected into the k -NN model constructed using the calibration data and the classification tool will predict the identity of the test samples based on the majority identity of the ' k ' nearest calibration samples (where k is a small odd number).

4.3.3.1 Predicting the caramel class and E150a formulation of test data

In this part of the research, k -NN classification was initially assessed to determine its ability for the prediction of caramel class (i.e. prediction of test samples as being either E150a, E150b, E150c, E150d or a burnt sugar) and so calibration Dataset 1 was used as the training set (see Table 4.1). A k value of 3 was implemented to construct the k -NN model using this training dataset (k -NN Model 1) and the data acquired from all test sets (Test Sets 1 – 5) were subsequently projected into the model to assess what class they would be predicted as. The results obtained from this data analysis have been provided within Figure 4.17, which clearly demonstrated that 100% of test samples were correctly assigned to their corresponding calibration class.

After this initial success, a second k -NN model (k -NN Model 2) was subsequently constructed using calibration Dataset 2 as the training set (i.e. taking forward just the E150a caramels) to determine whether individual E150a formulations could also be correctly assigned using k -NN classification. A k value of 3 was again implemented to construct the k -NN model and the E150a caramels from all of the test sets (Test Sets 1 – 5) were projected into the model. It was found that GLSW preprocessing was required to improve prediction in this case and so was implemented during construction of the k -NN Model 2 using an α value of 0.03. This tied in well with

earlier results obtained during HCA, which demonstrated clustering of the E150a formulations was better when GLSW preprocessing was implemented. The results obtained from this data analysis have been provided in Figure 4.18 and in this case it was found that 94% of the test samples were correctly assigned to their corresponding calibration category (these being the eight different E150a formulations included within calibration Dataset 2). The significance of these above findings in relation to each of the individual test sets is discussed in the subsections that follow.

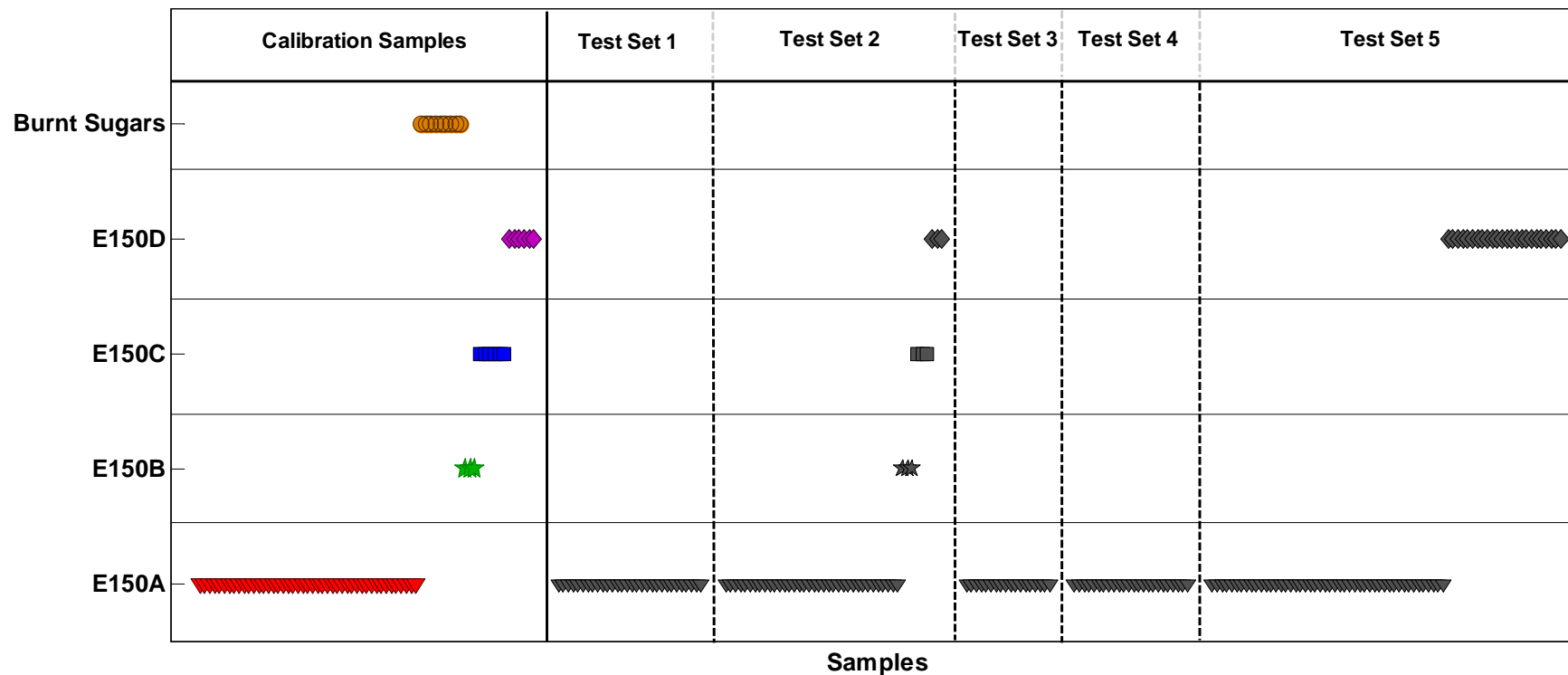


Figure 4.17: Results obtained after projecting the samples contained within Test Sets 1 – 5 into the k-NN classification model constructed using calibration Dataset 1 (k-NN Model 1). KEY: E150a calibration caramels (red triangles), E150b calibration caramels (green stars), E150c calibration caramels (blue squares), E150d calibration caramels (purple diamonds), Burnt Sugar calibration caramels (orange circles). The test samples are all coloured dark grey and their caramel class is portrayed by their symbol shapes (which correspond to the symbol shapes used for each caramel class within the calibration data).

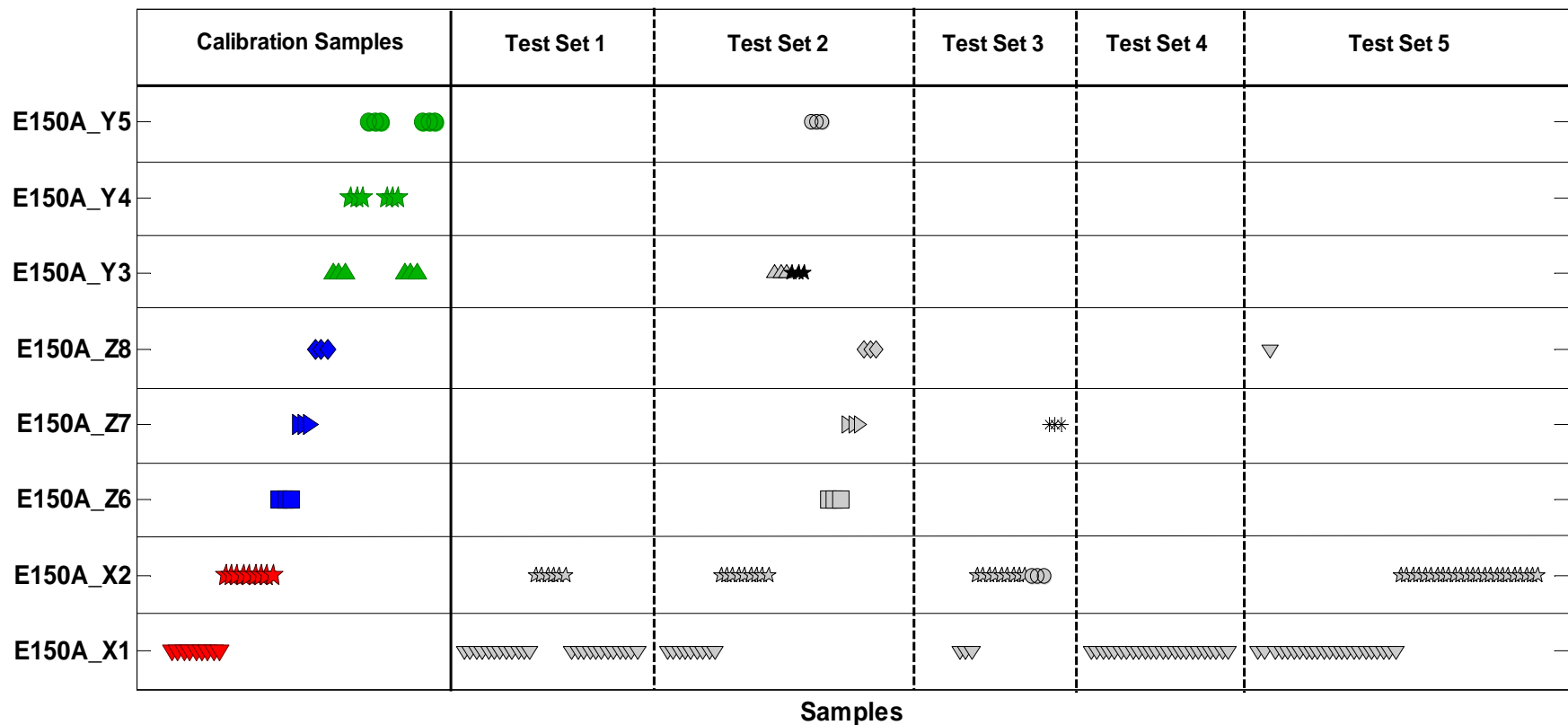


Figure 4.18: Results obtained after projecting the E150a samples contained within Test Sets 1 – 5 into the k-NN classification model constructed using calibration Dataset 2 (k-NN Model 2). KEY: E150A_X1 calibration caramels (red triangles), E150A_X2 calibration caramels (red stars), E150A_Y3 calibration caramels (green triangles), E150A_Y4 calibration caramels (green stars), E150A_Y5 calibration caramels (green circles), E150A_Z6 calibration caramels (blue squares), E150A_Z7 calibration caramels (blue triangles), E150A_Z8 calibration caramels (blue diamonds). The test samples are all coloured grey and their E150a formulation is portrayed by their symbol shapes (which correspond to the symbol shapes used for each E150a formulation within the calibration data). Any E150A_Y4 test samples have been portrayed as black stars to differentiate them from E150A_X2 test samples (grey stars).

Test Set 1 – Caramels in 40% ethanol

As discussed previously in section 4.3.1.2, Test Set 1 incorporated a selection of samples dissolved in 40% ethanol (the same background matrix as the calibration samples) and included: two batches of E150A_X1 already analysed as part of the calibration dataset (re-prepared and re-analysed); four completely new batches of E150a caramel (two E150A_X1 materials and two E150A_X2 substances); and four E150A_X1 caramels passed their date of expiry. When projected into *k*-NN Model 1, all of these samples were correctly assigned as being E150a caramels and on subsequent projection into *k*-NN Model 2, the different E150a formulations of all caramels were correctly predicted. These findings therefore demonstrated that this classification tool was robust to predict the identity of test caramel samples when dissolved in the same background matrix as the calibration data. Additional test samples covering caramels from classes other than E150a and of the remaining E150a formulations would be required to confirm this finding; however this preliminary study did indicate that *k*-NN classification has potential for the classification of caramel materials.

The caramel class and E150A formulation of the expired caramels were also correctly assigned and so indicated that *k*-NN classification would also not be affected by the introduction of ATR-MIR spectra from caramel samples that are at different stages of their shelf life.

Test Set 2 – Caramels in a typical Scotch Whisky matrix (Blend Whisky A)

Test Set 2 included a range of caramel materials dissolved in a typical blend whisky matrix (Blend Whisky A) and incorporated at least one caramel from each of the four E150 classes and at least one example from each of the eight different E150a formulations. On projection into *k*-NN Model 1, the caramel class of all samples was correctly predicted and when the E150a caramels were then projected into *k*-NN Model 2, it was found that all test samples (bar one) were subsequently assigned to the correct E150a formulation. Only the E150A_Y4 caramel was assigned to the wrong E150a formulation, being misclassified as E150A_Y3. This however can be linked to previous results (see section 3.3.1.2) which indicate that E150A_Y3 and

E150A_Y4 have very similar ATR-MIR profiles due to similarities in their manufacturing conditions. These findings demonstrated an improvement over those obtained previously to predict the identity of Test Set 2 samples using PCA with GLSW; *k*-NN classification being able to correctly predict both caramel class and E150a formulation despite the caramels being dissolved in a typical Scotch Whisky matrix. The influence of natural colour has clearly not affected ATR-MIR spectra to the extent where prediction using *k*-NN classification is affected; in other words the test samples are still nearest to their corresponding calibration samples. This data therefore also overcomes another issue identified with PCA with GLSW, where it was found that the addition of a preconcentration step during sample preparation of the test samples caused prediction to be affected. This does not appear to have caused a problem during *k*-NN classification, a finding that is reiterated again in the discussion of the Test Set 4 samples.

Test Set 3 – Caramels in Scotch Whisky with high natural colour (Blend Whisky B)

Test Set 3 incorporated a selection of caramels dissolved in a blend whisky containing a high degree of natural colour (Blend Whisky B): one E150A_X1 caramel; three E150A_X2 caramels; and one E150A_Y5 caramel. This test data set was therefore compiled to assess how the prediction of caramel identities would be affected when high levels of natural colour could interfere with ATR-MIR spectral features. On projection into *k*-NN Model 1 all of the caramels dissolved in Blend Whisky B were correctly predicted as E150a caramels, a vast improvement over the use of PCA with GLSW as a classification tool (which could not assign these samples to any class). Prediction of the E150a formulation of the Test Set 3 samples (*via* projection into *k*-NN Model 2) did however encounter a few misclassifications; although all of the E150A_X1 and E150A_X2 samples were correctly assigned to their corresponding calibration grouping, the E150A_Y5 samples were wrongly predicted as E150A_X2 caramels. These findings therefore indicated that although having excellent potential for caramels dissolved in typical blend whiskies, *k*-NN classification may encounter issues when predicting caramel identities if a high level of natural colour is present in the Scotch Whisky matrix. It would be interesting to

complete additional work in the future to test a wider range of caramels to see if this is a consistent issue when using k -NN classification and it would also be interesting to see whether accounting for the background whisky matrix in the calibration samples would remove this limitation.

An additional sample included in Test Set 3 also helped to highlight another potential drawback of k -NN classification. This sample incorporated Blend Whisky B without the addition of any caramel and it can be seen that in k -NN Model 1 this sample was predicted as being an E150a caramel, whilst in k -NN Model 2 this was assigned as an E150A_Z7 caramel. The major limitation of k -NN classification is therefore that it has to assign a test sample into one of the calibration categories and so if a test sample with an alternative source of colour was inputted this would not be picked up. This therefore introduces the potential for samples to be wrongly assigned as containing a particular caramel and may mean that suspect samples are wrongly predicted as containing authentic E150a if their colour source has not been accounted for during calibration.

Test Set 4 – Caramel solutions that vary in concentration

Test Set 4 was split into two subsets which each contained four E150a caramel solutions of E150A_X1 dissolved in 40% ethanol at different concentration levels (from an absorbance of 0.2 - 0.8 in increments of 0.2). Subset 1 pre-concentrated these samples to the same final volume (hence maintaining the concentration differences for ATR-MIR analysis) to assess whether k -NN classification could correctly predict sample identities despite the fact that changing caramel concentration has been shown previously to influence ATR-MIR spectra (see section 3.3.2.1). Subset 2 was made up of the same initial caramel solutions as for Subset 1 but these were pre-concentrated to provide the same final concentration for all samples prior to ATR-MIR analysis, leaving the only difference between the calibration and test samples as the additional preconcentration step during sample preparation. The purpose of this latter subset was therefore to assess/confirm whether k -NN classification could correctly predict sample identities despite this slight variation in sample preparation. When projected into k -NN Model 1, the samples

from both subsets of Test Set 4 were all correctly assigned as being E150a caramels and on subsequent projection into k -NN Model 2, all were correctly predicted as E150A_X1 caramels. These findings therefore demonstrated that prediction of caramel identities using k -NN classification was not affected by the influence of variation in caramel concentration on ATR-MIR spectra; neither was it affected by the addition of a sample preconcentration step required to obtain adequate spectra from solutions representing the colour level of real whiskies. It should be noted at this point however, that this test set only assessed one type of caramel colourant and so it would be interesting to undertake additional analyses in the future to confirm whether this would always be the case for caramels with different E150a formulations and also caramels of different class.

Test Set 5 – Caramels subjected to fade

As described already in section 4.3.1.2, Test Set 5 included eight samples each for three different caramel types (an E150A_X1, an E150A_X2 and an E150D_X11) that comprised of 3 control solutions and 5 samples varying in their degree of fade to provide a final sample with approximately 30% of its original colour level remaining (45% for the E150d caramel). On projection of the data for these Test Set 5 samples into k -NN Model 1, it was found that all samples (irrespective of their degree of fade) were assigned to the correct caramel class (Figure 4.17). When the E150a caramel solutions were then projected into k -NN Model 2, it was subsequently found that the E150A_X1 and E150A_X2 samples were all correctly assigned to their corresponding calibration grouping even when faded to the highest level assessed in this work. It should be noted here that one of the replicate spectra for an E150A_X1 control sample was actually misclassified as being an E150A_Z8 caramel. This can potentially be discounted as an outlier however as the identity of all of the other eight control spectra were correctly predicted. The findings obtained from this part of the study therefore indicated that k -NN classification could have the ability to correctly predict both caramel class and E150a formulation even if the caramel being analysed had undergone fading. It would be interesting to take this work further and confirm these findings for the remaining caramel classes (E150B and E150C) and for the other formulation of E150a. Future work looking at the process of fade when

caramels are dissolved in the Scotch Whisky matrix would also be interesting, to determine whether the affect of fade on natural colour would cause spectra to be affected differently when caramels are dissolved in Scotch Whisky.

4.3.3.2 Summary

Overall, the preliminary assessment of k -NN classification as a tool for predicting caramel identities has indicated that it has potential for this purpose. In contrast to PCA with GLSW, k -NN classification was able to correctly predict both the caramel class and E150a formulation of test data and in this preliminary study prediction was not affected by: caramels being dissolved in a typical Scotch Whisky matrix; variation in caramel concentrations; the addition of a preconcentration step during the preparation of test samples (not used for the preparation of calibration samples); and caramels subjected to an extreme level of fade. Despite these clear advantages of the k -NN classification tool over PCA with GLSW preprocessing, a few drawbacks were however identified, one of which could be quite major. The prediction of caramel identities using k -NN classification was found to deteriorate when caramels were dissolved in a blend whisky containing a high degree of natural colour. This however could potentially be improved upon or resolved if the features of natural colour were to be accounted for in the calibration model. The only potentially major downfall of k -NN classification identified was therefore down to the fact that it has to predict a test sample into one of the calibration categories (whichever one it is closest to). This means that samples with a colour source not accounted for within the calibration model would not be picked up and so introduces the potential for test or unknown samples to be misclassified as authentic when they might not be. This issue led to the investigation of an additional classification technique (PC-DFA) for the classification of caramel identities, which does not have to assign samples to one of the calibration categories unless it falls within a pre-assigned confidence limit (falls within an appointed threshold). PC-DFA could therefore potentially overcome this major limitation identified for k -NN classification and the findings obtained are discussed within the following section.

4.3.4 PC-DFA

As is the case with k -NN classification, PC-DFA is a supervised pattern recognition technique and so can be used to automatically predict the identity of test (or unknown) samples provided that a training set is available where the class membership of each sample is already known. As described previously in section 2.3.2.3, PC-DFA seeks out canonical variates that will maximise between group distances whilst reducing within group variation and is known to provide good classification when samples are linearly separable. A preliminary investigation into PC-DFA was therefore investigated within this research to assess its capabilities for the assignment of test caramel identities (both their caramel class and where relevant their E150a formulation). Time did not allow for an assessment of the prediction accuracies for test data using PC-DFA to be investigated and so the results that follow instead discuss visual interpretations of the PC-DFA measurement spaces for the different test datasets assessed.

4.3.4.1 Assigning caramel class and E150a formulation to test data

PC-DFA was initially assessed in this research to determine its potential for assigning the caramel class of test samples (Test Sets 1 – 5) and so calibration Dataset 1 was utilised to create a calibration model (PC-DFA Model 1). It should be noted at this point that only the spectral measurements labelled as calibration samples (and not validation samples) in Table 4.1 were utilised in the creation of this PC-DFA model, for ease of visualisation on the measurement space. After the initial assessment of the test data to assign its caramel class was completed, a second PC-DFA Model (PC-DFA Model 2) was subsequently created (using the samples contained within calibration Dataset 2) to determine the ability of this classification tool for the assignment of E150a formulations for all of the E150a classed caramels found within the test datasets. The results obtained from these analyses are discussed over the following subsections for each of the test datasets in turn.

Test Set 1 – Caramels in 40% ethanol

The ATR-MIR spectra acquired from the Test Set 1 samples were first projected into PC-DFA Model 1 to assess the ability of this classification tool for assigning the

caramel class of these test samples. Figure 4.19 illustrates the resulting measurement space and it was clearly observed that all of the test samples clustered in the same region as the E150a calibration cluster, the correct identity of these samples. On subsequent projection of the Test Set 1 samples onto the measurement space defined by PC-DFA Model 2, it was also found that each formulation of E150a overlaid well with its corresponding calibration grouping (Figure 4.20). These findings therefore indicated that PC-DFA has good potential for the prediction of caramel identities when dissolved in 40% ethanol (the same medium as for the calibration samples); correctly indicating the identity of re-prepared/re-analysed caramels, new caramel batches and those passed their expiry date, as being E150a caramels. As was the case for PCA with GLSW preprocessing however, future work with a much larger test dataset would be required to confirm these findings for those caramels not assessed.

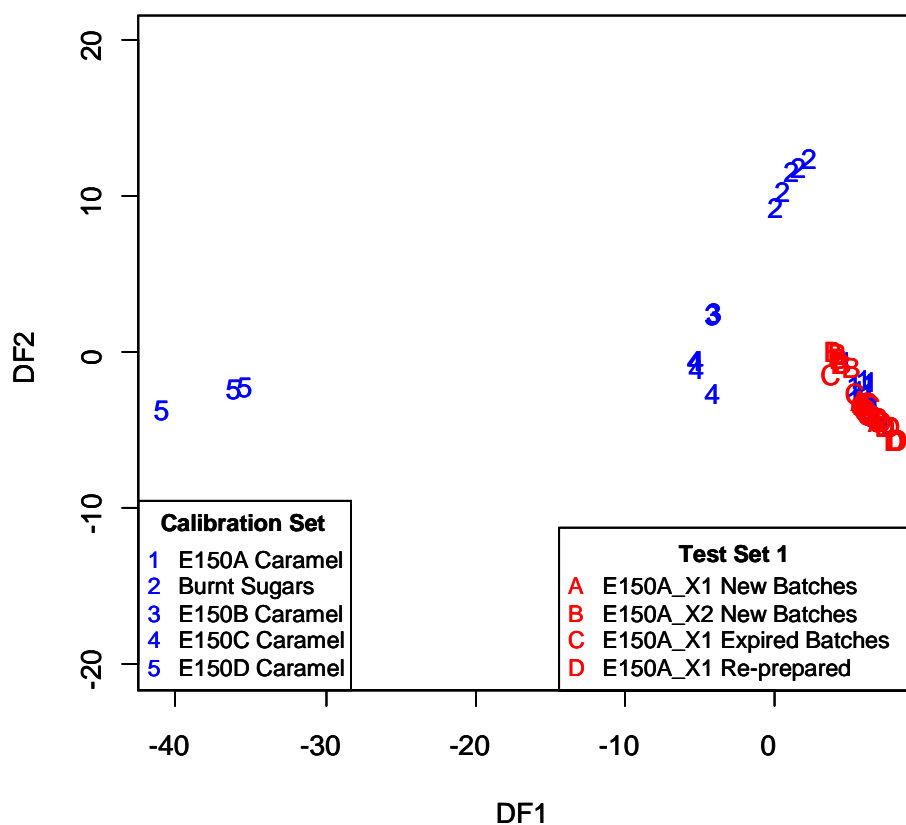


Figure 4.19: Projection of the Test Set 1 samples onto the measurement space defined by PC-DFA Model 1.

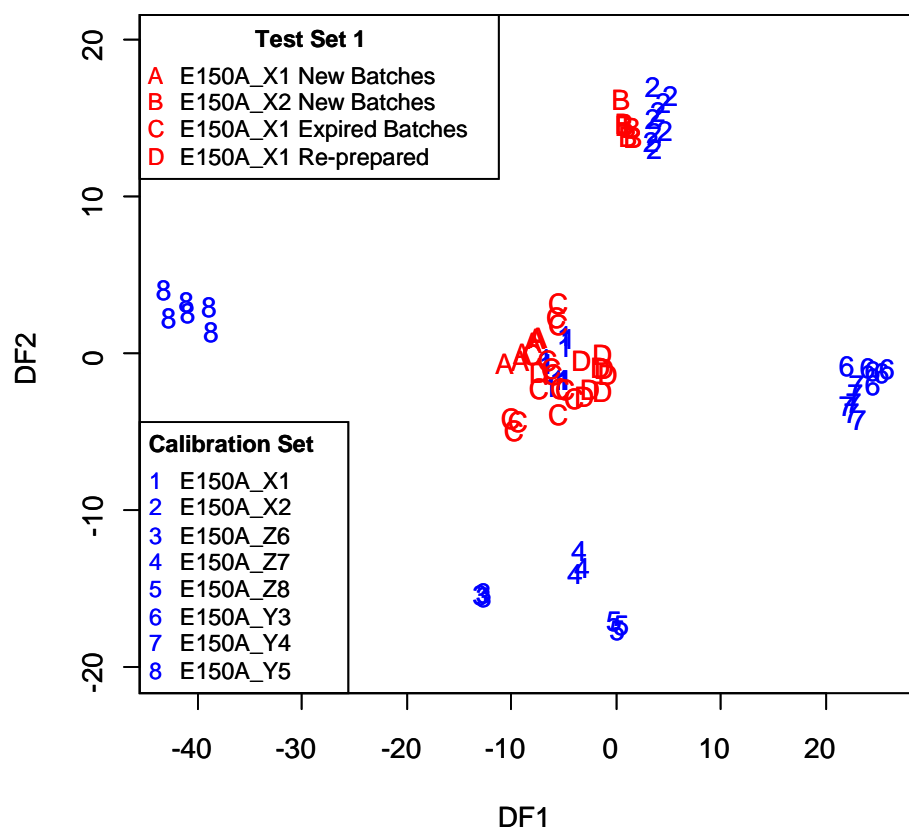


Figure 4.20: Projection of the Test Set 1 samples onto the measurement space defined by PC-DFA Model 2.

Test Set 2 & 3 – Caramels in the Scotch Whisky matrix

The Test Set 2 samples (incorporating a selection of E150a caramels dissolved in a typical blend whisky – the data for the other classes of caramel in this blend were not available at this point) were firstly projected into PC-DFA Model 1 to determine the ability of the data analysis tool for assigning the caramel class of these samples. The resulting PC-DFA measurement space has been provided in Figure 4.21 and it was clearly demonstrated that all test samples were found in very close proximity to the E150a calibration grouping. This indicated that even when dissolved in a typical Scotch Whisky, the correct caramel class of test/unknown samples could potentially be predicted using PC-DFA. The inclusion of additional test samples representing the other caramel classes would however be required to confirm if this was always the case.

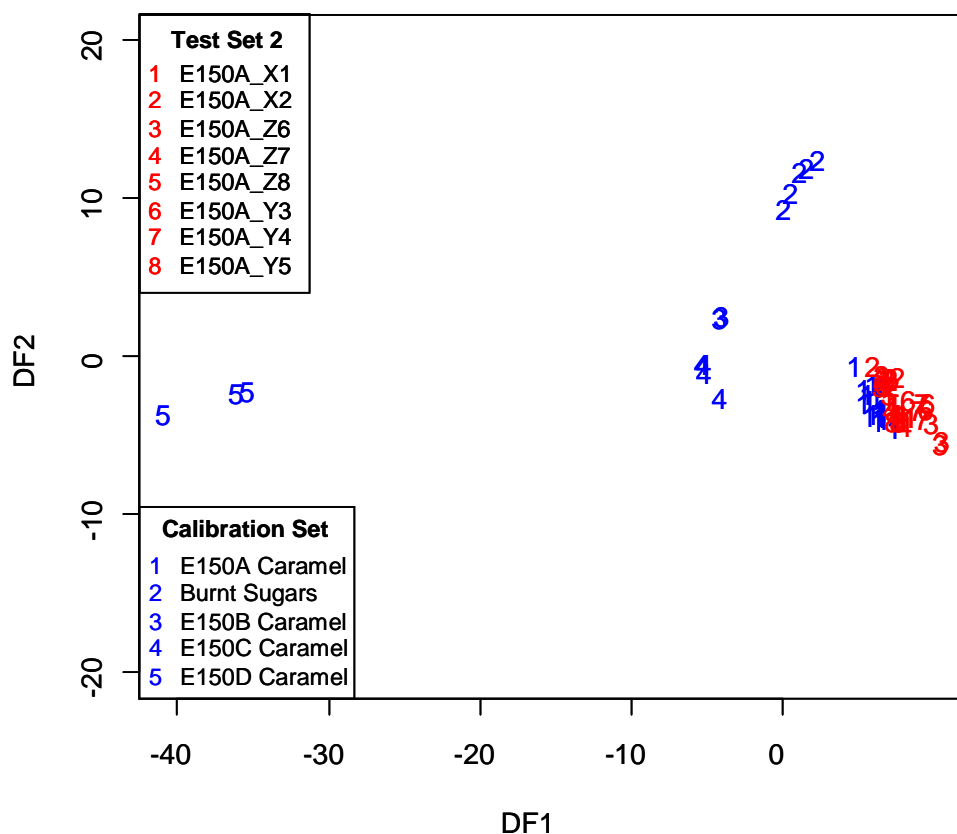


Figure 4.21: Projection of the Test Set 2 samples onto the measurement space defined by PC-DFA Model 1.

Projection of the Test Set 2 samples into PC-DFA Model 2 to assess prediction of their E150a formulation has been depicted within Figure 4.22 and it was found that although the test samples did not all overlay with their equivalent calibration grouping, they were at least found in a region of space closest in proximity to their corresponding calibration cluster. This finding therefore indicated that PC-DFA could potentially allow the correct prediction of E150a formulations, even when these caramel materials are dissolved in a typical Scotch Whisky. The shift in the test samples from their equivalent calibration groupings did however demonstrate that the background matrix of this typical Scotch Whisky is influencing ATR-MIR spectral features to the extent that the values obtained during PC-DFA are affected. Therefore, as was found for PCA with GLSW, classification of E150a formulations using PC-DFA would potentially need to account for the whisky matrix in the calibration model. This could also potentially be implemented to improve the classification of caramel class using PC-DFA if required, when caramels are dissolved in a typical Scotch Whisky.

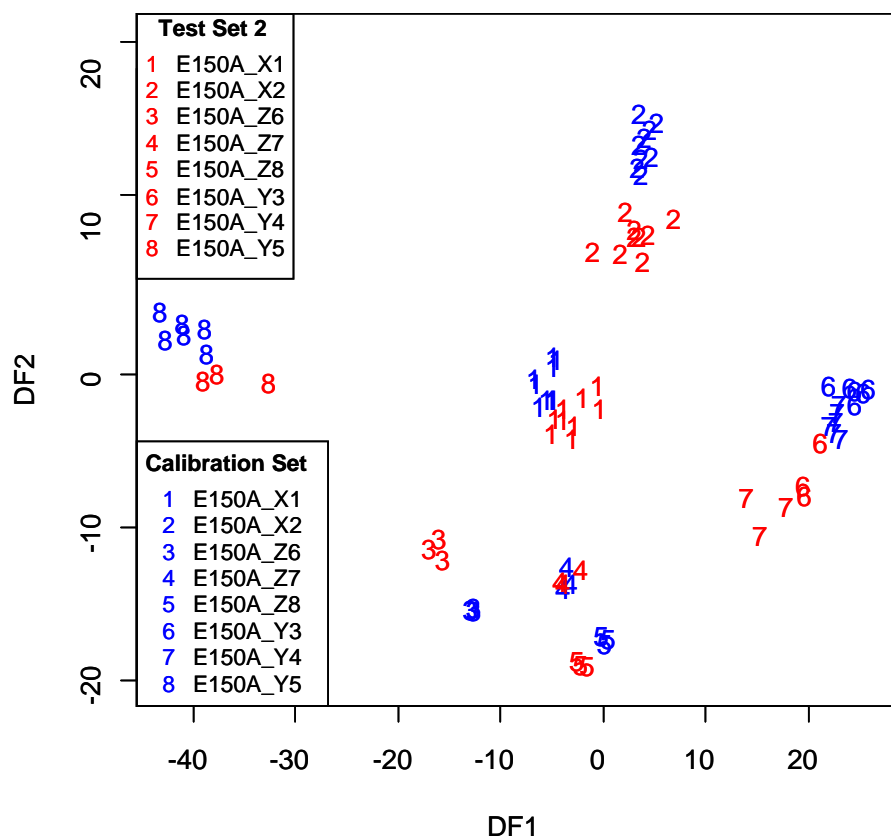


Figure 4.22: Projection of the Test Set 2 samples onto the measurement space defined by PC-DFA Model 2.

Projection of the Test Set 3 samples into both of the PC-DFA models also reiterated that the application of this classification technique for the prediction of caramel identities would require the background whisky matrix to be accounted for during calibration. As previously described, the Test Set 3 samples constitute three different types of E150a caramel dissolved in a blend whisky containing an extremely high degree of natural colour. Prediction using PC-DFA was found to be affected to an even greater extent in this case than previously observed for the Test Set 2 samples, in accordance with the increased influence of natural colour on spectral features for the darker blend. This can be seen within Figures 4.23 and 4.24 which show the Test Set 3 samples projected onto the measurement space for PC-DFA Model 1 and PC-DFA Model 2 respectively.

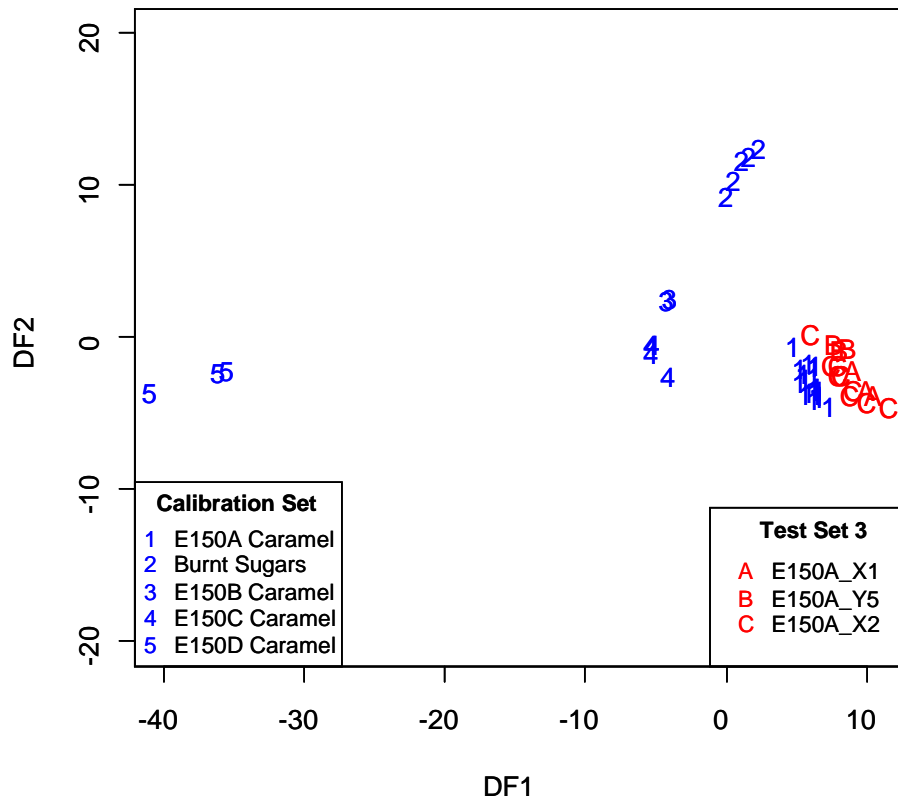


Figure 4.23: Projection of the Test Set 3 samples onto the measurement space defined by PC-DFA Model 1.

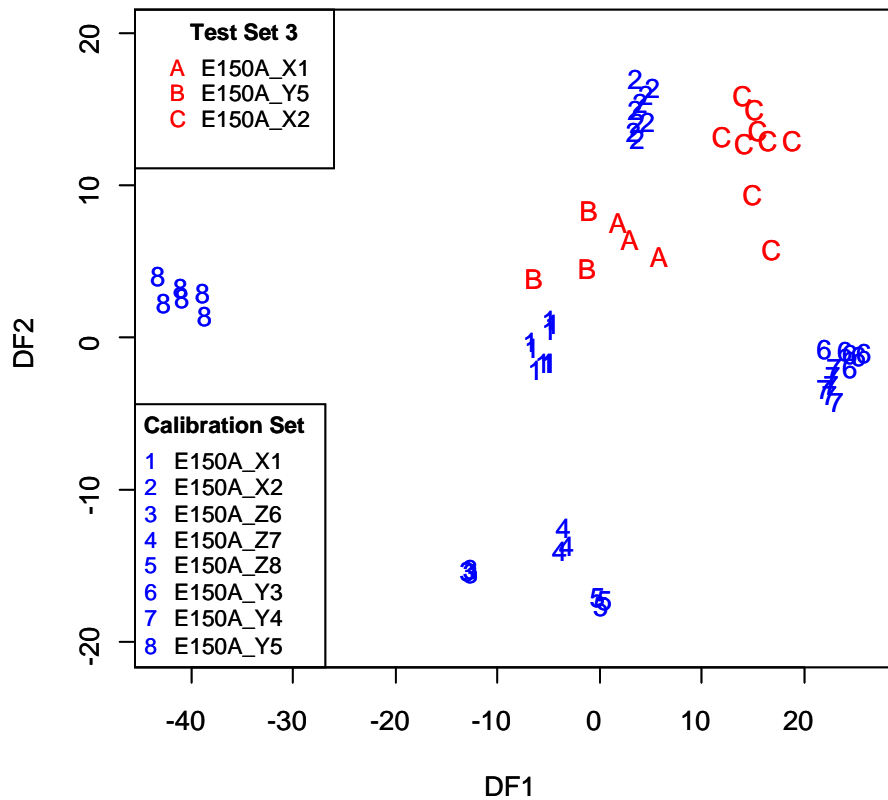


Figure 4.24: Projection of the Test Set 3 samples onto the measurement space defined by PC-DFA Model 2.

Test Set 4 – Variation in caramel concentration

As previously discussed earlier in this chapter, the Test Set 4 samples comprise of two subsets: ‘Subset 1’, incorporating four E150A_X1 caramel solutions at different concentrations; and ‘Subset 2’, being the same but accounting for these concentration differences and leaving the only difference with the calibration samples as an additional preconcentration step during sample preparation. The data acquired from the Test Set 4 samples were initially projected into PC-DFA Model 1 to assess whether these variable parameters would potentially affect the prediction of caramel class (all being E150a in this case) using this data analysis tool. The resulting measurement space has been provided within Figure 4.25 and it was clearly shown that although the Subset 2 samples overlaid reasonably well with the E150a calibration grouping, not all of the Subset 1 samples did. These findings therefore indicated that the prediction of caramel class using PC-DFA would potentially be affected by variations in caramel concentration; the additional preconcentration step used during sample preparation however, did not appear as if it would significantly influence class assignment. Additional samples would need to be assessed in the future to determine whether this were the case for the prediction of all E150 classes.

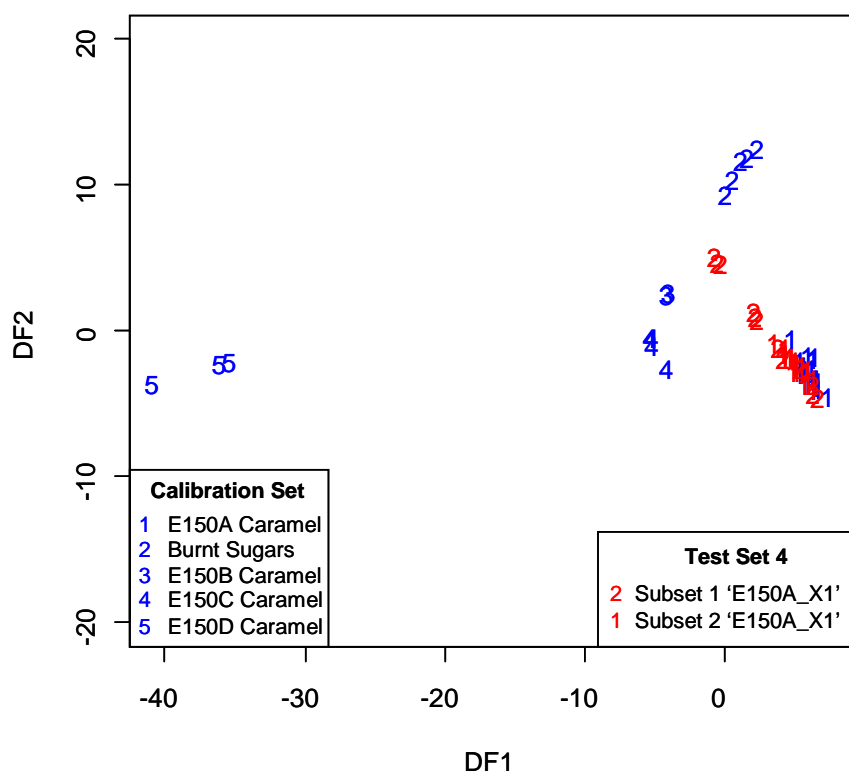


Figure 4.25: Projection of the Test Set 4 samples onto the measurement space defined by PC-DFA Model 1.

Projection of the Test Set 4 samples into PC-DFA Model 2 to assess prediction of their E150a formulation has been depicted within Figure 4.26 and it was found that although some samples overlaid well with their corresponding E150a calibration grouping (E150A_X1), a number of caramel solutions from both Subsets 1 and 2 were found to be situated significantly further away in the measurement space. This finding therefore indicated that the prediction of E150a formulation using PC-DFA would potentially be affected both if test samples vary in caramel concentration with respect to the calibration samples and also if they have been prepared using an additional preconcentration step.

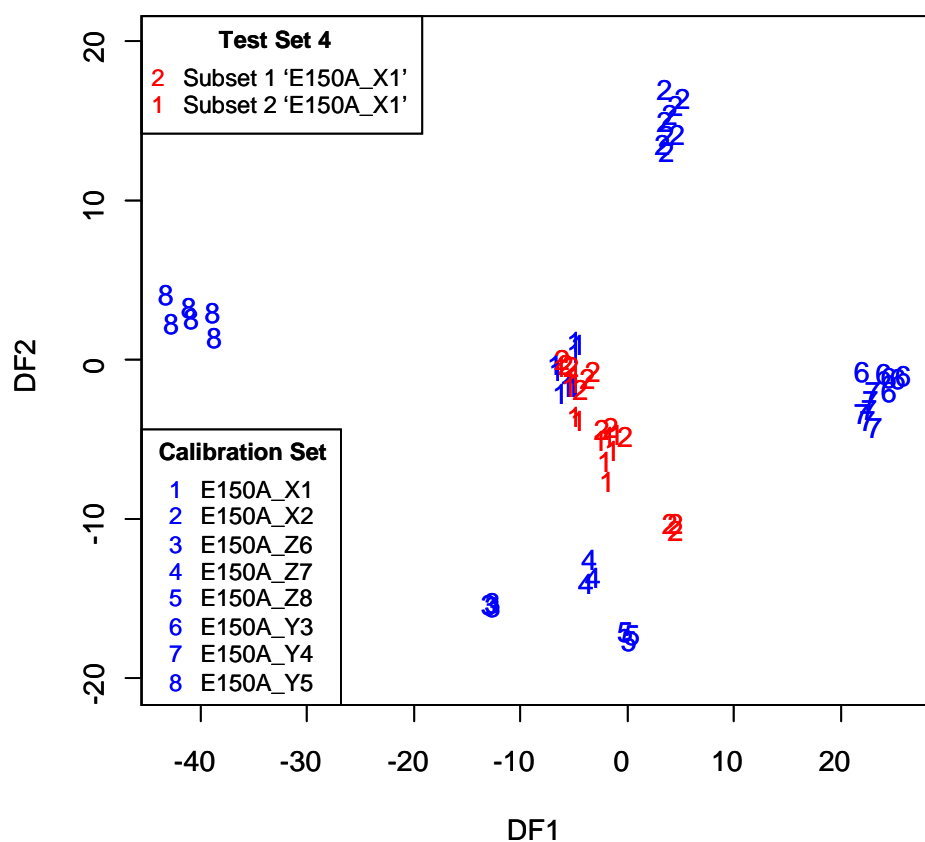


Figure 4.26: Projection of the Test Set 4 samples onto the measurement space defined by PC-DFA Model 2.

Test Set 5 – Caramel Fade

Figure 4.27 illustrates the Test Set 5 samples projecting into PC-DFA Model 1 to investigate the potential influence of caramel fade on the ability of this classification tool to predict the caramel class of test samples. As previously described, the Test Set 5 samples constituted solutions of an E150A_X1, an E150A_X2 and an

E150D_X11 subjected to varying degrees of fade. Figure 4.27 clearly demonstrated that the prediction of caramel class using PC-DFA would be affected by caramel fade. In the case of the E150a test caramels, all of the control samples (that had not been faded) overlaid very well with their corresponding calibration grouping but all of the faded E150a caramels (no matter the degree of fade) were found offset to the E150a calibration cluster (their DF1 scores generally increasing in accordance with fade). When the E150d caramel samples of Test Set 5 were considered, it was observed that all samples were offset from the E150d calibration grouping. It could therefore not be conclusively stated that caramel fade influenced the prediction of caramel class for E150d caramels, as the control samples were also apart from the relevant calibration cluster. This was tentatively put down to the small number of E150d samples incorporated within the calibration data (especially in comparison with the number of E150a calibration samples). It would be interesting to obtain a much larger set of calibration samples in the future to allow a more consistent representation of samples from each of the caramel classes. As E150a caramels are the only class legally permitted within Scotch Whisky, this was the reason behind a higher number of samples being available for this class and also why predictions were in general focussed on E150a test samples during this preliminary research.

Subsequent projection of the E150a samples of Test Set 5 into PC-DFA Model 2 demonstrated that the prediction of E150a formulation using PC-DFA would also be influenced by the fading process (Figure 4.28). Although the control samples of both the E150A_X1 and E150A_X2 caramels cluster together in quite close proximity to their corresponding calibration groupings, the positioning of the faded samples are varied. In the case of E150A_X1 it can be seen that as the level of fade is increased, both the DF1 and DF2 scores generally decrease away from the E150A_X1 calibration grouping. In the case of E150A_X2, fade does not appear to have as significant an affect. Only the E150A_X2 sample solution faded for seven days (to ~30% of its original colour level) was found in a region of the measurement space far away from the calibration samples that match its identity. Overall however, these findings indicated that prediction of E150a formulation would be affected by the implementation of test/unknown samples that have been subjected to fade.

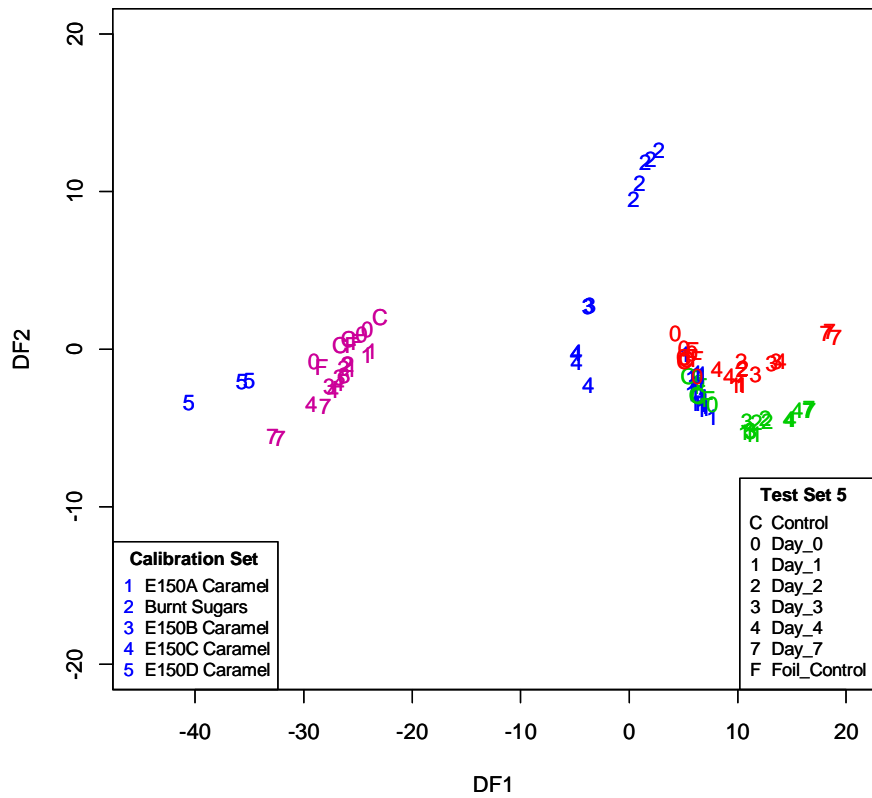


Figure 4.27: Projection of the Test Set 5 samples onto the measurement space defined by PC-DFA Model 1. KEY: E150A_X1 samples (green lettering), E150A_X2 samples (red lettering) and E150D_X11 samples (purple lettering).

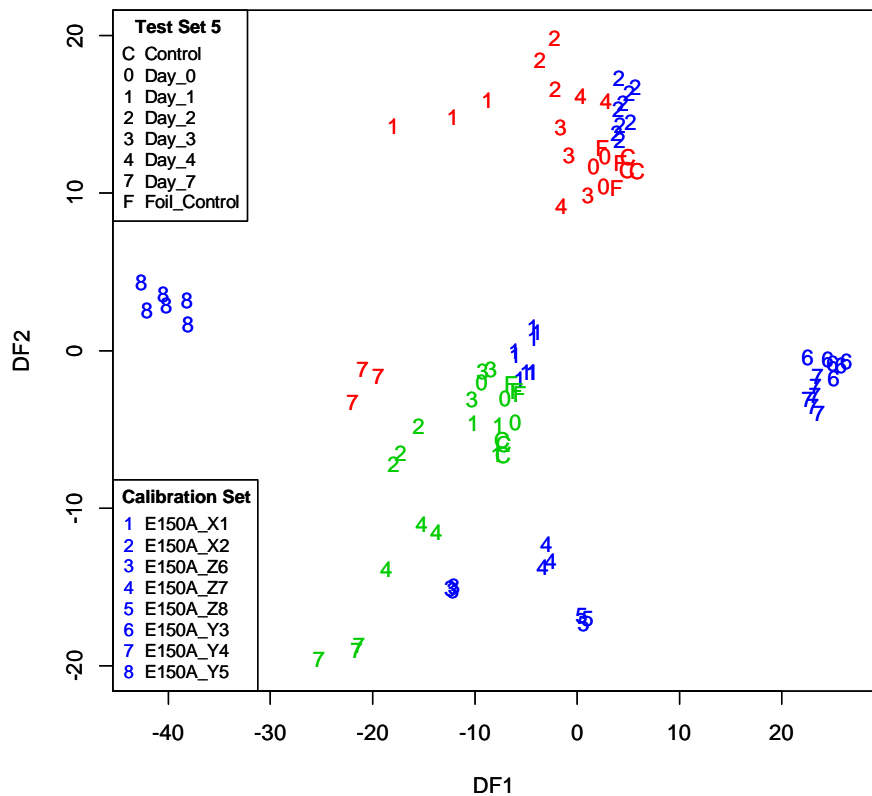


Figure 4.28: Projection of the Test Set 5 samples onto the measurement space defined by PC-DFA Model 2. KEY: E150A_X1 samples (green lettering) and E150A_X2 samples (red lettering).

4.3.4.1 Summary

Overall, the preliminary results presented above have indicated that PC-DFA could have good potential as a classification tool for predicting caramel identities in Scotch Whisky. The findings were however very similar to those previously observed when utilising PCA with GLSW preprocessing. When caramels were dissolved in the same matrix as the calibration samples (40% ethanol) assignment of caramel class and E150a formulation appeared to be reasonably successful, however if caramel materials were dissolved in a Scotch Whisky matrix it was found that this would likely need to be accounted for in the calibration model. In addition, it was found that the prediction of caramel class and E150a formulation using PC-DFA would also be affected by factors such as: the addition of a pre-concentration step during the preparation of test samples; any variation in caramel concentration between the calibration and test samples; and also if the test samples had been subjected to fade.

4.3.5 Prediction of Blend Whisky Identities using Classification Tools

Previous findings in Chapter 3 indicated that when caramels are dissolved in the Scotch Whisky matrix, the ATR-MIR spectra resulting from the dried sample residues are dominated by the caramel constituents. It was additionally found however, that natural colour components present in the whisky matrix also had an influence on spectra and so a preliminary study was undertaken to determine whether different blends on the market could be distinguished between using ATR-MIR analysis of dried sample residues, based on the differences caused by variation in natural colour components (see section 3.3.3). PCA was undertaken to examine this proposal for four blend whiskies and it was found that the ATR-MIR spectral features were too similar to allow discrimination between the four different blends. In other words the dominance of the caramel features would not permit samples to be differentiated between using PCA.

This section of the research therefore aimed to progress from these initial findings and determine whether discrimination between the four blends (and hence prediction of their identities based on characteristic ATR-MIR spectral features) could be improved *via* the application of more advanced data analysis techniques. To do this

the ATR-MIR data acquired previously for the four different blends were split into a 'calibration set' and a 'test set'; the former containing four batches of each blend and the latter containing one batch of each blend. After the construction of calibration models, prediction of the test sample identities was then attempted using each of the classification tools described previously within this Chapter (PCA with GLSW preprocessing, k-NN classification and PC-DFA) and all were found to improve discrimination between the four different blends in the calibration models. The best results were achieved however, using PC-DFA and so these have been depicted within Figure 4.29, which illustrates projection of the test data onto the PC-DFA calibration model. Figure 4.29 clearly demonstrates that distinction between the four different blends has been achieved, PC-DFA successfully maximising between group distances whilst reducing within group variation. This is a vast improvement compared to the previous findings where these data were analysed using PCA alone (see Figure 3.25 in section 3.3.3). Projection of the test data into the PC-DFA calibration model also demonstrated that in general, very good overlay was achieved between test samples and their corresponding calibration categories. Only the triplicate spectra of the Blend 3 test samples were found to be slightly separated from their equivalent calibration grouping, although they were still closest to this cluster and not mistaken for one of the other blends. The reason behind this separation for the Blend 3 test data is currently unclear and so it would be interesting to obtain additional test samples in the future to determine whether this was a consistent finding. This preliminary investigation however, has demonstrated that it could be possible to discriminate between Scotch Whisky products already on the market using ATR-MIR spectrometry and subsequently predict their identities using advanced data analysis techniques.

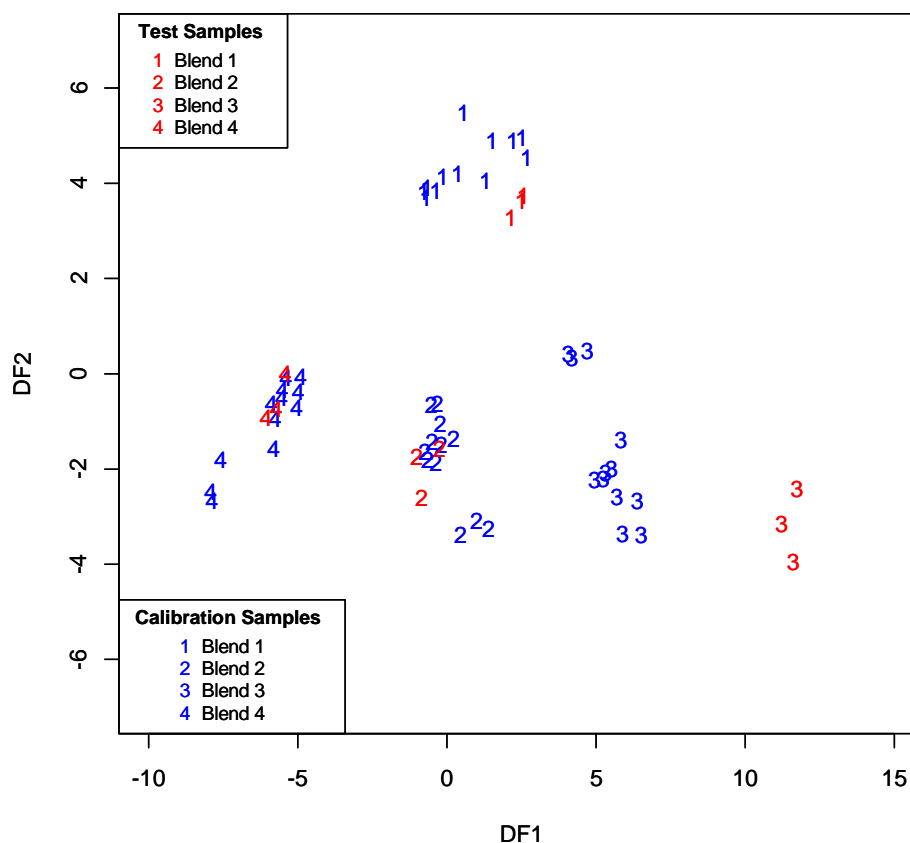


Figure 4.29: PC-DFA of the normalised first derivative spectra acquired from ATR-MIR analysis of the dried residues of four batches each of four blend whiskies (Blend 1 – 4). Data acquired from test data (incorporating one batch of each blend) has then been projected onto the measurement space. All samples have been analysed in triplicate.

4.4 Conclusions

The research presented within this chapter has successfully provided a comparison of different data analysis tools for the prediction of caramel identities (both their class and where relevant E150a formulation) based on the ATR-MIR spectral features acquired from dried sample residues. A selection of data analysis tools were investigated as part of this work and although one did not stand out at this point as being most successful, the advantages and limitations in terms of how they could be applied for future work were carefully compared. The data analysis tools PCA with GLSW preprocessing and PC-DFA would be the best to take forward for future studies and were found to provide very similar results within this preliminary research. Both were demonstrated to show excellent potential for the prediction of caramel identities when dissolved in 40% ethanol but it was indicated that the background matrix would need to be accounted for during calibration if

predicting/assigning caramel identities when dissolved in Scotch Whisky products. A number of additional studies would also need to be undertaken, using test samples representing a wider range of caramel types. In addition to this, predictions using both of these techniques were found to be affected by factors such as: variation in caramel concentrations between the calibration and test data; the addition of a pre-concentration step during the preparation of test samples; and also if a test caramel had been subjected to fade. Future work would therefore be required to determine whether these variable parameters could be accounted for either by adjusting sample preparation/ATR-MIR methodology or by adjusting the sample types incorporated within calibration models.

The data analysis tool *k*-NN classification was also investigated for the prediction of caramel identities within this research and showed very promising results. In contrast to the previous two techniques (PCA with GLSW preprocessing and PC-DFA) it was actually possible to correctly assign both the caramel class and E150a formulation of various test datasets using calibration samples dissolved in 40% ethanol (i.e. the pure caramel profiles) when: (1) samples were dissolved in a typical blend whisky matrix; (2) caramel concentration was varied; (3) samples were prepared using an additional pre-concentration step in comparison to the calibration data; and (4) when caramel materials had been faded. The only main difficulty encountered with *k*-NN classification was when attempting to predict the E150a formulation of test samples when dissolved in a blend whisky containing high levels of natural colour. In this case a selection of the test samples were misclassified and so indicated that in such an extreme situation, the background whisky matrix would potentially need to be accounted for during calibration. Despite the clear advantages of *k*-NN classification over the other two tools investigated, there was one major drawback that could limit its use for future work; *k*-NN classification has to appoint test data into one of the pre-assigned calibration categories and so this could cause misclassifications if the identity of a test or unknown sample was not accounted for within the calibration data. This could be a problem when assessing suspect samples within the Scotch Whisky industry where the origin of colour could be completely unknown.

Overall the main findings from this chapter have demonstrated the potential to utilise data analysis tools to predict the identity of caramel colourants when dissolved within Scotch Whisky, something that has never been done before. This would be extremely beneficial to the Scotch Whisky industry, particularly in terms of authenticity testing. It could allow the potential to confirm the presence (or absence) of a legally permitted caramel within a suspect product or alternatively, future whiskies could be spiked with E150a caramels manufactured to possess distinct signature profiles and so be used as markers for the positive identification of specific blends.

In addition to predicting caramel identities using classification techniques, part of the research undertaken within this chapter also investigated their ability to discriminate between blends already on the market and subsequently predict the identity of test samples. Using PC-DFA it was shown that four blends could be clearly distinguished between and on projection of test data into the calibration model, three of the four test samples very obviously overlaid with their corresponding calibration samples. These findings could be extremely beneficial for the Scotch Whisky industry, introducing the potential to use ATR-MIR spectrometry in combination with multivariate data analysis to confirm the authenticity/identity of market blends. Future work would be required in this area however, incorporating a much larger dataset and a wider variety of the available whisky products.

4.5 References

1. Y. Liu, Q. Jiang, T. Shi, T. Fei, J. Wang, G. Liu, Y. Chen, *Acta Agr. Scand. B-S P*, 2014, **64**, 267-281
2. B. M. Wise, J. M. Shaver, N. B. Gallagher, *Using clutter to improve pattern recognition, calibration and classification models*, at the Mediterranean Meeting: Application of Multivariate Analysis and Chemometry to Cultural Heritage and Environment, Taormina (Italy), 2010
3. B. M. Zorzetti, J. M. Shaver, J. J. Harynuk, *Anal. Chim. Acta*, 2011, **694**, 31-37
4. Q. Fu, X. He, G. Lin, H. Suo, C. Zhao, *Anal. Methods*, 2012, **4**, 1813-1819
5. R. P. Cogdill, C. A. Anderson, J. K. Drennen III, *AAPS PharmSciTech*, 2005, **6**, E284-E297
6. B. M. Wise, H. Martens, M. Høy, R. Bro, P. B. Brockhoff, *Calibration transfer by generalized least squares*, Eigenvector Research, Inc., Available online at: http://www.eigenvector.com/Docs/GLS_Standardization.pdf, Accessed January 2015
7. Q. Fu, J. Wang, G. Lin, H. Suo, C. Zhao, *J. Anal. Methods in Chem.*, 2012, **2012**, 1-7, Article ID 728128
8. U. K. Acharya, K. B. Walsh, P. P. Subedi, *J. Near Infrared Spec.*, 2014, **22**, 279-286
9. U. K. Acharya, K. B. Walsh, P. P. Subedi, *J. Near Infrared Spec.*, 2014, **22**, 287-295
10. O. Rozenstein, T. Paz-Kagan, C. Salbach, A. Karnieli, *IEEE J. Sel. Top. Appl.*, 2014, **Preprint**, 1-12
11. J. H. da Silva Taveira, F. M. Borém, L. P. Figueiredo, N. Reis, A. S. France, S. A. Harding, C. Tsai, *Food Res. Int.*, 2014, **61**, 75-82
12. V. Ulissi, F. Antonucci, C. Costa, P. Benicasa, P. Menesatti, *Agric. Eng. Int.:CIGR*, 2011, **13**, 1-7
13. S. Serranti, D. Cesare, F. Marini, G. Bonifazi, *Talanta*, 2013, **103**, 276-284
14. S. Serranti, D. Cesare, G. Bonifazi, *Biosyst. Eng.*, 2013, **115**, 20-30
15. M. Dotlich, R. M. Kattner, R. Roginski, J. Shaver, *American Pharmaceutical Review*, 2013, **16 (7)**

16. B. M. Wise, J. M. Shaver, N. B. Gallagher, *Orthogonalization Approaches for Data Preprocessing with Pharmaceutical, Petrochemical and Remote Sensing Applications*, unpublished conference paper at: APACT 13, 24-26 April 2013, Chester
17. *EigenGuide: Advanced Preprocessing 2 (GLS in classification)*, http://www.eigenvector.com/eigenguide.php?m=GLS_on_Olive_Oil, Accessed 05/02/2015
18. S. Sharma, M. Goodarzi, H. Ramon, W. Saeys, *Talanta*, 2014, **121**, 105-112
19. O. Beckonert, M. E. Bollard, T. M. D. Ebbels, H. C. Keun, H. Antti, E. Holmes, J. C. Lindon, J. K. Nicholson, *Anal. Chim. Acta*, 2003, **490**, 3-15
20. Y. Tikunov, A. Lommen, C. H. Ric de Vos, H. A. Verhoeven, J. Bino, R. D. Hall, A. G. Bovy, *Plant Physiol.*, 2005, **139**, 1125-1137
21. K Kim, P. Aronov, S. O. Zakharkin, D. Anderson, B. Perroud, I. M. Thompson, R. H. Weiss, *Mol. Cell. Proteomics*, 2009, **8**, 558-570
22. E. Holmes, R. L. Loo, J. Stamler, M. Bictash, I. K. S. Yap, Q. Chan, T. Ebbels, M. De Iorio, I. J. Brown, K. A. Veselkov, M. L. Davignus, H. Kesteloot, H. Ueshima, L. Zhao, J. K. Nicholson, P. Elliott, *Nature*, 2008, **453**, 396-400
23. Y. Dai, Z. Li, L. Xue, C. Dou, Y. Hou, L. Zhang, X. Qin, *J. Ethnopharmacol.*, 2010, **128**, 482-489
24. J. Taylor, R. D. King, T. Altmann, O. Fiehn, *Bioinformatics*, 2002, **18**, S241-S248
25. X. Wang, A. Zhang, Y. Han, P. Wang, H. Sun, G. Song, T. Dong, Y. Yuan, X. Yuan, M. Zhang, N. Xie, H. Zhang, H. Dong, W. Dong, *Mol. Cell. Proteomics*, 2012, **11**, 370-380
26. J-L. Chen. H-H. Liu, C-T. Chuang, *Mar. Pollut. Bull.*, 2015, In Press (Strategic planning to reduce conflicts for offshore wind development in Taiwan: A social marketing perspective), 12 pages
27. G. Stalidis, D. Karapistolis, A. Vafeiadis, *Procedia Soc. Behav. Sci.*, 2014, **175**, 106-113
28. K-Y. Wang, I-H. Ting, H-J. Wu, *J. Bus. Res.*, 2013, **66**, 1360-1366
29. I-C. Yeh, C-H. Lien, T-M. Ting, C-Hao. Liu, *Expert Syst. Appl.*, 2009, **36**, 11249-11256

30. B. S. Everitt, S. Landau, M. Leese, D. Stahl, *Cluster Analysis*, 5th Edition, John Wiley & Sons, Chichester, 2011
31. S. Gok, M. Severcan, E. Goormaghtigh, I. Kandemir, F. Severcan, *Food Chem.*, 2015, **170**, 234-240
32. M. De Luca, W. Terouzi, G. Ioele, F. Kzaiber, A. Oussama, F. Oliverio, R. Tauler, G. Ragno, *Food Chem.*, 2011, **124**, 1113-1118
33. J. M. Juardo, A. Alcázar, F. Pablos, M. J. Martin, A. G. González, *Talanta*, 2005, **66**, 1350-1354
34. E. A. F. Da Silva torres, M. L. Garbelotti, J. M. M. Neto, *Food Chem.*, 2006, **99**, 622-629
35. T. Yi, L. Zhu, W-L. Peng, X-C. He, H-L. Chen, J. Li, T. Yu, Z-T. Liang, Z-Z. Zhao, H-B. Chen, *LWT-Food Sci. Technol.*, 2015, **62**, 194-201
36. B. S. Everitt, S. Landau, M. Leese, D. Stahl, *Cluster Analysis*, 5th Edition, John Wiley & Sons, Chichester, 2011
37. J. B. Nikas, W. C. Low, *Comput. Meth. Prog. Bio.*, 2011, **104**, e133 – e147
38. M. P. Reser, K. A. Allott, E. Killackey, J. Farhall, S. M. Cotton, *Psychiatry Res.*, 2015, **229**, 819-827
39. J. F. McGuire, E. Nyirabahizi, K. Kircanski, J. Piacentini, A. L. Peterson, D. W. Woods, S. Wilhelm, J. T. Walkup, L. Scahill, *Psychiatry Res.*, 2013, **210**, 1198-1204
40. A. T. Bruni, J. A. Velho, A. S. L. Ferreira, M. J. Tasso, R. S. Ferrari, R. L. Yoshida, M. S. Dias, V. B. P. Leite, *J. Forensic Leg. Med.*, 2014, **26**, 29-38
41. X. Wang, D. Sheng, Z. Zhu, F. Xu, D. Huang, C. Yu, *Spectrochim. Acta A Mol. Biomol. Spectrosc.*, 2015, **141**, 94-98
42. C. Yu, C-Z. Wang, C-J. Zhou, B. Wang, L. Han, C-F Zang, X-H. Wu, C.S. Yuan, *J. Pharm. Biomed. Anal.*, 2014, **99**, 8-15
43. M. Kansiz, P. Heraud, B. Wood, F. Burden, J. Beardall, D. McNaughton, *Phytochemistry*, 1999, **52**, 407-417
44. G. Kos, H. Lohninger, R. Krska, *Anal. Chem.*, 2003, **75**, 1211-1217
45. R. Dell'Anna, P. Lazzeri, M. Frisanco, F. Monti, F. M. Campeggi, E. Gottardini, M. Bersani, *Anal. Bioanal. Chem.*, 2009, **394**, 1443-1452
46. S. Dudoit, J. Fridlyand, T. P. Speed, *J. Am. Stat. Assoc.*, 2002, **97**, 77-87

47. P. Anbeck, K. L. Vincken, G. S. Van Bochove, M. J. P. Van Osch, J. Van der Grond, *NeuroImage*, 2005, **27**, 795-804
48. P. Bhuvanewari, A. B. Therese, *Procedia Mat. Sci.*, 2015, **10**, 433-440
49. H-G. Acosta-Mesa, N. Cruz-Ramírez, R. Hernández-Jiménez, *Comput. Biol. Med.*, 2009, **39**, 778-784
50. R. M. Balabin, R. Z. Safieva, E. I. Lomakina, *Anal. Chim. Acta*, 2010, **671**, 27-35
51. R. M. Balabin, R. Z. Safieva, *Anal. Chim. Acta*, 2011, **689**, 190-197
52. A. R. Caneca, M. F. Pimentel, R. K. H. Galvão, C. E. da Matta, F. R. De Carvalho, I. M. Raimundo Jr., C. Pasquini, J. J. R. Rohwedder, *Talanta*, 2006, **70**, 344-352
53. P. S. Gromski, Y. Xu, K. A. Hollywood, M. L. Turner, R. Goodacre, *Metabolomics*, 2014, **11**, 684-695
54. E. Sikorska, T. Górecki, I. V. Khmelinskii, M. Sikorski, J. Koziol, *Food Chem.*, 2005, **89**, 217-225
55. P. Ritthiruangdej, S. Kasemsumran, T. Suwonsichon, V. Haruthaithanasan, W. Thanapase, Y. Ozaki, *Analyst*, 2005, **130**, 1439-1445
56. Q. Chen, J. Cai, X. Wan, J. Zhao, *LWT-Food Sci. Technol.*, 2011, **44**, 2053-2058
57. D. R. Cardoso, L. G. Andrade-Sobrinho, A. F. Leite-Neto, R. V. Reche, W. D. Isique, M. M. C. Ferreira, B. S. Lima-Neto, D. W. Franco, *J. Agric. Food Chem.*, 2004, **52**, 3429-3433
58. J. F. D. Kelly, G. Downey, V. Fouratier, *J. Agric. Food Chem.*, 2004, **52**, 33-39
59. H. B. Ding, R. J. Xu, *J. Agric. Food Chem.*, 2000, **48**, 2193-2198
60. E. Sikorska, T. Górecki, I. V. Khmelinskii, M. Sikorski, *Food Chem.*, 2006, **96**, 632-639
61. N. H. Beltrán, M. A. Duarte-Mermoud, M. A. Bustos, S. A. Salah, E. A. Loyola, A.I. Peña-Neira, J. W. Jalocha, *J. Food Eng.*, 2006, **75**, 1-10
62. L. A. Berrueta, R. M. Alonso-Salces, K. Héberger, *J. Chromatogr. A*, 2007, **1158**, 196-214
63. P. Gromski, H. Muhamadali, D. Ellis, Y. Xu, E. Correa, M. L. Turner, R. Goodacre, *Anal. Chim. Acta*, 2015, **879**, 10-23
64. R. M. Jarvis, A. Brooker, R. Goodacre, *Faraday Discuss.*, 2005, **132**, 281-292
65. H. AlRabiah, E. Correa, M. Upton, R. Goodacre, *Analyst*, 2013, **138**, 1363-1369

66. H. AlRabiah, Y. Xu, N. J. W. Rattray, A. A. Vaughan, T. Gibreel, A. Sayqal, M. Upton, J. W. Allwood, R. Goodacre, *Analyst*, 2014, **139**, 4193-4199
67. J. W. Allwood, D. I. Ellis, J. K. Heald, R. Goodacre, L. A. J. Muir, *Plant J.*, 2006, **46**, 351-368
68. J. W. Allwood, A. Clarke, R. Goodacre, L. A. J. Mur, *Phytochemistry*, 2010, **71**, 590-597
69. N. Nicolaou, R. Goodacre, *J. Dairy Sci.*, 2010, **93**, 5651-5660
70. R. Goodacre, E. Anklam, *J. Am. Oil Chem. Soc.*, 2001, **78**, 993-1000
71. P. S. Gromski, Y. Xu, E. Correa, D. Ellis, M. L. Turner, R. Goodacre, *Anal. Chim. Acta*, 2014, **829**, 1-8

5.0 UPLC TOF MS IN COMBINATION WITH STATISTICAL DATA ANALYSIS FOR THE IDENTIFICATION OF Caramel COMPONENTS

5.1 Introduction

5.1.1 Basis of this Study

It has been demonstrated in the preceding chapters that ATR-MIR spectrometry could be implemented as an analytical tool for profiling caramel colour. Characteristic MIR spectra were attained for different caramel materials (indicating that they vary in their non volatile composition) and as a result it was possible to predict when a particular caramel was present in a typical Scotch Whisky. For the reason that only E150a classed caramels are legally permitted in Scotch Whisky, ATR-MIR spectrometry could therefore be extremely beneficial to the Scotch Whisky industry in terms of counterfeit detection and one of the appealing features of the tool is that it has the potential for future adaption into portable instrumentation. Suspect samples could therefore be screened in the field to identify authentic products based on the confirmation of a specific colourant profile. Despite these appealing features, the main limitation of ATR-MIR spectrometry is that it provides little information relating to the exact chemical composition of caramel colour. Hence at this point, the identities of components responsible for spectral variation between caramels are still unknown. An understanding of the composition of different caramel materials could be extremely beneficial to the Scotch Whisky industry; as well as allowing a greater understanding of the composition of authentic colour, the ability to identify specific marker compounds in caramels could allow more comprehensive confirmation as to the origin of colour.

This chapter investigates the value of an ultra performance liquid chromatography (UPLC) system in combination with a time of flight (TOF) mass spectrometer as a tool for the identification of marker components within different caramel colourants. A selection of caramel samples were analysed prior to the commencement of this project (by Simon Cubbon of Waters Limited) and so this study focuses on the application of statistical data analysis software to demonstrate the value of UPLC

TOF MS for the analysis of caramels in Scotch Whisky. The review that follows investigates why individual components within caramel colourants have been difficult to characterise in the past and explains why UPLC TOF MS in combination with multivariate data analysis has been chosen as a means to assess this now.

5.1.2 UPLC-MS in Combination with Statistical Data Analysis for Differentiating Caramel Materials

Caramel colourants comprise a complex mixture of volatile and non volatile components and only the former fraction, accounting for approximately 5% of the total product, has been reasonably well characterised.¹⁻⁴ The majority of caramel composition therefore remains poorly understood and its elucidation in the past was impeded by analytical techniques that were insufficient at the time for the analysis of individual non volatile components within complex mixtures. Liquid chromatography (LC) is one such technique that has commonly been implemented in the past for profiling caramel colourants but was restricted by its level of development. Although it was possible to obtain chromatographic traces that were characteristic of the non-volatile fraction of different caramel materials (see section 3.1.2 for more details), the lack of resolution provided by separation science at the time meant that LC peaks were typically broad and unresolved.⁵⁻⁹ The complex mixture of components present within single peaks (and inadequate tools available to further investigate these components) therefore meant that features could not be linked to analytical composition.

The field of LC has greatly advanced from this in recent years and the development of UPLC has meant that chromatographic separations can now be employed with far superior resolution and much better sensitivity.¹⁰ To make the most of this enhanced performance however, it is now common practice for UPLC to be coupled with a mass spectrometer for detection purposes. Mass spectrometry (MS), which has also rapidly evolved over the last decade, can readily keep up with the speed and efficiency of UPLC separation and allows minimal dispersion of components. As well as UPLC-MS enabling the opportunity to better separate out components within complex mixtures, this instrumental set up therefore allows the subsequent

identification of component masses. UPLC-MS technology can therefore allow individual components within complex mixtures to be monitored whether their identities are previously known or not.^{11,12} In addition to permitting individual components to be monitored, recent developments made in the field of MS have also opened up the potential to assign structural identities to components that have been detected *via* UPLC-MS. Typically this is achieved using tandem MS where particular analytes are targeted within an initial mass analyser before being passed through a collision chamber to cause that component to fragment. Fragmentation patterns can then be monitored at a second mass analyser and such data can aid in the identification of compounds. The recent development of time of flight (TOF) mass analysers has also made this process easier by permitting component masses to be measured with very high sensitivity and accurate to ~ 1 mDa – potential molecular formulae can then be generated from data of this accuracy level.¹²

Due to these advancements in the fields of both LC and MS, analytical procedures based on UPLC-MS are now being regularly implemented within a variety of subject areas both to profile known analytes and also to help gain a greater understanding of the unknown components present within complex mixtures. These include applications within fields such as bioanalysis,¹³⁻¹⁶ drug analysis/drug metabolism studies¹⁷⁻²² and metabolomics/metabonomics.^{11,23-26} Although examples of UPLC-MS being utilised on its own for the analysis of caramel colourants could not be found in the literature, three recent publications by A. Golon *et al.* demonstrated that this type of analytical technology could have excellent potential to help profile non volatile components within caramel type materials.²⁷⁻²⁹ Each publication assessed caramel products being formed from different starting materials and the authors were able to generate lists of caramel components and their molecular formulae using a combination of high resolution mass spectrometry and liquid chromatography-tandem mass spectrometry. The data were then subjected to graphical interpretation tools that enabled a rough picture of structural trends and likely reaction mechanisms to be obtained, before the compositions of selected structures were confirmed using targeted LC-tandem mass spectrometry and direct infusion tandem MS experiments.

Although the above mentioned literature indicated that UPLC-MS has excellent potential for profiling individual components within complex mixtures (including caramels), determining what components are responsible for differences between such samples can be a very difficult task. One of the main reasons behind this is that for each sample being compared, a large number of analyte masses will be detected over a wide range of retention times, resulting in high dimensionality data that would be impossible to manually interpret. The processing of such data is therefore often simplified by the implementation of multivariate data analysis tools; principal component analysis (PCA) often being utilised as an initial exploratory technique. Examples of UPLC-MS in combination with PCA being applied to the analysis of caramel samples could not be found in the literature – indicating the novelty of attempting this – though examples were found that demonstrated the success of this approach for a wide range of other applications involving the analysis of complex mixtures.³⁰⁻⁴⁵ One of the most common applications of UPLC-MS in combination with multivariate statistics was found to be within the field of metabonomics, where this analytical approach has been commonly implemented to differentiate between healthy and diseased patients.⁴⁰⁻⁴⁵ The application of PCA to the UPLC-MS data also meant that potential biomarkers for these illnesses could be identified, as well as information relating to the metabolic pathways behind them. As an example, X. Zhao *et al.* were able to clearly distinguish between urine samples taken from cancer patients versus those acquired from healthy persons.⁴² This separation was based on the components present within each sample and examination of PCA loadings data enabled 15 biomarkers for cancer to be found. An additional highlight of this publication was that it included a comparison of the results obtained using UPLC-MS with those acquired using conventional LC-MS. The authors were able to clearly demonstrate that separation between sample groups was greatly improved when implementing UPLC-MS and a greater number of potential biomarkers were identified using this approach. Hence as a result of using UPLC, more information could be acquired about the components present within these complex samples.

A few other notable examples of UPLC-MS being used in combination with PCA to differentiate between complex samples based on their chemical compositions were

published by: Cheng *et al.*, who were able to clearly differentiate between five types of gelatine;³⁰ Xiao *et al.*, who demonstrated the potential to distinguish between samples of corn steep liquor prepared by different manufacturers;³¹ M. Zhou *et al.*, who highlighted the potential to differentiate between four organs of the Lotus Nelumbo plant;³² and G. Xie *et al.*, who were able to distinguish between three different varieties of a medicinal herb. In each of these cases, assessment of loadings data after PCA enabled components that were characteristic of each different sample group to be picked out – highlighting the potential of UPLC-MS as a tool for understanding more about individual components that are characteristic of different sample types.

The vast majority of the publications identified above were found to implement a UPLC system coupled to a TOF mass spectrometer, as this particular mass analyser was described as allowing all compounds within a sample to be analysed from a single injection. This therefore allowed a wide range of components to be considered simultaneously without them being specifically targeted. The very high mass accuracy of TOF analysis also meant that in some cases tentative structural identities could be assigned for components of interest. In many cases however, the identification of structures required additional MS analysis targeted to the component of interest and/or further analysis using NMR spectrometry.

5.1.3 Study Objectives

In this chapter, data acquired using a UPLC TOF MS system was analysed using statistical data analysis software to assess the technique's value to help unravel the composition of caramel colourants. The main objectives of the work were:

- To determine whether UPLC TOF MS could differentiate between the four caramel classes recognised for use in foodstuffs by the European Union.
- To find out whether components could be identified that were characteristic of each caramel class.
- To investigate whether the compositions of E150a caramels were consistent when different formulations were assessed.
- To examine whether caramel markers could still be observed when these materials were dissolved in Scotch Whisky and also to identify whether any interference might occur from components naturally present within Scotch Whisky.
- To assess whether the data acquired from the particular UPLC-MS system could be used in combination with the data analysis software to assign tentative structures to caramel components.

5.2 Experimental

5.2.1 Samples

Seven different caramel materials were assessed in this study, including four different types of E150a and one type of caramel from each of the remaining classes recognised by the European Union (E150b, E150c and E150d). All samples were dissolved in either 40% ethanol or a typical blend whisky (devoid of previous caramel addition and termed Blend W) to provide the 11 sample solutions described within Table 5.1. For each of these solutions, caramel was added to the chosen medium until the colour level matched that of a typical market blend – monitored with the use of absorbance measurements at 430 nm. Blend W containing no caramel was also analysed in this work for comparison purposes. It should also be noted here that all sample solutions were prepared at the Scotch Whisky Research Institute (Riccarton, Edinburgh, UK) prior to the commencement of this project.

Table 5.1: Descriptions of the 11 caramel solutions assessed within this study.

Sample Number	Sample Description	SWRI Reference Number
1	E150a (Type 1) dissolved in 40% ethanol	S11-1310
2	E150b dissolved in 40% ethanol	S11-1311
3	E150c dissolved in 40% ethanol	S11-1312
4	E150d dissolved in 40% ethanol	S11-1313
5	E150a (Type 2) dissolved in 40% ethanol	S11-1314
6	E150a (Type 3) dissolved in 40% ethanol	S11-1315
7	E150a (Type 4) dissolved in 40% ethanol	S11-1316
8	E150a (Type 1) dissolved in Blend W	S11-1317
9	E150b dissolved in Blend W	S11-1318
10	E150c dissolved in Blend W	S11-1319
11	E150d dissolved in Blend W	S11-1320

5.2.2 UPLC-MS

UPLC-MS analysis of the caramel solutions was undertaken by Simon Cubbon (Waters Ltd., Wilmslow, UK). Sample solutions were analysed without any

additional pre-treatment using a Waters ACQUITY UPLC, fitted with an ACQUITY HSS T3 column (100 x 2.1 mm i.d., 1.8 μm particle size). The column temperature was maintained at 40°C throughout analysis, whilst the sample chamber was kept at 10°C. Chromatographic separation was achieved using gradient conditions and 0.1% formic acid in water and 0.1% formic acid in methanol were used as the A and B solvents respectively. The chromatographic conditions used for this gradient separation have been provided in Table 5.2. Triplicate measurements were acquired for each sample solution using a 10 μL injection volume and the order of analysis was randomised to minimise the affects of cross contamination. A 50 μL injection loop was also implemented as a means to dilute the effects of ethanol.

Table 5.2: Gradient conditions employed for the analysis of caramel solutions.

Time (min)	Flow Rate (mL/min)	% A	% B
0.0	0.35	95	5
1.0		95	5
7.0		1	99
9.0		1	99
9.1		95	5
10.0		95	5

The ACQUITY UPLC was coupled to a Xevo G2 TOF mass spectrometer to allow mass analysis of high accuracy to be determined. The mass analyser was operated using electrospray ionisation in both positive and negative modes over the mass range of 50 to 1200 (m/z). MS^E data acquisition mode was also used meaning that both low and high energy data were simultaneously acquired. The former configuration results in no fragmentation of precursor ions, whereas the latter generates fragment ion data to aid in the assignment of structures based on their fragmentation data. External calibration was performed using leucine enkephalin and all data were acquired using MassLynx software (version 4.1) (Waters Ltd., Wilmslow, UK).

5.2.3 Data Analysis

The raw UPLC-MS data were processed using MarkerLynx XS, which is an Application Manager built into the MassLynx software (version 4.1; Waters Ltd., Wilmslow, UK). MarkerLynx used the proprietary ApexTrack algorithm to automatically detect chromatographic peaks and allowed the extraction and tabulation of exact mass and retention time (EMRT) pairs with associated intensities for all peaks detected over all samples. The main parameters implemented for this procedure were set as follows: retention time range of 0.7 – 9.6 min, mass range of 50 – 1200 (i.e. unrestricted), mass tolerance of 0.05 Da, marker intensity threshold of 1500 counts, mass window of 0.02 Da and retention time window of 0.05 min.

Once the raw data were processed as described above, PCA was used to compare samples based on the intensity values of the EMRT pairs. This multivariate data analysis was undertaken using the extended statistics package incorporated within the MarkerLynx Application Manager. Prior to PCA, all data were normalised to the total marker intensity and then subjected to pareto scaling. Other scaling methods were also examined in this research, including autoscaling (also known as unit variance) and mean centring, however pareto was generally found to allow the most successful sample separations.

5.2.3.1 Pareto scaling

The first step of pareto scaling is to mean centre the data being assessed, a process which shifts the origin of the measurement variables to the centroid (or mean value) of the data. Each variable is then divided by the square root of the standard deviation, which reduces the effect of large intensities to a greater extent than small ones, therefore making the most intense variables less dominant.^{46,47} Pareto scaling was therefore used in this research to account for the potentially large concentration range covered by caramel components. If scaling were not implemented, subsequent PCA models would be dominated by the components of highest concentration; however it might be the case that some of the less intense compounds would be useful in terms of allowing sample differentiation.⁴⁸ When literature relating to this topic was assessed, it was found that this scenario was commonly encountered in the field of

metabonomics and many examples were identified that demonstrated pareto scaling as a suitable solution.^{30,33,34,39,42,45} An additional advantage found to be associated with pareto scaling was that any baseline noise in data was not significantly enhanced.

5.2.4 Elemental Composition Analysis (ECA)

MassLynx contains an elemental composition tool that allows the prediction of molecular formulae to be automated within the software. The elemental composition method implemented in this research was set to return a maximum of 20 results and to contain no more than the following amounts of each of these atoms: 0 – 50 carbons; 0 – 100 hydrogens; 0 – 20 nitrogens; 0 – 20 oxygens; and 0 – 6 sulphurs. Other main parameters employed for ECA were: the mass tolerance, which was set at 10 ppm; the mass mode, set as monoisotopic; the electron state, which was set to even and odd electron ion; and the double bond equivalence range, which was set as -1.5 – 50.0.

5.3 Results and Discussion

5.3.1 UPLC-MS in combination with PCA to profile caramel composition

5.3.1.1 Caramels in 40% ethanol

Caramel class differentiation

Seven caramel materials (samples 1-7 in Table 5.1) were assessed in this work to determine whether their UPLC TOF MS profiles could be distinguished between and subsequently if components responsible for any differentiation could be picked out. The seven materials – incorporating four E150a caramels and one example from each of the remaining caramels classes – were initially assessed whilst dissolved in 40% ethanol to allow a comparison of profiles without any interference from components inherent to whisky. Once UPLC-MS analysis was completed (in triplicate for all samples), MarkerLynx software was then used to extract component information from the raw data in the form of EMRT pairs, along with the associated intensities of these components in each sample. This was undertaken separately for both the positive and negative ionisation data and 3161 EMRT pairs were obtained from the former, whilst 4397 were attained for the latter. PCA including all seven sample solutions in 40% ethanol was then carried out, the EMRT pairs in this case acting as the variables. The negative ionisation data were considered first and the resulting PC1 vs. PC2 scores plot has been provided in Figure 5.1 alongside the corresponding loadings data.

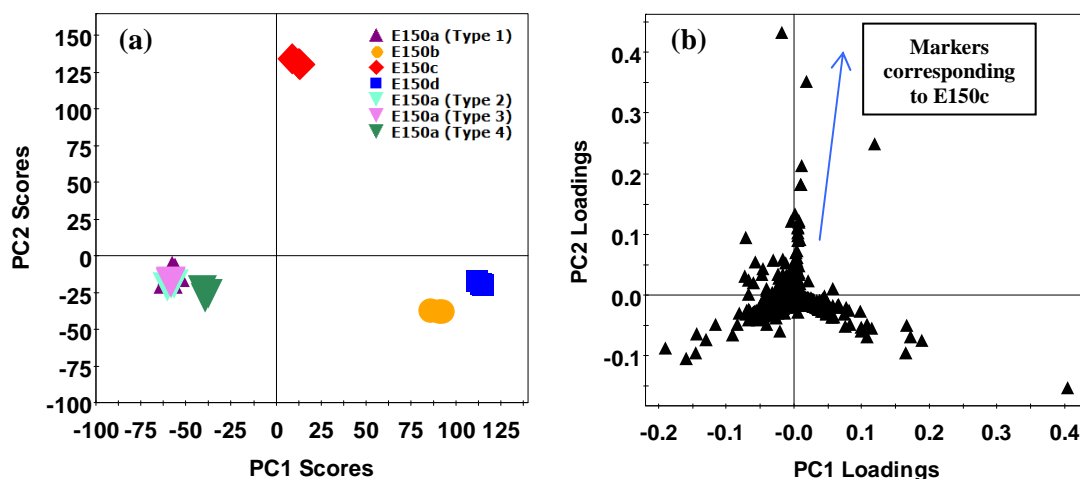


Figure 5.1: (a) PC1 vs. PC2 scores plot obtained from PCA of the negative ionisation data acquired from all seven caramels dissolved in 40% ethanol. Triplicate data were included for all samples. (b) Shows the corresponding (PC1 vs. PC2) loadings data.

It was seen from Figure 5.1a that differentiation between the four caramel classes was clearly possible based on the components detected using UPLC TOF MS under negative ionisation mode. The four different formulations of E150a caramel overlaid very closely together in the scores plot, whilst the samples representing the three remaining caramel classes (E150b, E150c and E150d) were generally found in distinct regions of the plot. This indicated that the compositional differences between caramel classes were more significant than within class variation, in this case in relation to E150a. The assessment of different caramel types within the E150b, E150c and E150d classes would be important in any future work to investigate the extent of within class variation for the remaining caramel classes.

In addition to the above observations from the PC1 *vs.* PC2 scores plot, further separation between certain caramel samples was achieved when additional PCs were considered. For instance, distinction between E150a (Type 4) and the other three E150a caramels was clearly achieved along the PC3 axis (Figure 5.2). When background information relating to E150a (Type 4) was assessed, it was identified that this sample was actually a burnt sugar. This helped to explain why the sample stood out so clearly compared to the other E150a caramels as the production processes implemented for burnt sugar manufacture – although very similar to the production of E150a – differ in the reactants that can be added to aid in the caramelisation process. The presence of different reactants during manufacture therefore highlights why the composition of the E150a caramels and the burnt sugar would be likely to differ. When PC4 was assessed, much clearer separation was achieved between the E150b and E150d classed caramels than was originally observed in the PC1 *vs.* PC2 scores plot; a finding depicted by Figure 5.3. It should be noted at this point however, that the analysis of additional batches of each caramel type would be required in the future to assess the consistency of caramel profiles and so confirm each of the above findings.

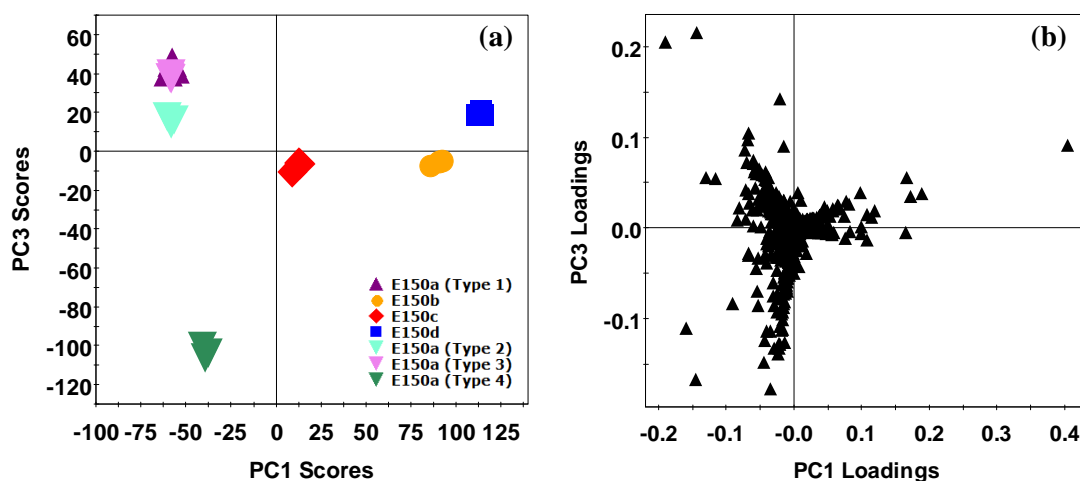


Figure 5.2: (a) *PC1 vs. PC3 scores plot obtained from PCA of the negative ionisation data acquired from all seven caramels dissolved in 40% ethanol. Triplicate data were included for all samples.* (b) *Shows the corresponding (PC1 vs. PC3) loadings data.*

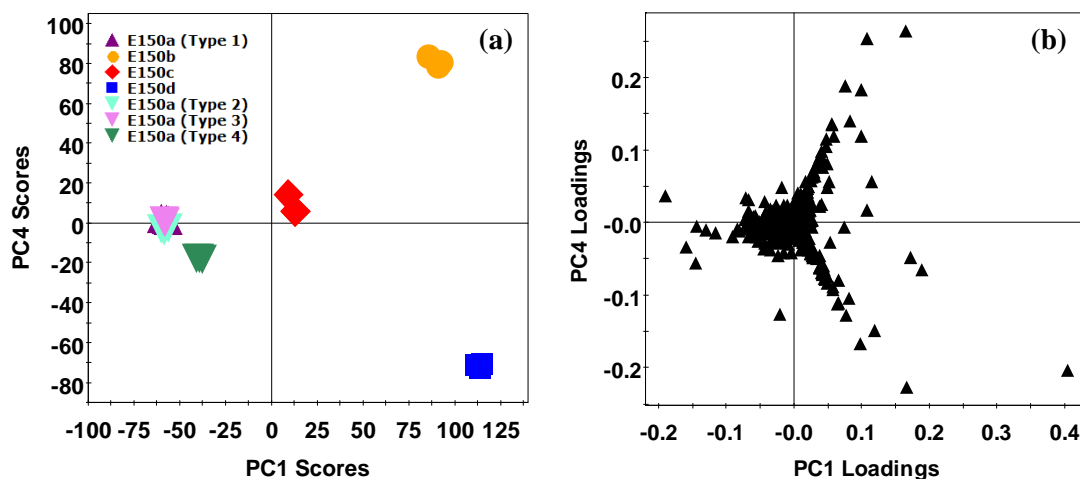


Figure 5.3: (a) *PC1 vs. PC4 scores plot obtained from PCA of the negative ionisation data acquired from all seven caramels dissolved in 40% ethanol. Triplicate data were included for all samples.* (b) *Shows the corresponding (PC1 vs. PC4) loadings data.*

The components responsible for the above mentioned findings were investigated by examination of loadings data that corresponded to each scores plot. The loadings data relating to the PC1 vs. PC2, PC1 vs. PC3 and PC1 vs. PC4 scores plots have been provided in Figures 5.1b, 5.2b and 5.3b respectively. Each triangular point within one of these loadings plots represents a different EMRT pair (or component) and data points clustered around the origin of a loadings plot are known to be common to all samples. As you move further from the centre however, these components will be present in fewer samples and so can be linked to any separation observed in the corresponding scores plots depending on their location. For instance in Figure 5.1b

the data points found towards the top of the loadings plot were most characteristic of E150c, as E150c samples clustered towards the top of the corresponding scores plot (Figure 5.1a). From the data presented in each of the loadings plots above it was therefore possible to identify components that were characteristic of each different caramel class and these potential marker compounds have been summarised in Table 5.3. The intensity levels of each selected component were compared over all samples with the use of trend plots to ensure compounds were essentially unique to a particular caramel class; all components listed are therefore either completely distinct to their associated caramel class (at the concentration analysed) or present in their associated category at significantly elevated levels compared to the other samples. The trend plots constructed for marker components 7 and 52 have been included in Figures 5.4 and 5.5 respectively as examples of this selection process.

Table 5.3: Marker components of different caramel classes – from negative ionisation data.

Marker Number	Retention Time (min)	Mass¹	Associated Class
1*	0.98	377.0847	E150A Types 1-4
2	1.00	383.1001	
3*	1.02	341.1084	
4*	1.07	503.1611	
5*	1.08	323.0976	
6	1.08	429.1245	
7*	0.95	305.0636	E150A Types 1-3
8*	0.96	269.0873	
9	1.01	366.1085	
10*	1.01	179.0553	
11*	1.04	281.0873	
12	1.05	177.0396	
13	1.33	251.0764	
14	1.08	531.1557	E150A Type 4 (confirmed as being a BS)
15	1.08	693.2087	
16	1.32	693.2079	
17	1.33	855.2613	
18	1.34	809.2551	

¹ The mass quoted is the component mass minus one proton (a result of using negative ionisation).

* Labels the components that were most clearly visible/most intense when the same caramels were dissolved in a typical blend matrix (Blend W).

Table 5.3 cont.: Marker components of different caramel classes – from negative ionisation data.

Marker Number	Retention Time	Mass¹	Associated Class
19	3.00	449.1294	E150A Type 4 (confirmed as being a BS)
20	3.20	477.1243	
21	3.32	477.1240	
22	3.83	441.1036	
23*	0.96	202.0036	E150B
24	0.97	329.0538	
25*	0.97	359.0648	
26*	0.98	345.0491	
27*	0.98	168.9803	
28	0.99	285.0279	
29*	1.00	210.9909	
30*	1.00	255.0172	
31*	1.01	182.9959	
32	1.08	330.9795	
33*	1.33	251.0234	
34	1.33	279.0174	
35*	1.34	237.0067	
36	1.35	293.0331	
37	1.35	321.0283	
38	3.05	273.0066	
39	3.75	361.0235	
40	0.92	261.1089	E150C
41	0.93	305.1346	
42*	0.95	184.0608	
43*	0.99	339.0738	
44*	0.99	338.0769	
45	1.29	165.0399	
46*	1.29	303.1194	
47*	1.29	213.0877	
48*	1.30	349.1250	
49	1.33	207.0503	
50	1.35	333.1292	
51	0.82	246.9888	E150D
52*	0.93	270.9581	
53*	0.93	258.9580	
54*	0.94	226.0384	
55*	0.96	385.0914	

Table 5.3 cont.: Marker components of different caramel classes – from negative ionisation data.

Marker Number	Retention Time	Mass¹	Associated Class
56	1.00	431.0428	E150D
57*	1.01	235.0389	
58	1.07	415.0454	
59*	1.07	225.0067	
60	1.34	146.9749	
61*	1.34	247.0389	
62*	1.34	349.0710	
63	1.35	160.9908	
64*	0.90	321.1298	E150C and E150D
65	0.90	435.1220	
66	0.97	405.0700	E150B and E150D
67*	0.98	243.0173	
68*	0.99	241.0017	
69	0.99	213.0065	
70*	1.00	197.0106	
71	1.01	227.0218	
72	1.02	167.0009	E150B and E150D
73	1.05	391.0001	
74*	1.05	194.9961	
75*	1.08	164.9855	
76*	1.34	191.0087	

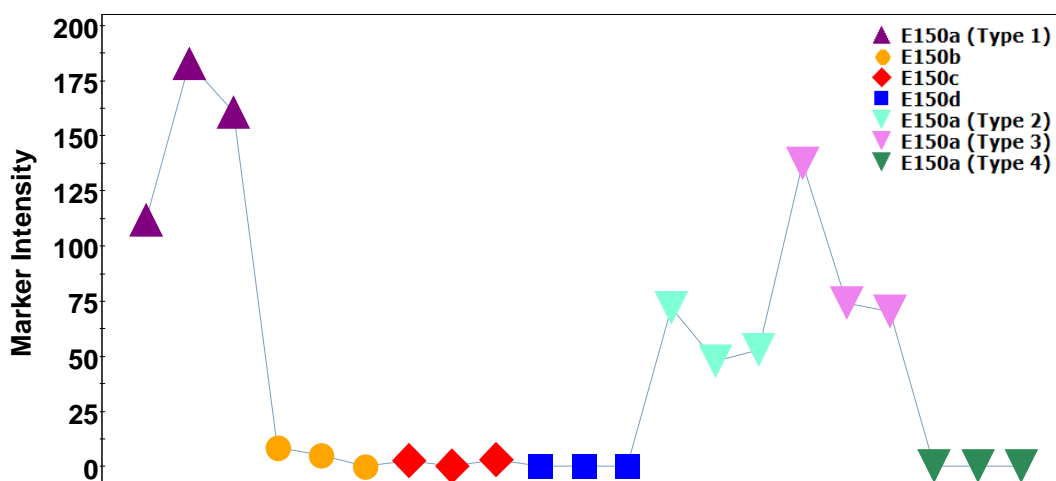


Figure 5.4: Trend plot of the component with retention time of 0.95 minutes and mass of 305.0636 (marker compound 7) showing the intensity of this component across the seven caramel samples dissolved in 40% ethanol. Triplicate data included for each sample solution.

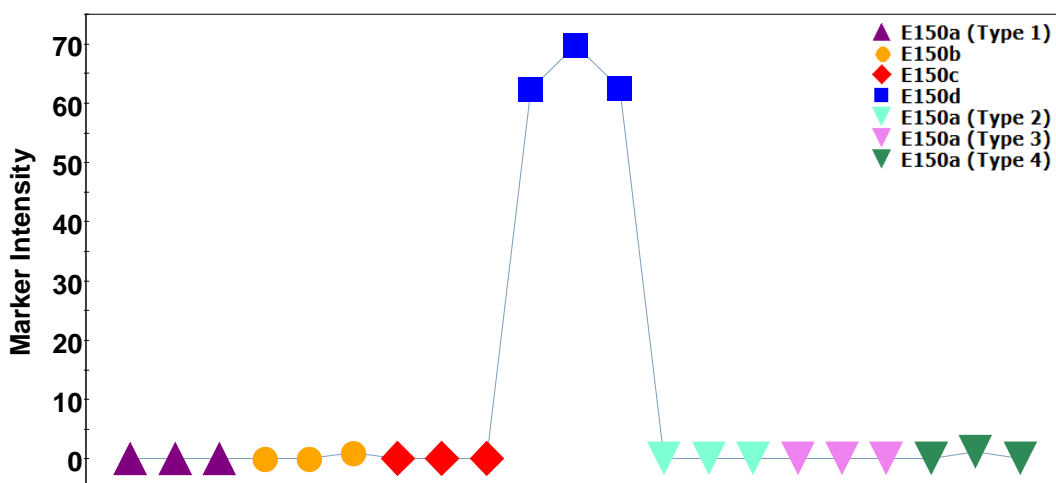


Figure 5.5: Trend plot of the component with retention time of 0.93 minutes and mass of 270.9581 (marker compound 52) showing the intensity of this component across the seven caramel samples dissolved in 40% ethanol. Triplicate data included for each sample solution.

As shown in Table 5.3, a number of components identified from the negative ionisation data were also found to be present within two of the caramel classes; either in both E150b and E150d or in both E150c and E150d. It was thought that this could be due to the common reactants that can be added to these caramel classes during their manufacture; sulphite reactants for the former two classes and ammonium based reactants for the latter. This will be discussed in more detail in section 5.3.2.1, where potential elemental compositions for the marker components have been investigated.

When the positive ionisation data were considered it was again possible to differentiate between the four caramel classes based on the detected EMRT pairs

using PCA (although not as easily as with the negative ionisation data). The PC1 vs. PC2 scores plot (shown in Figure 5.6a) clearly distinguished both the E150c and E150d caramels from each other as well as from the other samples assessed; in this plot however the E150a caramels and the E150b sample were not separated from each other. The PC3 axis still did not allow distinction of these latter materials but instead enabled E150a Type 4 (now confirmed as being a burnt sugar) to be differentiated from all other samples (Figure 5.7a). It was not until PC4 was then assessed that E150b could be distinctly separated from the remaining samples (Figure 5.8a).

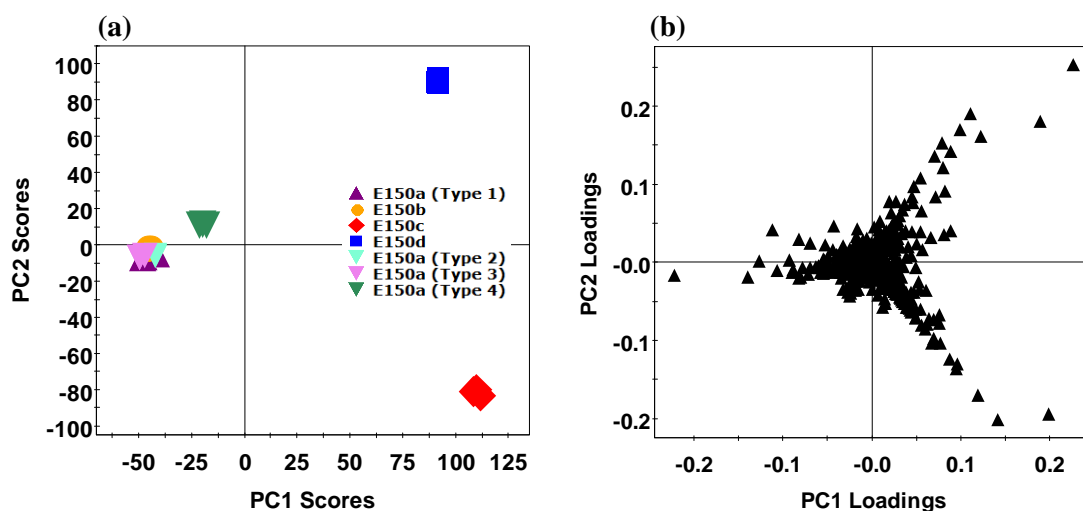


Figure 5.6: (a) PC1 vs. PC2 scores plot obtained from PCA of the positive ionisation data acquired from all seven caramels dissolved in 40% ethanol. Triplicate data were included for all samples. (b) Shows the corresponding (PC1 vs. PC2) loadings data.

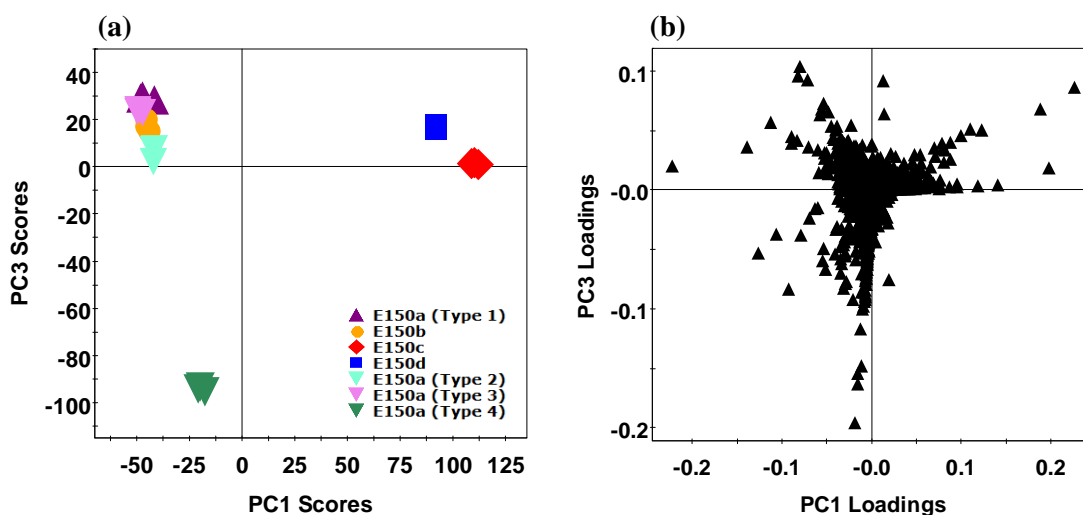


Figure 5.7: (a) PC1 vs. PC3 scores plot obtained from PCA of the positive ionisation data acquired from all seven caramels dissolved in 40% ethanol. Triplicate data were included for all samples. (b) Shows the corresponding (PC1 vs. PC3) loadings data.

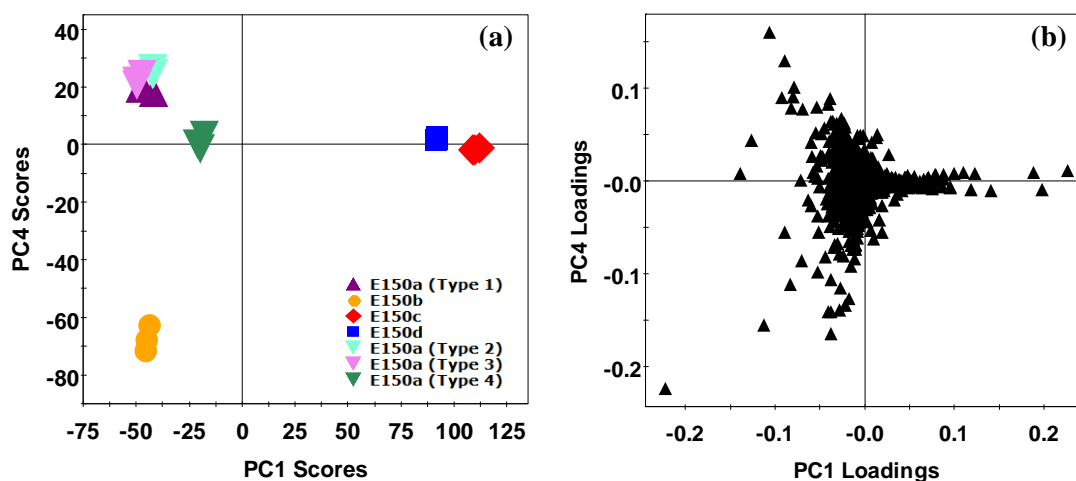


Figure 5.8: (a) *PC1 vs. PC4 scores plot obtained from PCA of the positive ionisation data acquired from all seven caramels dissolved in 40% ethanol. Triplicate data were included for all samples.* (b) *Shows the corresponding (PC1 vs. PC4) loadings data.*

The components responsible for these observations were again investigated *via* loadings data using the same approach implemented previously for the negative ionisation data. The loadings plots corresponding to the PC1 vs. PC2, PC1 vs. PC3 and PC1 vs. PC4 scores plots have been provided in Figures 5.6b, 5.7b and 5.8b respectively. From these data it was possible to identify additional components that were characteristic of certain caramel classes and these have been summarised in Table 5.4. Overall, the positive ionisation data provided fewer marker components than the negative ionisation data for caramels of different class. This indicated that the majority of components responsible for caramel differentiation possessed functional groups that more readily lose a proton, such as carboxylic acids ($\text{R-CO}_2\text{H} \rightarrow \text{R-CO}_2^-$) and alcohols ($\text{R-OH} \rightarrow \text{R-O}^-$). These are known to be common functional groups in saccharides and so this potentially explains these findings in relation to caramel differentiation. The highest amount of information from the positive ionisation data (in terms of characteristic components picked out) was attained for the E150c classed caramel (potentially due to the presence of amines, resulting from the addition of ammonium compounds during production, that will more readily receive a proton) and also for the E150a caramel that had been previously confirmed as a burnt sugar (E150a Type 4). It was difficult however, to attain much information about the other E150a caramels using the positive ionisation data, which was due to the close proximity in the majority of scores plots of these materials with the E150b caramel. Any components found as being common to all E150a caramels were

therefore also found to be present in the E150b caramel at significant (but typically lower) levels. These components have been recorded separately in Table 5.5.

Table 5.4: Marker components of different caramel classes – from positive ionisation data.

Marker Number	Retention Time (min)	Mass¹	Associated Class
1	2.71	127.0397	E150A Type 4 (Burnt Sugar)
2	3.01	471.0904	
3	3.28	309.0378	
4	3.70	163.0758	
5	3.81	414.1395	
6	3.89	163.0758	
7	4.10	257.0427	
8	4.10	109.0290	
9	4.10	235.0628	
10	4.10	273.0181	
11	4.11	249.0817	
12	4.47	371.0533	
13	7.70	339.2895	
14	0.95	383.0665	E150B
15	1.07	307.0474	
16	1.08	225.0785	
17	1.32	259.0801	
18	1.32	275.0592	
19	1.50	385.1107	
20	3.33	165.0547	
21*	0.90	319.1509	E150C
22*	0.92	303.1558	
23	0.93	259.1292	
24	0.93	333.1662	
25*	0.95	317.1706	
26	0.96	273.1448	
27*	0.97	243.1342	
28	0.99	287.1605	
29*	0.99	213.1242	
30*	0.99	301.1400	
31*	1.06	227.1395	

¹ The mass quoted is the component mass plus one proton (a result of using positive ionisation).

* Labels the components that were most clearly visible/most intense when the same caramels were dissolved in a typical blend matrix (Blend W).

Table 5.4 cont.: Marker components of different caramel classes – from positive ionisation data

Marker Number	Retention Time (min)	Mass¹	Associated Class	
32	1.09	153.1027	E150C	
33*	1.34	289.1401		
34*	3.10	199.1084		
35	0.93	210.0437	E150D	
36*	0.97	387.1084		
37*	0.99	305.1349		
38*	1.01	237.0550		
39*	1.07	369.0966		
40	1.08	251.1035		
41	1.24	272.1133		
42*	1.34	110.0609		
43	2.98	269.1134		
44*	0.91	323.1455		E150C and E150D
45*	0.94	335.1453		
46*	0.95	173.0929		
47*	0.97	277.1399		
48	0.98	467.1874		
49	1.02	321.1299		
50*	1.03	233.1140		
51	1.04	187.1084		
52	1.06	275.1248		
53	1.06	245.1141		
54*	1.18	126.0556		
55	1.19	108.0449		
56*	1.29	305.1354		

Table 5.5: Components prominent in E150a caramels but also found in the E150b assessed.

Marker Number	Retention Time (min)	Mass¹	Component Information
1	0.95	293.0849	Highest in E150a caramels Types 1 & 3. Also present in E150b & E150a Type 2 at lower intensity. Absent from E150a Type 4.
2	0.98	365.1063	Present at high levels in all E150a caramels (Types 1 - 4). Also in E150b at a similarly high intensity.
3	0.99	219.0279	Highest in E150a caramels Types 1 - 3. Also in E150b & E150a Type 4 at lower levels.
4	1.00	343.1241	Highest in E150a caramels Types 1 - 3. Also in E150b at lower level. Absent from E150a Type 4.
5	1.01	381.0804	Highest in all E150a caramels (Types 1 – 4). Also in E150b at much lower levels.
6	1.11	363.0699	Highest in all E150a caramels (Types 1 - 4). Also in E150b but at much lower levels.
7	1.11	347.0952	Present at high levels in all E150a caramels (Types 1 - 4). Also in E150b but at much lower level.
8	3.09	127.0398	Highest in E150a caramels Types 2 - 4. Also in E150a Type 1 and E150b at lower intensity.
9	3.10	109.0293	Highest in E150a caramels Types 2 - 4. Also in E150a Type 1 and E150b at lower intensity.

¹ The mass quoted is the component mass plus one proton (a result of using positive ionisation).

E150a differentiation

As shown in the previous subsection, when PCA was undertaken to compare all seven caramel materials the three different types of E150a (E150a Type 4 now being classed as a burnt sugar instead) were generally found to cluster closely together both when negative and positive ionisation data were separately considered. This tight grouping of the E150a caramels was maintained within all of the scores plots previously shown, indicating that different types of E150a caramel had consistent compositions when their UPLC TOF MS profiles were compared with samples from other caramel classes. In other words the different E150a caramels contained many common components that were not present in E150b, E150c and E150d caramels. This however could only be concluded for the particular caramels analysed in this study and a wider range of samples would be required to confirm whether this would always be the case.

Despite the above observation, it was possible to distinguish one of the E150a caramels from the other two when using the PCA model previously constructed using the positive ionisation data, containing all seven sample solutions in 40% ethanol. E150a Type 2 could be separated out along the PC5 axis as demonstrated within Figure 5.9a. Examination of the corresponding loadings data (Figure 5.9b) identified one primary component that was responsible for this distinction. This marker has been highlighted within a red box in Figure 5.9b and had a retention time of 0.97 minutes and a mass of 258.1097. The trend plot for this component has also been provided in Figure 5.10, which clearly demonstrates that this compound is predominantly characteristic of E150a Type 2.

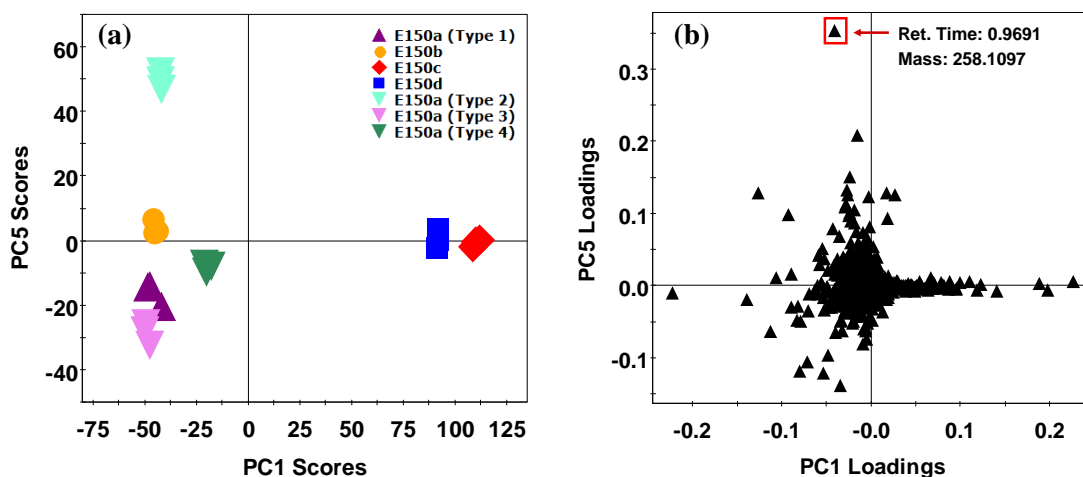


Figure 5.9: (A) *PC1 vs. PC5 scores plot obtained from PCA of the positive ionisation data acquired from all seven caramels dissolved in 40% ethanol. Triplicate data were included for all samples.* (B) *Shows the corresponding (PC1 vs. PC5) loadings data.*

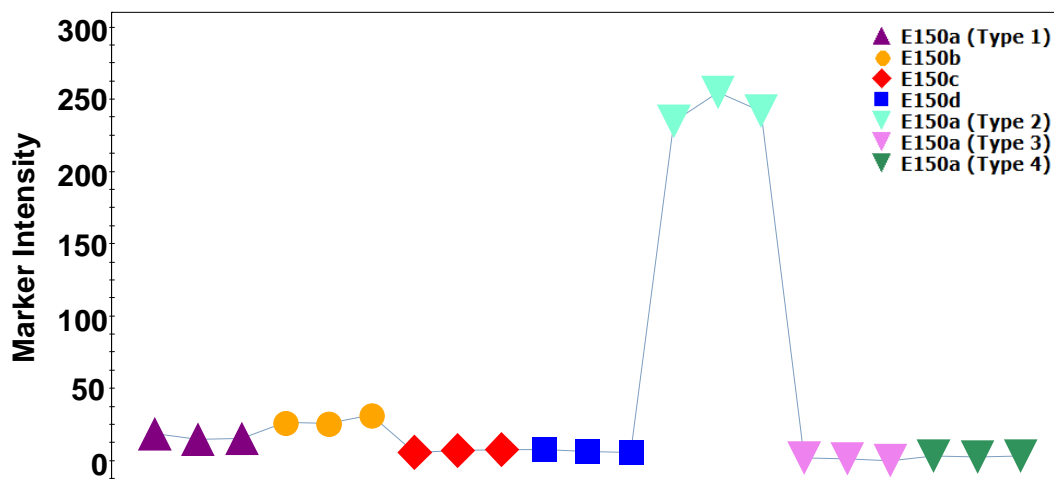


Figure 5.10: *Trend plot of the component with retention time 0.97 minutes and mass of 258.1097 showing the intensity of this component across the seven caramel samples dissolved in 40% ethanol. Triplicate data included for each sample solution.*

PCA incorporating only the three E150a caramels was next performed for both the negative and positive ionisation data to determine whether further separation could be attained between these materials using models focused on this caramel class only. The resulting PC1 vs. PC2 scores plots have been given in Figures 5.11a and 5.11b for the negative and positive ionisation data respectively. These plots indicated that the positive ionisation data provided clearest separation between the three E150a caramels assessed; each type being situated in a distinct region of the relevant scores plot (Figure 5.11b). This indicated that the compounds responsible for E150a differentiation were those containing functional groups more readily able to accept a proton. Consistency was also obtained between triplicate measurements. The

loadings data corresponding to the PC1 vs. PC2 scores plot attained from the positive ionisation data has been provided in Figure 5.12 and was used to allow the components responsible for differentiation between E150a caramels to be examined.

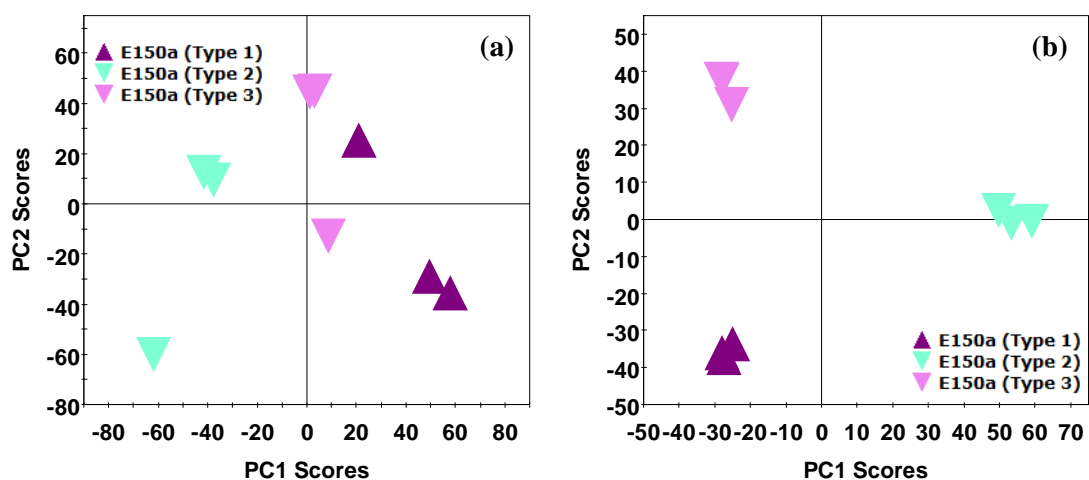


Figure 5.11: PC1 vs. PC2 scores plots obtained from PCA of E150a Types 1 - 3 dissolved in 40% ethanol using (a) negative ionisation data and (b) positive ionisation data. In both cases, triplicate data were included for all samples.

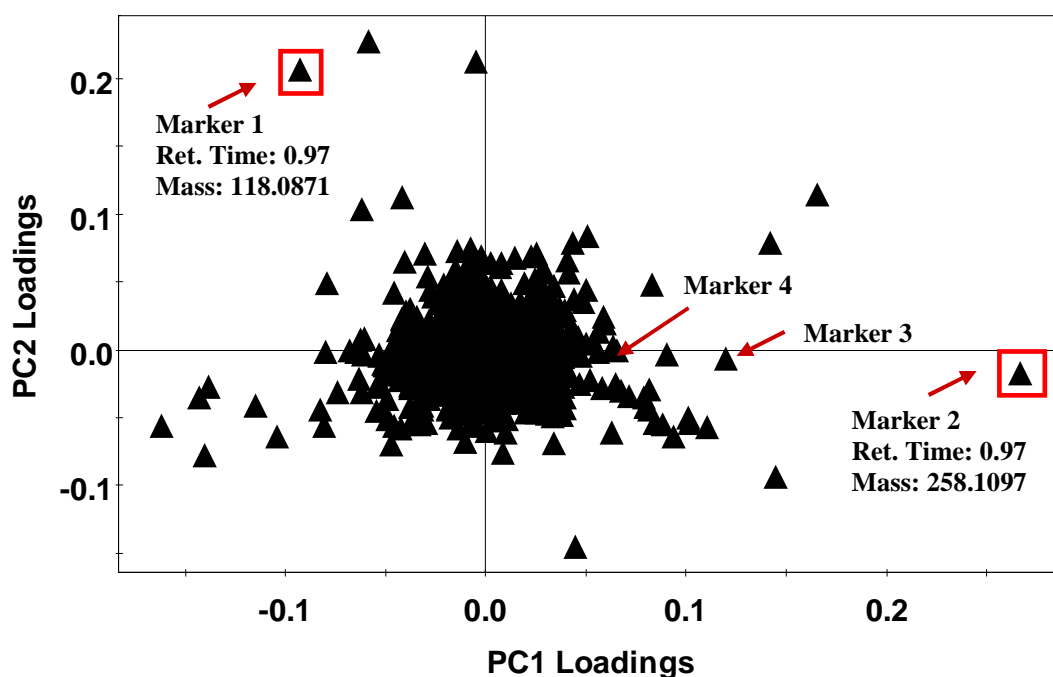


Figure 5.12: PC1 vs. PC2 loadings data obtained from PCA of E150a Types 1 - 3 dissolved in 40% ethanol using positive ionisation data. Triplicate measurements included for all samples. Markers of interest have been numbered for future reference within the document.

The two most notable components picked out from the loadings data shown in Figure 5.12 have been highlighted with red boxes. These components had masses of

118.0871 (Marker 1) and 258.1097 (Marker 2) and by the assessment of trend plots were found to be virtually unique to E150a Type 3 and E150a Type 2 respectively. The latter of these components was the same one picked out previously from PCA incorporating all seven caramel materials in 40% ethanol analysed using positive ionisation data (PC1 vs. PC5 as shown in Figure 5.9). The trend plot for Marker 2 can therefore be found in Figure 5.10, whilst the trend plot for Marker 1 has been provided in Figure 5.13. A few other components were identified from the loadings data that were predominantly characteristic of the E150a Type 2 caramel, though these were present at lower intensities than Marker 2. These additional components have been labelled as Markers 3 and 4 in Figure 5.12 and were found to have masses of 104.1080 (RT of 0.91 mins) and 420.1626 (RT of 0.99 mins) respectively. When the trend plots for these components were examined however (plots not shown), it was found that they appeared in caramels other than the E150a class. Marker 3 for instance was present in the E150d caramel at a higher intensity, whilst Marker 4 was also present in the E150b caramel although comparably this was at a very low level. This would not necessarily be an issue however, if the caramel present had already been initially confirmed as one from the E150a class.

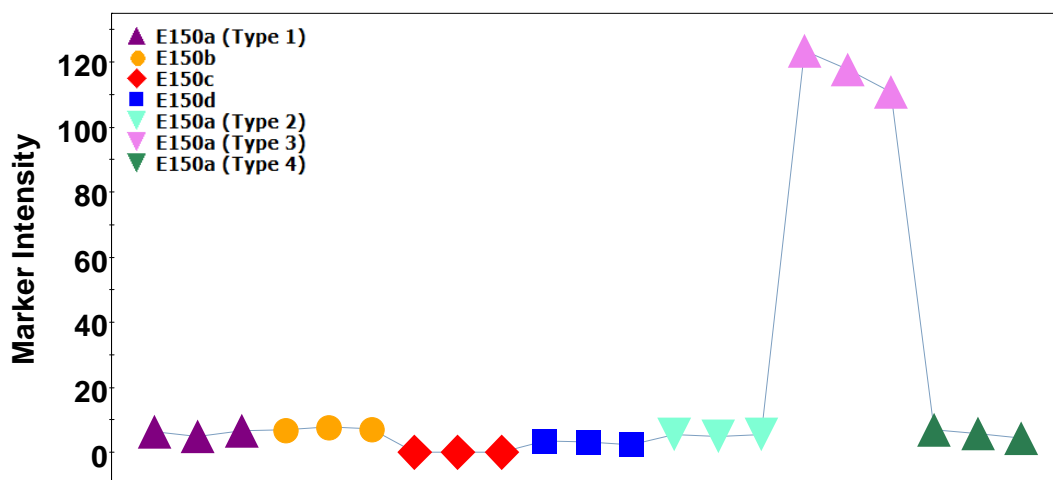


Figure 5.13: Trend plot of the component with retention time 0.97 minutes and mass of 118.0871 showing the intensity of this component across the seven caramel samples dissolved in 40% ethanol. Triplicate data included for each sample solution.

It was difficult to find any further components that were unique to a particular type of E150a. The other components that were primarily responsible for the observed separations in the PC1 vs. PC2 scores plot (Figure 5.11b) were instead present in two

or more of the E150a caramels and it was distinct differences in intensity levels of these compounds that allowed the different E150a types to be clearly distinguished. For example, the majority of the markers found towards the bottom left corner of the loadings plot were generally highest in E150a Type 1 but were also found at lower levels in one or both of the other E150a caramels.

The above findings indicated that it might be possible to use UPLC TOF MS to confirm the identity of a particular E150a caramel based on the presence and intensity of selected marker components. To be sure of this however, additional batches of each caramel type would need to be included in the model to ensure consistency of composition from batch to batch. Analysis of a wider range of E150a caramels would also be interesting to identify whether the majority of E150a products possess unique UPLC TOF MS profiles. In addition to this (as was found within the ATR-MIR chapter; more specifically in section 3.3.1.2) it would also be interesting to determine exactly what changes in the manufacturing process cause any sample differentiation between E150a caramels. If this can be identified then E150a manufacture could potentially be manipulated in the future to create materials with distinct UPLC TOF MS profiles. The presence of a particular E150a in a Scotch Whisky product could then be confirmed in the laboratory using this technology to monitor for specific marker components.

5.3.1.2 Caramels in the whisky matrix (Blend W)

The results so far have indicated that caramels of different class and also E150a products of different formulation can be clearly distinguished between (using PCA) based on the presence and intensity of characteristic marker compounds detected using UPLC TOF MS. To enable the presence of a particular caramel to be identified when dissolved in a Scotch Whisky however, it would be extremely important to understand whether inherent whisky components might interfere with the ability of this tool to detect marker compounds. When dissolved in Scotch whiskies, characteristic caramel components could become diluted or masked to the extent where they are no longer clearly visible, or alternatively, it could be the case that the presence of a caramel would be mistakenly assigned if the chosen markers already

occurred naturally within the Scotch Whisky being analysed. These possibilities were investigated in this research for the case of a typical blend whisky matrix, by dissolving a selection of caramels in Blend W.

Four of the caramel materials previously considered were assessed in this part of the study: E150a (Type 1) and each of the samples representing the three remaining caramel classes (incorporating solutions 8 to 11 in Table 5.1). This was to facilitate a preliminary study to initially identify whether caramels of different class could still be distinguished when inherent whisky components might interfere with the UPLC-MS profiles. Each caramel was dissolved in Blend W (devoid of previous caramel addition) until the final colour level matched that of a typical market blend, so that caramel components would be present at a level representative of real products. Once prepared, all solutions – along with Blend W containing no caramel – were analysed in triplicate using UPLC TOF MS and data were acquired in both negative and positive ionisation modes. MarkerLynx software was then used to extract EMRT pairs from both datasets and 2739 were obtained from the negative data whilst 6677 were attained from the positive. Two separate PCA models were then constructed from these data in turn (including all five samples in each case) and the resulting PC1 vs. PC2 scores plots have been included in Figures 5.14a and 5.15a for the negative and positive ionisation data respectively.

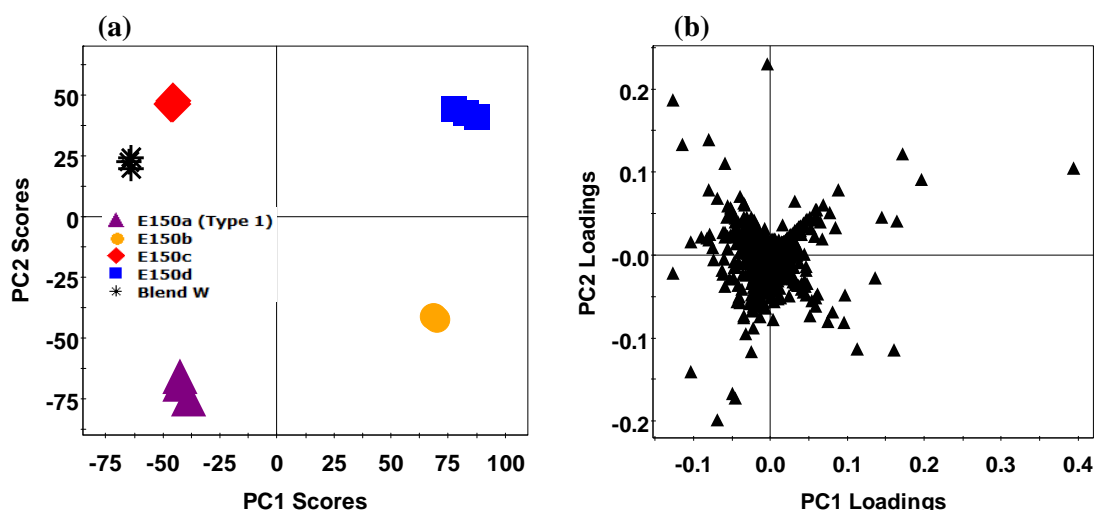


Figure 5.14: (a) PC1 vs. PC2 scores plot obtained from PCA of the negative ionisation data acquired from all four caramels dissolved in Blend W and Blend W prior to caramel addition. Triplicate data were included for all samples and (b) shows the corresponding (PC1 vs. PC2) loadings data.

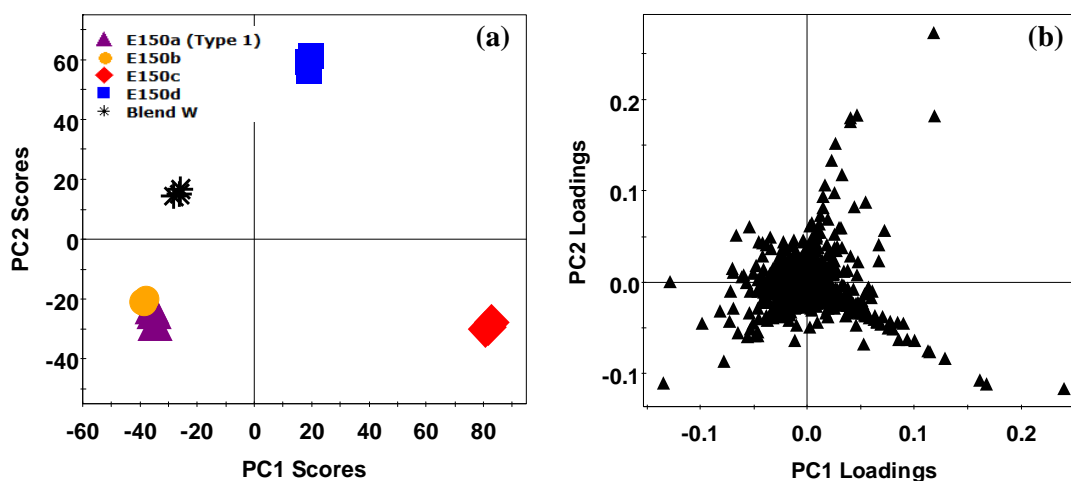


Figure 5.15: (a) PC1 vs. PC2 scores plot obtained from PCA of the positive ionisation data acquired from all four caramels dissolved in Blend W and Blend W prior to caramel addition. Triplicate data were included for all samples and (b) shows the corresponding (PC1 vs. PC2) loadings data.

In both cases it was shown that all four caramel solutions in Blend W were clearly separated from the blend alone. This demonstrated that components characteristic of caramel materials did not appear to be completely masked (if at all) by the matrix of a typical blended whisky. It was however, only possible to clearly distinguish between all four caramel classes using the negative ionisation data, as demonstrated in Figure 5.14a. When the positive ionisation data were considered, the E150a and E150b caramels could no longer be separated when dissolved in Blend W, even when additional PCs were assessed (plots not shown). This latter finding indicated that some of the components previously identified as being unique to one of these caramel classes may have been diluted to the extent where they were no longer clearly visible when these materials were dissolved at a typical level in a standard Scotch Whisky.

The loadings data corresponding to each scores plot were assessed to understand what variables (or in other words components) were responsible for the above observations. The loadings from the negative ionisation data (shown in Figure 5.14b) were considered first and it was found that the components responsible for separation between the four caramel classes matched up well with those previously identified as suitable markers of different classes when the same caramels were dissolved in 40% ethanol (see Table 5.3 for reference). The marker components of different caramel classes that were the most clearly visible when caramels were dissolved in the typical

blend matrix have been labelled in Table 5.3 where relevant. The markers not labelled in this way in the table were still found when the caramels were dissolved in Blend W but at lower intensity levels.

The loadings data corresponding to the PC1 vs. PC2 scores plot attained from the positive ionisation data have been included in Figure 5.15b. When these data were assessed it was found that marker compounds characteristic of the E150c and E150d caramels were the easiest to pick out. It was possible to detect all of the components previously identified as suitable markers for these caramel types when the same materials had been dissolved in 40% ethanol (see Table 5.4 for reference). The marker components that were visible at the highest intensity levels when these two caramel types were dissolved in Blend W have been highlighted in Table 5.4. From Figure 5.15b, it was also possible to detect the compounds that were previously found as being common to E150c and E150d and the markers that were most intense in this case have again been labelled in Table 5.4.

The bottom left hand region of the loadings plot acquired from the positive ionisation data (Figure 5.15b) was next examined to investigate why the E150a and E150b caramels could no longer be separated when dissolved in the typical blend whisky matrix. It was only possible to find the components that were previously identified as being common to both E150a and E150b (recorded in Table 5.5); the components previously identified as being unique to E150b (shown in Table 5.4) could no longer be found amongst those furthest from the centre of the loadings plot. Examination of trend plots demonstrated that some of the E150b marker components were still present when that caramel was dissolved in Blend W, however they were at intensity levels that were very close to zero. This observation indicated that the components characteristic of the E150b classed caramel would be almost completely masked by the background matrix of a typical Scotch Whisky (at the concentration implemented) when analysed using positive ionisation mode.

Trend plots were used next to determine whether any of the marker components (from both the negative and positive ionisation data) also occurred naturally within Blend W, in which case the suitability of a marker for confirming the presence of a

particular caramel might come into question. It was found however, that all compounds previously identified as being suitable markers of different caramel materials were not generally inherent within the typical blend whisky matrix assessed. The trend plot for marker 62 from Table 5.3, showing its intensity across the five samples analysed in this part of the study, has been provided in Figure 5.16 as an example. It was clearly seen from this figure that marker 62 was not inherent to Blend W and remained only characteristic of the E150d caramel assessed in this research.

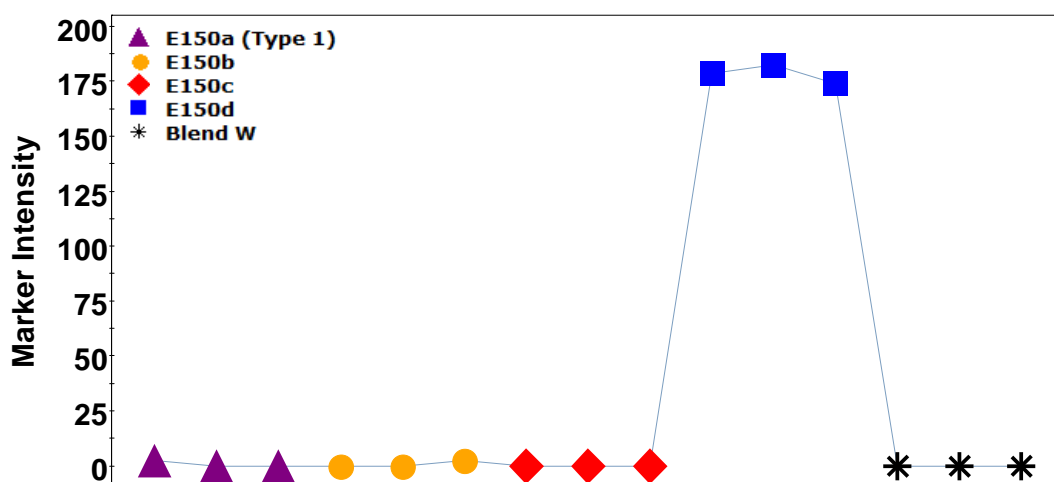


Figure 5.16: Trend plot of the component with retention time of 1.34 minutes and mass of 349.0710 (marker compound 62 –Table 5.3) showing the intensity of this component across the four caramel samples dissolved in Blend W and Blend W as it was prior to any caramel addition. Triplicate data included for each sample solution.

In the few cases where components were found to occur naturally in Blend W (markers 27 and 76 for the negative ionisation data (Table 5.3) and markers 3, 5, 8 and 9 from Table 5.5 for the positive ionisation data), the intensity of those compounds were always considerably higher in the sample containing the relevant caramel. The trend plots for markers 76, 3 and 5 have been included in Figures 5.17, 5.18 and 5.19 respectively to demonstrate this point. The three marker compounds whose trend plots have not been shown were found to occur naturally in even lower levels still.

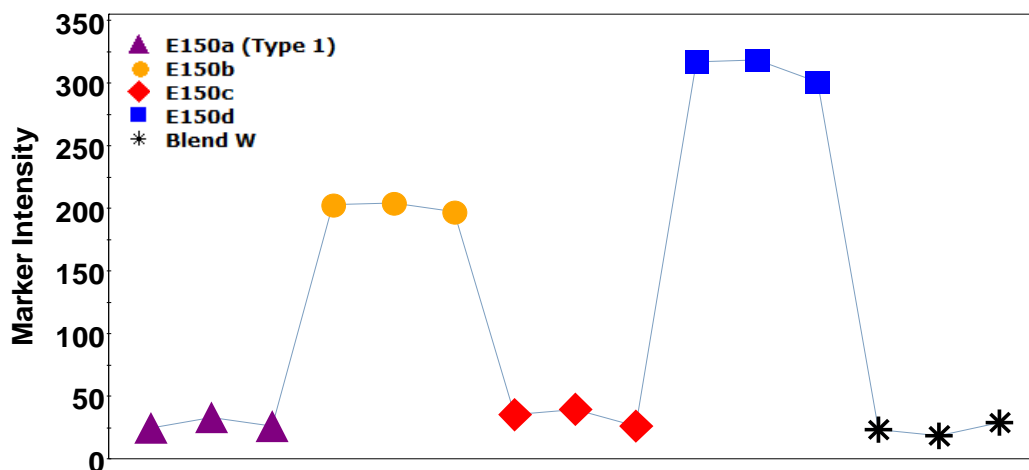


Figure 5.17: Trend plot of the component with retention time of 1.34 minutes and mass of 191.0087 (marker compound 76 –Table 5.3) showing its intensity across the caramel samples dissolved in Blend W (and Blend W alone). Triplicate data included for each sample solution.

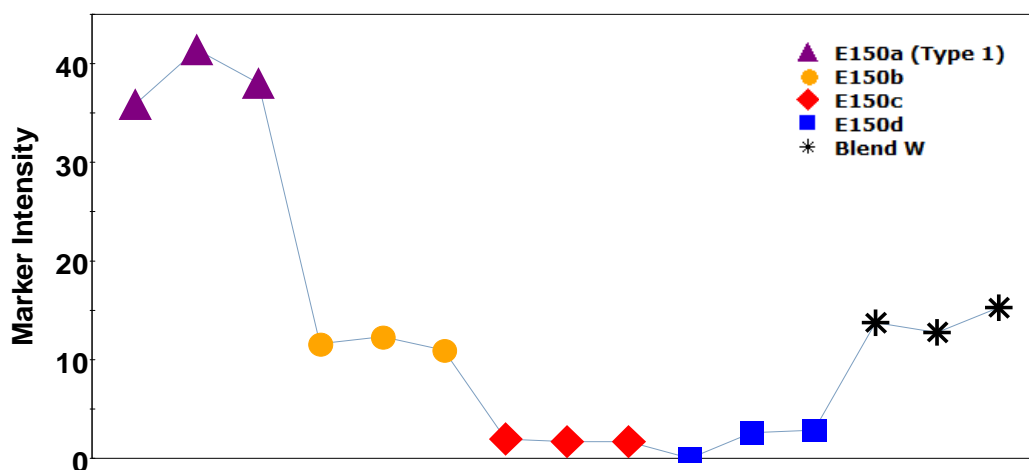


Figure 5.18: Trend plot of the component with retention time of 0.99 minutes and mass of 219.0279 (marker compound 3 –Table 5.5) showing its intensity across the caramel samples dissolved in Blend W (and Blend W alone). Triplicate data included for each sample solution.

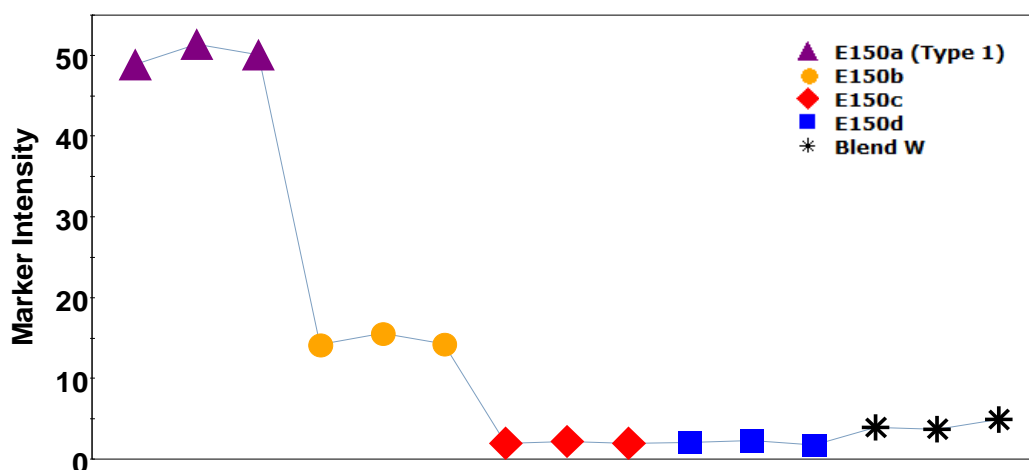


Figure 5.19: Trend plot of the component with retention time of 1.01 minutes and mass of 381.0804 (marker compound 5 –Table 5.5) showing its intensity across the caramel samples dissolved in Blend W (and Blend W alone). Triplicate data included for each sample solution.

Overall this part of the research has demonstrated that it was possible to assess the influence of a blend matrix on the ability of UPLC TOF MS to detect characteristic caramel components. This particular study however, only investigated samples where caramels had been dissolved in a typical blend matrix and at a concentration to provide a level of colour similar to that of the average blend on the market. If UPLC TOF MS was to be implemented in the Scotch Whisky industry to confirm the presence of caramel colourants, additional studies would be required to assess the suitability of the components identified in this work for different scenarios (i.e. for different caramel concentrations and blend matrices).

5.3.2 The Application of MarkerLynx Software for Structural Elucidation

5.3.2.1 Elemental composition analysis

The use of a TOF mass analyser within this research enabled component masses to be detected with ppm mass accuracy. Elemental composition analysis (ECA) could therefore be performed to provide potential molecular formulae for compounds. This procedure (ECA) is an automated feature within the MarkerLynx software and so was applied to the majority of components identified earlier as being characteristic of different caramel materials (details of the method parameters for ECA have been provided in section 5.2.4). In all cases however, multiple elemental compositions were returned and so it was attempted to manually prioritise the proposed formulae for all components based on a number of factors: (a) how closely the mass of the predicted composition matched that of the mass provided by the instrument (<1.0 mDa difference is normally considered); (b) the i-FIT value obtained, which compares the theoretical isotope distribution of the suggested formula against the isotope pattern observed experimentally; (c) the likelihood of the proposed formula being related to a plausible structure. Table 5.6 illustrates some of the most conceivable formulae acquired for selected markers that were previously listed for different caramel materials analysed under negative ionisation mode. The components taken forward to this point (from Table 5.3) were generally those that were most clearly visible when caramels were dissolved within the typical blend matrix.

Table 5.6: The most plausible elemental compositions attained for selected components found as being characteristic of different caramel materials – from negative ionisation data.

Retention Time (min)	Mass ¹	Associated Caramel Class	Potential Composition(s)*
0.96	269.0873	E150A	C ₉ H ₁₈ O ₉
1.01	179.0553		C ₆ H ₁₂ O ₆
1.02	341.1084		C ₁₂ H ₂₂ O ₁₁
1.07	503.1611		C ₁₈ H ₃₂ O ₁₆
1.08	323.0976		C ₁₂ H ₂₀ O ₁₀
0.97	359.0648	E150B	C ₁₁ H ₂₀ O ₁₁ S
0.98	345.0491		C ₁₀ H ₁₈ O ₁₁ S
0.98	168.9803		C ₃ H ₆ O ₆ S
1.00	210.9909		C ₅ H ₈ O ₇ S
1.00	255.0172		C ₇ H ₁₂ O ₈ S
1.01	182.9959		C ₄ H ₈ O ₆ S
0.95	184.0608	E150C	C ₈ H ₁₁ NO ₄
0.99	339.0738		C ₁₆ H ₁₂ N ₄ O ₅
1.29	303.1194		C ₁₂ H ₁₉ N ₂ O ₇ (OR C ₁₁ H ₁₄ N ₉ O ₂)
1.29	213.0877		C ₉ H ₁₄ N ₂ O ₄ (OR C ₇ H ₁₂ N ₅ O ₃)
1.30	349.1250		C ₁₃ H ₂₂ N ₂ O ₉
0.93	270.9581	E150D	C ₆ H ₈ O ₈ S ₂
0.93	258.9580		C ₅ H ₈ O ₈ S ₂
0.93	226.0384		C ₆ H ₁₃ NO ₆ S
1.07	225.0067		C ₆ H ₁₀ O ₇ S
1.34	146.9749		C ₄ H ₄ O ₄ S
1.34	247.0389		C ₈ H ₁₂ N ₂ O ₅ S
1.35	160.9908		C ₅ H ₆ O ₄ S
0.90	321.1298	E150C and E150D	C ₁₂ H ₂₂ N ₂ O ₈
0.98	243.0173	E150B and E150D	C ₆ H ₁₂ O ₈ S
0.99	241.0017		C ₆ H ₁₀ O ₈ S
0.99	213.0065		C ₅ H ₁₀ O ₇ S
1.02	167.0009		C ₄ H ₈ O ₅ S
1.05	194.9961		C ₅ H ₈ O ₆ S
1.08	164.9855		C ₄ H ₆ O ₅ S

¹ The mass quoted is the component mass minus one proton (a result of using negative ionisation).

* One proton has been added to each formula to account for the one removed during negative ionisation

An interesting observation made from the elemental compositions recorded in Table 5.6 was that the elements present in each formula corresponded well with those that would originate from the materials that are legally permitted during manufacture of the four different caramel classes; each caramel class having a different set of restrictions in place for their production as set out by the EU Directive 2008/128/EC (see section 1.4.2 for more details).⁴⁹ The markers relating to E150b for example, were all shown as being likely to contain sulphur (but not nitrogen), reflecting the use of sulphites during manufacture but the restriction of ammonium compounds. The E150c components on the other hand were indicated as containing nitrogen but not sulphur, reflecting the use of ammonium compounds but not sulphites during production. E150a caramels, which cannot be produced with either ammonium compounds or sulphites, were shown to incorporate markers that did not contain either nitrogen or sulphur in their proposed compositions. The E150d components all contained sulphur (reflecting the use of sulphites during production) but also contained nitrogen in a few cases. This latter observation therefore corresponded well to the fact that ammonium compounds can also be implemented during the production of E150d classed caramels. It was also found that markers common to two caramel classes (i.e. either E150c and E150d or E150b and E150d) contained elements (nitrogen or sulphur) that reflected the common materials permitted for use during the manufacture of each of these caramel groupings: ammonium compounds for the former combination and sulphites for the latter.

It is possible that the elemental compositions given in Table 5.6 may not denote the correct formulae in all cases, as multiple possibilities were initially produced when ECA was undertaken. They do however act as good starting points for the determination of component structures as they were selected due to them being the most plausible formulae according to the criteria mentioned earlier in the section. If on further investigation however, these formulae do not represent the actual composition of a component, the next most likely elemental composition provided by the software would need to be assessed.

5.3.2.2 Structural elucidation

Once ECA has been completed, any chosen molecular formula can be searched against online databases (in this case using MarkerLynx) to find potential structures that would match the proposed composition. In the majority of cases however, this search provides quite a large number of suitable structures, making the assignment of the correct structure quite complex. The particular instrumental set up used for this research however (incorporating MS^E data acquisition), acquired fragmentation patterns for all components as well as the mass information for the precursor ion. Any potential compound structures can therefore be assessed using MassFragment; a tool within the MarkerLynx software that can compare the most likely fragment ions relating to a proposed structure with those that have been observed experimentally (see section 2.2.3 for more details). This tool can therefore aid in the assignment of a structure to an unknown component of interest.

The implementation of the above procedure for structural elucidation can be a very difficult task. One initial issue found was that quite a high number of matching structures can be proposed for a single molecular formula and each of these has to be manually inputted into the MassFragment tool in turn – an extremely time consuming process. This may then have to be repeated for different molecular formulae (suggested during ECA) if none of the fragmentation patterns can be matched up with those acquired experimentally. Further difficulties can also be encountered when multiple isomers are suggested for a component, as these often have similar fragmentation patterns and so are difficult to distinguish between. Personal judgement also has to be used to identify whether a structure fits well with the raw experimental data.

Another issue with assigning component structures is commonly encountered when complex mixtures such as caramels and whiskies are assessed. In this situation it is likely that many sample analytes will co-elute from the chromatographic system, which could lead to certain peaks within relevant mass spectra being mistaken as fragments by the MassFragment software, when they are in fact related to a completely different component. Structures that could potentially be a good match

would therefore be discounted by the analyst due to poor correlation between the proposed and experimental fragmentation patterns. A better approach for structural elucidation would therefore be to firstly isolate the components of interest before fragmentation patterns are assessed. Isolating components would also allow additional tools such as NMR spectrometry to be used as a means to aid with confirming assigned structures – restrictions with time and resources meant that this could not be achieved within the scope of this project but such an approach should be considered for any future work.

The issue of co-eluting analytes could also influence isotope patterns in mass spectra, if the masses of such components are very close together. This would throw off *i*-FIT values used as a means to select plausible formulae during ECA and so could mean that the correct elemental composition is initially missed. This would significantly hamper attempts to structurally elucidate components of interest.

In addition to each of the abovementioned issues, even if a plausible structure can be identified from the MassFragment software, this does not necessarily make it the correct assignment. The identity of a component would subsequently need to be confirmed, which can be done by further fragmentation studies on the isolated component and/or by comparing the mass and retention time of the component with a reference standard analysed under the same conditions. Again however, time and resource restrictions meant this could not be achieved within this project. An attempt has been made however to use the tools within MarkerLynx to understand as much as possible about the structures of a selection of the E150a components. These components have been discussed in turn within the following subsections. These examples were included to demonstrate the capabilities of the UPLC TOF MS technology, however before further time is exerted on assigning component identities, it would be important to analyse numerous additional batches of each caramel sample - to confirm the suitability of all components as markers for particular caramel classes.

E150a component with a mass of 341.1084 (RT of 1.02 minutes)

The most plausible elemental composition suggested for this component was $C_{12}H_{22}O_{11}$ and when searched against online databases a number of potential structures were proposed. The top hit returned by the software was sucrose, however literature indicated that E150a classed caramels should contain very little of this material, if any at all.⁵⁰ The other proposed structures returned from the search were therefore examined and the vast majority were found to be disaccharides, generally with similar conformations to sucrose. Each of these structures was subsequently implemented into MassFragment in turn to determine which would provide a fragmentation pattern that would best fit the one observed experimentally. When this was undertaken however, a high number of the suggested structures were well fitted with the experimental results, which was likely due to the structural similarities between the proposed materials. Many of the sugars had the same general backbone but differed mainly in either stereochemistry or the positioning of just a few functional groups – meaning that each provided very similar fragments. At this point therefore, the most information that could confidently be deduced about this E150a marker was that it is very likely to be a disaccharide sugar. Some of the potential identities of this component are: β -lactose, β -maltose, α,α -trehalose; cellobiose; lactulose; kojibiose; 6-O- α -D-Mannopyranosyl- α -D-mannopyranose; and various other isomers/stereoisomers of these materials. The MassFragment results acquired for β -lactose have been provided in Figure 5.20 to demonstrate how well its most likely fragments matched up with those observed experimentally. The main peaks observed in the mass spectrum were clearly shown to relate to plausible fragments of β -lactose with very good mass accuracy. Each of the other sugars returned similar fragments when submitted to MassFragment, matching the experimental data well and with good mass accuracy. It was therefore not possible to use personal judgement to pick out the correct assignment for this E150a marker at this point. A lot of future work (of the type described in section 5.4.2.2) would therefore be required to confirm the correct identity of this marker.

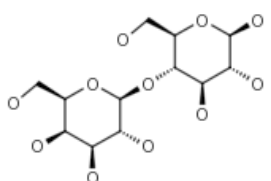
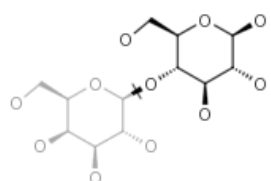
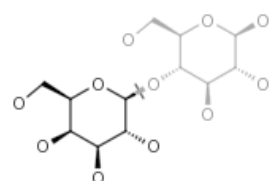
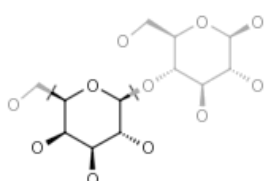
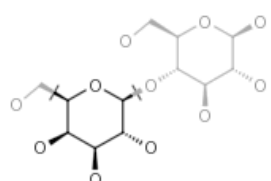
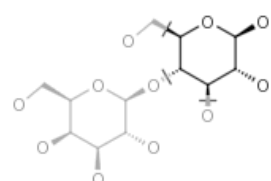
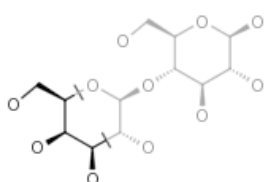
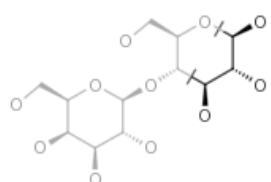
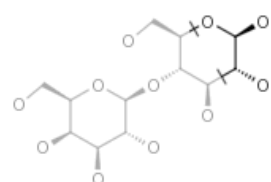
<p>341.1085 \sim (+1H) Chiral</p>  <p>341.1084 (+0.1.mDa) $C_{12}H_{21}O_{11}$ (-none)</p>	<p>179.0559 \sim (+2H) Chiral</p>  <p>179.0556 (+0.3.mDa) (S:0.5, B:1) $C_6H_{11}O_6$ (-$C_6H_{10}O_5$)</p>	<p>161.0452 \sim (+0H) Chiral</p>  <p>161.0450 (+0.2.mDa) (S:0.5, B:1) $C_6H_9O_5$ (-$C_6H_{12}O_6$)</p>
<p>131.0350 \sim (+1H) Chiral</p>  <p>131.0344 (+0.6.mDa) (S:1.5, B:2) $C_5H_7O_4$ (-$C_7H_{14}O_7$)</p>	<p>129.0193 \sim (-1H) Chiral</p>  <p>129.0188 (+0.5.mDa) (S:1.5, B:2) $C_5H_5O_4$ (-$C_7H_{16}O_7$)</p>	<p>113.0242 \sim (+0H) Chiral</p>  <p>113.0239 (+0.3.mDa) (S:2.0, B:3) $C_5H_5O_3$ (-$C_7H_{16}O_8$)</p>
<p>101.0239 \sim (-1H) Chiral</p>  <p>101.0239 (+0.0.mDa) (S:3.0, B:2) $C_4H_5O_3$ (-$C_8H_{16}O_8$)</p>	<p>89.0240 \sim (+1H) Chiral</p>  <p>89.0239 (+0.1.mDa) (S:3.0, B:2) $C_3H_5O_3$ (-$C_9H_{16}O_8$)</p>	<p>75.0094 \sim (+1H) Chiral</p>  <p>75.0082 (+1.2.mDa) (S:3.0, B:2) $C_2H_3O_3$ (-$C_{10}H_{18}O_8$)</p>

Figure 5.20: MassFragment results returned from β -lactose (structure in top left box). The masses of experimentally observed fragments are provided in bold in the top left corner of each box whilst the masses of the likely fragments (pictured in each box) are listed underneath each structure.

E150a component with a mass of 179.0553 (RT of 1.01 minutes)

The most plausible elemental composition suggested for this component was $C_6H_{12}O_6$ and when searched against online databases a large number of potential structures were again proposed. When these structures were compared, it became clear that this component was very likely to be a monosaccharide, with D-Glucose being the top hit. Other possible identities were: hex-2-ulose; D-Fructose; D-Tagatose; D-Sorbose; and a variety of other hexoses. The fragmentation pattern of D-Glucose appeared to provide a very good fit with the fragments observed

experimentally and the MassFragment results for this compound have therefore been provided in Figure 5.21 to demonstrate this finding.

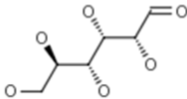
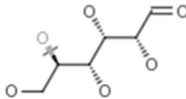
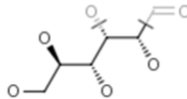
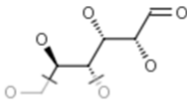
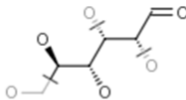
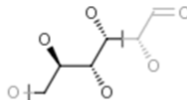
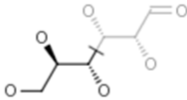
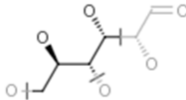
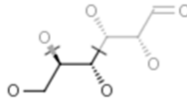
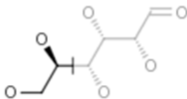
<p>179.0553 \sim (+1H) Chiral</p>  <p>179.0556 (-0.3.mDa) $C_6H_{11}O_6$ (-none)</p>	<p>161.0451 \sim (+0H) Chiral</p>  <p>161.0450 (+0.1.mDa) (S:0.5, B:1) $C_6H_9O_5$ (-H₂O)</p>	<p>131.0345 \sim (-1H) Chiral</p>  <p>131.0344 (+0.1.mDa) (S:1.5, B:2) $C_5H_7O_4$ (-CH₄O₂)</p>
<p>129.0196 \sim (-1H) Chiral</p>  <p>129.0188 (+0.8.mDa) (S:1.5, B:2) $C_5H_5O_4$ (-CH₆O₂)</p>	<p>113.0245 \sim (+0H) Chiral</p>  <p>113.0239 (+0.6.mDa) (S:2.0, B:3) $C_5H_5O_3$ (-CH₆O₃)</p>	<p>101.0242 \sim (-1H) Chiral</p>  <p>101.0239 (+0.3.mDa) (S:1.5, B:2) $C_4H_5O_3$ (-C₂H₆O₃)</p>
<p>89.0241 \sim (+0H) Chiral</p>  <p>89.0239 (+0.2.mDa) (S:1.0, B:1) $C_3H_5O_3$ (-C₃H₆O₃)</p>	<p>85.0292 \sim (+0H) Chiral</p>  <p>85.0290 (+0.2.mDa) (S:2.0, B:3) $C_4H_5O_2$ (-C₂H₆O₄)</p>	<p>71.0138 \sim (-1H) Chiral</p>  <p>71.0133 (+0.5.mDa) (S:1.5, B:2) $C_3H_3O_2$ (-C₃H₈O₄)</p>
<p>59.0137 \sim (+0H) Chiral</p>  <p>59.0133 (+0.4.mDa) (S:1.0, B:1) $C_2H_3O_2$ (-C₄H₈O₄)</p>		

Figure 5.21: MassFragment results returned from glucose (structure in top left box). The masses of experimentally observed fragments are provided in bold in the top left corner of each box whilst the masses of the likely fragments (pictured in each box) are listed underneath each structure.

To confirm the identity of this particular E150a marker however, additional work would be required. The component should be analysed alongside a reference standard for comparison and also isolated so that either further fragmentation studies could be undertaken and/or NMR analysis. It should be noted here that a number of the other monosaccharides conforming to the molecular formula of $C_6H_{12}O_6$ could also represent the correct identity of this E150a marker however, as there are a lot of similarities in their structures.

E150a component with a mass of 503.1611 (RT of 1.07 minutes)

The most plausible elemental composition suggested for this component was $C_{18}H_{32}O_{16}$ and so this molecular formula was subsequently searched against online databases using MarkerLynx. One of the top hits returned in this case was raffinose (which is a trisaccharide sugar) and when its structure was submitted to MassFragment a good match was obtained between the likely fragments of this compound and those that were observed experimentally. The MassFragment results for raffinose have therefore been provided in Figure 5.22, however not all fragments have been included – this was for clarity as the large size of this molecule meant there were a very high number of fragments. The majority of other proposed structures returned from the database search were also trisaccharide sugars (e.g. melezitose, β -gentiotriose, and various isomers/sterioisomers of such sugars) and many of these gave similar fragmentation patterns to raffinose – consequently providing reasonable matches with the fragments actually observed. Further experiments would therefore be required to confirm the correct structural identity of this component, however it does seem very likely that this E150a marker has the conformation of a trisaccharide.

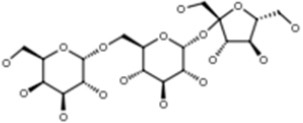
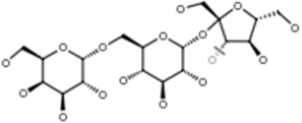
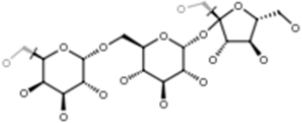
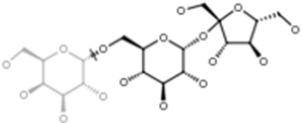
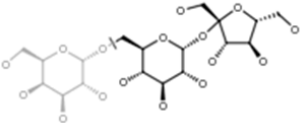
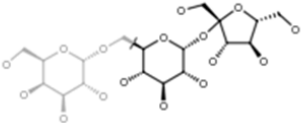
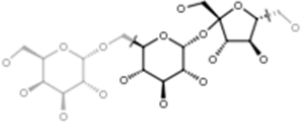
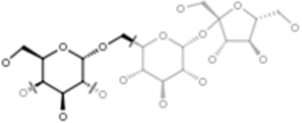
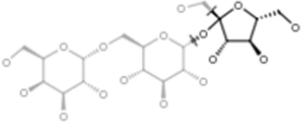
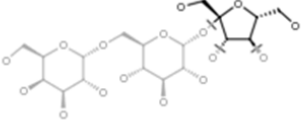
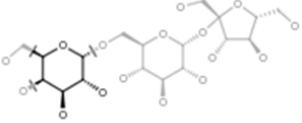
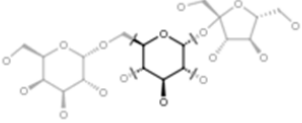
<p>503.1628 \neg (+1H) Chiral</p>  <p>503.1612 (+1.6.mDa) $C_{18}H_{31}O_{16}$ (-none)</p>	<p>485.1515 \neg (+0H) Chiral</p>  <p>485.1506 (+0.9.mDa) (S:0.5, B:1) $C_{18}H_{29}O_{15}$ (-H₂O)</p>	<p>443.1413 \neg (+3H) Chiral</p>  <p>443.1401 (+1.2.mDa) (S:2.0, B:2) $C_{16}H_{27}O_{14}$ (-C₂H₄O₂)</p>
<p>341.1087 \neg (+2H) Chiral</p>  <p>341.1084 (+0.3.mDa) (S:0.5, B:1) $C_{12}H_{21}O_{11}$ (-C₆H₁₀O₅)</p>	<p>323.0976 \neg (+0H) Chiral</p>  <p>323.0978 (-0.2.mDa) (S:0.5, B:1) $C_{12}H_{19}O_{10}$ (-C₆H₁₂O₆)</p>	<p>311.0980 \neg (+2H) Chiral</p>  <p>311.0978 (+0.2.mDa) (S:1.0, B:1) $C_{11}H_{19}O_{10}$ (-C₇H₁₂O₆)</p>
<p>281.0872 \neg (+3H) Chiral</p>  <p>281.0873 (-0.1.mDa) (S:2.0, B:2) $C_{10}H_{17}O_9$ (-C₈H₁₄O₇)</p>	<p>155.0346 \neg (-2H) Chiral</p>  <p>155.0344 (+0.2.mDa) (S:2.0, B:3) $C_7H_7O_4$ (-C₁₁H₂₄O₁₂)</p>	<p>149.0453 \neg (+3H) Chiral</p>  <p>149.0450 (+0.3.mDa) (S:1.5, B:2) $C_5H_9O_5$ (-C₁₃H₂₂O₁₁)</p>
<p>127.0386 \neg (+0H) Chiral</p>  <p>127.0395 (-0.9.mDa) (S:1.5, B:3) $C_6H_7O_3$ (-C₁₂H₂₄O₁₃)</p>	<p>113.0243 \neg (+0H) Chiral</p>  <p>113.0239 (+0.4.mDa) (S:2.0, B:3) $C_5H_5O_3$ (-C₁₃H₂₆O₁₃)</p>	<p>99.0445 \neg (+3H) Chiral</p>  <p>99.0446 (-0.1.mDa) (S:2.5, B:4) $C_5H_7O_2$ (-C₁₃H₂₄O₁₄)</p>

Figure 5.22: MassFragment results returned from raffinose (structure in top left box). The masses of experimentally observed fragments are provided in bold in the top left corner of each box whilst the masses of the likely fragments (pictured in each box) are listed underneath each structure.

5.4 Conclusions

The research presented within this chapter has demonstrated that UPLC TOF MS in combination with statistical data analysis software has excellent potential for profiling caramel colourants. Characteristic profiles were obtained for different caramel materials and it was possible, using PCA, to differentiate between the four caramel classes based on the components detected using UPLC-MS. This finding was achieved when both negative and positive ionisation data were separately considered, however the former was found to give slightly improved sample distinction in this case. It was also demonstrated that different types of E150a caramel had quite similar profiles when materials representing all caramel classes were incorporated during PCA – indicating that between class variation was much more significant than within class variation in the case of E150a caramels. When only E150a caramels were compared using PCA however, it was possible to distinguish between the three different types included within this study – the best results being obtained from the UPLC TOF MS data acquired using positive ionisation mode.

In addition to being able to distinguish between different caramel materials, the examination of relevant loadings data also allowed the components responsible for the above observations to be picked out (as EMRT pairs). As a result, it was possible to find compounds within this research that were unique to or predominantly associated with each of the four caramel classes. A few components were also detected that were characteristic of different E150a materials. When selected caramels were then dissolved in a typical whisky matrix, the majority of these markers could still be clearly observed; the markers not being masked by the whisky matrix and not being found to occur naturally in a typical blend. These data therefore demonstrated that UPLC TOF MS could potentially be applied within the Scotch Whisky industry to confirm sample authenticity, by monitoring for specific marker compounds known as being characteristic of legally permitted E150a. Further experiments would be required in the future however, to assess the influence of different blend matrices and caramel concentrations on the detection of marker compounds. It should also be noted here that only one batch of each caramel material

was assessed in this work and so additional batches of all samples would be required in the future to confirm the consistency of caramel profiles.

As well as the ability to pick out potential markers, the particular software implemented within this research enabled attempts to be made at structural elucidation based on the accurate mass details acquired as a result of TOF analysis. The use of elemental composition analysis enabled plausible molecular formulae to be proposed for markers of different caramel classes and after searching these against online databases, a number of possible chemical structures could be identified for certain components. Although many difficulties were found when assigning the exact chemical structures to components, it was possible to confidently assign three E150a markers as being sugars (a mono-, a di- and a tri- saccharide) and to give tentative structural identities to these components using the MassFragment tool. Isolating these compounds and subjecting them to additional analyses (such as further fragmentation studies and NMR) would be required in the future to confirm structural identities.

This latter part of the research has demonstrated that UPLC TOF MS could be extremely useful as a tool for understanding more about the identity of the individual components that make up caramel colourants and also how composition varies between different caramel materials. This is an area of research that has been severely limited in the past due to a lack of sufficiently developed analytical techniques being available to profile individual components within such complex mixtures. The research presented in this chapter is therefore novel and introduces technology that could have a lot of potential in the future for understanding more about the non volatile composition of caramel colourants (and other complex mixtures).

5.5 References

1. P. Tomasik, M. Palasiński, S. Wiejak, *Adv. Carbohydr. Chem. Biochem.*, 1989, **47**, 203-278
2. L. Cottier, G. Descotes, C. Neyret, H. Nigay, *Ind. Aliment. Agric.*, 1989, **106**, 567-570
3. P. Tomasik, *Caramel*, in *Encyclopaedia of Food Science. Food Technology and Nutrition*, (eds) R. Macrae; R. K. Robinson; M. J. Sadler, Academic Press, San Diego, 1993
4. J. Defaye, J. M. García Fernández, *Carbohydr. Res.*, 1994, **256**, C1-C4
5. B. H. Licht, K. Shaw, C. Smith, M. Mendoza, J. Orr, D. V. Myres, *Food Chem. Toxicol.*, 1992, **30(5)**, 365-374
6. B. H. Licht, Shaw, C. Smith, M. Mendoza, J. Orr, D. V. Myres, *Food Chem. Toxicol.*, 1992, **30(5)**, 375-382
7. J. S. Coffey, L. Castle, *Food Chem.*, 1994, **51**, 413-416
8. J. S. Coffey, H. E. Nursten, J. M. Ames, L. Castle, *Food Chem.*, 1997, **58(3)**, 259-267
9. L. Ciolino, *J. Agric. Food Chem.*, 1998, **46**, 1746-1753
10. M. E. Swartz, *J. Liq. Chromatogr. Relat. Technol.*, 2005, **28**, 1253-1263
11. J. Schappler, S. Rudaz, J. Veuthey, D. Guillarme, *Coupling UHPLC with MS: The Needs, Challenges, and Applications*, in *Ultra-High Performance Liquid Chromatography and its Applications*, (ed) Q. A. Xu, John Wiley & Sons, New Jersey, 2013
12. Z. Xiong, Y. Deng, F. Li, *Ultra-High Performance Liquid Chromatography – Mass Spectrometry and its Application*, in *Ultra-High Performance Liquid Chromatography and its Applications*, (ed) Q. A. Xu, John Wiley & Sons, New Jersey, 2013
13. R. N. Xu, L. Fan, M. J. Rieser, T. A. El-Shourbagy, *J. Pharmaceut. Biomed.*, 2007, **44**, 342-355
14. F. Gosetti, E. Mazzucco, M. C. Gennaro, E. Marengo, *J. Chromatogr. B.*, 2013, **927**, 22-36
15. F. Badoud, E. Grata, L. Perrenoud, L. Avois, M. Saugy, S. Rudaz, J. L. Veuthey, *J. Chromatogr. A.*, 2009, **1216**, 4423-4433

16. F. Gosetti, E. Mazzucco, M. C. Gennaro, *UHPLC Determination of Drugs of Abuse in Human Biological Matrices*, in *Ultra-High Performance Liquid Chromatography and its Applications*, (ed) Q. A. Xu, John Wiley & Sons, New Jersey, 2013
17. G. Jiang, J. R. Stenzel, R. Chen, D. Elmashni, *UHPLC/MS Analysis of Illicit Drugs*, in *Ultra-High Performance Liquid Chromatography and its Applications*, (ed) Q. A. Xu, John Wiley & Sons, New Jersey, 2013
18. R. Kostiaainen, T. Kotiaho, T. Kuuranne, S. Auriola, *J. Mass Spectrom.*, 2003, **38**, 357-372
19. N. J. Clarke, D. Rindgen, W. A. Korfmacher, . A. Cox, *Anal. Chem.*, 2001, **73**, 430-439
20. F. Li, F. J. Gonzalez, X. Ma, *Acta Pharma. Sin. B*, 2012, **2**, 118-125
21. X. H. Sun, L. L. Niu, X. Q. Li, X. M. Lu, F. M. Li, *J. Pharma. Biomed. Anal.*, 2009, **50**, 27-34
22. R. Nicoli, S. Martel, S. Rudaz, J. L. Wolfender, J. L. Veuthey, P. A. Carrupt, D. Guillarme, *Expert Opin. Drug Disc.*, 2010, **5**, 475-489
23. X. Lu, X. Zhao, C. Bai, C. Zhao, G. Lu, G. Xu, *J. Chromatogr. B*, 2008, **866**, 64-76
24. G. Theodoridis, H. G. Gika, I. D. Wilson, *Metabolomics*, 2008, **27**, 251-260
25. F. Chen, J. Xue, L. Zhou, S. Wu, Z. Chen, *Anal. Bioanal. Chem.*, 2011, **401**, 1899-1904
26. H. G. Gika, G. A. Theodoridis, I. D. Wison, *J. Chromatogr. A*, 2008, **1189**, 314-322
27. A. Golon, N. Kuhnert, *J. Agric. Food Chem.*, 2012, **60**, 3266-3274
28. A. Golon, N. Kuhnert, *J. Food Sci. Eng.*, 2012, **2**, 625-641
29. A. Golon, N. Kuhnert, *Food Funct.*, 2013, **4**, 1040-1050
30. X. L. Cheng, F. Wei, X. Y. Xiao, Y. Y. Zhao, Y. Shi, W. Liu, P. Zhang, S. C. Ma, S. S. Tian, R. C. Lin, *J. Pharmaceut. Biomed.*, 2012, **62**, 191-195
31. X. Xiao, Y. Hou, Y. Liu, Y. Liu, H. Zhao, L. Dong, J. Du, Y. Wang, G. Bai, G. Luo, *Talanta*, 2013, **107**, 344-348
32. M. Zhou, M. Jiang, X. Ying, Q. Cui, Y. Han, Y. Hou, J. Gao, G. Bai, G. Luo, *Plos One*, 2013, **8**, 1-11

33. G. Xie, Y. Ni, M. M. Su, Y. Y. Zhang, A. H. Zhao, X. F. Gao, Z. Liu, P. G. Xiao, W. Jia, *Metabolomics*, 2008, **4**, 248-260
34. R. Plumb, M. D. Jones, P. D. Rainville, J. K. Nicholson, *J. Chromatogr. Sci.*, 2008, **46**, 193-198
35. Y. Zhao, P. Chen, L. Lin, J. M. Harnly, L. Yu, Z. Li, *Food Chem.*, 2011, **126**, 1269-1277
36. J. Sun, P. Chen, *Anal. Bioanal. Chem.*, 2011, **399**, 1877-1889
37. I. D. Wilson, J. K. Nicholson, J. Castro-Perez, J. H. Granger, K. A. Johnson, B. W. Smith, R. S. Plumb, *J. Proteome Res.*, 2005, **4**, 591-598
38. R. Plumb, J. H. Granger, C. L. Stumpf, K. A. Johnson, B. W. Smith, S. Gaultitz, I. D. Wilson, J. Castro-Perez, *Analyst*, 2005, **130**, 844-849
39. H. G. Gika, G. A. Theodoridis, I. D. Wilson, *J. Chromatogr. A.*, 2008, **1189**, 314-322
40. J. Zhang, L. Yan, W. Chen, L. Lin, X. Song, X. Yan, W. Hang, B. Huang, *Anal. Chim. Acta*, 2009, **650**, 16-22
41. X. Wang, H. Lv, H. Sun, L. Liu, B. Yang, W. Sun, P. Wang, D. Zhou, L. Zhao, S. Dou, G. Zhang, H. Cao, *J. Pharmaceut. Biomed.*, 2008, **48**, 1161-1168
42. X. Zhao, W. Wang, J. Wang, J. Yang, G. Xu, *J. Sep. Sci.*, 2006, **29**, 2444-2451
43. S. Inagaki, T. Noda, J. Z. Min, T. Toyooka, *J. Chromatogr. A.*, 2007, **1176**, 94-99
44. J. Chen, W. Wang, S. Lv, P. Yin, X. Zhao, X. Lu, F. Zhang, G. Xu, *Anal. Chim. Acta*, 2009, **650**, 3-9
45. S. Su, J. Duan, P. Wang, P. Liu, J. Guo, E. Shang, D. Qian, Y. Tang, Z. Tang, *J. Proteome Res.*, 2013, **12**, 852-865
46. R. A. van den Berg, H. C. J. Hoefsloot, J. A. Westerhuis, A. K. Smilde, M. J. Van der Werf, *BMC Genomics*, 2006, **7**, 142-156
47. B. Worley, R. Powers, *Curr. Metabolomics*, 2013, **1**, 92-107
48. S. Cubbon, Ph.D Thesis, University of York, 2007
49. EU Commission Directive 2008/128/EC, <http://eur-lex.europa.eu/legal-content/EN/TXT/?qid=1418823300247&uri=CELEX:32008L0128>, Accessed 17/12/2014
50. R. I. Aylott, W. M. MacKenzie, *J. Inst. Brew.*, 2010, **116**, 215-229

6.0 UPLC TOF MS IN COMBINATION WITH STATISTICAL DATA ANALYSIS FOR PROFILING NON VOLATILE COMPONENTS IN SCOTCH WHISKY

6.1 Introduction

6.1.1 Basis of this Study

Chapter 5 demonstrated the success of UPLC TOF MS for the analysis of individual components within caramel colourants and using PCA it was possible to find compounds that were characteristic of different caramel materials. As a result of these findings it was then possible to identify when a particular caramel colourant was present in a Scotch Whisky, by monitoring for these marker components. From an assessment of the literature it became clear that this work represented one of the first examples of UPLC-MS being combined with multivariate statistics for the analysis of Scotch whiskies and so raised the question as to what else this tool could offer to the Scotch Whisky industry. The work completed in this chapter has therefore been undertaken to determine whether UPLC TOF MS in combination with PCA could be implemented for a wider range of applications involving Scotch Whisky. Such analyses could both complement and broaden the data provided by existing tools applied for the analysis of Scotch. The review that follows explains why LC-MS has been disfavoured in the past and highlights some recent examples demonstrating the success of UPLC-MS within the spirits industry.

6.1.2 UPLC in combination with MS as a tool for profiling Scotch Whisky

Techniques based on chromatography are commonly implemented for analysing Scotch whiskies and both liquid chromatography (LC) and gas chromatography (GC) have been employed for profiling components within this spirit.¹⁻⁷ When used as stand alone techniques however, it is typical to simply monitor known components using these tools, as peak identities can only be confirmed by comparisons with reference standards. It is therefore extremely difficult to profile new components using chromatographic tools on their own and so to resolve this it has become common for LC/GC to be combined with mass spectrometry (MS) as a mode of

detection.³ This approach enables component masses to be determined after component separation and as a result known components can be easily monitored based on their masses and the identity of unknown or new components can potentially be elucidated – especially with recent advancements in the field of MS.⁴⁻⁶

MS has been implemented in the Scotch Whisky industry for many years; however GC has traditionally been preferred over LC as the preceding tool employed for component separation.^{1,4-6} The reasons behind this preference in the past were due to better separation efficiency and much improved reproducibility associated with GC when combined with MS detection. These factors also meant that the availability of searchable reference libraries that aid with component identification were far superior for GC-MS analysis. The main limitation of GC-MS for profiling Scotch Whisky is that not all components present in the spirit will be picked up using this technique. For instance, GC is not well suited for the analysis of compounds that are non volatile or for those that are thermally labile. There are also potential issues when using GC-MS in relation to precursor ions fragmenting to the extent where component identification from libraries becomes ambiguous.

LC-MS could potentially overcome the above issues associated with GC-MS and so help to provide a fuller understanding of the chemical composition of Scotch Whisky. Its implementation has been restricted in the past however, due to the aforementioned limitations. In recent years the fields of both LC and MS have greatly advanced making LC-MS increasingly more popular. The development of UPLC has resulted in the ability to achieve component separations with far superior efficiency and also reproducibility, whilst the application of TOF mass spectrometers can allow untargeted components to be measured with very high sensitivity (accurate to ~1 mDa). Potential molecular formulae can be generated from data of this accuracy level, a factor that has aided in the assignment of component identities using LC-MS. In addition, the introduction of more advanced software packages that link to online databases has also helped to simplify the processing of complex datasets using LC-MS.

Due to the dominance of GC-MS in the past, there are few publications available that have implemented LC-MS for the analysis of alcoholic beverages such as Scotch Whisky. Most examples have only emerged in recent years and the majority of these focus on a means to monitor for the presence of and sometimes quantity of known or specifically targeted components.⁸⁻¹⁵ These papers include implementation of LC-MS for the analysis of polyphenols in wines and rum,⁸⁻¹⁰ the determination of ethyl carbamate in wines and spirits,^{11,12} the identification of artificial sweeteners in spirits and beers,¹³ and also for the analysis of dipeptides in various alcoholic beverages.¹⁴ The general consensus from each of these papers is that the advancements made in LC-MS technology over recent years has made its implementation much more appealing for these applications. Good resolution, high sensitivity, short analysis times, low solvent consumption and reduced sample preparation are all described as being desirable features of this tool. A selection of the papers also demonstrate the potential advantage of LC-MS for the elucidation of structures of unknown peaks that are encountered in chromatographic traces.^{9,10,14}

Although the above publications demonstrate the growing use of LC-MS in the spirits industry, their primary purpose was not to assess the technique's potential for profiling unknown components. In fact, only a single publication could be found in the literature that had implemented LC-MS technology for the analysis of untargeted components, as a means to gain a greater understanding of the chemical composition of the beverage under investigation. This paper, by T. Collins *et al.*, demonstrates the use of UPLC coupled to a quadrupole time of flight mass analyser to compare the non volatile compositions of 63 commercial American whiskeys.¹⁶ The instrumental set up that was employed allowed the detection of approximately 7600 different components across all samples – although this number was manually reduced to simplify subsequent data analysis. These non volatile components were then used to model differences among the whiskey samples using discriminant analysis and it was possible to distinguish between whiskeys of different type. Blended American whiskeys were clearly separated from all others in the dataset and the majority of Tennessee whiskeys could be distinguished from bourbon and rye products. In addition to this it was possible to differentiate between whiskey samples from

different producers and also those of different age. The important components responsible for these findings were also identified in this research by examination of loadings data that corresponded to the relevant discriminant analysis model. These data therefore highlight the potential of UPLC-MS for understanding more about the non volatile compositions of alcoholic beverages. Another advantage of the untargeted analysis used in the work presented by T. Collins *et al.* is that samples were directly injected into the UPLC-MS system without any prior sample preparation. The majority of previous examples that monitored for specific components required an additional preparation step prior to analysis by LC-MS to extract and isolate the components of interest.

A similar approach to T. Collins *et al.*¹⁶ has been adopted for the work presented in this chapter, where UPLC TOF MS in combination with PCA has been assessed as an untargeted tool to further elucidate the non volatile composition of Scotch Whisky and hence increase understanding of the processes involved in its production.

6.1.3 Study Objectives

In this chapter, data acquired using a UPLC TOF MS was analysed using statistical data analysis software to assess the techniques value for profiling the non volatile components in Scotch Whisky. A range of samples relating to different aspects of Scotch Whisky production were assessed within this work and the main objectives were to determine whether UPLC TOF MS in combination with PCA could be used to:

- Differentiate between whisky samples that varied only by their maturation age.
- Distinguish between samples taken from casks of different history (i.e. first fill *vs.* second fill and sherry cask *vs.* bourbon cask).
- Separate whiskies that have been artificially matured from those with authentic maturation profiles.
- Differentiate between different whisky products on the market (i.e. multiple blends and a malt whisky).
- Find out whether characteristic components could be identified for samples within each of the above scenarios to help gain a greater understanding of the processes behind authentic Scotch Whisky production.
- Discover whether sample fade may impact analysis or alternatively whether the technique could be used to identify components relating to the fading process.
- Identify when common adulterants such as sucrose, vanillin and methanol have been added to a whisky product.

6.2 Experimental

6.2.1 Samples

Twenty three samples were assessed in this study, chosen to represent a variety of different sample types typically encountered within the Scotch Whisky industry. The details of each sample are summarised in Table 6.1. Within this table, samples have also been divided into multiple subsets, each assessing a different aspect of Scotch Whisky production or another scenario of interest to the industry. The samples within subset 'A' were grouped together to assess how profiles compare when whiskies have been matured in casks of different history. Subset 'B' was put together to investigate how whisky composition is affected by variation in maturation age. Subset 'C' included wood extracts that had been acquired using a variety of different solvents (details of their production provided in section 6.2.1.1). These samples therefore represented cases of artificial maturation and their comparison with authentically matured samples could be useful in the field of counterfeit detection. Subset 'D' grouped together multiple samples of a typical blend (Blend C) subjected to different conditions. One of the samples incorporated the blend as normal; another sample was forcibly faded to see whether information could be acquired about this particular process; and the final three Blend C samples were spiked with different compounds commonly found in adulterated whiskies, to see whether they could easily be detected. The final group of samples, Subset 'E', included a range of different blend products (and one malt whisky) to see whether different whiskies could be discriminated between.

It should be noted at this point that all samples were provided by the Scotch Whisky Research Institute (Riccarton, Edinburgh, UK).

Table 6.1: Descriptions of the 23 samples assessed within this study. Each sample has been designated within a specific subset.

Sample Number	Sample Subset	Sample Description	SWRI Number
1	‘A’	<i>Whisky from a first fill sherry cask</i> (from Distillery X and 7 years 8 months old)	S11-1418
2		<i>Whisky from a refilled sherry cask</i> (from Distillery X and 7 years 10 months old)	S11-1419
3		<i>Whisky from a first fill bourbon cask (FFBC)</i> (from Distillery X and 7 years 5 months old)	S11-1420
4		<i>Whisky from a refilled bourbon cask</i> (from Distillery X and 7 years 7 months old)	S11-1421
5	‘B’	<i>Whisky aged for 3 years 5 month</i> (from Distillery V and a FFBC)	S11-1346
6		<i>Whisky aged for 6 years 2 months</i> (from Distillery V and a FFBC)	S11-1347
7		<i>Whisky aged for 9 years 6 months</i> (from Distillery V and a FFBC)	S11-1348
8		<i>Whisky aged for 12 years 4 months</i> (from Distillery V and a FFBC)	S11-1349
9	‘C’	Wood extract acquired using water	S11-1422
10		Wood extract acquired using ethanol	S11-1423
11		Wood extract acquired using ethyl acetate	S11-1424
12	‘D’	Blend C	S11-1330
13		Blend C with added sucrose (2000 ppm)	S11-1324
14		Blend C with added vanillin (50 ppm)	S11-1325
15		Blend C with added methanol (6000 ppm)	S11-1326
16		Blend C subjected to forced fade by 25%	S11-1327
17	‘E’	Blend A	S11-1328
18		Blend B	S11-1329
12		Blend C	S11-1330
19		Blend D	S11-1331
20		Blend E	S11-1332
21		Blend F	S11-1333
22		Blend G	S11-1390
23		Malt H	S11-1334

6.2.2.1 Preparation of the solvent extracts (samples 9 – 11)

Solvent extracts were prepared by the SWRI from toasted American oak wood that had been treated at 190°C for 60 minutes. For each of the three samples being prepared, 3 g of wood was extracted using 180 mL of solvent for 6 hours in a Soxhlet extractor (Quickfit EX5/53). The three samples were prepared using each of the following solvents in turn: water, ethanol and ethyl acetate. Once extraction was complete, the three samples were treated slightly differently. The ethyl acetate extract was firstly evaporated to dryness using a rotary evaporator (bath temperature set to 35°C), before being reconstituted in 40 mL of ethanol. This solution was then diluted to 40% ethanol using UHQ water. The ethanol extract was reduced in volume to 100 mL (again using a rotary evaporator) and then diluted to 40% ethanol using UHQ water. Finally, the water extract was simply diluted with ethanol (Analar) so that the final concentration of the sample was 40% ethanol.

6.2.2 UPLC-MS

UPLC-MS analysis of all samples was undertaken prior to the commencement of this project by Simon Cubbon (Waters Ltd., Wilmslow, UK). The analysis itself was completed on the same occasion as the caramel solutions that were discussed in Chapter 5. The UPLC-MS conditions of operation can therefore be found within section 5.2.2.

6.2.3 Data Analysis

Data were processed using MarkerLynx XS (built into MassLynx software (version 4.1; Waters Ltd., Wilmslow, UK)), which was implemented to automatically extract and tabulate components from the raw UPLC-MS data. Detected components were recorded as EMRT pairs and the intensity of each compound was listed over all samples. The main parameters that were implemented within the software for component extraction were set as follows: retention time range of 0.7 – 9.6 min, mass range of 50 – 1200 (i.e. unrestricted), mass tolerance of 0.05 Da, marker intensity threshold of 1500 counts, mass window of 0.02 Da and retention time window of 0.05min. These conditions were identical to those used when UPLC-MS data from caramel solutions were assessed in Chapter 5 (see section 5.2.3).

As in Chapter 5, once the raw data were processed PCA was used to compare samples based on the intensity values of the detected EMRT pairs. This procedure was undertaken using the extended statistics package incorporated within the MarkerLynx Application Manager. Prior to PCA, all data were normalised to the total marker intensity and then subjected to pareto scaling. This scaling method and the reasons behind its use have been described previously in section 5.2.3.1.

6.3 Results and Discussion

The research presented within this section describes the results of a preliminary study undertaken to assess the benefits of UPLC TOF MS for a variety of applications within the Scotch Whisky industry. A range of samples, split into particular subsets as assigned in section 6.2.1, were assessed within the work and the results that follow have therefore been divided into subsections to discuss the different sample groupings in turn. *(It is important to note here that any mass values quoted within the following results will be less one proton if taken from negative ionisation data and will contain an extra proton if taken from positive ionisation data).*

6.3.1 Profiling Whiskies with Different Cask History – ‘Subset A’

As discussed previously in Chapter 1 (section 1.4.1.1), the composition of a Scotch Whisky is known to be affected by the history of the cask used during maturation; typically a cask will previously have been used for either the storage of sherry or bourbon and it can either be the first time that a cask has been filled with Scotch Whisky or a cask could have been refilled. A quick review of literature indicated that some work has been done in the past to investigate the compositional changes that occur during the maturation process due to differences in cask history but many of these have targeted specific components and so a lot of information still remains unknown.^{4,5,17,18} The work completed in this part of the study has therefore aimed to determine whether UPLC TOF MS (in combination with statistical data analysis) could be suitable as a non-targeted approach to further elucidate, in this case, the non-volatile components responsible for compositional differences caused by variations in cask history.

Sample Subset ‘A’ was assessed in this part of the study (see Table 6.1) and incorporated four whisky samples that varied in their cask history. The samples included one whisky from a first fill sherry cask, a second whisky from a refilled sherry cask, a whisky from a first fill bourbon cask and a whisky from a bourbon cask that had been refilled. All of the samples were acquired from the same distillery and had been matured for approximately the same amount of time so that other potential sources of variation were kept as consistent as possible. Once analysed

using UPLC-MS, detected components were extracted from the raw data using MarkerLynx software and tabulated alongside their associated intensities. This was undertaken for data acquired using both negative and positive ionisation modes and 1468 EMRT pairs were attained from the former whilst 2636 were obtained from the latter. PCA was then undertaken separately for both datasets and the PC1 vs. PC2 scores plot acquired from the negative ionisation data has been provided in Figure 6.1 alongside the corresponding loadings data.

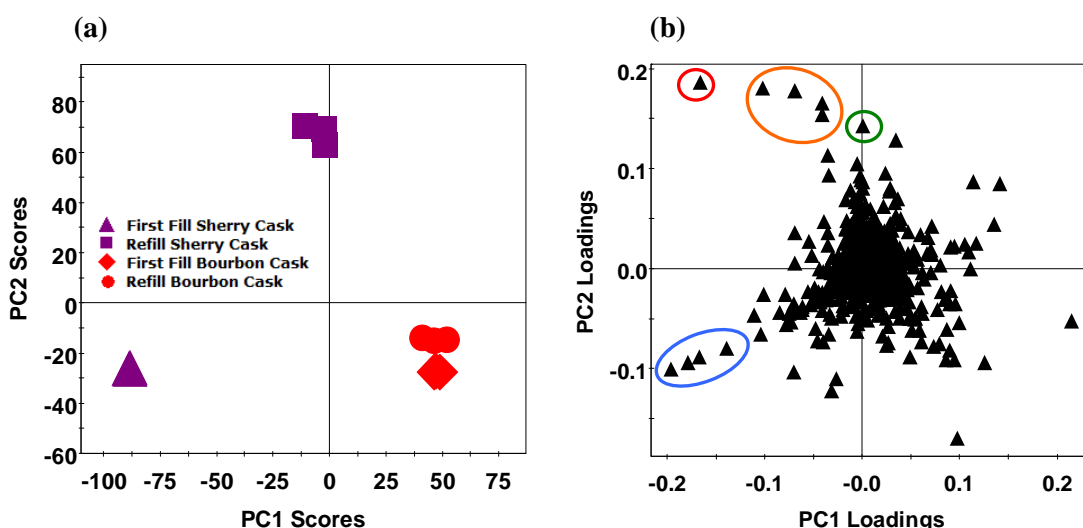


Figure 6.1: (a) PC1 vs. PC2 scores plot obtained from PCA of the negative ionisation data acquired from the four samples incorporated within Subset A. Triplicate data included for all samples. (b) Shows the corresponding (PC1 vs. PC2) loadings data. Certain EMRT pairs have been enclosed within coloured circles to allow them to be referred to in future text.

Figure 6.1a demonstrates that the two sherry cask samples can clearly be distinguished from the two samples originating from ex-bourbon casks, based on the components detected using UPLC TOF MS in negative ionisation mode. In addition to this, further separation was achieved between the first fill and refill sherry cask samples; it was not possible however to clearly differentiate the first fill and refill bourbon cask samples in this case.

The examination of corresponding loadings data (Figure 6.1b) enabled components responsible for the above separations to be investigated and a number of compounds could be picked out that were characteristic of different cask histories. Components with both highly negative PC1 and PC2 loadings (found towards the bottom left hand corner of the loadings plot) were identified as being predominantly associated with the first fill sherry cask sample. The four components highlighted with a blue circle

in Figure 6.1b were all significantly higher in intensity within the first fill sherry cask compared to the other three sample types. This finding is depicted by the trend plot provided in Figure 6.2, which shows the intensity levels of these four components over all sample measurements – the mass and retention time details of each component have been included in the figure. Other components predominantly characteristic of the first fill sherry cask sample were found within the loadings plot; however those four that have been highlighted were the most influential.

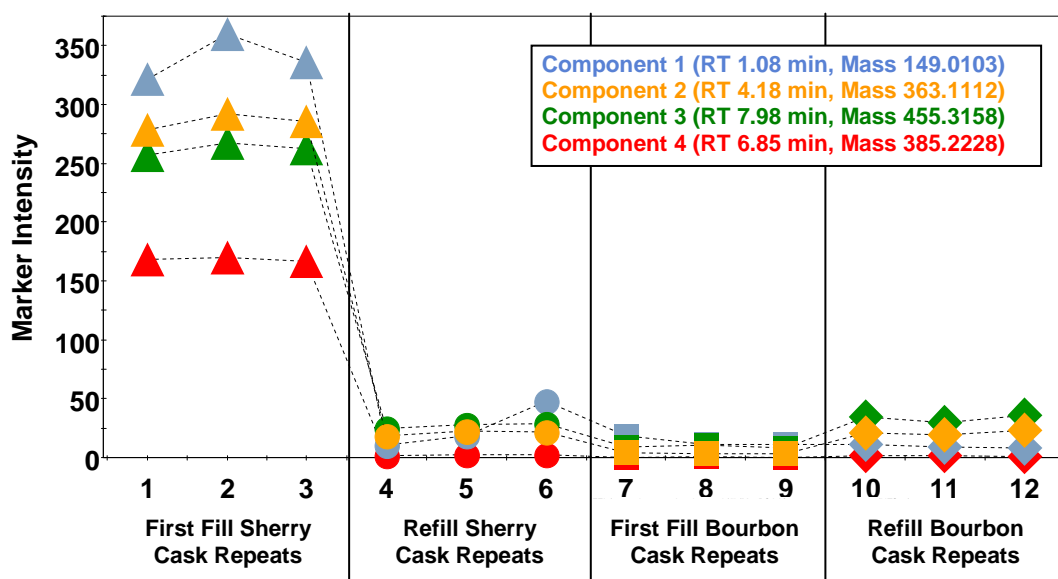


Figure 6.2: Trend plot showing the intensity levels of four components across the samples incorporated by 'Subset A'. The plot demonstrates that these components were most characteristic of the first fill sherry cask sample. TriPLICATE data included for each sample.

Further components characteristic of sherry casks were also identified from the top left hand quadrant of the loadings plot shown in Figure 6.1b. The point enclosed within a red circle on the plot for instance was found at similar levels within both the first fill and refilled sherry casks but was comparably much lower within the two bourbon cask samples. The trend plot for this component (with retention time of 5.91 mins and mass of 517.3160) has been provided in Figure 6.3 to highlight this observation. The components encircled in orange in Figure 6.1b were also found in both of the sherry cask samples at much higher levels than in the bourbon cask samples, they were however most intense within the refilled sherry cask sample. This was related to an increase in the value of the PC1 loadings (compared to the red circled marker) to become less negative, taking them closer to the region of the

loadings plot that corresponded to the position of the refilled sherry cask on the scores plot. When the PC1 loadings became very close to zero (and the PC2 loadings remained highly positive), components were predominantly characteristic of the refilled sherry cask sample. The compound emphasised within a green circle in the loadings plot (with retention time of 4.40 mins and mass of 253.0349) was the most unique to the refilled sherry cask and its trend plot has been included in Figure 6.4 to demonstrate this finding.

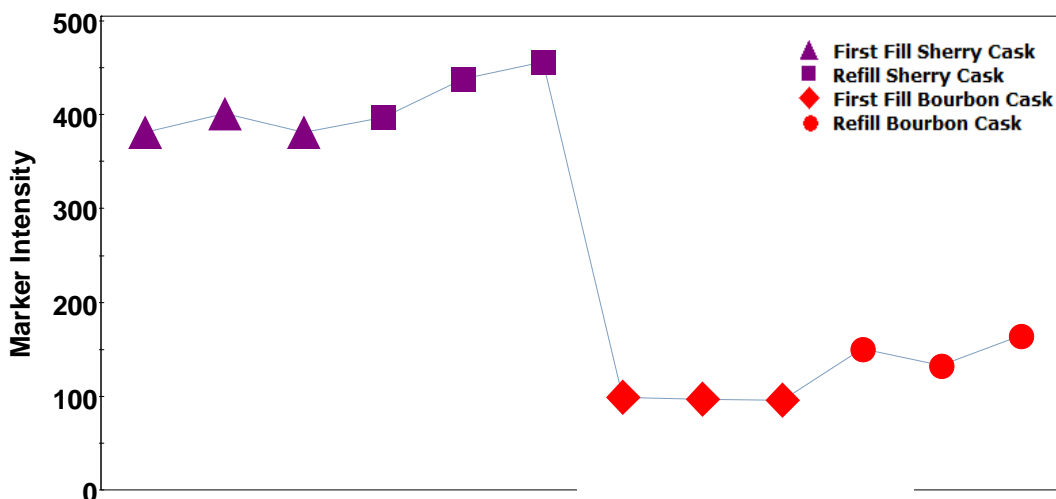


Figure 6.3: Trend plot of the component with retention time of 5.91 minutes and mass of 517.3160 showing its intensity across the four samples contained within Subset 'A'. Triplicate data included for each sample.

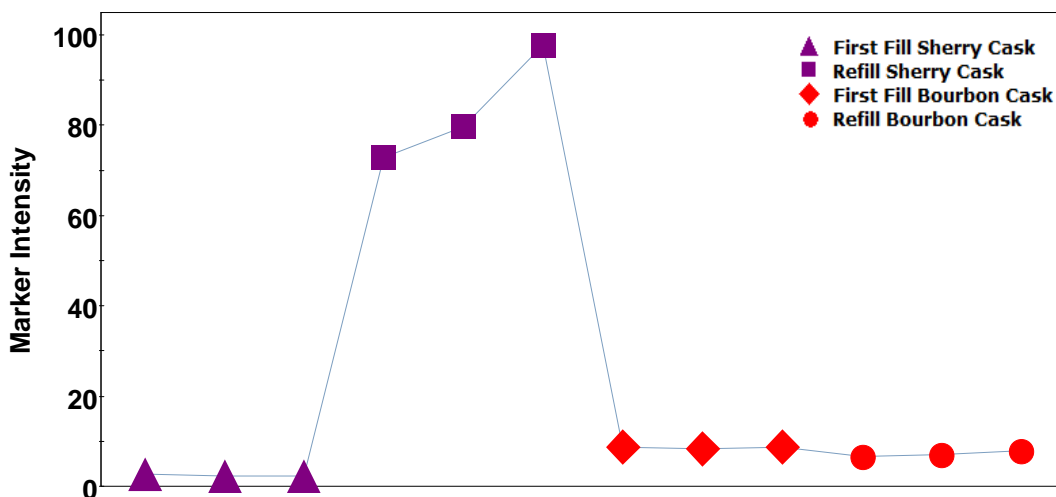


Figure 6.4: Trend plot of the component with retention time of 4.40 minutes and mass of 253.0349 showing its intensity across the four samples contained within Subset 'A'. Triplicate data included for each sample.

The bottom right hand quadrant of the loadings plot (shown in Figure 6.1b) held the most information relating to components that allowed the two bourbon cask samples to be separated from the sherry cask samples. It was possible to find a few compounds that were predominantly found within the two bourbon cask samples as opposed to the sherry cask samples and the most notable of these had a retention time of 0.94 minutes and a mass of 225.0608. The trend plot for this component has been included in Figure 6.5 to show how its intensity varied across the four samples incorporated by Subset 'A'.

Another interesting finding from these negative ionisation data was that within the top right hand quadrant of the loadings plot, quite a few components were found that as well as being common to both the bourbon cask samples, were also present within the whisky from the refilled sherry cask. This could potentially indicate that when sherry casks are refilled, the maturation process within this cask type might begin to have some similarities with maturation inside ex bourbon casks. As an example, Figure 6.6 has been included to provide a trend plot of one such component (with a retention time of 6.85 minutes and a mass of 297.2430).

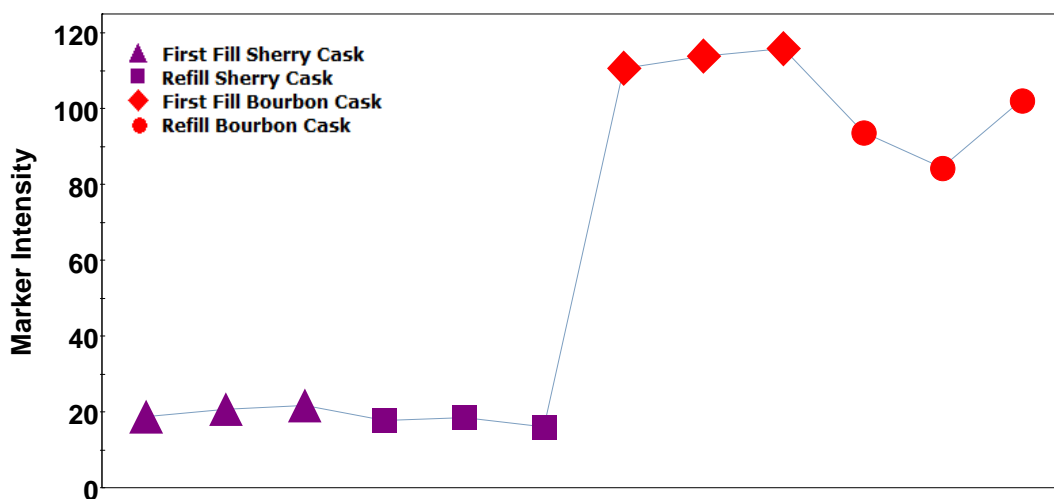


Figure 6.5: Trend plot of the component with retention time of 0.94 mins and mass of 225.0608 showing its intensity across the four samples contained within Subset 'A'. Triplicate data included for each sample.

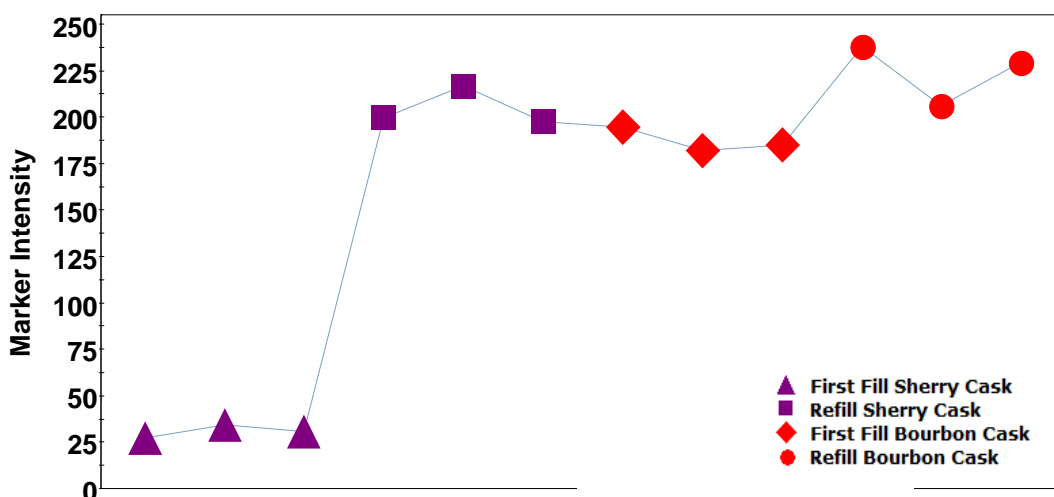


Figure 6.6: Trend plot of the component with retention time of 6.85 mins and mass of 297.2430 showing its intensity across the four samples contained within Subset 'A'. Triplicate data included for each sample.

When PCA was undertaken using the data acquired from positive ionisation, the findings were similar to those already obtained from the negative ionisation data. For instance, it was possible to clearly distinguish the two sherry cask samples from the two bourbon cask samples and the first fill and refilled sherry cask samples could be clearly separated from each other. Some additional components characteristic of certain cask histories could therefore be acquired by interpretation of relevant loadings data (components not shown within this preliminary study). One additional observation from the positive ionisation data was that separation between the first fill and refilled bourbon cask samples was slightly improved. It was still difficult however to extract components that were clearly characteristic of one or the other of these two samples. The PC1 vs. PC2 scores plot attained from the positive ionisation data has been provided in Figure 6.7a to help visualise the above observations. The corresponding loadings data are given in Figure 6.7b.

Another interesting observation from Figure 6.7a was that the two bourbon cask samples and the refilled sherry cask sample all had very similar PC1 scores, whilst the PC1 scores for the first fill sherry cask measurements were significantly different. This suggested that the former three samples contained common components that were not present in the first fill sherry cask whisky. As alluded to previously when the negative ionisation data were considered, this could indicate that when refilled,

maturation within an ex sherry cask might undergo some processes that are similar to those occurring when ex bourbon casks are used.

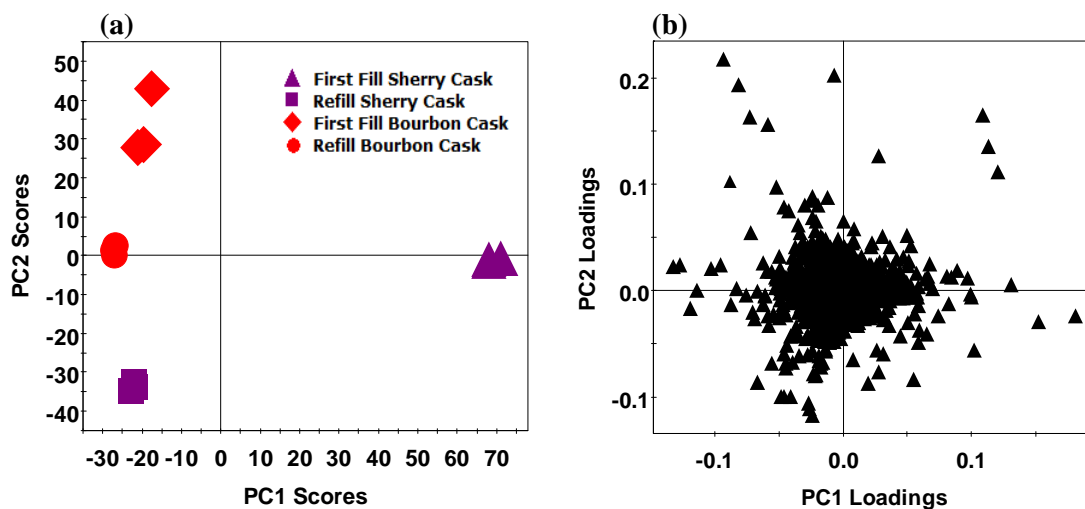


Figure 6.7: (a) PC1 vs. PC2 scores plot obtained from PCA of the positive ionisation data acquired from the four samples incorporated within Subset A. Triplicate data included for all samples. (b) Shows the corresponding (PC1 vs. PC2) loadings data.

Overall, the findings from this initial study have demonstrated that UPLC TOF MS (in combination with statistical data analysis) has excellent potential as a tool for differentiating between whisky samples of different cask history. In addition, this analytical approach allowed components characteristic of different cask types to be identified and so the tool could prove very useful in terms of understanding more about the processes behind maturation. It should be noted however, that a much larger data set incorporating multiple batches of each sample would be required to assess the consistency of these results. The addition of multiple batches would also mean that further PCA models could be constructed separately for the sherry cask samples and the bourbon cask samples, which may then allow the first fill and refilled bourbon casks to be better distinguished between (as this was not clearly achieved within this preliminary work). It should also be noted that the work completed in this section only considered whisky from a single distillery and all samples were of a similar maturation age. Additional experiments would therefore be required in the future to assess what affect changing these circumstances might have on the ability of UPLC TOF MS to distinguish whiskies matured in casks of different history.

6.3.2 Profiling Whiskies with Different Maturation Ages – ‘Subset B’

The Scotch Whisky Regulations of 2009 stipulate that a Scotch Whisky must be matured for a minimum time period of three years.¹⁹ The maturation age of products can therefore vary above this time period and it is not uncommon for maturation to occur over periods of ten years (and also for much longer than this). As discussed previously in Chapter 1 (section 1.3.5), a vast number of reactions occur during the maturation process, resulting in major changes to the chemical composition of the spirit. These changes are known to depend on the length of time that a whisky is matured for and so Scotch whiskies of different maturation age will vary in their final composition. Work has been undertaken in the past to try and understand the processes occurring during maturation and the level of colour and specific, known cask extractives have been used as easy to measure markers for the length of maturation.¹⁸ The majority of important reactions however have so far remained unidentified and so the work completed in this part of the study aimed to identify whether UPLC TOF MS (in combination with statistical data analysis) could be used as a non-targeted tool to increase knowledge of maturation in terms of any compositional changes that occur due to differences in whisky maturation age.

Sample Subset ‘B’ was investigated in this part of the study and incorporated four whisky samples that varied in the length of time that they had been matured (see Table 6.1 for specific details). All of the samples were matured in first fill bourbon casks and were obtained from the same distillery so that other potential sources of variation in composition could be kept as consistent as possible. After analysis using UPLC TOF MS (under both negative and positive ionisation modes), MarkerLynx software was used to extract and tabulate detected components from the raw data. PCA models were then constructed separately for the positive and negative ionisation datasets to compare the compositions of all four samples (measured in triplicate); 1468 components were incorporated within the negative ionisation data set, whilst 2751 were present within the positive. The positive ionisation data yielded slightly better results and so these data have been considered initially in the following text. The PC1 vs. PC2 scores plot acquired from the positive ionisation data has been provided in Figure 6.8 along with the corresponding loadings plot.

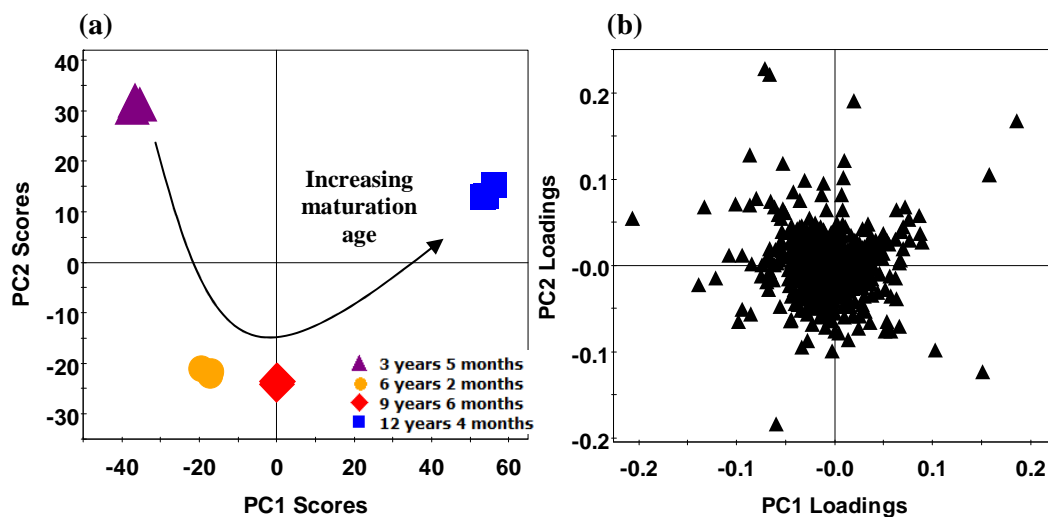


Figure 6.8: (a) PC1 vs. PC2 scores plot obtained from PCA of the positive ionisation data acquired from the four samples incorporated within Subset B. Triplicate data included for all samples. (b) Shows the corresponding (PC1 vs. PC2) loadings data.

The scores plot depicted within Figure 6.8a demonstrated that clear separation was achieved between the four samples of different maturation age, based on the components detected using UPLC TOF MS operated in positive ionisation mode. A distinct pattern was observed along the PC1 axis, where the scores were clearly shown to increase as maturation age increased. Further differentiation was also seen along the PC2 axis; the 3 year 5 month old and 12 year 4 month old samples possessing similar positive PC2 scores, whilst the 6 year 2 month old and 9 year 6 month old samples had PC2 scores that were negative and similar in value to each other.

The components responsible for the above observations were subsequently investigated by examination of corresponding loadings data (shown in Figure 6.8b) and it was possible to pick out a number of components whose intensity levels clearly varied as a result of differences in maturation age. Components with highly negative PC1 loadings and also highly positive PC2 loadings were found to be most intense within the whisky sample matured for the shortest amount of time (3 years and 5 months). Examination of the top left hand quadrant of the loadings plot therefore enabled components to be identified that decreased in intensity as maturation time lengthened (in this case from approximately 3 to 12 years). A compound that eluted at a retention time of 8.43 minutes with a mass of 283.2643

was one notable example of such a component. The trend plot for this compound, comparing its intensity over the four samples incorporated within Subset 'B', has been provided in Figure 6.9 to illustrate how the level of this component gradually decreased as maturation age increased. This same pattern was also observed for a number of other components within the top left hand quadrant of the loadings plot and so these data could indicate that compounds have been detected that are being used up in reactions occurring during the maturation process.

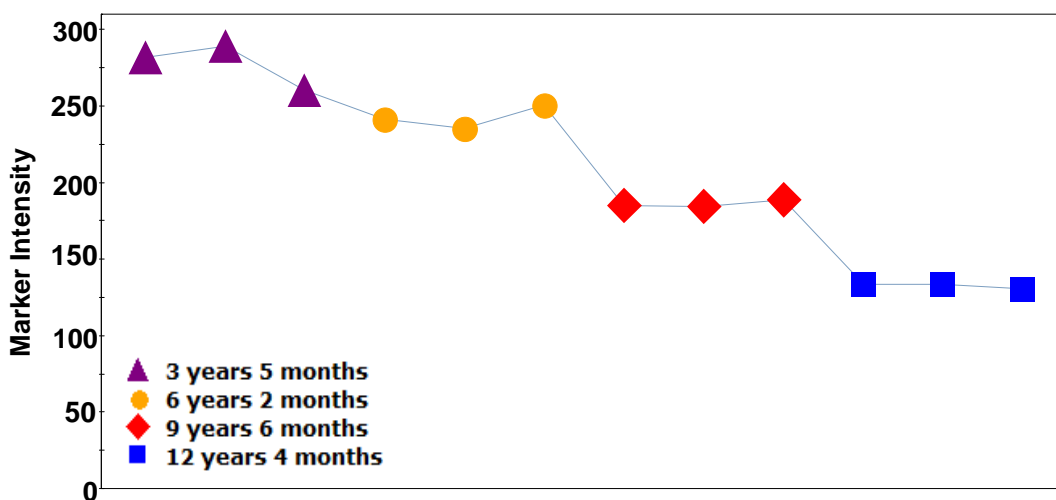


Figure 6.9: Trend plot of the component with retention time of 8.43 minutes and a mass of 283.2643 showing its intensity across the four samples contained within Subset 'B'. Triplicate data included for each sample.

In addition to finding components that gradually decreased in intensity as maturation age increased, compounds were detected within the loadings data that clearly increased over time (typically found within the bottom right hand quadrant of the loadings plot). These components could therefore be reaction products that are forming during maturation, in this case under the cask conditions covered by the four samples assessed within Subset 'B'. The most notable component found to increase in intensity in accordance with maturation age had a retention time of 3.98 minutes and a mass of 249.1137. The trend plot for this compound has been included within Figure 6.10 to illustrate its level over the four components contained within Subset 'B'.

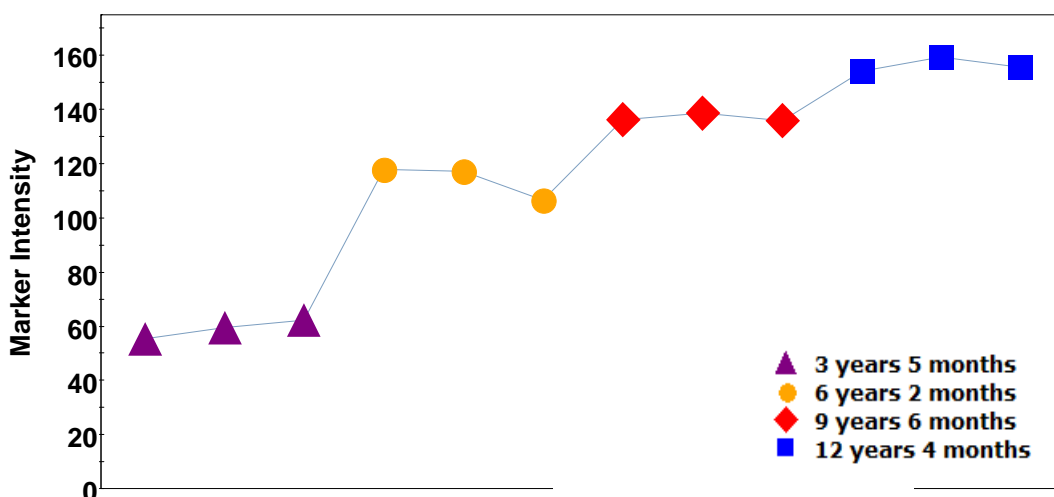


Figure 6.10: Trend plot of the component with retention time of 3.98 minutes and a mass of 249.1137 showing its intensity across the four samples contained within Subset 'B'. Triplicate data included for each sample.

A number of other interesting components were found within the loadings data (provided in Figure 6.8b) that varied in intensity as a result of differences in the maturation age of samples. Some components were found that tended to be present in high levels until reaching a particular maturation age, at which point they decreased quite sharply and levelled off. Figures 6.11 and 6.12 illustrate trend plots for two such components, each decreasing in intensity between two of the maturation ages covered by Subset 'B' and reaching a steady level. Components were also found that followed the opposite trend; i.e. they were initially present at low levels until reaching a specific maturation age, at which point their intensity increased and levelled off. These findings could potentially indicate that UPLC TOF MS could provide information about the timescale over which certain maturation reactions might occur.

Components responsible for separation along the PC2 axis of the scores plot were also investigated by examination of the corresponding loadings data and the component with the most negative PC2 loading was found to follow an interesting trend. This compound was observed at similar levels within the whisky samples of approximately 6 and 9 years old, whilst being present in the other two samples at comparably much lower levels. It therefore appeared as though this component initially increased in concentration in accordance with maturation age before reaching a steady level and then eventually decreasing in intensity. The trend plot for

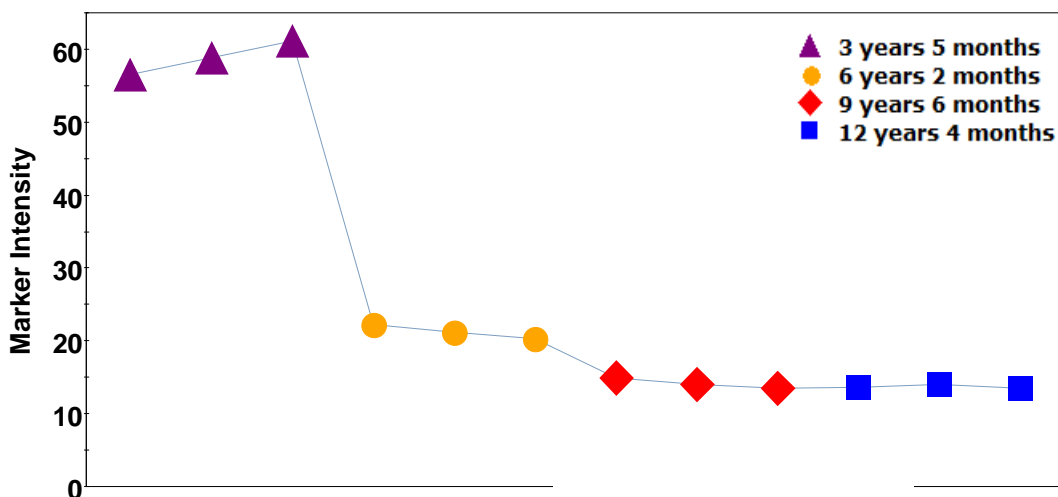


Figure 6.11: Trend plot of a component with retention time of 4.83 minutes and a mass of 197.0798 showing its intensity across the four samples contained within Subset 'B'. (Triplicate data included for each sample.) The plot demonstrates that the intensity of this component begins to level of at approximately 6 years into the maturation process.

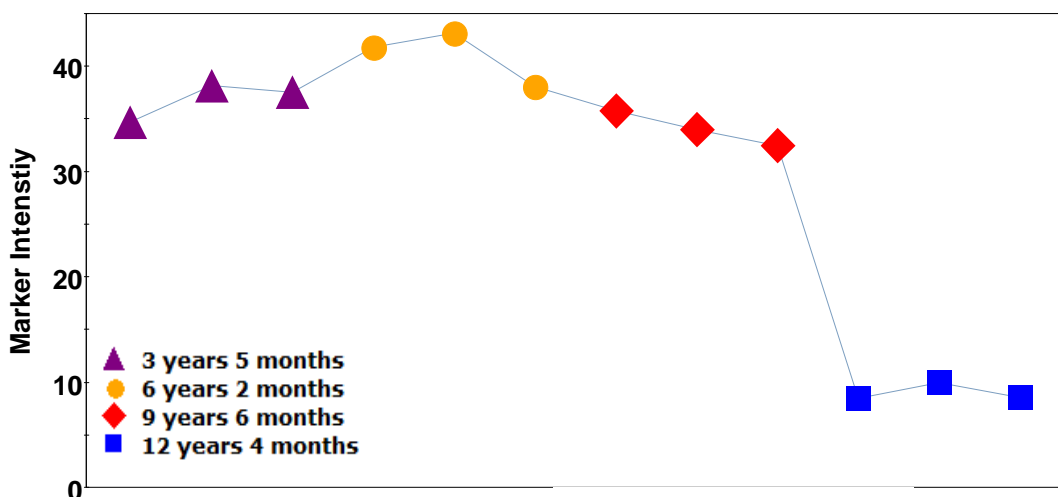


Figure 6.12: Trend plot of a component with retention time of 0.97 minutes and a mass of 187.0602 showing its intensity across the four samples contained within Subset 'B'. (Triplicate data included for each sample.) The plot demonstrates that the intensity of this component only begins to decrease after approximately 9 years of maturation.

this component has been included in Figure 6.13 to demonstrate its variation in intensity over the four samples of different maturation age. A few other components with the most negative PC2 loadings also followed this intensity pattern. In addition to this, it was found that compounds with the most positive PC2 loadings followed the opposite trend; being most intense in both the youngest and oldest maturation samples but being present at lower intensities within the middle two samples. A component with a mass of 309.2798 (retention time of 8.63 minutes) for instance, steadily decreased in intensity over the first 9 years after which point its level began

to increase again (visualised by the trend plot provided in Figure 6.14). These findings corresponded well with the positioning of samples in the scores plot.

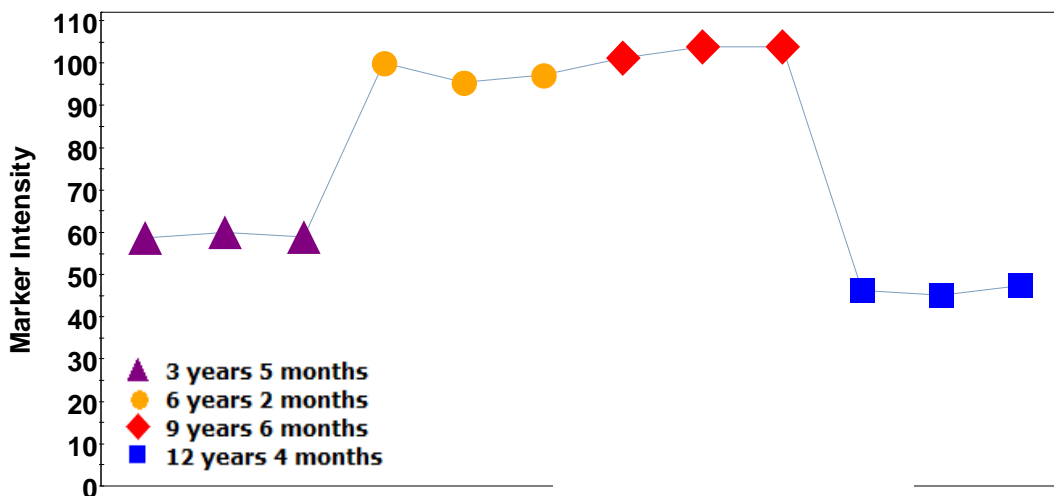


Figure 6.13: Trend plot of a component with retention time of 7.31 minutes and a mass of 323.2596 showing its intensity across the four samples contained within Subset 'B'. Triplicate data included for each sample.

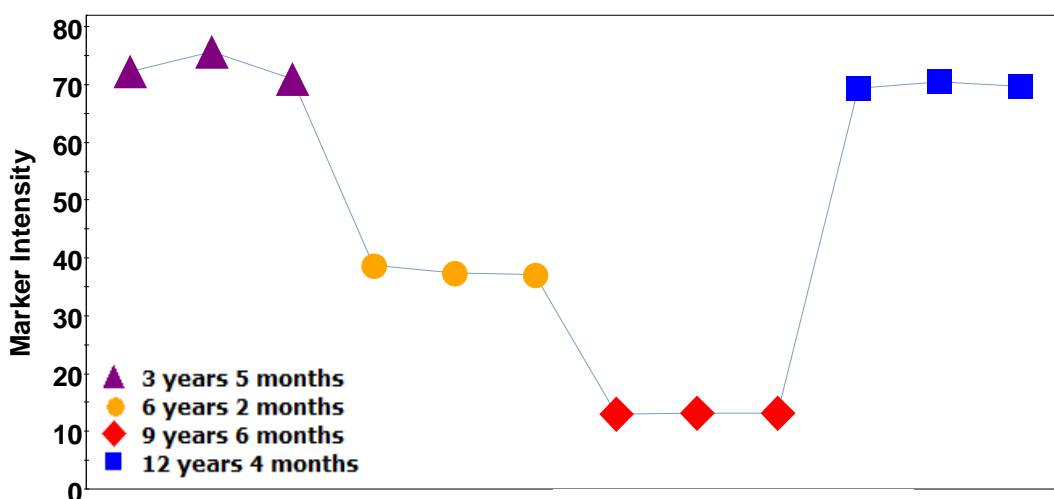


Figure 6.14: Trend plot of a component with retention time of 8.63 minutes and a mass of 309.2798 showing its intensity across the four samples contained within Subset 'B'. Triplicate data included for each sample.

When PCA was undertaken using the negative ionisation data, the findings were similar to those already described above for the positive ionisation data. The PC1 vs. PC2 scores plot acquired from the negative ionisation data has been included in Figure 6.15 for reference alongside the corresponding loadings data. As was found previously with the positive ionisation data, a clear trend was observed along the PC1 axis; in this case however PC1 scores clearly decreased as maturation age

increased. Separation of samples along the PC2 axis was also found to match the pattern previously observed when the positive ionisation data were considered. Due to the similarities of the two scores plots, it was consequently possible to identify components from the negative ionisation loadings data (Figure 6.15b) that showed similar changes in intensity (in accordance with maturation age), as those that have already been highlighted. These have not been included at this point however, as the positive ionisation data provided better examples.

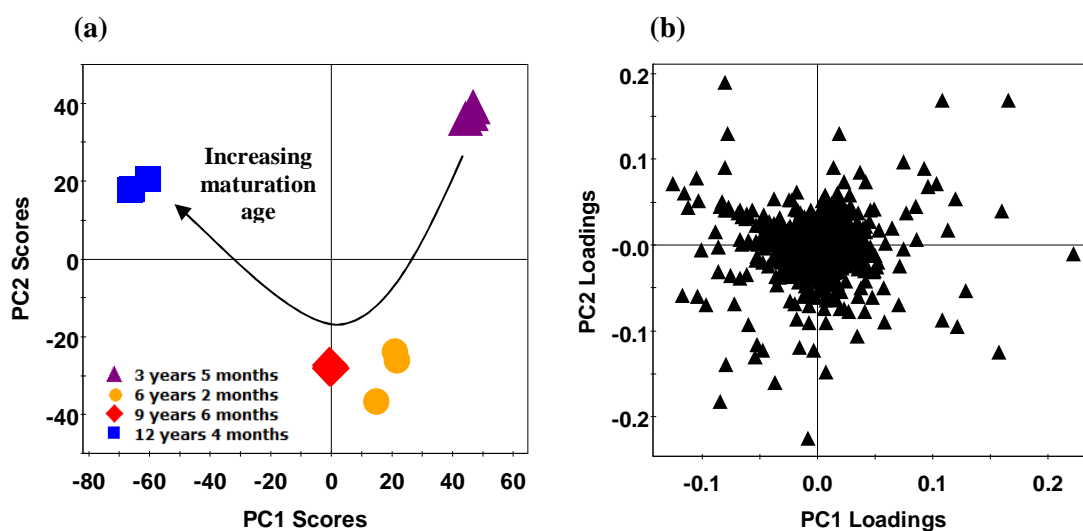


Figure 6.15: (a) PC1 vs. PC2 scores plot obtained from PCA of the negative ionisation data acquired from the four samples incorporated within Subset B. Triplicate data included for all samples. (b) Shows the corresponding (PC1 vs. PC2) loadings data.

Overall, the findings presented in this section have demonstrated that UPLC TOF MS (in combination with statistical data analysis) could be extremely beneficial as a tool to help increase knowledge of the compositional changes that occur during maturation as the time whisky spends in the cask increases. It has been possible to distinguish between samples of different maturation age and a number of components associated with this differentiation could be easily identified. Again however, it should be noted that additional batches of each sample incorporated within Subset 'B' would be required to assess the consistency of profiles. In addition, as all of the samples assessed in this piece of work were from the same cask type and acquired from the same distillery, further experiments would be required in the future to identify the applicability of UPLC TOF MS to assess compositional changes resulting from variation in maturation age under different cask conditions. It would also be interesting to analyse samples that cover maturation timescales other than the

one assessed above, to see whether information could be obtained about reactions that might occur over shorter or longer time periods.

6.3.3 Comparison of ‘Authentic’ vs. ‘Simulated’ Maturation Profiles – ‘Subset C’

The maturation process undertaken during the production of Scotch Whisky is legally required to adhere to the stipulations set out within the Scotch Whisky Regulations of 2009.¹⁹ The details of these conditions have been outlined previously in Chapter 1 (section 1.2) and part of the legislation dictates that Scotch whiskies must be matured in oak casks for a period not less than three years. This time that the spirit spends within the cask has a huge influence on the final composition of the whisky and is ultimately when the majority of important colour and flavour related components are formed. The minimum three year maturation requirement for Scotch Whisky however, is a factor that potential counterfeiters want to avoid and so it has been known for them to try and mimic the process of authentic maturation but over a significantly shorter timescale. A common way in which this has been achieved is *via* the use of solvent extracts. Such a process would typically involve the extraction of components from a piece (or pieces) of wood by having it in contact with a particular solvent, heated to a temperature close to its boiling point. The solvent material can then be evaporated off and the resulting residue dissolved in 40% ethanol. The product that is formed in this case will therefore have a similar colour to authentically matured whisky and the use of wood within the process means that an attempt has been made to simulate the composition of an authentic whisky. The common features that the simulated product might then share with one that has undergone natural maturation often makes these counterfeit samples difficult to detect and so the aim of this part of the study was to identify whether UPLC TOF MS (in combination with statistical data analysis) could potentially be used as a tool to differentiate between ‘authentic’ vs. ‘artificial’ maturation.

Sample Subset ‘C’ was the main focus of this part of the study and incorporated three different solvent extracts prepared from shavings of toasted American oak wood (for specific sample details see section 6.2.1). These samples therefore represented

examples of simulated maturation and in this work their UPLC TOF MS profiles were compared with those attained from the whisky samples contained within subsets 'A' and 'B'; both of these latter sample groupings representing cases of authentic Scotch Whisky maturation. PCA was undertaken to compare all of these samples, based on the component information extracted from the raw UPLC-MS data using MarkerLynx software. Separate models were constructed for the positive and negative ionisation datasets and it was found that the former provided slightly better results. The PC1 vs. PC2 scores plot attained from the positive ionisation data has therefore been provided in Figure 6.16 alongside its corresponding loadings data.

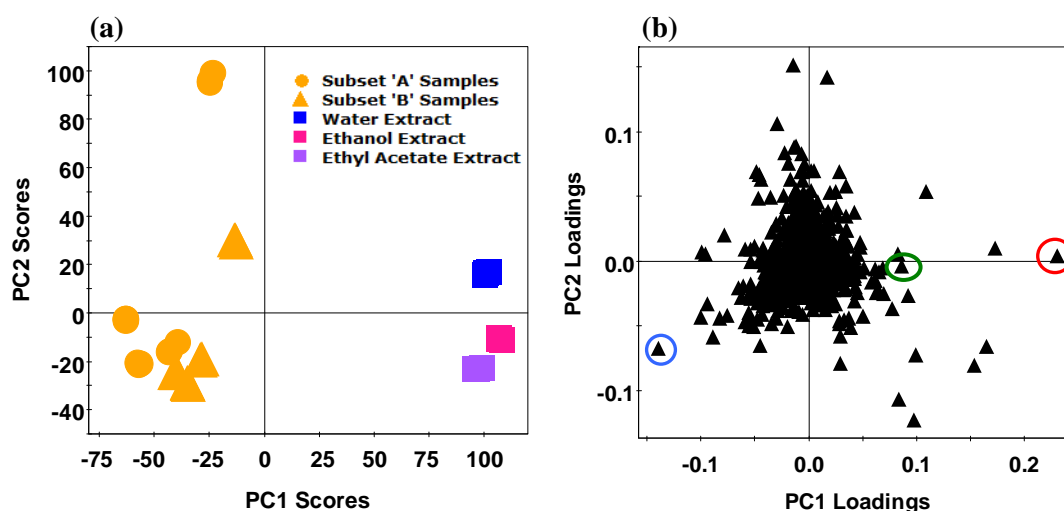


Figure 6.16: (a) PC1 vs. PC2 scores plot obtained from PCA of the positive ionisation data acquired from the samples included in Subsets 'A', 'B' and 'C', to compare the profiles obtained from authentic maturation with those of solvent extracts. Triplicate data included for all samples. (b) Shows the corresponding (PC1 vs. PC2) loadings data.

Figure 6.16a clearly demonstrated that it was possible to distinguish between authentically matured samples (ranging in their cask history and age) and solvent extracts along the PC1 axis, based on the components detected using UPLC TOF MS in positive ionisation mode. Examination of the corresponding loadings data (Figure 6.16b) subsequently allowed a selection of interesting components to be identified that were associated with this sample separation. Components with the highest PC1 loadings for instance, were found to be predominantly associated with all three of the solvent extracts, corresponding with the position of these samples on the scores plot. One of the most notable components found as being highly elevated in intensity within the solvent extracts (highlighted with a red circle in Figure 6.16b) had a mass

of 209.0822 and a retention time of 4.34 minutes. The trend plot for this component has been provided in Figure 6.17 to demonstrate its intensity across all samples from Subsets 'A – C'. Another interesting observation taken from this trend plot was that this particular component, although comparably much lower in the authentically matured samples, was present at the next highest level within the sample matured for the longest time (12 years and 4 months). This indicated a component that if extracted *via* authentic maturation would take many years to form but whose extraction was clearly significantly accelerated under the stronger conditions of the simulated maturation process being addressed. A number of other components with high PC1 loadings followed similar intensity patterns and the trend plot of the component highlighted with a green circle in the loadings data has been provided in Figure 6.18 as another example. Although the trend plots of other similar components have not been included, the exact mass and retention time (RT) details of the most influential compounds have been given as follows: component with a mass of 179.0715 (RT of 4.37 minutes); compound with a mass of 249.1132 (RT of 4.84 minutes); component with a mass of 213.0770 (RT of 3.95 minutes); and a compound with mass of 183.0666 (RT of 4.12).

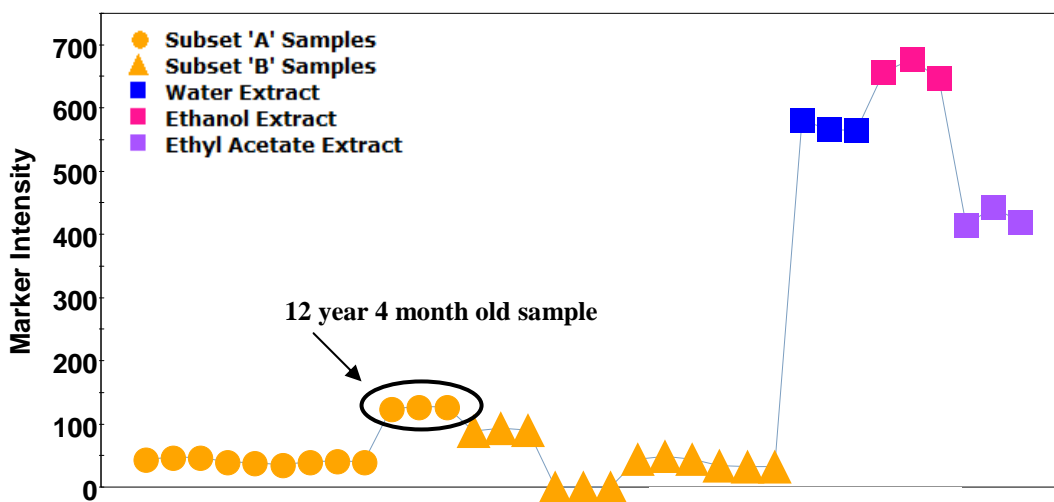


Figure 6.17: Trend plot of a component with retention time of 4.34 minutes and a mass of 209.0822 showing its intensity across the samples contained within Subsets 'A – C'. Triplicate measurements included for each sample.

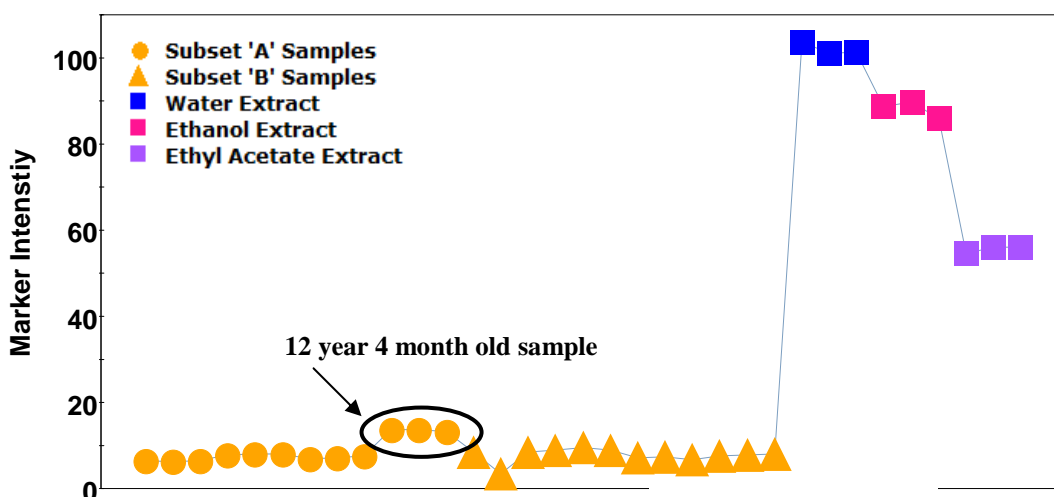


Figure 6.18: Trend plot of a component with retention time of 3.87 minutes and a mass of 227.0925 showing its intensity across the samples contained within Subsets 'A - C'. Triplicate measurements included for each sample.

As well as the presence of components that were highly elevated within the three solvent extracts, it was also possible to identify compounds from the loadings data that were present within all of the authentically matured samples, whilst being absent from (or present in considerably lower levels within) those that were artificially matured. Such components had highly negative PC1 loadings and the most notable compound showing this intensity pattern has been highlighted with a blue circle within Figure 6.16b. The trend plot for this component, showing its intensity over all samples within Subsets 'A - C', has also been provided in Figure 6.19. On closer inspection it turned out that this component (with mass of 283.2643 and RT of 8.43 minutes) had already been picked out as an interesting marker in a previous section of this Chapter; being found to gradually decrease in intensity as maturation age increased within a first fill bourbon cask (Figure 6.9). Other components with highly negative PC1 loadings that followed the same intensity pattern as this component included: a compound with a mass of 201.1861 (RT of 7.20 minutes); a component with a mass of 311.2950 (RT of 9.11 minutes); a compound with a mass of 307.2645 (RT of 8.20); and a component with mass of 229.2173 (RT of 7.74 minutes).

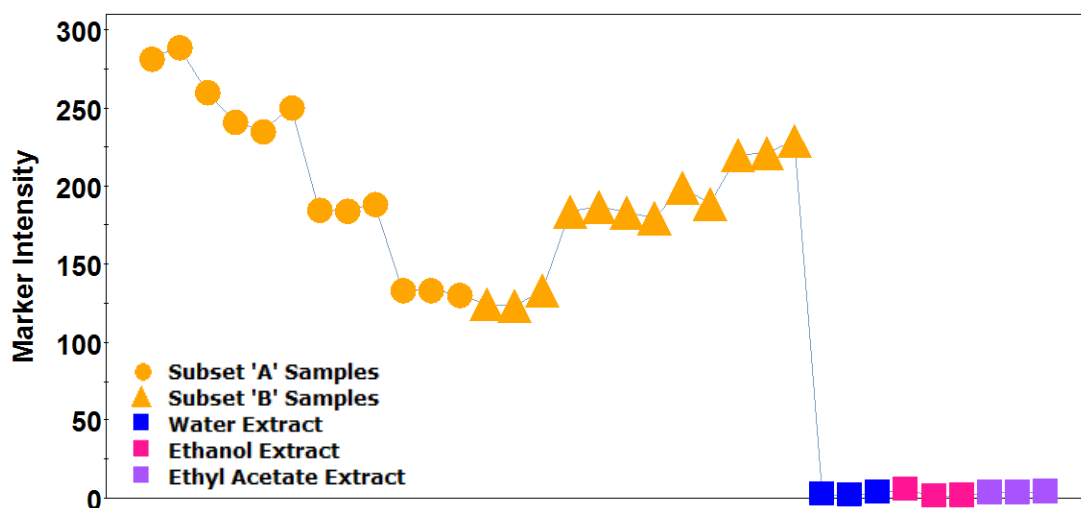


Figure 6.19: Trend plot of a component with retention time of 8.43 minutes and a mass of 283.2643 showing its intensity across the samples contained within Subsets 'A – C'. Triplicate measurements included for each sample.

The PC1 vs. PC2 scores plot acquired from the negative ionisation data has been provided in Figure 6.20a and it showed very similar separation along the PC1 axis as was observed previously for the positive ionisation dataset. Examination of the corresponding loadings data (Figure 6.20b) therefore allowed the identification of some components that were highly elevated within the solvent extracts and some compounds that were present within the authentically matured samples but generally absent from the samples of simulated maturation or present at comparably low levels. The details of these components have not been discussed at this point however, as the positive ionisation data provided better examples for the purposes of this preliminary study.

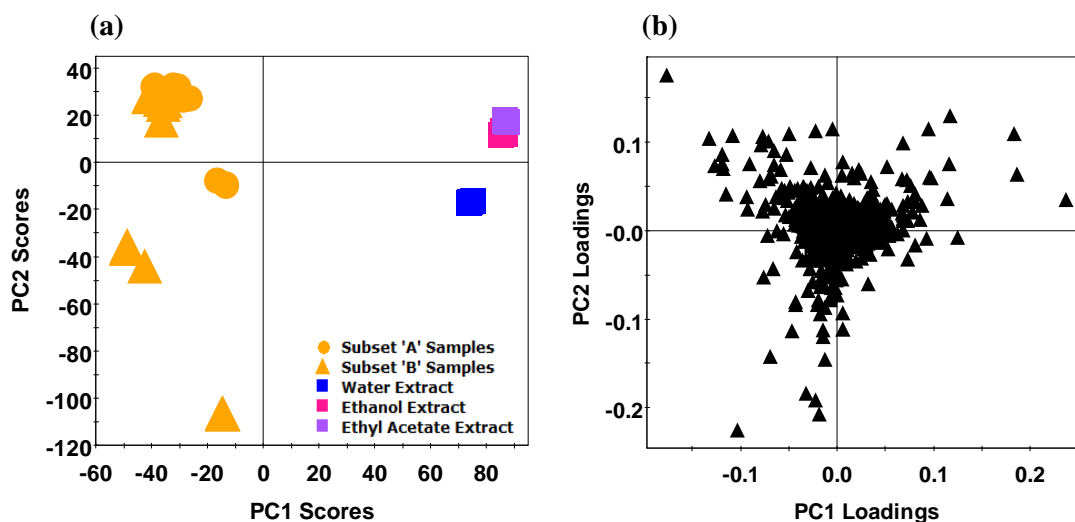


Figure 6.20: (a) PC1 vs. PC2 scores plot obtained from PCA of the negative ionisation data acquired from the samples included in Subsets 'A', 'B' and 'C', to compare the profiles obtained from authentic maturation with those of solvent extracts. Triplicate data included for all samples. (b) Shows the corresponding (PC1 vs. PC2) loadings data.

Overall this study has demonstrated that UPLC TOF MS (in combination with statistical data analysis) has the potential to distinguish between products that have been authentically matured within oak casks and samples that have been artificially matured with the use of solvents to extract components from wood shavings. Particular components responsible for the differences observed in the profiles could also be identified and so UPLC TOF MS would be an extremely useful tool both to identify cases of simulated maturation and also to allow a greater understanding of the processes occurring during maturation (both natural and simulated). Additional batches of the solvent extracts would be required to confirm the consistency of UPLC TOF MS profiles and future experiments would also be required to assess the effect of changing extraction method parameters on the resultant simulated maturation profiles (e.g. changing the type/quantity of wood or the timescale of the extraction process). Details of the extraction procedure used in this work can be found in section 6.2.1.1. Future work would also be required to ensure that any marker components identified would show consistent trends for cases of natural maturation that have not been covered by the samples incorporated within Subsets 'A' and 'B'. The samples from the former subset only covered whiskies of different cask history from a single distillery and the samples from the latter only covered a particular range of maturation ages for a single cask type.

6.3.4 Detecting common adulterants and understanding the affect of fade

The work completed within this part of the study assessed the samples of Subset 'D', which incorporated five samples of a particular blend (Blend C) that had been subjected to different conditions. Three of the samples had each been spiked with one of the following common adulterants: vanillin at 50 ppm; sucrose at 2000 ppm; and methanol at 6000 ppm. Compared to the levels that would naturally be observed in Scotch whiskies, these concentrations represented elevated amounts; such high levels often being indicative of a counterfeit whisky. Another sample within this subset had been forcibly faded to 25% of its original colour to see what affect this might have on whisky profiles and also whether any information could be obtained about the fading process. The remaining sample within Subset 'D' was one of Blend C that had been unaltered and was included for comparison purposes. After UPLC TOF MS analysis and extraction of component information using MarkerLynx software, the five samples were compared using PCA; separate models being constructed for the negative and positive ionisation data. The PC1 vs. PC2 scores plot acquired from the negative ionisation data has been included within Figure 6.21 alongside the corresponding loadings data.

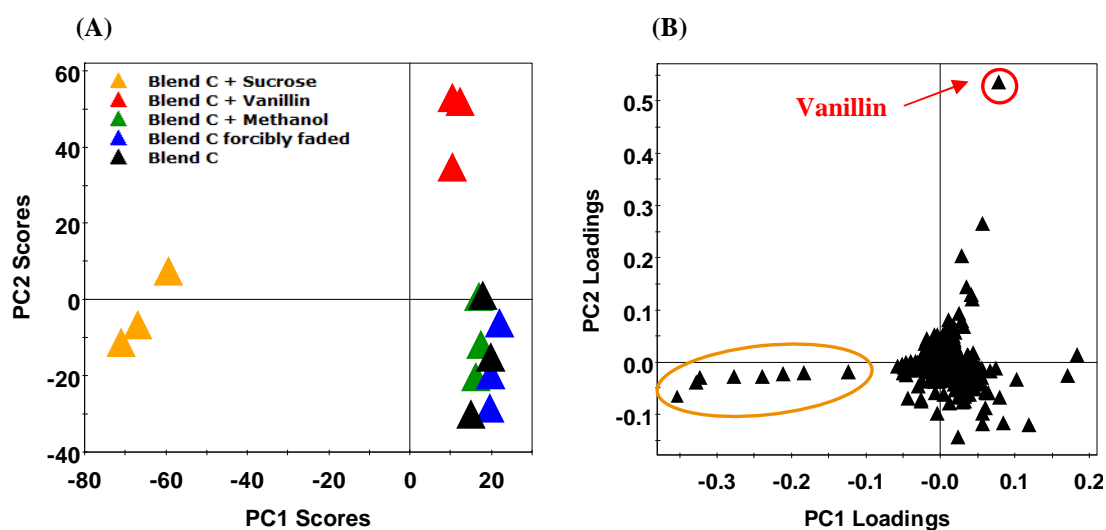


Figure 6.21: (A) PC1 vs. PC2 scores plot obtained from PCA of the negative ionisation data acquired from the five samples incorporated within Subset 'D'. Triplicate measurements included for all samples. (B) Shows the corresponding (PC1 vs. PC2) loadings data.

Figure 6.21a demonstrated that the samples of Blend C spiked with either vanillin or sucrose could be clearly distinguished from the unaltered blend, indicating the ability of UPLC TOF MS to monitor for the presence of these two components at elevated

levels in Scotch Whisky. Vanillin was easily identified within the corresponding loadings data (Figure 6.21b) and has been highlighted within a red circle. The trend plot obtained for this compound has been provided in Figure 6.22 and clearly showed the elevated concentration of vanillin within the spiked sample. It was also clear from this plot that UPLC TOF MS was sensitive enough to detect vanillin at its natural level within Blend C; with comparably lower but consistent intensities being observed within the four other samples assessed.

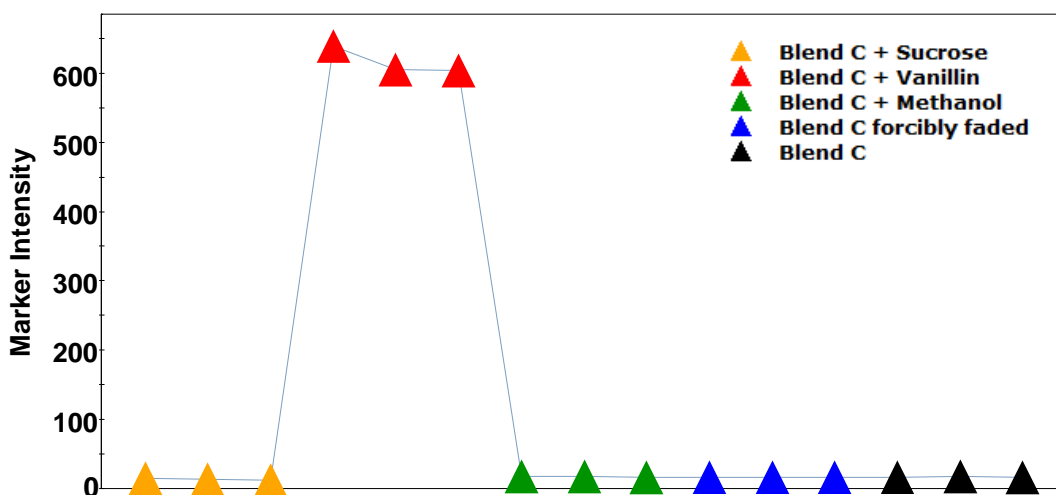


Figure 6.22: Trend plot of vanillin (mass of 151.0392 under negative ionisation) eluting with a retention time of 4.10 minutes, showing its intensity across the four samples contained within Subset 'D'. Triplicate measurements included for all samples.

Although the sucrose spiked blend was also clearly distinct within the scores plot, sucrose itself was a little more difficult to pick out from the loadings data. As can be seen from Figure 6.21b, a number of components appeared to be characteristic of the Blend C sample containing added sucrose (highlighted within an orange ellipse). Slightly unexpectedly, two of these components were found to have a mass that matched sucrose and so one hypothesis was that different conformations of sucrose were being detected (as nothing else was added to the sample other than sucrose). When the trend plots for these two components were compared however (Figure 6.23), the findings were quite difficult to explain. One of the components was found to be completely absent from the remaining samples and this was the expected trend for sucrose; Aylott and MacKenzie describing that it should generally be absent within typical Scotch whiskies.²⁰ The other component with the same mass however, appeared naturally at much higher levels and it was unclear as to why this was –

unless something has been formed (with the same mass) that also appears naturally in blends (potentially from E150a as on closer inspection this component had previously been highlighted as a marker for this caramel class (see Table 5.3)). Due to the difficulties in explaining this finding, it would be very interesting at this point to repeat the analysis of these samples to see if the observations remained consistent. One other possible explanation could be that something has occurred as a result of the particular instrumentation (or data analysis parameters) implemented, as this behaviour of sucrose appeared very unusual. For instance it may be the case that during chromatography, sucrose has eluted over a slightly broader timescale than would typically be expected using this instrumentation and so would be picked up as two separate components by the MarkerLynx software due to the narrow retention time window set for component extraction (see section 6.2 for settings). It could therefore just be a coincidence that one of the points picked up above happened to occur at the same retention time as something naturally present within blends (potentially originating from the E150a caramel) that is not sucrose but has exactly the same mass. Some of the other components found within the orange ellipse were much easier to tentatively identify: one appeared to be a dimer of sucrose, being exactly double in mass; and two others looked like adducts formed during the ionisation process, their masses being 45 units larger than the two ‘sucrose’ compounds and so potentially indicating $[M + \text{HCOO}]^-$.

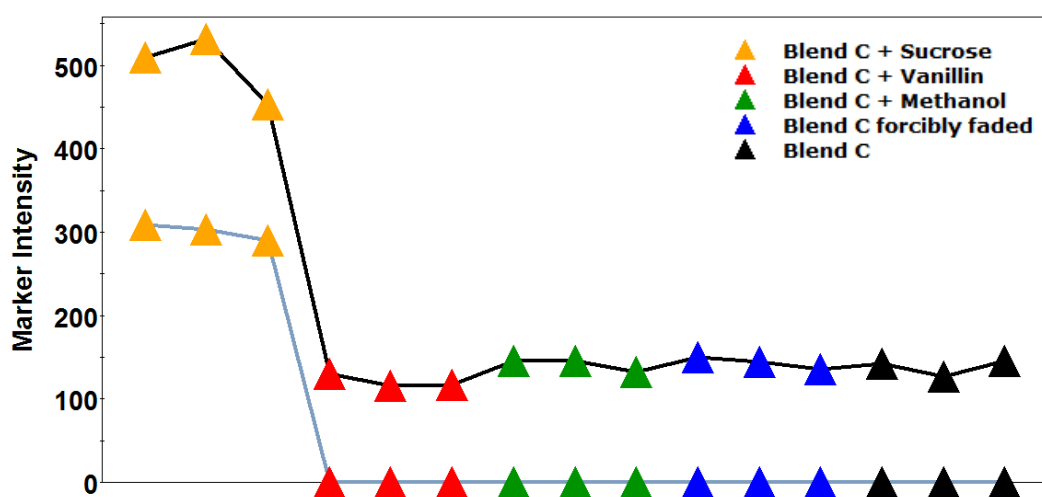


Figure 6.23: Trend plot showing the intensity levels of two components across the samples incorporated by Subset ‘D’. The component where samples are linked with a black line had a mass of 341.1084 and a retention time of 1.02 minutes, whilst the component where samples are linked with a pale blue line had a mass of 341.1085 and a retention time of 1.11 minutes. Triplicate measurements of each sample are included.

The data depicted by Figure 6.21a also demonstrated that the UPLC TOF MS profile of Blend C was unaffected by the process of fade in this case, the faded and the unaltered Blend C samples overlaying within the same region of the scores plot. This could be very useful information to the industry as it would mean that analyses with this technique, if carried out in negative ionisation mode, could be undertaken without having to account for the fading process as a potential means of compositional variation. Further work would be required however to confirm whether this finding would be true for other blend matrices and for higher levels of fade. The negative ionisation data also demonstrated that Blend C spiked with high levels of methanol could not be distinguished. This was not surprising however as it is likely that any excess methanol would have eluted in the solvent front (removed for the purposes of data analysis) and also the low mass of the compound would not have been detected within the mass range set within this experimental work. The same results were therefore encountered when positive ionisation data were considered; the blend spiked with methanol could not be distinguished from the unaltered blend using UPLC TOF MS.

The PC1 vs. PC2 scores plot attained from the positive ionisation data has been included in Figure 6.24 alongside corresponding loadings data. As with the negative ionisation data, elevated levels of vanillin were easily detected, however in this case high levels of added sucrose were not observed. The latter finding indicated that sucrose was not well suited for ionisation under the positive mode. Another key difference observed from the positive ionisation scores plot was that the sample of Blend C faded by a factor of 25% could now be separated from the remaining samples. This indicated that, whilst negative ionisation mode could be used for analysis free from the influence of fade, positive ionisation mode could potentially be used as an investigative tool to find out more about the components and reactions involved with the fading process of whisky. This was investigated for Blend C by examination of the loadings data provided in Figure 6.24b, from which a number of interesting components could be identified that were clearly related to the fading process. Components with the most positive PC2 scores were found to provide the most information, being found in significantly reduced levels within the faded

whisky compared to the other four Blend C samples. These could therefore represent components that have been broken down or degraded as a result of the fading process. The most notable compound that followed this intensity pattern had a mass of 249.1137 (retention time of 3.98 minutes) and its trend plot has been provided in Figure 6.25 to demonstrate this finding. Other components found to follow a similar trend (all of which had high positive PC2 loadings) were: a compound with a mass of 323.2596 (RT of 7.31 minutes); a component with a mass of 193.0507 (RT of 4.18 minutes); a component with a mass of 209.0822 (RT of 4.34 minutes); and a component with mass of 459.1421 (RT of 3.98 minutes).

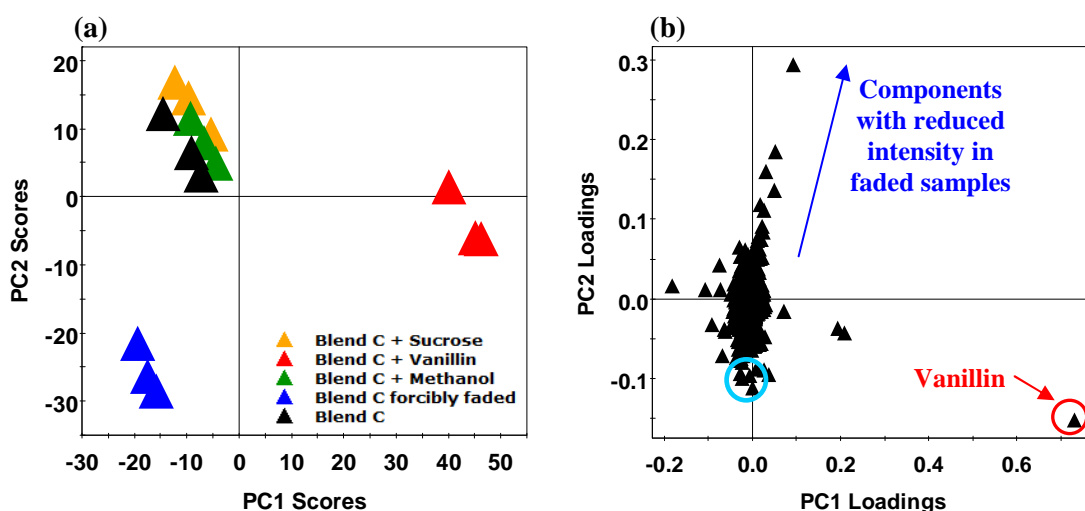


Figure 6.24: (a) PC1 vs. PC2 scores plot obtained from PCA of the negative ionisation data acquired from the five samples incorporated within Subset 'D'. Triplicate measurements included for all samples. (b) Shows the corresponding (PC1 vs. PC2) loadings data.

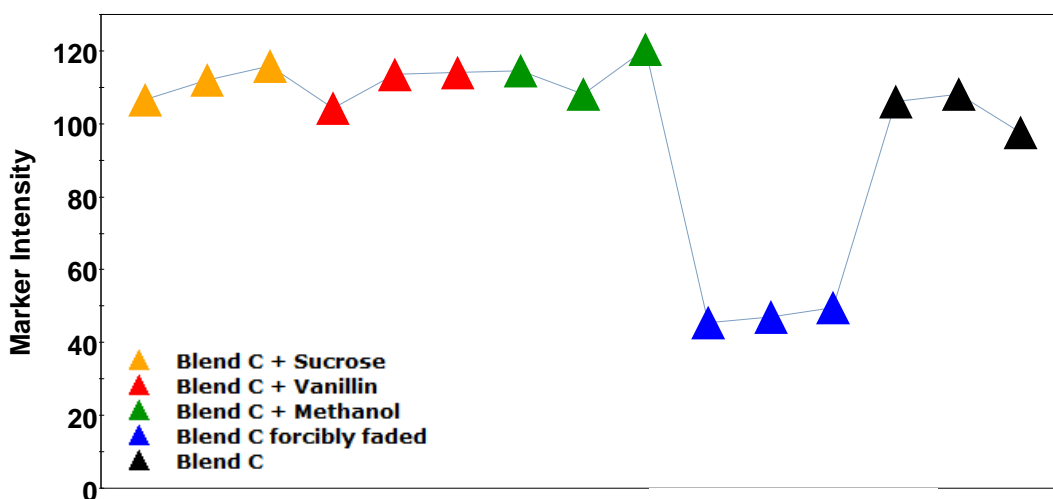


Figure 6.25: Trend plot of a component with retention time of 3.98 minutes and a mass of 249.1137 showing its intensity across the samples contained within Subset 'D'. Triplicate measurements included for each sample.

As well as the presence of components that were clearly reduced in intensity as a result of the fading process, it was also possible to find a few compounds from the loadings data that were present in higher levels within the faded whisky compared to the four other Blend C samples. These components had the most negative PC2 loadings (encircled in pale blue within Figure 6.24b) and could potentially represent products forming as a result of degradation reactions relating to fade; it should also be noted here though, that these compounds were present in quite low levels and already had low intensities prior to any fade. One such component had a mass of 141.0552 and a retention time of 4.52 minutes and its trend plot has been provided in Figure 6.26 for reference.

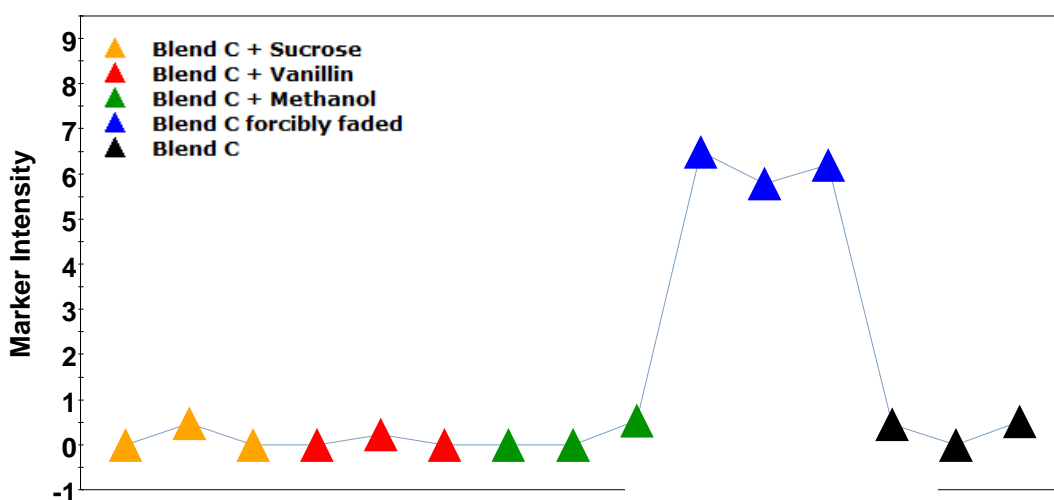


Figure 6.26: Trend plot of a component with retention time of 4.52 minutes and a mass of 141.0552 showing its intensity across the samples contained within Subset 'D'. Triplicate measurements included for each sample.

Overall, the positive ionisation data indicated that UPLC TOF MS could be useful as a tool to increase knowledge of the fading process that can occur to Scotch whiskies. Using Blend C as an example, a number of components could be identified that either decreased or increased in intensity as a result of the fading process. It should also be noted here though, that this does not mean that all components related to the fading process have been detected using UPLC TOF MS, as some may have been missed if they are not easily ionised under the conditions employed. Future experiments implementing additional batches of faded vs. non faded samples of Blend C would also be required to determine whether consistent results would be obtained to those of the preliminary study described above. It would also be

important to assess the fading process in relation to other blend products to see whether similar components remain responsible for sample distinction. In addition to this, as the samples analysed in this part of the study were of a caramel containing blend, it is currently unclear as to whether the components being detected originated from the spirit itself or from the E150a caramel. It would therefore be interesting in the future to profile (a) faded E150a caramel samples dissolved in 40% ethanol and (b) faded whiskies containing no caramel, to see how the composition of each would change individually as a result of fade.

6.3.5 Blend Discrimination – ‘Subset E’

Subset ‘E’ was included within this study to get an idea as to whether UPLC TOF MS had the potential to discriminate between different whiskies on the market, and so be used as a tool to understand more about the compositional differences between these products. A selection of seven blends and one malt whisky were analysed as part of this work and their UPLC TOF MS profiles were compared using PCA; based on the component information extracted using MarkerLynx software. The PC1 vs. PC2 scores plots constructed separately from the negative and positive ionisation data have been provided in Figures 6.27a and 6.27b respectively.

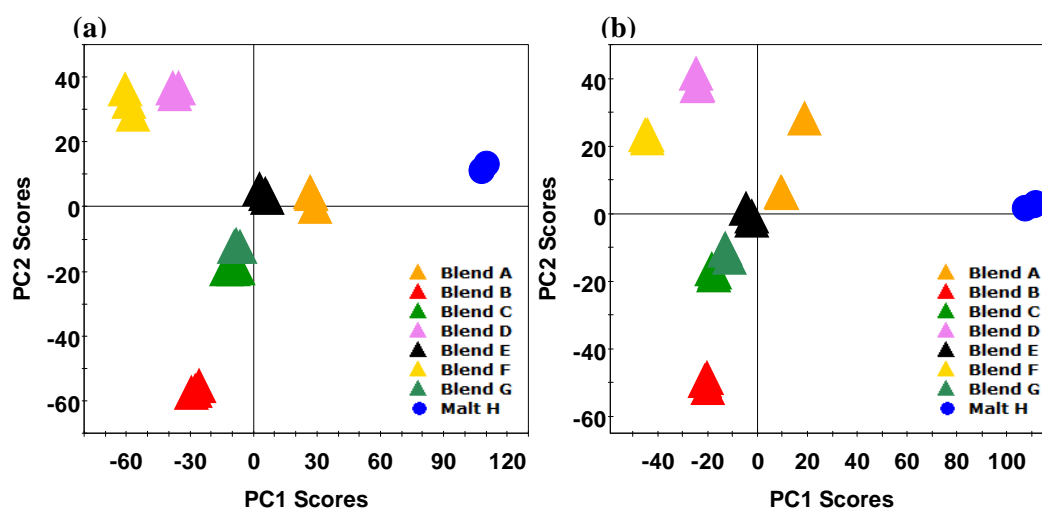


Figure 6.27: PC1 vs. PC2 scores plots obtained from PCA of all samples from Subset ‘E’ using (a) negative and (b) positive ionisation data. Triplicate measurements included for all samples.

Both scores plots showed very similar patterns of separation and the clearest distinction between the samples occurred along the PC1 axis, where the malt was

clearly separated from all blends. Corresponding loadings data were subsequently examined to identify which components were responsible for this observation; only the information acquired from the negative ionisation data will be discussed at this point however, as it provided better examples for the purposes of this preliminary study. The loadings plot acquired from the negative ionisation data has therefore been provided in Figure 6.28 and it was found that components with the highest PC1 loadings were predominantly associated with Malt H.

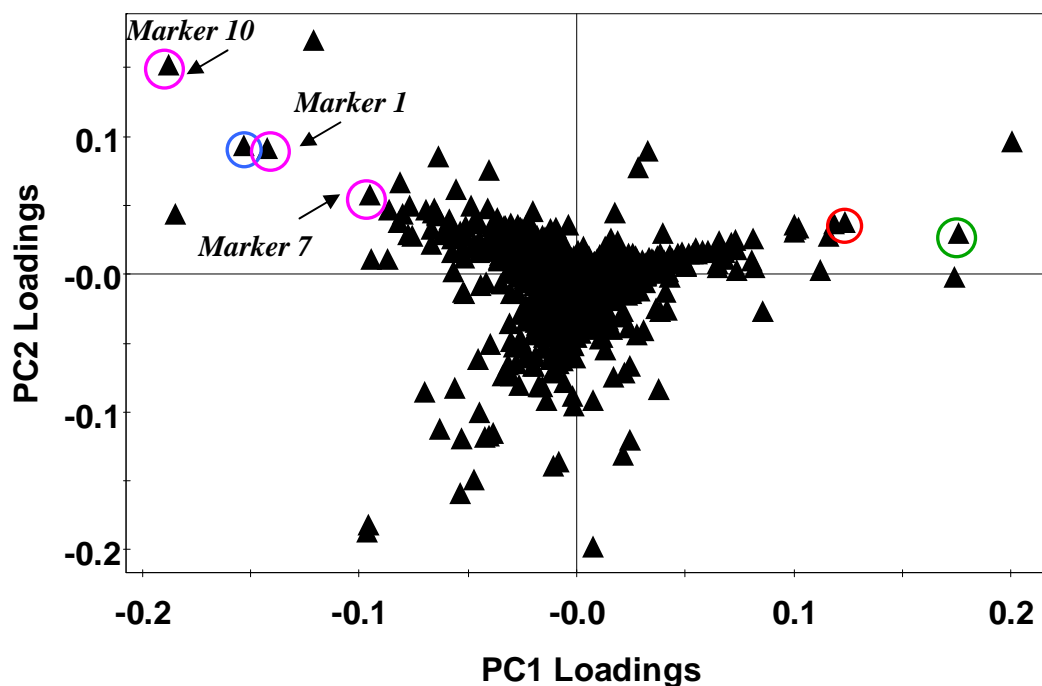


Figure 6.28: PC1 vs. PC2 loadings plot obtained from PCA of the negative ionisation data acquired from the samples incorporated within Subset ‘E’. The marker numbers that label the pink circled components refer to the compounds contained within Table 5.3 in Chapter 5.

One of the most notable components characteristic of Malt H has been highlighted within a red circle in Figure 6.28. The mass of this compound was 363.1112 (retention time of 4.18 minutes) and its trend plot has been provided in Figure 6.29, to demonstrate its intensity across the samples included within Subset ‘E’. It was clear from the trend plot that this component was present in much higher levels within Malt H than in any of the seven blend products. On closer inspection it turned out that this particular component had already been picked out as an interesting marker within this Chapter; being primarily associated with the first fill sherry cask sample compared to the casks of other history (see section 6.3.1). When background

information on Malt H was investigated, the whisky was identified as being a Macallan product; supporting why this ‘sherry cask marker’ was able to help distinguish the malt, as this brand of whisky is known to typically contain a high degree of spirit from sherry casks. In further accordance with this finding, when the loadings data were examined in more detail, it was also determined that the majority of components previously identified as being associated with sherry casks clearly influenced the separation of Malt H along the PC1 axis. The components with masses of 149.0103, 385.2228, 455.3158 and 517.3160 were all found to have PC1 loadings close to or higher than a value of 0.1. As well as these components, a number of additional compounds were present that helped to distinguish Malt H from the seven blends. One example (encircled in green within Figure 6.28) had a mass of 124.9907 (RT of 1.29 minutes) and its trend plot has been provided in Figure 6.30 to demonstrate its comparably high intensity within Malt H compared to the seven blends. Although not previously included as a component characteristic of sherry casks, on closer inspection the level of this compound again appeared to be much higher in the two sherry cask samples within subset ‘A’ than in the two bourbon cask samples. This again highlighted that a large number of the components allowing Malt H to be distinguished from the blends originated from it containing high levels of whisky from sherry casks.

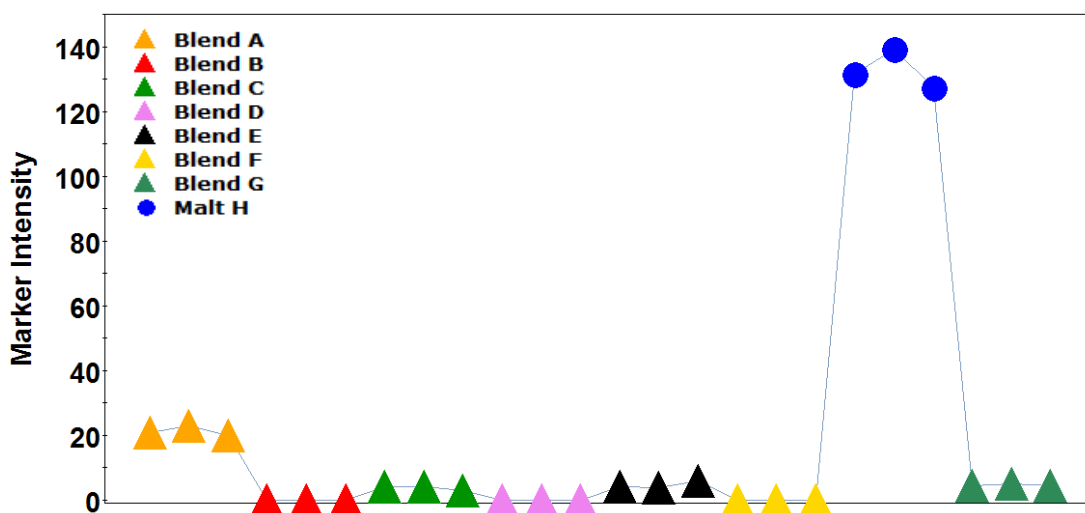


Figure 6.29: Trend plot of a component with retention time of 4.18 minutes and a mass of 363.1112 showing its intensity across the blends and malt contained within Subset ‘E’. Triplicate measurements included for each sample.

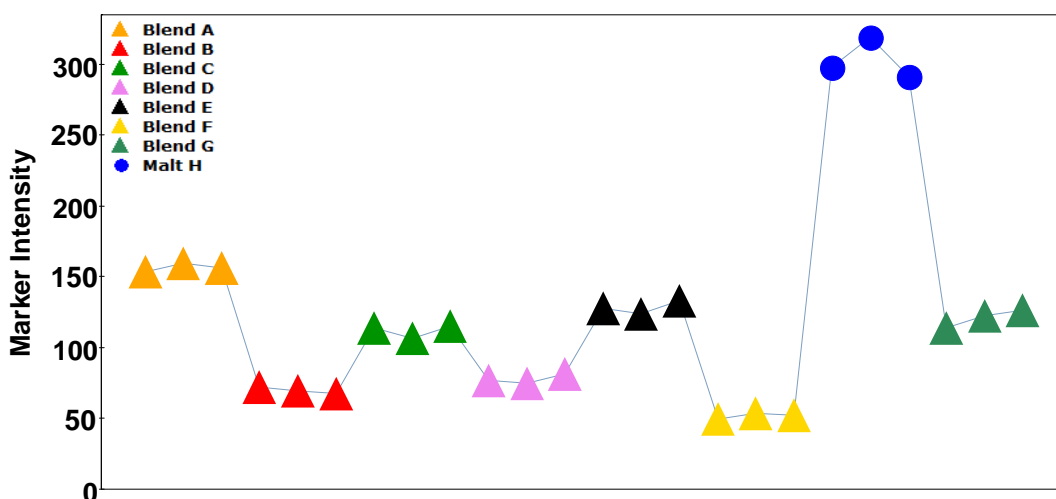


Figure 6.30: Trend plot of a component with retention time of 1.29 minutes and a mass of 124.9907 showing its intensity across the blends and malt contained within Subset 'E'. Triplicate measurements included for each sample.

As well as the presence of components present in high levels within Malt H, it was also possible to identify compounds from the loadings data that were high in all of the blends but either absent or present in significantly lower levels within Malt H. These components all had highly negative PC2 scores and the component encircled in blue within Figure 6.28 provided a good example. The trend plot for this compound – including its mass and retention time details – has been provided in Figure 6.31 to demonstrate its presence within all blend products but its near complete absence from the malt. When investigated in more detail, the fact that this component stood out was really interesting, as it had already been highlighted within Chapter 5 as a marker characteristic of all E150a caramels assessed (see section 5.4.1.1 – Table 5.3). When the loadings plot was assessed further, a number of other components previously identified as markers of E150a caramel were clearly found to influence the separation along PC1 between the seven blends and the malt. These components included the markers 1, 7 and 10 (numbered according to Table 5.3) and each has been encircled in pink within Figure 6.28 and labelled. As well as these data indicating that the presence of E150a caramel can be detected within real blends on the market (using marker components detected by UPLC TOF MS), blend products could potentially be differentiated from malts based on markers originating from (and unique to) E150a caramel.

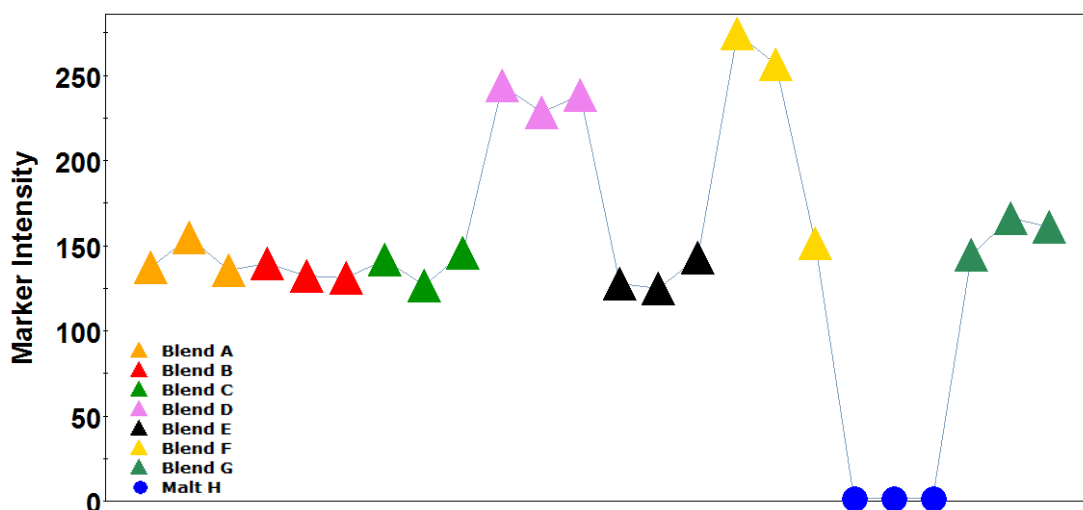


Figure 6.31: Trend plot of a component with retention time of 1.02 minutes and a mass of 341.1084 showing its intensity across the blends and malt contained within Subset 'E'. Triplicate measurements included for each sample.

The scores plot previously depicted in Figure 6.27a demonstrated that as well as the potential to differentiate all blends from the malt, there was also a certain degree of separation between the seven different blend products included in Subset 'E'. These compositional differences were slightly easier to interpret by removing Malt H from the PCA model and the new PC1 vs. PC2 scores plot attained has been provided in Figure 6.32 alongside the corresponding loadings data.

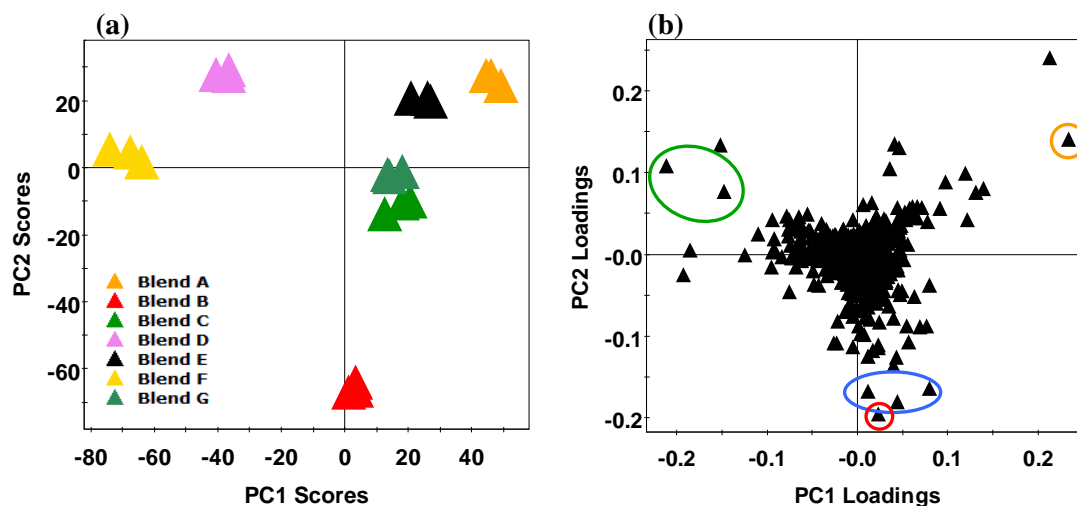


Figure 6.32: (a) PC1 vs. PC2 scores plot obtained from PCA of the negative ionisation data acquired from only the seven blends contained within Subset 'E'. Triplicate measurements included for all samples. (b) Shows the corresponding (PC1 vs. PC2) loadings data.

Blend B was shown to be the most distinct within Figure 6.32a and examination of the corresponding loadings data (Figure 6.32b) enabled the components responsible

for this observation to be investigated. Components present at the highest intensity levels within Blend B had the most negative PC2 loadings and one of the clearest examples has been highlighted by a red circle within Figure 6.32b. This component had a mass of 373.2590 (retention time of 5.97 minutes) and its trend plot has been provided in Figure 6.33 to show its intensity across the seven blends. The trend plot demonstrated that although this component was common to all blends, it was present at its highest level within Blend B. The components encircled in blue within Figure 6.32b were also found to be present at their highest levels within Blend B and had masses of 197.0447 (RT of 4.10 minutes), 297.2430 (RT of 6.85 minutes) and 515.2126 (RT of 5.11 minutes). On closer inspection, the middle of these three components was identified as one previously picked out in section 6.3.1; being common to the first fill and refilled bourbon casks as well as the refilled sherry cask of Subset 'A'. This pattern of intensities within the Subset 'A' samples was also observed for the above component of mass 373.2590 as well. The component of mass 515.2126 was also quite interesting; being primarily associated with both first fill and refilled bourbon casks and present only at extremely low levels if at all within in the two sherry cask samples. These observations indicated that non volatile cask congeners detected by UPLC TOF MS could be useful markers to investigate compositional differences between different blend products.

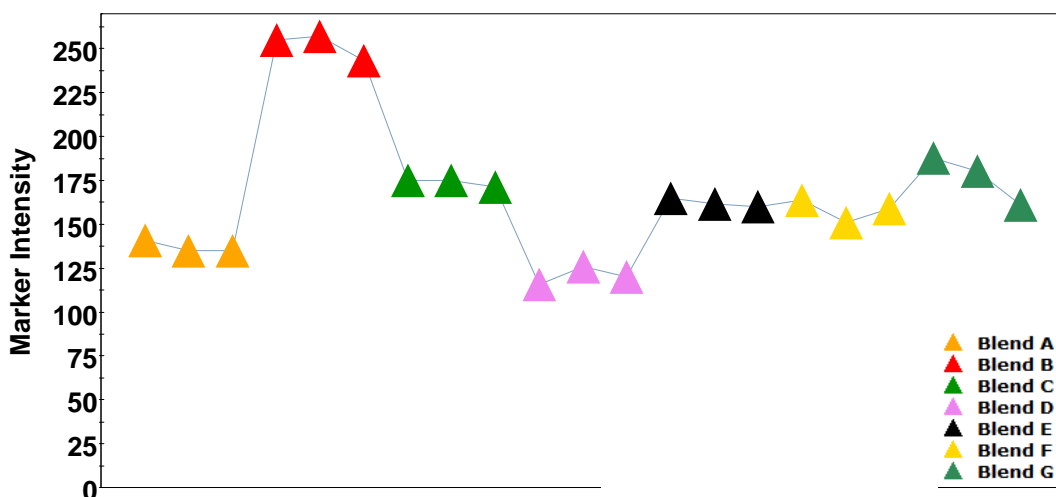


Figure 6.33: Trend plot of a component with retention time of 5.97 minutes and a mass of 373.2590 showing its intensity across the seven blends contained within Subset 'E'. Triplicate measurements included for each sample.

Examination of the loadings data in Figure 6.32b also allowed components present in higher levels within Blends D and F to be found; these two samples both appearing quite close together in the top left hand quadrant of the corresponding scores plot (Figure 6.32a). Two such components (encircled in green in Figure 6.32b) were those that had been previously highlighted as being characteristic of E150a caramel: 179.0553 and 341.1084. The trend plot for the latter has therefore been included previously in Figure 6.31 whilst the trend plot for the former is now provided in Figure 6.34. Both plots demonstrated that these components are clearly most intense within Blends D and F. Such findings could therefore indicate that these two blends contain the highest amounts of E150a caramel and that this is the primary parameter that distinguishes them from the other blends.

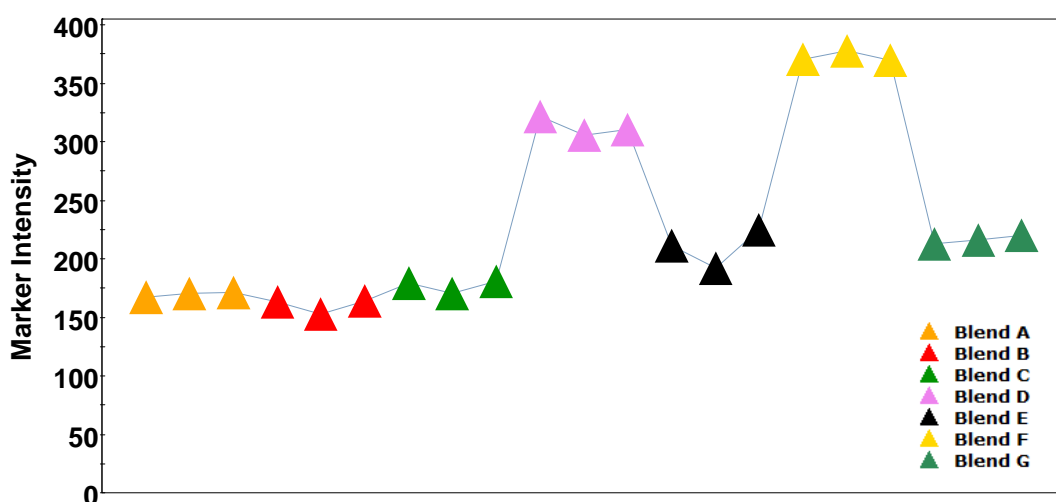


Figure 6.34: Trend plot of a component with retention time of 1.01 minutes and a mass of 179.0553 showing its intensity across the seven blends contained within Subset 'E'. Triplicate measurements included for each sample.

The remaining blends within Subset 'E' (Blends A, C, E and G) were slightly more difficult to distinguish based on their UPLC TOF MS profiles; all appeared in quite close proximity to each other within the scores plot. One component could be picked out however that appeared to be higher in these four blends than the other three (highlighted with an orange circle in Figure 6.32b). This component had a mass of 517.3160 (retention time of 5.91 minutes) and its trend plot has been provided in Figure 6.35 to demonstrate this intensity pattern across the seven blends. As explained previously, this component has been identified as being predominantly characteristic of sherry casks rather than bourbon casks and so this finding indicates

that Blends A, C, E and G potentially contain higher percentages of sherry cask whisky than the other three blends. A few other components were found that followed this same intensity pattern (as well as being primarily associated with sherry casks) emphasising this point. UPLC TOF MS could therefore be an extremely useful tool to understand the components responsible for compositional variations between different blends and also the origins of such compounds.

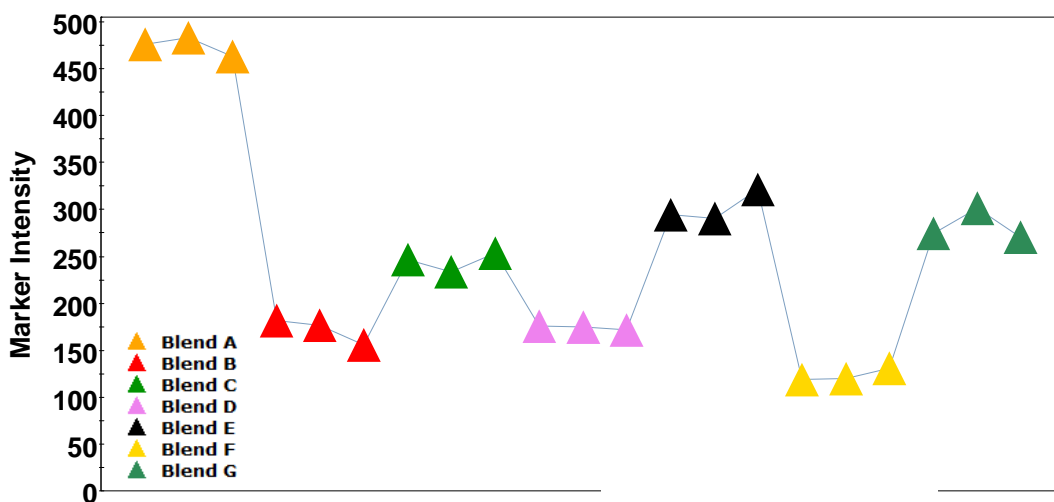


Figure 6.35: Trend plot of a component with retention time of 5.91 minutes and a mass of 517.3160 showing its intensity across the seven blends contained within Subset 'E'. Triplicate measurements included for each sample.

Overall, the findings obtained within this part of the study have demonstrated that UPLC TOF MS has excellent potential for investigating non volatile components responsible for compositional differences between different whisky products on the market. It was shown that as well as having the ability to distinguish between different blend products, this tool could differentiate the malt from all of the blends included within this analysis. It would be interesting to include other malt products within future studies to confirm whether this would always be possible. Additional malt samples would also allow an investigation as to whether different malt products could be distinguished between using UPLC TOF MS. It should also be noted at this point that multiple batches of all samples would need to be assessed in the future to investigate the consistency of profiles from batch to batch. The inclusion of multiple batches of samples would also mean that a variety of other PCA models could be constructed (more robustly) to focus on the comparisons of particular blends. This

might help to further distinguish blends that have proven difficult to separate when a wide variety of products are included in the model.

6.4 Conclusions

The research presented within this Chapter has demonstrated that UPLC TOF MS in combination with statistical data analysis software has excellent potential for a variety of applications within the Scotch Whisky industry. Characteristic profiles were obtained for a wide range of whisky samples and by implementing PCA it has been possible to distinguish between these different sample types based on the components that have been detected. Differentiation was achieved between whiskies that differed in their cask history; whiskies that were matured for different lengths of time; samples that containing elevated levels of the common adulterants sucrose and vanillin; a faded whisky *versus* its non faded equivalent; samples that had been artificially matured using solvent extraction from a variety of whiskies that were authentically matured; different blend whiskies; and a range of blends from a particular malt product.

The particular software implemented also enabled the components responsible for the above observations to be examined and as a result a number of interesting compounds were found that were characteristic of the different scenarios. One application of UPLC TOF MS within the Scotch Whisky industry could therefore be to analyse for particular marker compounds that could provide important information about the particular product or sample under investigation; whether this be to assess characteristics such as maturation age, cask history, or authenticity, or simply to understand more about the compositional variation of different blends (or malts). The potential of advanced software packages to help unravel the chemical composition of marker components could also be extremely beneficial and would mean that UPLC TOF MS could allow a greater understanding of many processes relevant to the Scotch Whisky industry; the findings in this chapter indicated that the technology could assess maturation reactions and the process of whisky fade. At this stage, structural elucidation of components identified in this research has not been attempted however, as a number of future experiments would initially be required

(containing additional batches of all samples) to ensure the consistency of UPLC TOF MS profiles. In addition, as indicated throughout the results, a number of future experiments would also be required to account for particular factors that may affect the profiles of specific samples.

The findings presented in this Chapter represent novel research, with UPLC TOF MS not having been implemented for analyses within the Scotch Whisky industry before. This preliminary work has therefore introduced technology that could greatly broaden and compliment knowledge of the composition of Scotch Whisky. One of the primary advantages of this tool is that it has the ability to monitor a variety of components that would not be detected using the traditionally preferred GC-MS. This preference of GC-MS in the past has also been the case throughout the spirits industry and so this preliminary investigation, as well as demonstrating benefits in relation to Scotch Whisky analysis, could potentially highlight the advantages of this tool to a much wider audience.

6.5 References

1. R. Aylott, *Whisky analysis*, in *Whisky: Technology, Production and Marketing*, (eds) I. Russell; G. Stewart, Elsevier, Oxford, 2nd Edition, 2014
2. R. Aylott, A. H. Clyne, A. P. Fox, D. A. Walker, *Analyst*, 1994, **119**, 1741-1746
3. A. J. Buglass, D. J. Caven-Quantril, *Analytical Methods*, in *Handbook of Alcoholic Beverages: Technical, Analytical and Nutritional Aspects (Volume II)*, (ed) A. Buglass, John Wiley & Sons, Chichester, 2011
4. J. M. Conner, A. Paterson, J. R. Piggott, *J. Sci. Food Agr.*, 1992 **60**, 349-353
5. J. R. Piggott, J. M. Conner, A. Paterson, J. Clyne, *Int. J. Food Sci. Tech.*, 1993, **28**, 303-318
6. J. Clyne, J. M. Conner, A. Paterson, J. R. Piggott, *Int. J. Food Sci. Tech.*, 1993, **28**, 69-81
7. S. J. Withers, J. R. Piggott, J. M. Conner, A. Paterson, *J. Inst. Brew.*, 1995, **101**, 359-364
8. J. Gruz, O. Novák, M. Strnad, *Food Chem.*, 2008, **111**, 789-794
9. E. L. Regalado, S. Tolle, J. A. Pino, P. Winterhalter, R. Menendez, A. R. Morales, J. L. Rodríguez, *J. Chromatogr. A.*, 2011, **1218**, 7358-7364
10. M. De Rosso, A. Panighel, A. D. Vedova, L. Stella, R. Flamini, *J. Agric. Food Chem.*, 2009, **57**, 1915-1920
11. E. Deák, A. Gyepes, É. Stefanovits-Bányai, M. Demovics, *Food Res. Int.*, 2010, **43**, 2452-2455
12. P. Alberts, M. A. Stander, A. De Villiers, *Food Addit. Contam. A*, 2011, **28**, 826-839
13. R. A. Lorenzo, M. T. Pena, P. Fernández, P. González, A. M. Carro, *Food Control*, 2014, **47**, 43-52
14. K. Takahshi, M. Tokuoka, H. Kohno, N. Sawamura, Y. Myoken, A. Mizuno, *J. Chromatogr. A.*, 2012, **1242**, 17-25
15. G. Chiva-Blanch, M. Urpi-Sarda, M. Rotchés-Ribalta, R. Zamora-Ros, R. Llorach, R. M. Lamuela-Raventós, R. Estruch, C. Andrés-Lacueva, *J. Chromatogr. A.*, 2011, **1218**, 698-705
16. T. Collins, J. Zweigenbaum, S. E. Ebeler, *Food Chem.*, 2014, **163**, 186-196

17. J. M. Conner, K. Reid, G. Richardson, *SPME analysis of flavour components in the headspace of scotch whisky and their subsequent correlation with sensory perception*, in *Gas Chromatography-Olfactometry: The State of the Art*, (eds) J. Leland; P. Schieberle; A. Buettner; T. Acree, American Chemical Society, USA, 2001
18. J. Conner, *Maturation*, in *Whisky: Technology, Production and Marketing*, (eds) I. Russell; G. Stewart, Elsevier, Oxford, 2nd Edition, 2014
19. *Scotch Whisky Regulations 2009*,
<http://www.legislation.gov.uk/uksi/2009/2890/made>, Accessed 25/11/2014
20. R. I. Aylott, W. M. MacKenzie, *J. Inst. Brew.*, 2010, **116**, 215-229

7.0 CONCLUSIONS AND FUTURE WORK

7.1 Conclusions

The primary objective set out at the beginning of this research was to investigate and develop analytical approaches that could be used to profile and understand more about Scotch Whisky colour (originating both from the legally permitted E150a caramel and also that derived naturally during maturation). ATR-MIR spectrometry and LC-MS were investigated as potential techniques for this purpose and multivariate data analysis tools were implemented to interpret the results acquired.

ATR-MIR was initially assessed to profile caramel colourants, to determine whether unique profiles could be obtained for different caramel materials. Caramels were firstly dissolved in 40% ethanol to mimic the medium of a typical Scotch Whisky and it was determined that characteristic profiles could be obtained by drying the sample solutions directly onto the ATR crystal – this allowed the otherwise dominating features of ethanol and water to be removed. By implementing this methodology to analyse different caramel colourants, it was possible to clearly distinguish between the four caramel classes recognised for use in foodstuffs by the EU (E150a, E150b, E150c and E150d). In addition to this it was found that ATR-MIR spectrometry also had the ability to differentiate between a selection of E150a caramels produced using different conditions of manufacture. These findings were maintained when the same caramel materials were dissolved in a typical Scotch Whisky (subject to no prior caramel addition), indicating that the dried residues of this spirit would be dominated by the colourant added. Despite this finding, it was also found that natural whisky colour did have some influence on the spectra of dried residues when caramels were dissolved within this product. Additional studies were therefore undertaken using ATR-MIR spectrometry to assess how the spectral profiles of caramels (when dissolved in Scotch whiskies) would be affected by variation in the background whisky matrix and it was found that differentiation between E150a caramels was still possible even when a high level of natural colour was present. Other factors that were found to influence the ATR-MIR spectral

features of dried caramel residues were the process of caramel fade and variations in caramel concentration.

After it was established that ATR-MIR spectrometry had the ability to obtain characteristic profiles of different caramel colourants, a number of multivariate data analysis tools were investigated to determine whether it would be possible to predict the identity of test/unknown caramel solutions based on their unique spectral features. PCA with GLSW preprocessing, HCA, *k*-NN classification and PC-DFA were all compared for this purpose and although one did not stand out at this point as being the most successful, each was found to have its own associated advantages and disadvantages to be considered. PCA with GLSW preprocessing and PC-DFA both showed very similar findings: they demonstrated excellent potential for the prediction of caramel identities (both class and E150a formulation) when dissolved in 40% ethanol, however it was found that the background matrix of any whisky would need to be accounted for during calibration to allow more successful predictions when caramels are dissolved in a Scotch Whisky. It was also found that the prediction of caramel identities using these two data analysis tools would likely be influenced by factors such as variation in caramel concentrations between calibration and test data and also if a test caramel had been subjected to fade. Studies undertaken using *k*-NN classification were found to overcome all of these potential limitations associated with PCA with GLSW and PC-DFA, *k*-NN classification however had its own major drawback in that test data has to be appointed to one of the pre-assigned calibration categories. This would result in misclassifications if the identity of a test/unknown sample was not accounted for within the calibration data – a potentially significant problem if being used to assess suspect whisky samples where the origin of colour would most likely be completely unknown.

An additional study undertaken using PC-DFA demonstrated the potential to differentiate between four real blend products already on the market based on their dried residue profiles (obtained *via* ATR-MIR spectrometry) and the potential to predict the identity of test blend samples was clearly shown. It would be interesting to undertake future work in this area using a much bigger sample set, to see whether

blend discrimination using ATR-MIR spectrometry is possible using a much wider range of Scotch Whisky products.

A wide range of samples relevant to the Scotch Whisky industry were analysed using LC-MS prior to the commencement of this project and so the primary objective of this research was to determine the potential of this tool for profiling the non-volatile components of Scotch Whisky by the application of multivariate data analysis tools to the data. Caramel colourant profiles were assessed initially in this work and it was possible to clearly distinguish between the four caramel classes based on the components detected using LC-MS. It was also possible to differentiate between three different types of E150a included within this study and both findings were maintained when caramels were dissolved in a typical Scotch Whisky as opposed to 40% ethanol. These findings therefore complemented those attained already when ATR-MIR spectrometry was used to profile caramel colourants, however the advantage of using LC-MS over ATR-MIR is that the former can allow the individual components responsible for sample differentiation to be investigated. It was therefore possible in this part of the research to pick out specific marker compounds that were either unique to or predominantly associated with different caramel materials and not present in/masked by the typical background whisky matrix. An attempt was also made using advanced software to structurally elucidate these compounds and hence confirm the identity of certain caramel markers. It was possible to confidently assign three E150a markers as sugars and tentative structures for these compounds were suggested. These compounds would however need to be isolated and subjected to additional analyses (further fragmentation studies and NMR) to confirm their structural identities.

Additional studies undertaken using the LC-MS dataset demonstrated that it was possible to use this technique to differentiate between: whiskies that differed in their cask history; whiskies that were matured for different lengths of time; samples that contained elevated levels of the common adulterants sucrose and vanillin; a faded whisky *vs.* its non faded equivalent; samples that had been artificially matured from a variety of whiskies that were authentically matured; different blend whiskies; and a

range of blends from a particular malt. It was also possible to pick out a number of interesting components that were responsible for these observed distinctions.

7.2 Comments and Suggestions for Future Work

Overall, the above findings relating to ATR-MIR spectrometry could be extremely beneficial to the Scotch Whisky industry, particularly in terms of counterfeit detection; authentic products could potentially be identified based on the confirmation of a specific colourant profile being present (or absent). The fact that different E150a caramel materials can be clearly differentiated between using ATR-MIR spectrometry also opens up the potential for E150a caramels with unique spectral profiles to be spiked into different blend products to act as markers for authenticity. At this point of the research however, the manufacturing conditions responsible for spectral variation could not be pinpointed as limited information was available about the caramels from the manufacturers. One key piece of future work that would therefore be extremely interesting to undertake would be to obtain and analyse a set of caramels with known manufacturing conditions, to investigate whether spectral variations could be attributed to particular manufacturing parameters. It would then potentially be possible to control/manipulate E150a manufacture in the future to create legally permitted caramels with distinct signature profiles that could be used as authenticity markers in blends. A much larger dataset would be recommended for this work to be taken forward, incorporating samples covering a wide range of manufacturing variables (keeping any parameters not being assessed consistent). Multiple replicates of each sample type would also be important to ensure consistency of profiles for each set of conditions considered.

Another key area of future work would be to investigate the potential to miniaturise/adapt the ATR-MIR instrumentation into a portable device to open up the possibility for it to be taken into the field; as indicated by the preliminary findings within this research, such a tool could be used to screen suspect samples based on their colourant profile. There is currently a growing requirement for such portable devices within the Scotch Whisky industry and this is one of the key advantages of ATR-MIR over LC-MS; although it has been shown in this research that the latter

can provide a more comprehensive assessment of whisky composition, it is a laboratory based tool and so could not be implemented as a field device for quick screening purposes. Recommendations as to considerations that should be taken when developing the ATR-MIR methodology into a portable device have been included in Appendix 8.3.

Other areas of future work that could be undertaken in relation to profiling Scotch Whisky colour using ATR-MIR have been summarised below:

- Only single batches of caramel types E150b, E150c and E150d were assessed in this research when distinguishing between caramel classes. An area of future work would therefore be to obtain multiple batches of additional types of caramels from these classes to investigate whether they would still group together and also remain distinguished from other classes.
- Caramel profiles were also only assessed within two Scotch Whisky matrixes (one typical and one representing a much higher level of natural colour). It would therefore be interesting to assess a wider range of whisky matrixes to see what influence their natural colour components would have on caramel profiles. For instance, would all whiskies with a typical level of natural colour influence spectra to the same or a similar extent?
- Only a single or a few types of caramel were examined when investigating the influence of the following factors on caramel profiles: high levels of natural colour, caramel concentration and caramel fade. Future work could therefore assess other caramel types to see whether findings remained consistent.
- Preliminary work in this research demonstrated that natural colour will also influence the ATR-MIR spectral features of dried whisky residues and an area of future work could be to determine whether whiskies that contain no caramel will possess unique features depending on their natural colour profiles. This could be particularly useful for distinguishing between malt whiskies, the majority of which do not contain E150a caramel.

- It would also be interesting to determine whether the developed ATR-MIR methodology could be used to profile and investigate cask variables based on natural colour profiles. Natural colour is known to be influenced by factors such as cask history (e.g. the use of ex-sherry casks *vs.* ex-bourbon casks and first fill *vs.* refill casks), maturation age and cask fill strength. The ability to distinguish between different cask variables could be used to provide information – for cask or bottle samples – as to the wood policy used for their production. Obtaining a greater understanding how cask variables influence natural colour could also be used to identify the maturation potential of a particular cask and to evaluate and optimise various procedures available for cask regeneration.

In relation to predicting the identity of test caramels when dissolved in Scotch whiskies, it was identified that the background whisky matrix would likely have to be accounted for in the calibration model to allow successful predictions. A key piece of future work would therefore be to construct new calibration models consisting of samples dissolved in a typical Scotch Whisky and predict the identity of fresh test samples (dissolved in the same whisky) to confirm whether predictions could be improved when using PCA with GLSW and PC-DFA as classification tools. A much bigger sample set would also be required to ensure that test samples representing all types of caramels within the calibration dataset are being assessed. The number of test samples utilised within this research were restricted in their availability but were deemed suitable to allow preliminary studies to be undertaken.

The use of LC-MS to analyse the non volatile constituents of Scotch whiskies is relatively novel and the results obtained from the LC-MS data analysis within this research have provided an excellent preliminary overview as to how this technique could be utilised within the Scotch Whisky industry. Being a preliminary study however, means that only a small sample set spanning a range of sample types was initially utilised, typically incorporating only a single example of each sample type (analysed in triplicate). It would therefore be extremely interesting to split this research into a number of subprojects each focusing on one of the different factors initially assessed within this preliminary research (e.g. caramel colourants, cask

history, maturation age, authentic vs. natural maturation, etc...) and obtain multiple batches of the samples initially assessed/any other samples deemed relevant. This would allow confirmation of these initial findings in terms of the sample differentiation observed and also in terms of whether the marker components identified for different sample types are consistently observed. Once the identity of suitable markers has been confirmed, it would then be extremely interesting to take structural elucidation further and assign tentative structures to all marker components using the advanced LC-MS software. It would subsequently be recommended that components of interest be isolated and their structural identities confirmed using additional fragmentation studies and techniques such as NMR.

Overall it has been demonstrated that LC-MS would be an extremely beneficial tool for understanding more about the non volatile composition of Scotch Whisky (which would incorporate components relating to colour – both caramel colour and natural colour). This is an area where there is currently very little knowledge within the industry and this is due to GC-MS being traditionally preferred for compositional analysis. The advances made in LC-MS technology in recent years however have made it very appealing for profiling complex mixtures and so as well as highlighting its potential within the Scotch Whisky industry, the results from this research indicate that this technology could potentially be used on a much wider scale throughout the spirits industry where GC-MS has traditionally been preferred.

8.0 APPENDICES

8.1 Calculating Reconstitution Volume

When samples were being prepared for the concentration study it was found that the original ATR-MIR methodology (pre-concentrating samples from 6 mL to 300 μ L) did not provide consistent profiles when solutions of the same caramel were prepared at different concentrations in 40% ethanol. This was unexpected due to the fact that all data were normalised, a process that should have accounted for any concentration differences and so provide consistent spectra. To account for this issue encountered with the original ATR-MIR methodology, when samples of different starting concentration were to be considered they were all reconstituted in different volumes during the pre-concentration step to ensure that the final concentration before analysis was theoretically equivalent. An example of the calculations used to determine the appropriate reconstitution volume in these cases has been provided below.

The desired final concentration (C_2) for sample solutions was calculated based on what was originally obtained after pre-concentrating an average whisky (with absorbance of 0.55 at 430 nm) from 6000 μ L to 300 μ L. This was calculated as shown below using Equation 8.1, where C_1 is the initial concentration (before the pre-concentration step), V_1 is the volume taken of this initial solution, C_2 is the final concentration (after pre-concentration) and V_2 is the final volume. Concentration values in this case have been replaced with the absorbance values at 430 nm as the two are linearly proportional.

$$C_1V_1 = C_2V_2 \quad \text{Equation: 8.1}$$

$$0.55 \times 6000 = C_2 \times 300$$

$$C_2 = 11$$

The reconstitution volume required to prepare all future sample solutions was subsequently calculated to provide this final concentration ($C_2=11$) – although it should be noted that this is not a true absorbance value but rather a theoretical value

to scale others to in order to achieve equivalent final concentrations. If a caramel solution therefore had an initial absorbance (C_1) of 0.2 for example, the reconstitution volume (V_2) can be calculated as follows (a starting volume (V_1) of 6000 μL was always used):

$$C_1V_1 = C_2V_2$$

$$0.2 \times 6000 = 11 \times V_2$$

$$V_2 = 109 \mu\text{L}$$

8.2 Scores and Loadings Data for Additional PCs

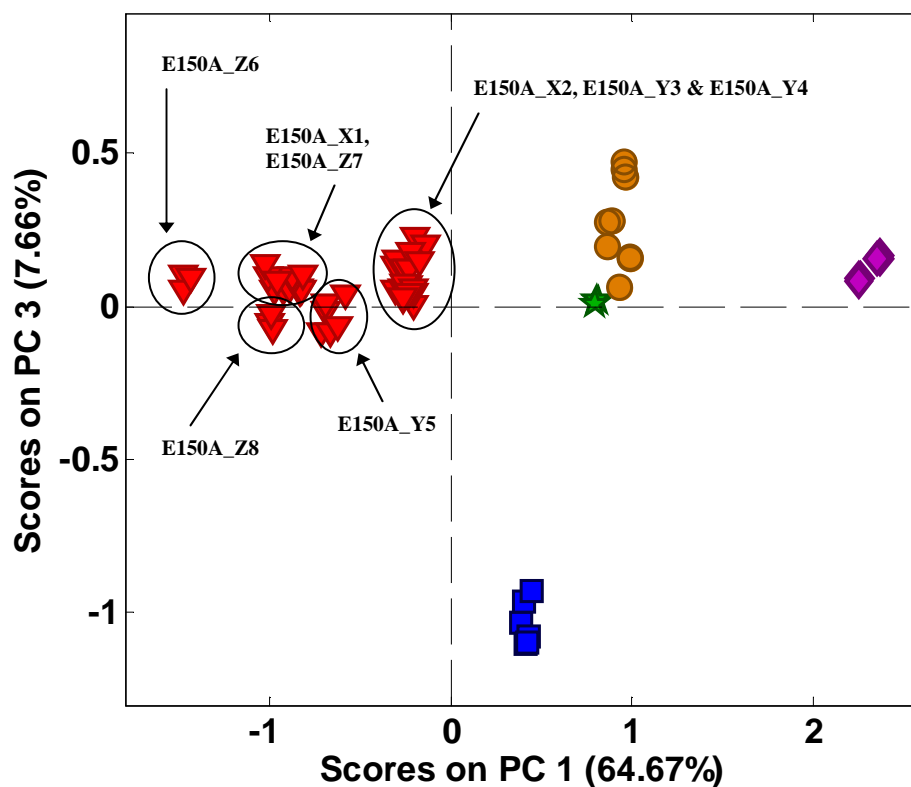


Figure 8.1: PC1 vs. PC3 scores plot obtained from PCA of the ATR-MIR spectra acquired from all fifteen E150A caramels (red triangles), one batch of E150B_X9 (green stars), two batches of E150C_10 (blue squares), two batches of E150D_11 (purple diamonds) and the three burnt sugar materials (orange circles). Sample details can be found in Table 3.1 and each sample was dissolved in 40% ethanol and analysed in triplicate.

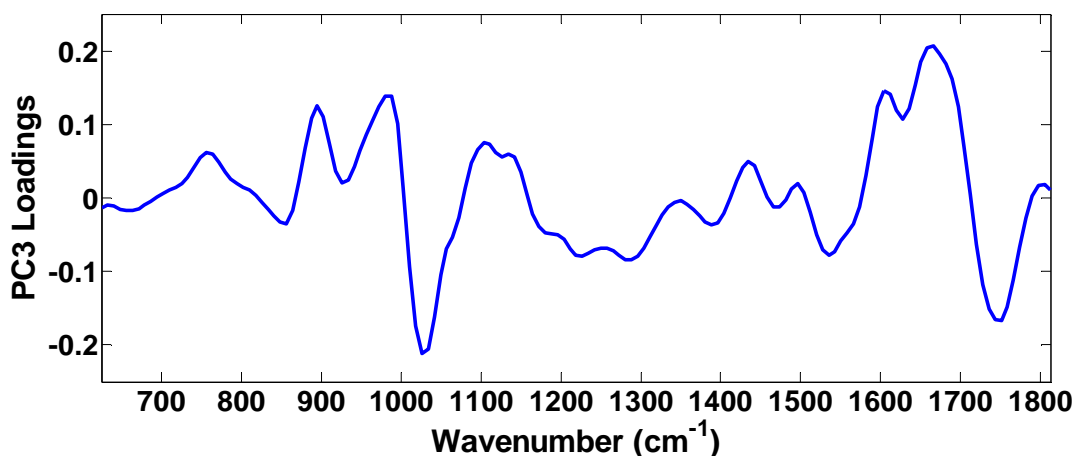


Figure 8.2: PC3 loadings acquired from PCA of the ATR-MIR spectra acquired from all 23 samples described in Table 3.1, when dissolved in 40% ethanol and analysed in triplicate.

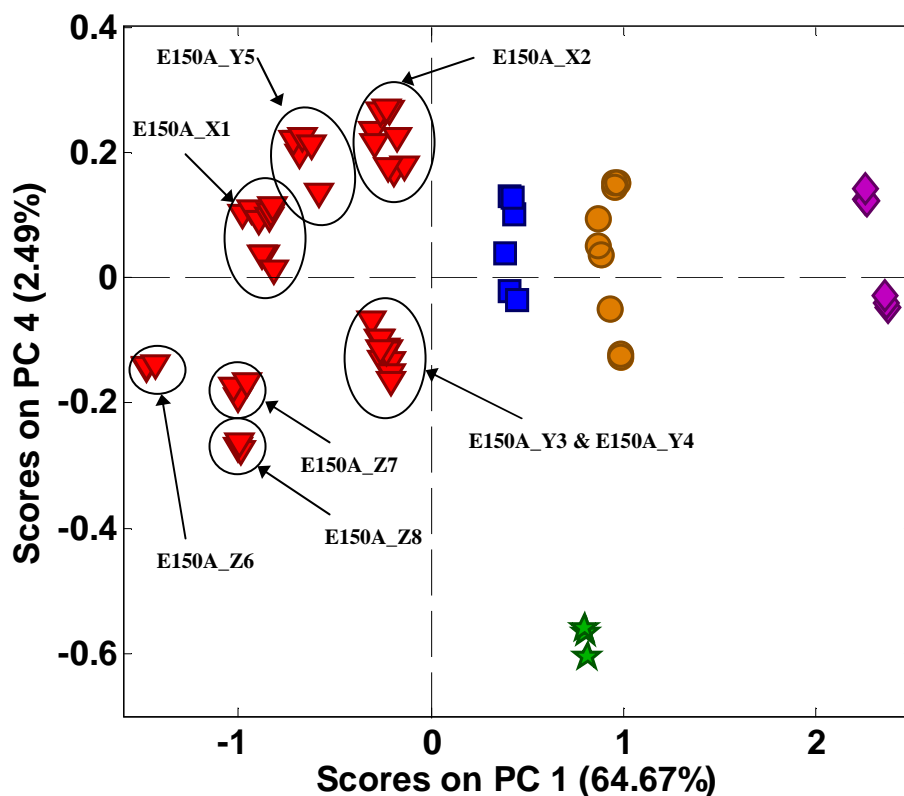


Figure 8.3: PC1 vs. PC4 scores plot obtained from PCA of the ATR-MIR spectra acquired from all fifteen E150A caramels (red triangles), one batch of E150B_X9 (green stars), two batches of E150C_10 (blue squares), two batches of E150D_11 (purple diamonds) and the three burnt sugar materials (orange circles). Sample details can be found in Table 3.1 and each sample was dissolved in 40% ethanol and analysed in triplicate.

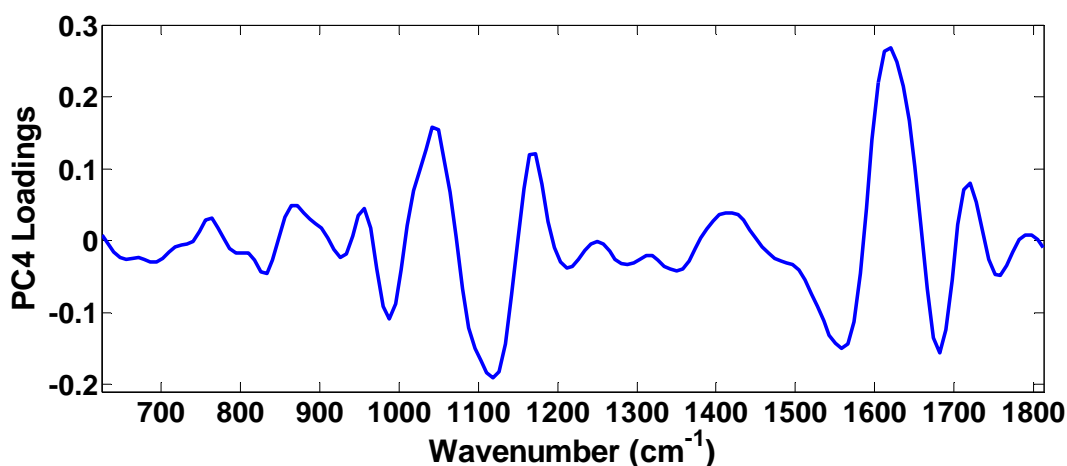


Figure 8.4: PC4 loadings acquired from PCA of the ATR-MIR spectra acquired from all 23 samples described in Table 3.1, when dissolved in 40% ethanol and analysed in triplicate.

8.3 Considerations and Recommendations for ATR-MIR Instrument Development

Table 8.1: Table of the considerations and recommendations for developing a portable ATR-MIR device for field testing whiskies using the methodology developed in this research.

Consideration	Resulting Recommendation
Instrumentation needs to be developed that is practical as a portable device.	The fibre optic probe set up would not be the most suitable for a portable device; an ATR system with a 'drop in' sample chamber might be more appropriate.
Samples with the colour level of a typical blend (~0.5 at 430nm) currently require a pre-concentration step to get spectra of adequate absorbance.	It would be much more practical and time effective if instrumentation could be devised that incorporated the pre-concentration step as part of the analysis procedure. One suggestion could be to incorporate a heating element or an air flow to dry samples onto the ATR crystal.
Spectral differences have been observed when comparing profiles of dried residues just after switching the heat lamp off with when the probe head has returned back to room temperature.	Would it be possible/feasible to include a means to rapidly cool the device back to room temperature for measurements? or Would it be possible to dry samples in a reasonable timeframe without the use of heat (e.g. with an air flow)?
The size of the sample chamber would need to reflect the volume of liquid required for adequate spectra to be obtained.	Based on current pre-concentration (6000uL to 300uL and then taking 10uL of this to dryness), then if samples were introduced directly into the sample chamber, the equivalent factor would be from 200uL to dryness. Need to consider if this would this change if crystal parameters changed (e.g. no. of bounces)

Table 8.1 cont.: Table of the considerations and recommendations for developing a portable ATR-MIR device for field testing whiskies using the methodology developed in this research.

Consideration	Resulting Recommendation
Initial research has indicated that different concentrations of the same sample will affect spectral features, even when data is normalised.	Can different calibration models perhaps be created for different concentration ranges (e.g. low/typical/high) and selected by the analyst according to the sample being considered?
Samples are currently injected manually onto the ATR crystal and there is no means of sample containment, both of which could be affecting dried residue concentration and introducing a source of spectral variation.	Can the sample compartment be adapted so that sample droplets can be deposited more consistently over the ATR crystal (e.g. incorporate a sample well around the crystal)? Would an automated sample introduction be more appropriate/a practical development?
As sample concentration has been shown to influence spectral features it would be important to ensure that no sample material is lost on the sides of any sample chamber when drying.	Could Teflon or another similar material potentially be used to coat the walls of the sample chamber/the sample well to prevent samples from sticking?
The sample compartment/sample well would need to be cleaned between each measurement. Can an easy cleaning mechanism be devised?	One suggestion could be to incorporate a chamber set up with disposable tips at the crystal that can be removed after each sample analysis.
It would be an additional benefit/provide an additional application if any developed instrumentation could also be used to determine ethanol concentration.	It might therefore be beneficial to devise a way that the sample chamber can be sealed/covered to allow an initial ethanol concentration to be determined without sample evaporation.
What data analysis would need to be performed/how can this be implemented?	Ease of implementation – the instrument will not necessarily be used by scientific personnel.